NTIS Pavement and Geometric
Design Criteria for Minimizing
Hydroplaning, Final Report
FHWA-RD-79-31

December 1979

EDC Library Ref. No. 1107

DISCLAIMER

These materials are available in the public domain and are not copyrighted. Engineering Dynamics Corporation (EDC) copies and distributes these materials to provide a source of information to the accident investigation community. EDC makes no claims as to their accuracy and assumes no liability for the contents or use thereof.

PB80146194

NTIS
Information is our business.

PAVEMENT AND GEOMETRIC DESIGN CRITERIA FOR MINIMIZING HYDROPLANING FINAL REPORT

TEXAS A&M UNIVERSITY
COLLEGE STATION, TX

DEC 79

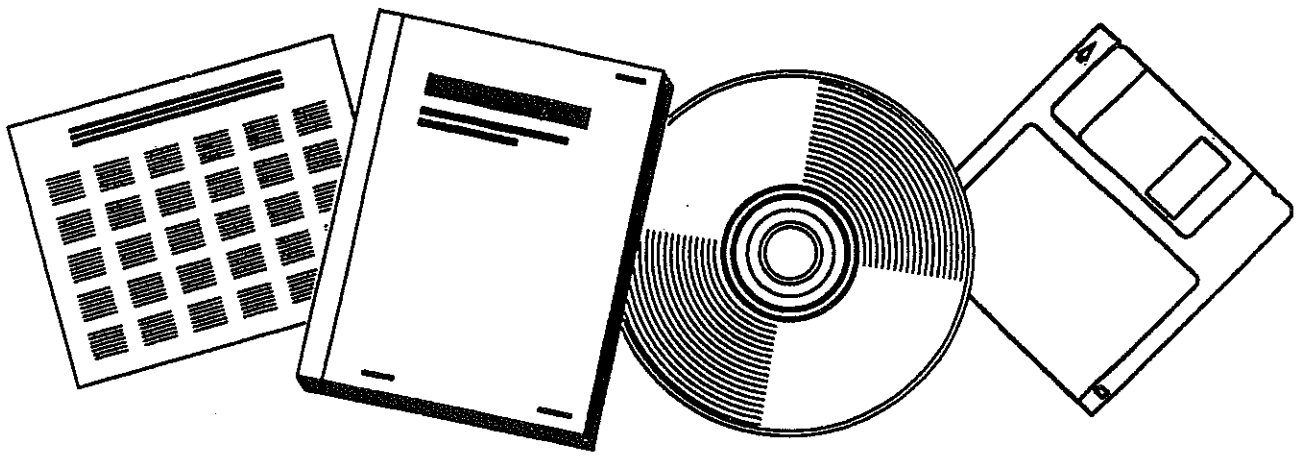

U.S. DEPARTMENT OF COMMERCE
National Technical Information Service

PB80146194

Report No. FHWA-RD-79-31

PAVEMENT AND GEOMETRIC DESIGN CRITERIA FOR MINIMIZING HYDROPLANING

December 1979
Final Report

Document is available to the public through the National Technical Information Service, Springfield, Virginia 22161

Prepared for
FEDERAL HIGHWAY ADMINISTRATION
Offices of Research & Development
Structures & Applied Mechanics Division
Washington, D.C. 20590

REPRODUCED BY
NATIONAL TECHNICAL
INFORMATION SERVICE
U. S. DEPARTMENT OF COMMERCE
SPRINGFIELD, VA. 22161

FOREWORD

This is a report of an investigation of factors that affect vehicle hydroplaning. It involves design criteria related to pavement texture, cross slope, rutting, drainage, rainfall likelihood, vehicle control, and traction.

Laboratory and full scale tests were conducted to determine the influence of pavement conditions on the hydroplaning phenomenon. The experiments were followed by analytic analyses and data interpretation to provide sound evaluation.

Limited distribution of the full report is being made primarily to research personnel.

Charles F. Scheffey
Director, Office of Research
Federal Highway Administration

Notice

This document is disseminated under the sponsorship of the U. S. Department of Transportation in the interest of information exchange. The United States Government assumes no liability for its contents or use thereof.

The contents of this report reflect the views of the authors, who are responsible for the facts and the accuracy of the data presented herein. The contents do not necessarily reflect the official views or policy of the Department of Transportation.

This report does not constitute a standard, specification, or regulation.

The United States Government does not endorse products or manufacturers. Trademarks or manufacturers' names appear herein only because they are considered essential to the object of this document.

Technical Report Documentation Page

1. Report No.	2. Government Accession No.	3. Recipient's Catalog No.
FHWA-RD-79-31		PB 80 146194

4. Title and Subtitle	5. Report Date
PAVEMENT AND GEOMETRIC DESIGN CRITERIA FOR MINIMIZING HYDROPLANING	December 1979
	6. Performing Organization Code
	8. Performing Organization Report No.

7. Author(s)	10. Work Unit No. (TRAIS)
B. M. Gallaway, D. L. Ivey, G. Hayes, W. B. Ledbetter, R. M. Olson, D. L. Woods and R. F. Schiller, Jr.	FCP 31H2-212

9. Performing Organization Name and Address	11. Contract or Grant No.
Texas Transportation Institute Texas A&M University College Station, Texas 77843	Contract DOT-FH-11-8269

12. Sponsoring Agency Name and Address	13. Type of Report and Period Covered
Federal Highway Administration Offices of Research and Development HRS-12 Washington, D.C. 20590	Final Report Phase II
	14. Sponsoring Agency Code 80929

15. Supplementary Notes

FHWA Contract Manager: Glenn G. Balmer (HRS-12)

16. Abstract

A comprehensive literature review, multistate questionnaire, mathematical modeling, computer simulation, field testing and data correlations were used to establish criteria relating to geometric and pavement surface characteristics to minimize highway hydroplaning.

More specifically, the authors have covered in detail the empirical indications of hydroplaning as determined from interpretation of hard data developed with a spin-down trailer in a hydroplaning trough, skid number trailers including drag link and torque, and extensive tire and pavement testing under simulated and natural rain. Precise measurements of surface drainage were examined and equations relating pavement texture, cross slope and rainfall were developed. Random and patterned textures covering the complete range of real-world pavements were included.

A determination of deficiencies in existing surface drainage design methodology for sag-vertical curves was conducted by state surveys and representative sites were studied and innovative answers supplied.

A summary of criteria to reduce hydroplaning is presented along with recommendations for construction of flexible and rigid pavements to minimize hydroplaning.

Extensive field studies of open-graded surfaces under simulated and natural rain confirm the high level performance of such surfaces, including tire-to-surface contact, reduction of splash and spray, and flatter friction vs. speed gradients.

Report No. FHWA-RD-79-30 is a technical summary of this report.

17. Key Words	18. Distribution Statement
skid number, texture, available friction, hydroplaning, tire-pavement interaction, pavement surface design, criteria, cross slope, driver requirements, math model, computer simulation, flow-phenomena, rainfall intensity	No restriction. This document is available through the National Technical Information Service, Springfield, Virginia 22161

19. Security Classif. (of this report)	20. Security Classif. (of this page)	21. No. of Pages	22. Price
Unclassified	Unclassified		

Form DOT F 1700.7 (8-72) Reproduction of completed page authorized

METRIC CONVERSION FACTORS

Approximate Conversions to Metric Measures

Symbol	When You Know	Multiply by	To Find	Symbol
	LENGTH			
in	inches	*2.5	centimeters	cm
ft	feet	30	centimeters	cm
yd	yards	0.9	meters	m
mi	miles	1.6	kilometers	km
	AREA			
in^2	square inches	6.5	square centimeters	cm^2
ft^2	square feet	0.09	square meters	m^2
yd^2	square yards	0.8	square meters	m^2
mi^2	square miles	2.6	square kilometers	km^2
	acres	0.4	hectares	ha
	MASS (weight)			
oz	ounces	28	grams	g
lb	pounds	0.45	kilograms	kg
	short tons (2000 lb)	0.9	tonnes	t
	VOLUME			
tsp	teaspoons	5	milliliters	ml
Tbsp	tablespoons	15	milliliters	ml
fl oz	fluid ounces	30	milliliters	ml
c	cups	0.24	liters	l
pt	pints	0.47	liters	l
qt	quarts	0.96	liters	l
gal	gallons	3.8	liters	l
ft^3	cubic feet	0.03	cubic meters	m^3
yd^3	cubic yards	0.76	cubic meters	m^3
	TEMPERATURE (exact)			
°F	Fahrenheit temperature	5/9 (after subtracting 32)	Celsius temperature	°C

*1 in = 2.54 (exactly). For other exact conversions and more detailed tables, see NBS Misc. Publ. 286, Units of Weights and Measures, Price $2.25, SD Catalog No. C13.10:286.

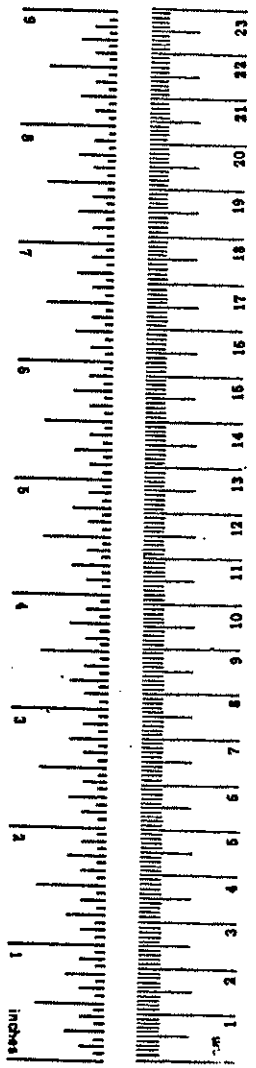

Approximate Conversions from Metric Measures

Symbol	When You Know	Multiply by	To Find	Symbol
	LENGTH			
mm	millimeters	0.04	inches	in
cm	centimeters	0.4	inches	in
m	meters	3.3	feet	ft
m	meters	1.1	yards	yd
km	kilometers	0.6	miles	mi
	AREA			
cm^2	square centimeters	0.16	square inches	in^2
m^2	square meters	1.2	square yards	yd^2
km^2	square kilometers	0.4	square miles	mi^2
ha	hectares (10,000 m^2)	2.5	acres	
	MASS (weight)			
g	grams	0.035	ounces	oz
kg	kilograms	2.2	pounds	lb
t	tonnes (1000 kg)	1.1	short tons	
	VOLUME			
ml	milliliters	0.03	fluid ounces	fl oz
l	liters	2.1	pints	pt
l	liters	1.06	quarts	qt
l	liters	0.26	gallons	gal
m^3	cubic meters	35	cubic feet	ft^3
m^3	cubic meters	1.3	cubic yards	yd^3
	TEMPERATURE (exact)			
°C	Celsius temperature	9/5 (then add 32)	Fahrenheit temperature	°F

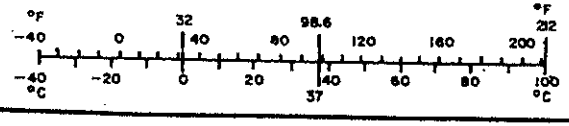

PREFACE

This is the report issued following a two-phase study under Contract DOT-FH-11-8269, which deals with "Pavement and Geometric Design Criteria for Minimizing Highway Hydroplaning".

The report presents criteria developed by a seven-man team for pavement surface texture and cross slope and suggestions for modifications in pavement geometrics to minimize hydroplaning.

The recommendations presented can be adapted to suit the road situations of the various states taking into account terrain, traffic, weather and available materials.

ACKNOWLEDGMENTS

The authors wish to express their appreciation to Mr. Glenn G. Balmer, Contact Representative of the Federal Highway Administration, for his assistance in securing vital background information for the study and for his counsel and devoted interest in assuring the successful execution of the objectives of the study.

The secretarial and technical staff of the Materials Division, the Safety Division and the Structures Division are commended for the preparation of the manuscript. Particular commendation is made to Sylvia Velasco for her dedicated effort to the successful execution of the report.

TABLE OF CONTENTS

Chapter		Page
	INTRODUCTION	1
I	THE PHENOMENON OF HYDROPLANING	3
II	DETERMINING THE PROBABILITY OF SELECTED RAINFALL INTENSITIES	21
	General	21
	Determination of Rainfall Characteristics	22
	Selection of Representative Stations	27
	Selection of Representative Years for Rainfall Analysis	27
	Analysis of Detailed Rainfall Records	30
	Determining the Probability of Specific Rainfall Intensities	35
III	HYDROPLANING AND TRACTION TESTS UNDER CONTROLLED CONDITIONS	51
	Test Conditions	51
	Preliminary Tests on Grooved PCC	51
	Summary of Observations from Preliminary Tests on Grooved PCC	61
	Tests on Asphalt Surfaces	61
	Tests in Free-Standing Pools ("Puddles")	72
	General Observations	77
IV	MINIMIZING HYDROPLANING CONDITIONS ON PORTLAND CEMENT CONCRETE SURFACES	79
	Introduction	79
	Water Depth Prediction on PCC Surfaces for Multilane Roadways	79
	Skid Resistance and Cornering Slip on Textured PCC Surfaces	84
	Discussion and Conclusions	98
V	TIRE-PAVEMENT INTERACTIONS ON OPEN-GRADED FRICTION COURSES IN SIMULATED AND NATURAL RAINFALL	101
	Introduction	101
	Review of Recent Literature	101
	Field Experiments by TTI	119
	Tire-Pavement Interaction on OGFC	121
	Discussion of Performance of Open Mixes in Simulated Rain	126
	Macrotexture of SH-21 OGFC	144
	Performance of OGFC Under Natural Rain	148
	Natural Rainfall on Open-Graded and Dense Surfaces in Austin, Texas	163
	Fort Worth Pavements in Natural Rain	163
	Natural Rainfall on OGFC in Beaumont	171
	Natural Rainfall on OGFC in Bryan on SH-21	178

TABLE OF CONTENTS (continued)

Chapter		Page
	General Conclusions and Summary Statements	186
	Economic Factors	193
VI	PAVEMENT DRAINAGE	196
	Field Investigations of Puddle and Texture Depth	196
	Test Procedures	196
	Findings	201
	Water Depths on Multilane Highways with Different Cross Slopes	209
	Example Calculation for Theoretical Water Depth	213
VII	DESIGN OF SAG-VERTICAL CURVES TO REDUCE HYDROPLANING	217
	Design Criteria for Drainage of Sag-Vertical Curves	217
	Innovative Drainage Concepts for Sag-Vertical Curves	217
	Objectives	218
	Generalized Work Plan	218
	Assumptions	219
	Findings from Drainage Path Analysis	232
	Recommended Remedial Treatments for Sag-Vertical Curves Subject to Flooding	240
VIII	CRITERIA TO REDUCE HYDROPLANING	243
IX	SUMMARY AND CONCLUSIONS	253
REFERENCES		260
Appendix A		264
Appendix B		274

LIST OF TABLES

Table		Page
1	Equations to predict hydroplaning speed	4
2	Computed and observed hydroplaning speeds	10
3	Sequence of operations	22
4	Average yearly rainfall for Illinois, 1942 through 1972	28
5	The average rainfall of selected stations as grouped by rainfall ranges	31
6	Data from Figure 17	36
7	Summary of individual rainfall analyses from nine data stations in Illinois	37
8	Summary of individual rainfall analyses from nine data stations in Alabama	38
9	Duration of threshold intensities for one year	42
10	Summary of rainfall exposure time in four states	43
11	Peak forces and percent spindown traversing "puddles" shown in Figures 51 through 56	73
12	Concrete test section texture depths	87
13	Cornering slip equations	92
14	Swiss classification of road surfaces	107
15	Macrotexture of OGFC surfaces SH-21	149
16	Comparative performance of open mixes under various conditions	150
17	Performance of open-graded friction courses on SH-21 Brazos County in natural rain	159
18	Properties of field cores from SH-21 open-graded surfaces	162
19	Locations of test sites in Texas	197
20	Surface texture depth	202
21	Comparison of theoretical water depths with water depths from the empirical equation at several points along the slope	216
22	Tentative sag vertical curve drainage design criteria based on a survey of existing practice	218
23	Required thickness of open-graded pavement for selected rainfalls, inches (mm)	228

LIST OF TABLES (continued)

Table		Page
24	Allowable wheel path depressions	231
25	Evaluation of innovative systems	239
26	Ranking of innovative surface-drainage systems for practicality	239
27	Recommended remedial treatment for sag-vertical curves subject to flooding	241
28	Recommended treatment for sag-vertical curves in new construction	241
29	Variables influencing hydroplaning	246
30	Example design rainfall intensities	248
31	Example allowable combination of pavement drainage parameters	249

LIST OF FIGURES

Figure		Page
1	Estimated free rolling minimum full dynamic hydroplaning speed for passenger tires	5
2a	Wheel freely rolling on dry surface	7
2b	Wheel not turning, 100% spindown condition	7
3	Data scatter for hydroplaning equation	11
4	Influence of four parameters on hydroplaning speed	12
5a	Deterioration of available friction with speed	13
5b	Possible range of hydroplaning speeds	13
6	Observed values of skid numbers compared to calculated values of spindown	16
7	Variation of water depth during rainmaker SN tests	17
8	60 mph skid numbers vs. texture depths	18
9	Resistance due to the displacement of water as a function of velocity for different water depths	20
10	Isolines of mean annual precipitation	23
11	Isolines of mean annual precipitation	24
12	Isolines of mean annual precipitation	25
13	Tentative criterion for acceptable variation in annual	26
14	Statewide average annual rainfall frequency diagram	29
15	Average of selected stations annual rainfall frequency diagram	32
16	Frequency diagrams for selected stations	33
17	Incremental rainfall recording	34
18	Probability of a given rainfall of intensity I or greater vs rainfall intensity I	39
19	Influence of trace rainfall duration on probability curves, Alabama data	40
20	Percent of typical calendar year having rainfall of intensity I or greater	44
21	Determination of percent time of exposure to > 0.01 in/h rain	45
22	Percent of all accidents occurring during wet weather vs annual rainfall	46
23	Duration of rainfall events of nominally 1/2 in/h intensity	48

LIST OF FIGURES (continued)

Figure		Page
24	Influence of different theoretical rainfall patterns on the simplifying assumption	49
25	Hydroplaning trough	52
26	Test run in the hydroplaning trough	52
27	Locked-wheel horizontal force from force transducer vs. 5th wheel vehicle speed	54
28	Horizontal force from torque transducer vs. 5th wheel vehicle speed	55
29	Freewheeling horizontal force vs. 5th wheel speed	56
30	Freewheeling horizontal force vs. 5th wheel speed	57
31	Locked-wheel skid number vs. speed	58
32	Percent spindown vs. vehicle speed	59
33	Spinup time vs. 5th wheel vehicle speed	60
34	Increase in stopping distance due to hydroplaning	62
35	Comparison of open-graded and slurry seal surfaces	63
36	Comparison of open-graded and slurry seal surfaces	63
37	Comparison of open-graded and slurry seal surfaces	64
38	Comparison of open-graded and slurry seal surfaces	64
39	Comparison of open-graded and slurry seal surfaces	65
40	Comparison of open-graded and slurry seal surfaces	65
41	Comparison of open-graded and slurry seal surfaces	66
42	Comparison of open-graded and slurry seal surfaces	66
43	Comparison of open-graded and slurry seal surfaces	68
44	Comparison of open-graded and slurry seal surfaces	68
45	Comparison of open-graded and slurry seal surfaces	69
46	Comparison of open-graded and slurry seal surfaces	69
47	Comparison of open-graded and slurry seal surfaces	70
48	Comparison of open-graded and slurry seal surfaces	70
49	Comparison of open-graded and slurry seal surfaces	71
50	Comparison of open-graded and slurry seal surfaces	71
51	Puddle "A"	74
52	Puddle "B"	74

LIST OF FIGURES (continued)

Figure		Page
53	Puddle "C"	75
54	"Puddles" used in short-duration hydroplaning tests	75
55	Tow-vehicle splash and wake entering puddle "B"	76
56	Severe splash and spray (some self-generated) obscuring test trailer	76
57	Water depth vs. drainage length for concrete surfaces and old equation	80
58	Water depth vs. drainage length for longitudinal and transverse textures	82
59	Water depth vs. drainage length for combined data and old equation	83
60	Water depth vs. time after cessation of rainfall	85
61	Effect of vehicle speed on skid number for tread depth of 11/32 in and texture depth of 0.030 in	88
62	Effect of vehicle speed on skid number for tread depth of 2/32 in and water depth of 0.00 in	89
63	Michigan's tire-pavement friction tester	90
64	Cornering slip number vs. vehicle speed for ASTM tire E501 at a 4^{o} slip angle	94
65	Cornering slip number vs. slip angle for ASTM tire E501 at 55 mph	95
66	Cornering slip number vs. slip angle for various tire types	96
67	Cornering slip number vs. texture depth for ASTM standard tire E501 with full (11/32 in) and low (2/32 in) tread depth at hydroplaning conditions	97
68	Cornering slip number vs. slip angle for all surfaces	99
69	Classification of surface types	103
70	Frequency distribution of the friction coefficients on German highways and motorways	103
71	Pavement cross section at transition from tangent to superelevated curve	106
72a	Texture depth characteristic	106
72b	Coefficient of friction in relation to speed for different water depths	106
73	Frequency distribution of locked-wheel braking-force coefficients of 200± road surfacing	107

LIST OF FIGURES (continued)

Figure		Page
74	Percentage draining as a function of crossfall	108
75	Rainfall and discharge as function of time	108
76	Lines of flow at a transition curve	110
77	Outflow meter shows traffic effects on open-graded friction course	113
78	Skid resistance of plant mix surface course	113
79	Effects of limestone filler on asphalt hardening rate	115
80	Coefficient of friction as function of the speed on various pavements	115
81	Test layout and rain gage locations - SH-21	122
82	Cross slope of the finished OGFC on SH-21 was checked at regular intervals during construction	123
83	During construction mat thickness was monitored closely on SH-21 Brazos County	123
84	Testing OGFC at 30 mph (48 km/h) on SH-21 Brazos County	124
85	Water was supplied to the rain simulator on SH-21 by two 5000-gallon (19 m^3) tankers	124
86	Prior to testing, water depths for each fixed rainfall intensity were carefully measured	125
87	Testing OGFC at 55 mph (88 km/h) on SH-21 Brazos County	125
88	Skid number vs. speed from ASTM standard test method E274	127
89	Skid number vs. water depth for ASTM standard tire E501 with 11/32 in tread depth on Section 1, outside wheel path of outside lane	127
90	Skid number vs. water depth for ASTM standard tire E501 with 11/32 in tread depth on Section 2, outside wheel path of outside lane	129
91	Skid number vs. water depth for ASTM standard tire E501 with 11/32 in tread depth on Section 3, outside wheel path of inside lane	129
92	Skid number vs. water depth for ASTM standard tire E501 with 11/32 in tread depth on Section 3, outside wheel path of outside lane	130
93	Skid number vs. water depth for ASTM standard tire E501 with 11/32 in tread depth on Section 4, outside wheel path of outside lane	130

LIST OF FIGURES (continued)

Figure		Page
94	Skid number vs, water depth for steel-belted radial (SBR) with 2/32 in tread depth on Section 1, outside wheel path of outside lane	131
95	Skid number vs. water depth for steel-belted radial (SBR) with 2/32 in tread depth on Section 2, outside wheel path of outside lane	131
96	Skid number vs. water depth for steel-belted radial (SBR) with 2/32 in tread depth on Section 3, outside wheel path of outside lane	132
97	Skid number vs. water depth for steel-belted radial (SBR) with 2/32 in tread depth on Section 3, outside wheel path of inside lane	132
98	Skid number vs, water depth for steel-belted radial (SBR) with 2/32 in tread depth on Section 4, outside wheel path of outside lane	133
99	Skid number vs, water depth for glass-belted bias-ply tire (F-78-14) with 2/32 in tread on Section 1, outside wheel path of outside lane	133
100	Skid number vs, water depth for glass-belted bias-ply tire (F-78-14) with 2/32 in tread depth on Section 2, outside wheel path of outside lane	135
101	Skid number vs, water depth for glass-belted bias-ply tire (F-78-14) with 2/32 in tread depth on Section 3, outside wheel path of outside lane	135
102	Skid number vs, water depth for glass-belted bias-ply tire (F-78-14) with 2/32 in tread depth on Section 3, outside wheel path of inside lane	136
103	Skid number vs, water depth for glass-belted bias-ply tire (F-78-14) with 2/32 in tread depth on Section 4, outside wheel path of outside lane	136
104	Skid number vs, water depth for glass-belted bias-ply wide tire (G-60-14) with 2/32 in tread depth on Section 1, outside wheel path of outside lane	137
105	Skid number vs, water depth for glass-belted bias-ply wide tire (G-60-14) with 2/32 in tread depth on Section 2, outside wheel path of outside lane	137
106	Skid number vs. water depth for glass-belted bias-ply wide tire (G-60-14) with 2/32 in tread depth on Section 3, outside wheel path of outside lane	138

LIST OF FIGURES (continued)

Figure		Page
107	Skid number vs. water depth for glass-belted bias-ply wide tire (G-60-14) with 2/32 in tread depth on Section 3, outside wheel path of inside lane	138
108	Skid number vs. water depth for glass-belted bias-ply wide tire (G-60-14) with 2/32 in tread depth on Section 4, outside wheel path of outside lane	140
109	Skid number vs. water depth for ASTM standard tire E501 with 2/32 in tread depth on Section 2 with simulated sealed shoulder, outside wheel path of outside lane	140
110	Skid number vs. water depth for steel-belted radial (SBR) with 2/32 in tread depth on Section 2 with simulated sealed shoulder, outside wheel path of outside lane	141
111	Skid number vs. water depth for glass-belted bias-ply tire with 2/32 in tread depth on Section 2 with simulated sealed shoulder, outside wheel path of outside lane	141
112	Skid number vs. water depth for glass-belted bias-ply wide tire (G-60-14) with 2/32 in tread depth on Section 2 with simulated sealed shoulder, outside wheel path of outside lane	142
113	Skid number vs. water depth for glass-belted bias-ply tire (F-78-14) and steel belted radial (FR-78-14) having 11/32 in tread depth and inflated to 24 psi. Testing done on Section 2, outside wheel path of outside lane	142
114	Skid number vs. water depth for glass-belted bias-ply tire (F-78-14) and steel belted radial (FR-78-14) having 5/32 in tread depth and inflated to 24 psi. Testing done on Section 2, outside wheel path of outside lane	143
115	Skid number vs. water depth for glass-belted bias-ply tire (F-78-14) inflated to 24 psi. Testing done on Section 2, outside lane, outside wheel path	143
116	Skid number vs. water depth for belted-bias ply tire (F-78-14) on Section 2 at various positions across the lane	145
117	Skid number vs. speed for all sections, average of ASTM E501 tire only	145
118	Skid number vs. speed for all sections, average of ASTM E501 tire only	146
119	Skid number vs. speed for all sections, average of all tires except ASTM E501	146
120	Skid number vs. speed for all sections, average of all tires except ASTM E501	147

LIST OF FIGURES (continued)

Figure		Page
121	Model surface used to examine runoff from multilane pavements	149
122	Recession curves 9 ft - flow length slope = 4%	152
123	Recession curve 9 ft - flow length slope = 8%	152
124	Recession curves 14 ft - flow length slope = 4%	153
125	Recession curves 18 ft - flow length slope = 4%	153
126	Recession curves 18 ft - flow length slope = 8%	154
127	Recession curves 28 ft - flow length slope = 0.5%	154
128	Recession curves 28 ft - flow length slope = 4%	155
129	Recession curves 28 ft - flow length slope = 8%	155
130	Average recession curves for slope = 8%; 9 ft, 18 ft and 28 ft flow lengths	156
131	Average recession curves for slope = 4%; 9 ft and 18 ft flow lengths	156
132	Value of discharge after 6 minutes with respect to cutoff supply rate, σ	160
133	Average skid numbers in natural rain of various intensities on SH-21 OGFC for outside lane, outside wheel path (O.O.) and inside lane, outside wheel path (I.O.)	162
134	Modified U. S. Corps of Engineers Waterways Experiment Station permeameter values for field cores from SH-21 open-graded surfaces	162
135	Austin, Texas, U. S. 290 open-graded friction course on crest vertical curve	164
136	Austin, Texas, U. S. 290 OGFC 3 minutes after rain ceased	164
137	Austin, Texas, U. S. 290, 10 minutes after rainfall ceased on open mix	165
138	Austin, Texas, U. S. 290 open-graded surface 3/4 inch (19 mm) thick after skid trailer lockup	165
139	Austin, Texas, U. S. 290 open-graded friction course in 0.06 in/h (1.5 mm/h) rainfall before wheel lockup	166
140	Austin, Texas, U. S. 290 "light" rain	166
141	Austin, Texas, U. S. 290 dense pavement in 0.06 in/h (1.5 mm/h) rainfall - locked wheel skid tests	167
142	Austin, Texas, U. S. 290 5 minutes after rainfall ceased on dense pavement	167

LIST OF FIGURES (continued)

Figure		Page
143	Austin, Texas, U. S. 290, 10 minutes after rainfall ceased on dense pavement	168
144	Fort Worth, Texas, I-30, open-graded surface 3/4 inch (19 mm) thick in 0.04 in/h (1 mm/h) rainfall	168
145	Fort Worth, Texas, I-30, 0.04 in/h (1 mm/h) rainfall	169
146	Fort Worth, Texas, open-graded lightweight aggregate surface about 3/4 inch (19 mm) thick in 0.04 in/h (1 mm/h) rainfall	169
147	Fort Worth, Texas, I-30, open-graded surface on compound curve in 0.04 in/h (1 mm/h) rainfall	170
148	Fort Worth, Texas, I-30, concrete pavement	170
149	Fort Worth, Texas, Hulen Street, portland cement concrete on 0.04 in/h (1 mm/h) rainfall	172
150	Fort Worth, Texas, I-30, concrete pavement in 0.03 in/h (0.8 mm/h) rainfall	172
151	Fort Worth, Texas, I-30, concrete pavement in 0.03 in/h (0.8 mm/h)	173
152	Fort Worth, Texas, I-30, open-graded friction course in 0.03 in/h (0.8 mm/h) rainfall on downgrade to sag-vertical curve	173
153	Fort Worth, Texas, I-30, lightweight aggregate open mix in 0.03 in/h (0.8 mm/h) rainfall	174
154	Fort Worth, Texas, I-20, during 0.03 in/h (0.8 mm/h) rainfall	174
155	Fort Worth, Texas, I-20, during 0.03 in/h (0.8 mm/h) rainfall	175
156	Fort Worth, Texas, I-20, rhyolite aggregate open mix in 0.02 in/h (0.5 mm/h)	175
157	Fort Worth, Texas, I-20, OGFC utilizing rhyolite	176
158	Fort Worth, Texas, I-20, during 0.02 in/h (0.5 mm/h) rainfall	176
159	Fort Worth, Texas, I-20, open mix using rhyolite aggregate rainfall 0.02 in/h (0.5 mm/h)	177
160	Beaumont, Texas, I-10, open mix in 0.25 in/h (6.4 mm/h) rainfall	177
161	Beaumont, Texas, I-10, open-graded surface in 0.25 in/h (6.4 mm/h) rainfall	179
162	Beaumont, Texas, I-10, open-graded surface in 0.25 in/h (6.4 mm/h) rainfall	179
163	Beaumont, Texas, SH-87, open mix in 0.05 in/h (1.3 mm/h) rainfall	180

LIST OF FIGURES (continued)

Figure		Page
164	Beaumont, Texas, SH-87, open-graded friction course in 0.05 in/h (1.3 mm/h) rainfall	180
165	Beaumont, Texas, SH-87, open mix including the shoulder effective in 0.05 in/h (1.3 mm/h) rainfall	181
166	Beaumont, Texas, I-10, open mix shortly after heavy shower (about 3 minutes)	181
167	Beaumont, Texas, SH-87, open mix made from crushed trap rock	183
168	Natural rain 0.02 in/h (0.5 mm/h) on OGFC SH-21 Brazos County at intersection of Section No. 4	183
169	Natural rain 0.02 in/h (0.5 mm/h), SH-21 Brazos County Section No. 2	184
170	Natural rain 0.08 in/h (2 mm/h) OGFC SH-21 Brazos County Section No. 3	184
171	Natural rain 0.08 in/h (2 mm/h) on westbound dense pavement (SH-21); cross slope about 1 percent	185
172	Natural rain 0.08 in/h (2 mm/h) Section No. 3, SH-21 Brazos County	185
173	Natural rain of 0.08 in/h (2 mm/h) OGFC SH-21 Brazos County	187
174	Natural rain of 0.08 in/h (2 mm/h) on SH-21 Section No. 3	187
175	Natural rain 0.2 in/h (5 mm/h) SH-21 Brazos County Section No. 1	188
176	Natural rain 0.2 in/h (5 mm/h) SH-21 Brazos County Section No. 3 in foreground; Section No. 4 in background	188
177	Dense surface on SH-21 with 1 percent cross slope in 0.2 in/h (5 mm/h) rainfall	189
178	Natural rain of 0.3 in/h (7.6 mm/h) on SH-21 Section 3 outside lane	189
179	Natural rain 0.25 in/h (6.4 mm/h) SH-21 Brazos County Section No. 1	190
180	Natural rain 0.25 in/h (6.4 mm/h) on OGFC SH-21 Brazos County Section No. 3 in foreground and Section No. 4 in background	190
181	SH-21 open-graded friction course Section 3 in 0.4 in/h (10 mm/h) rainfall	191
182	Splash and spray on SH-21 Section 3 in 0.6 in/h (15 mm/h) rainfall	191

LIST OF FIGURES (continued)

Figure		Page
183	Natural rainfall 0.8 in/h (20 mm/h) intensity on SH-21 Section 4	192
184	Trailing test trailer at 55 mph (88 km/h) in 0.8 in/h (20 mm/h) rainfall	192
185	Influences of increasing anti-polishing characteristics on pavement friction	194
186	Step gauge details	198
187	Positive puddle depth ($\Delta > H$)	199
188	Negative puddle depth ($\Delta < H$)	199
189	Cross section of traveled way	200
190	Relative frequency of cross slopes	203
191	Cumulative percentage of cross slopes	204
192	Relative frequency of puddle depth	205
193	Cumulative percentage of puddle depth	206
194	Relative frequency of texture depth	207
195	Cumulative percentage of texture depth	208
196	Texture depth as a function of surface material, measurement technique, and measurement location	210
197	Typical values of surface texture as measured by putty test	211
198	Laminar flow conditions	212
199	Example of comparative water depths on multilane highways with different cross slopes	214
200	Surface transverse slotted pipe, System A	220
201	Surface drop inlets, System B	221
202	Subsurface drop inlet, System C	222
203	Subsurface directional berm, System D	223
204	Subsurface cross-slope drainage, System E	224
205	Subsurface channel drainage, System F	225
206	Subsurface individual-lane drainage, System G	226
207	Longitudinal cross section	227
208	Thickness of open-graded pavements	228
209	Basic geometry of wheel path depression	230
210	Critical grade analysis	232

LIST OF FIGURES (continued)

Figure		Page
211	Rainfall intensity vs, critical grade	233
212	Rainfall intensity vs. critical grade	234
213	Rainfall intensity vs, critical grade	235
214	Rainfall intensity vs. critical grade	236
215	Rainfall intensity vs, critical grade	237
216	Approximate distribution of texture depths in one state, comparison of 1967 and 1977 data	244
217	Curves of zero water depth for an intensity of 0.25 in/h	250
218	Curves of zero water depth for an intensity of 0.5 in/h	250
219	Curves of zero water depth for intensities of 0.75 and 1.0 in/h	251

INTRODUCTION

Hydroplaning is an event that has been widely misunderstood. In relation to its importance to highway safety, published opinions vary widely. One extreme is that hydroplaning has no significant influence on accidents due to relatively low traffic speeds. The other extreme is that hydroplaning has a great influence on wet-weather accidents. The truth must be that both of these opinions are correct at different specific highway sites. In the general case, the truth must lie somewhere between these extremes. Hydroplaning will be shown to be a fairly low probability event, primarily due to the fact the high intensity rainfalls necessary to flood a pavement are low probability events. The nature of the event, however, is so hazardous when it does occur, that criteria for surface design to reduce the probability of hydroplaning are warranted.

Some of the earliest investigations and technical reports on hydroplaning came from NACA and its successor NASA and were primarily concerned with hydroplaning of aircraft during landings. In this connection, the U. S. Army Air Corps and its successor U. S. Air Force also did valuable work. Later the Road Research Laboratory in Great Britain began investigations related to automobiles. Concurrent with this research, the Americans and Germans studied tires and road surfaces to seek their own answers. Most recently, the Highway Research Board, now the Transportation Research Board, the National Cooperative Highway Research Program and the FHWA have encouraged and are financing studies related to tire-pavement interaction and hydroplaning, studies that are bringing the "state of the art" to a most respectable level.

The following subjects cover the main areas where good information has been found or developed.

1. The definition of full dynamic hydroplaning conditions.
2. The definition of changes in available friction as full hydroplaning is approached as a function of a variety of textural conditions, both random and patterned.
3. The definition of road surface geometry and how it affects the accumulation of water under various environmental conditions.

4. The interrelationship of different methods of measuring hydroplaning.
5. The performance of open-graded friction courses during rainfall conditions.
6. The probability of different conditions relating to hydroplaning such as tire condition and rainfall intensity.
7. The influence of various pavement cross slopes on driver workload and performance, as indicated by vehicle accelerations and friction demand levels.
8. Determination of the drainage properties of sag vertical curves and innovative drainage concepts for these geometric situations.

In Chapter VIII of this document indications of the range and frequency of important factors such as tread depth, tire pressure, surface texture, cross slope and rainfall intensity are used to develop design criteria. Curves are developed, based on a capability to predict water depth from given geometric and environmental conditions, which can be used to determine appropriate combinations of pavement cross slope and texture depth during periods of specified rainfall intensity. "Design" rainfall intensities are discussed on page 248.

The implementation of criteria and recommendations for surface texture and pavement cross slope to minimize hydroplaning has the potential for a significant impact on the high wet-weather accident toll. The information contained in this report justifies this action. Further, it is hoped that the means used to accomplish this reduction may be extended to other nations that are now experiencing similar problems.

CHAPTER I

THE PHENOMENON OF HYDROPLANING

Hydroplaning is the separation of the tire from the road surface by a layer of fluid. On a microscopic scale all operational conditions may involve some degree of partial hydroplaning as long as there is any significant amount of water present. On a macroscopic scale, however, this zone can be defined as occurring during those operational conditions when there is some significant degree of penetration of a water wedge between the tire and pavement contact area.

Hydroplaning of pneumatic-tired vehicles has been divided into three categories by Horne (1). These categories are

1. viscous hydroplaning,
2. dynamic hydroplaning and
3. tire tread rubber reversion hydroplaning.

Viscous and dynamic hydroplaning are the important types of hydroplaning insofar as passenger cars are concerned as tire-tread-reversion hydroplaning occurs only when heavy vehicles such as trucks or airplanes lock their wheels when moving at high speeds on wet pavements with macro but little microtexture. Viscous hydroplaning may occur at any speed and with extremely thin films of water. Browne (2) states that viscous hydroplaning occurs only on surfaces where there is little microtexture. A thin film of water remains between the tire and pavement since there is insufficient pavement microtexture to promote the breakdown of the water film.

A variety of equations has been developed to predict the speed at which hydroplaning will occur. These equations are summarized in Table 1. The first equation is of value primarily as a definition of the phenomenon of viscous hydroplaning rather than as a prediction of viscous hydroplaning speeds. Equations 2 through 5 all predict the dynamic hydroplaning minimum speed. Equations 2, 3 and 5 have limitations, primarily because they were derived independently of the surface texture characterization. Equation 4 does consider one aspect of pavement texture through the factor K_1, but K_1 must be determined empirically if the equation is expected to be accurate. Equation 4 must be used in conjunction with Figure 1 in order to estimate hydroplaning speed. The procedure is to determine the unit groove capacity (UGC), then determine the proper position on the chart for either of the two stated combinations of cross slope and drainage-path length by selecting a specific rainfall intensity. It should be noted that this predictive method is not comprehensive in terms of combinations of cross slope, pavement texture and drainage-path length, but is limited to the two combinations tested. Another aspect of the wet-weather safety problem which has a definite interaction with the speed most drivers are content to drive is that of visibility. Yeager (3) also includes an estimate of this characteristic for different intensities of rainfall in Figure 1.

One of the most significant studies of the influence of tread design on hydroplaning speed was conducted by Gengenbach (4). In this study he

Table 1. Equations to predict hydroplaning speed

Equation	Definition of Variables	References
1. $V_H \geq L/\Delta T_{sf}$	V_H = minimum speed necessary for viscous hydroplaning L = the length of the tire footprint region ΔT_{sf} = the amount of time necessary for the water film thickness to be sufficiently reduced so that contact is made between the tread rubber and the pavement microasperities	Browne (2)
2. $V_H = 1.8\sqrt{P_{IN}}$ * $V'_H = 6.35\sqrt{P_{IN}}$	V_H = the limiting dynamic hydroplaning speed in m/s V'_H = the limiting dynamic hydroplaning speed in km/h P_{IN} = the tire inflation pressure in kilopascals (kPa)	Horne and Joyner (5)
3. $V_P = 0.592\sqrt{\frac{228F_v}{\rho A_G C_{L,S}}}$	V_P = hydroplaning speed in mph F_v = vertical ground force ρ = fluid density A_G = tire contact area $C_{L,S}$ = hydroplaning lift coefficient	Horne and Dreher (6)
4. $V_H = f(UGC)$ $UGC = \frac{K_1}{W_T}\sum_{i=1}^{n} w_i d_i$	V_H = hydroplaning speed in mph (The function of UGC, f(UGC), is given graphically by Yeager.) K_1 = weighting factor to consider lateral grooving and blading n = number of ribs w_i and d_i = individual widths and depths of each groove as obtained dynamically on a wet glass plate W_T = effective width of tread	Yeager (3)
5. $V = 508\sqrt{\frac{Q}{B\ t\ C_H}}$	V = hydroplaning speed in km/h Q = wheel load in kg B = maximum width of contact patch in mm t = thickness of water film in mm C_H = hydroplaning left coefficient	Gengenbach (4)

*Metric conversion of $V_P = 10.35\sqrt{P}$ in which P is the tire inflation pressure in psi and V_P is in mph (5,2)

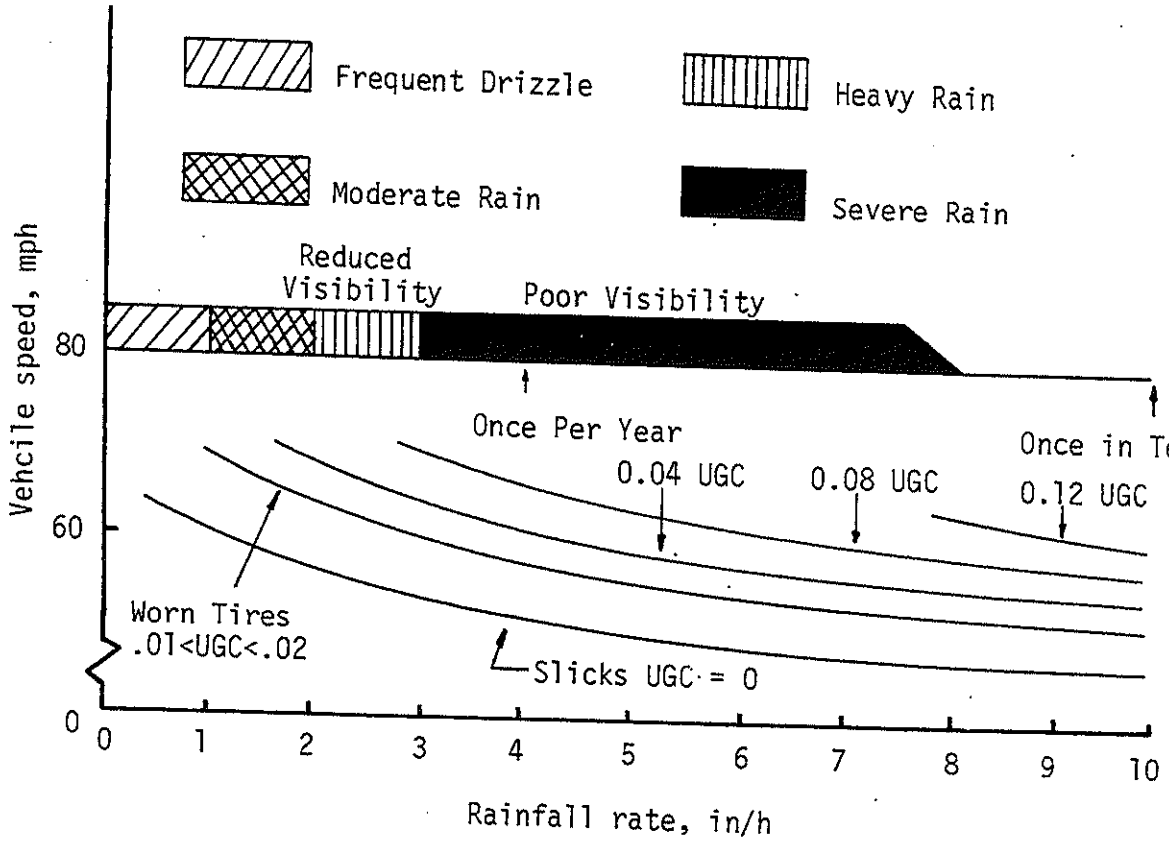

(after R. W. Yeager (3))

Metric Conversion:

1 in/h = 25.4 mm/h
1 in = 25.4 mm
1 ft = 0.305 m
1 mph = 1.609 km/h

Water depth (in)											
	0.030	0.045	0.057	0.067	0.075	0.082	0.088	0.093	0.097	0.101	2.1% Slope, 11 ft Drainage Length
	0.045	0.060	0.072	0.082	0.092	0.102	0.110	0.117	0.124	0.130	1.56% Slope, 22 ft Drainage Length

Figure 1. Estimated free rolling minimum full dynamic hydroplaning speed for passenger tires (conditions: relatively smooth surface, rounded footprint, and rated inflations and loads)

compared seven conventional bias-ply tires with a variety of tread patterns designed and cut into the tire so that the total volume of grooves was constant (groove-area ratio was 20 percent).

One conclusion not drawn by Gengenbach seems appropriate here. While for bald tires hydroplaning was observed at water depths as low as 0.01 in (0.3 mm) for treaded tires, no hydroplaning data have been found in the report for water depths less than 0.08 in (2 mm). Evidently, for the low values of texture between 0.005 and 0.008 in (0.13 and 0.20 mm), treaded tires did not hydroplane at water depths less than 0.08 in (2 mm). It is noted that there was space for almost all the water in the contact patch within the grooves. It should be understood that Gengenbach's tests were conducted in a drum facility where very small water depths could be controlled with extreme precision. On highway surfaces dynamic hydroplaning by tires with minimal (<2/32 in) (<1.6 mm) tread depths was not achieved whenever the average water depth was less than 0.06 in (1.5 mm).

In addition to the findings of research efforts already cited, the authors are fortunate in that several research projects relating either directly or indirectly to hydroplaning have been recently completed. These projects proved to be useful in the development of a quantitative definition of partial hydroplaning conditions.

The study directly related to hydroplaning, HPR-147 (7), is an extensive empirical study of tires, pavements and water depths which compare closely to real highway conditions. The water depths are all over 0.1 in (2.5 mm) and therefore extend the information available to the larger water depth conditions. These tests show a range of full dynamic hydroplaning speeds from 45 to 77 mph (72 to 124 km/h).

In developing the body of data in HPR-147 the indication of hydroplaning which was used was the spindown of a test wheel when moved in a freely rolling condition over a section of pavement covered by a significant layer of water. Spindown is usually given in percent as dictated by the following equation:

$$SD = \frac{\omega_d - \omega_w}{\omega_d} (100) \qquad \text{Eq (6)}$$

where

ω_d = rotational velocity of the rolling wheel when on a dry surface

ω_w = rotational velocity of the wheel after spinning down due to contact with a flooded pavement.

Figure 2 will be used to illustrate the forces acting on the tire in two extreme conditions: (a) freely rolling on a dry surface and (b) the condition of 100 percent spindown when the tire is sliding over a water surface with little, if any, direct contact between tire and pavement surface. At 100 percent spindown, the rotational velocity of the tire is equal to zero.

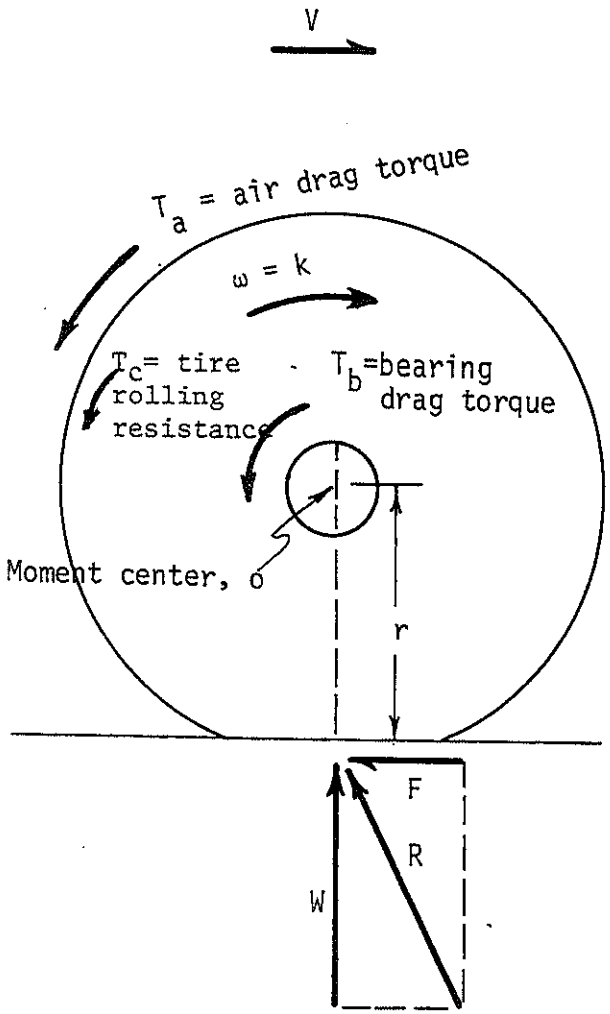

Figure 2 (a). Wheel freely rolling on dry surface

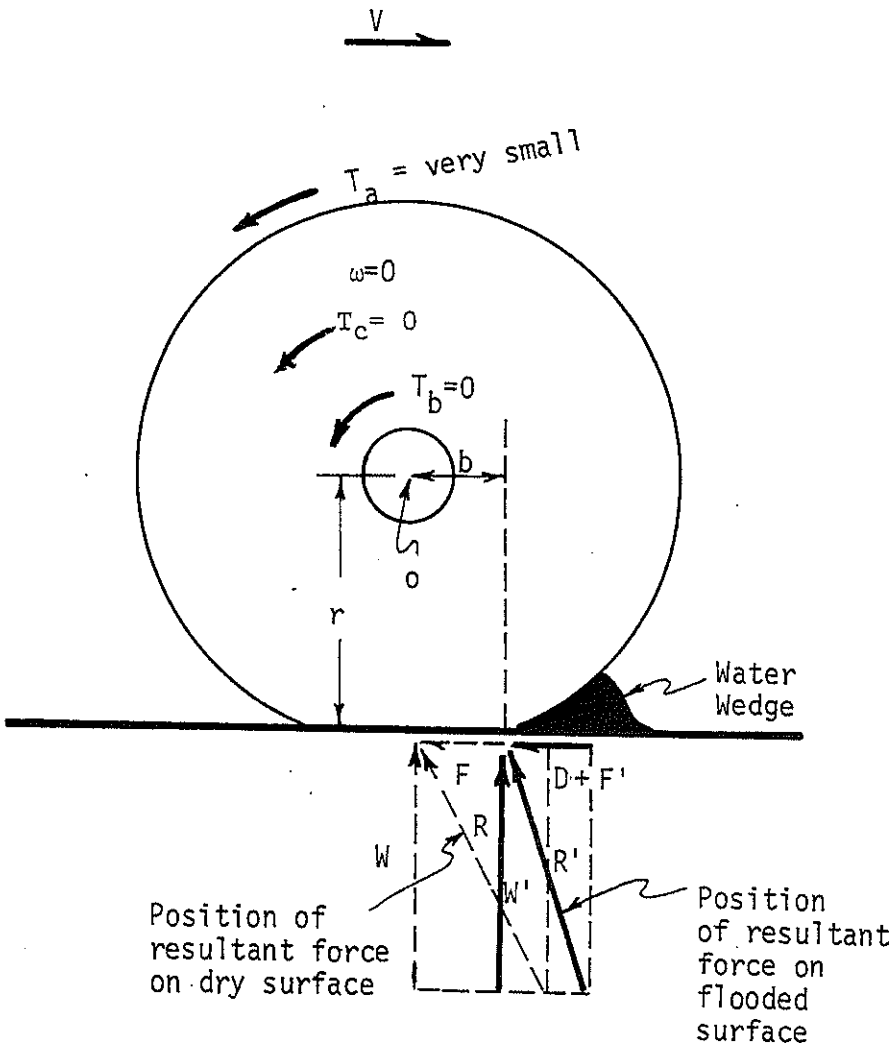

Figure 2 (b). Wheel not turning, 100% spindown condition

In the freely rolling condition with the rotational velocity a constant, K, a summation of moments about the center of the wheel is given by

$$Ta + Tb + Tc = Fr$$

when the vertical component, W, of the resultant force, R, is assumed to pass through the moment center, O, or to pass so close to it that the torque induced by W is negligible. Thus, in order for the tire to rotate at the constant value of ω, without significant contact zone slip, only enough friction needs to be developed to overcome the retarding effects of rolling resistance, which includes bearing friction and air drag. Thus, the value of F is small with respect to W. Up to 60 mph (97 km/h) the rolling resistance is generally less than 2 percent of W (8).

In the 100 percent spindown condition, a condition considered to be indicative of full dynamic hydroplaning, the resultant force, R, changes to some degree in magnitude; but the major change is in its line of action. These changes are caused by 1) the destruction of friction between tire and pavement surface, 2) the development of pressure on the tire in the region of contact with the water wedge and 3) the development of a hydrodynamic drag force on the tire-water interface.

The resultant force, R', can still be resolved into two components, the vertical, W', equal to the weight supported by the wheel and the horizontal force, D + F'. Hydrodynamic drag, D, is due to the inertia of the water over and through which the tire is sliding. F' is some small remaining value of tire-pavement friction. Now the moment summation gives

$$W'b = (D + F')r.$$

Thus, the change in line of action of R' produces a counterclockwise torque due to W which counteracts the torque due to D. Stated another way the line of action of R' moves to a position which includes the moment center, O, resulting in negligible net torque on the wheel.

In interpreting the meaning of hydroplaning data developed under HPR-147, it was concluded that significant control forces between the tire and the pavement did not exist at high values of wheel spindown, i.e., over 50 percent. Further, the difference in vehicle velocity between 100 percent spindown and 50 percent spindown when expressed in mph (test vehicle speed) was so small that 10 percent spindown was chosen as the indicator of hydroplaning. Further testing during this study indicated that almost full dynamic hydroplaning was present with as little as 10 percent spindown. In order to make maximum use of the test data, it was necessary to develop a general equation that would allow the vehicle speed to be predicted as a function of SD and of the variables denoting test conditions. The parameters were as follows:

1. V, vehicle speed in mph ((km/h)/1.609)
2. TD, tread depth in 32nds of an inch (mm x 32/25.4)
3. TXD, texture depth in inches (mm/25.4), silicone putty method
4. WD, water depth (above the asperities in inches (mm/25.4))

5. P, tire pressure in psi (6.895 kPa)

6. SD, spindown percent.

Based on data from approximately 1,300 tests and the curves of SD vs V which fit these data for specific test conditions, 1,038 points were selected at SD values of 10, 30 and 60 percent. The equation which produced the best fit to these data is as follows:

$$V = SD^{0.04}\ P^{0.3}\ (TD + 1)^{0.06}\ A \qquad \text{Eq. (7)}$$

where A is the greater of

$$\frac{10.409}{WD^{0.06}} + 3.507 \quad \text{and} \quad \left[\frac{28.952}{WD^{0.06}} - 7.817\right]\ TXD^{0.14}.$$

In this case the greater value of A would always be used.

Figure 3 shows how the data are fit by Equation 7. Approximately 99 percent of the observations lie within plus or minus 5 mph (8 km/h) of the predicted value. The value of the calculated correlation coefficient is 0.85.

To illustrate the influence of the different parameters on the relationship between vehicle velocity and spindown, Figures 4a through 4d were plotted using Equation 7. Shown progressively are the influences of water depth (Figure 4a), tread depth (Figure 4b), tire pressure (Figure 4c) and texture depth (Figure 4d).

Limited direct evaluation of Equation 7 is provided by tests of two vehicles on flooded surfaces. Table 2 shows a comparison of hydroplaning speeds predicted by Equation 7, the column labeled "Computed Speed", with speeds at which it was observed that the vehicle was subject to negligible control forces, "Observed Speeds". The correspondence of these predicted and observed hydroplaning speeds is excellent considering the variations associated with full-scale vehicle tests, but is limited in the range of variables included. It was further noted that the deterioration of control forces occurred rather gradually over a range of about 20 mph (32 km/h), shown in Figure 5a, as full hydroplaning conditions were approached. What makes hydroplaning seem an abrupt occurrence is that on a straight tangent very little friction is required to maintain direction, usually less than 0.1. However, the final deterioration of friction from 0.1 to 0 takes place in a range of only 1 or 2 mph (2 or 3 km/h) or can take place due to only a slight increase in water depth, or decrease in texture.

To depict the likely range in hydroplaning speed which may occur in the traffic mix along a highway, consider the following relatively extreme cases:

Vehicle 1	Vehicle 2
WD = 0.1 in (2.5 mm)	WD = 0.1 in (2.5 mm)
TD = 9/32 in (7.14 mm)	TD = 0 in
TXD = 0.15 in (3.81 mm)	TXD = 0.01 in (0.25 mm)
P = 36 psi (250 kPa)	P = 18 psi (125 kPa)

Table 2. Computed and observed hydroplaning speeds

Vehicle	Surface (No)	Texture Depth (in)	Average Water Depth (in)	Tread Depth (32nds in)	Tire Pressure (psi)	Computed Speed (mph)	Observed Speed (mph)
1964 Ford	2	0.014	0.10	8	26	53	53-57
1971 Ford	10	0.033	0.15	8	27	53	49-55
1971 VW	10	0.033	0.15	2	21	46	47-52

Surface Number 2 - Jennite Flush Seal
Surface Number 10 - Siliceous Rock Hot Mix

Metric Conversion: 1 in = 25.4 mm
1/32 in = 0.79 mm
1 psi = 6.895 kPa
1 mph = 1.609 km/h
1 psi = 6.895 kPa

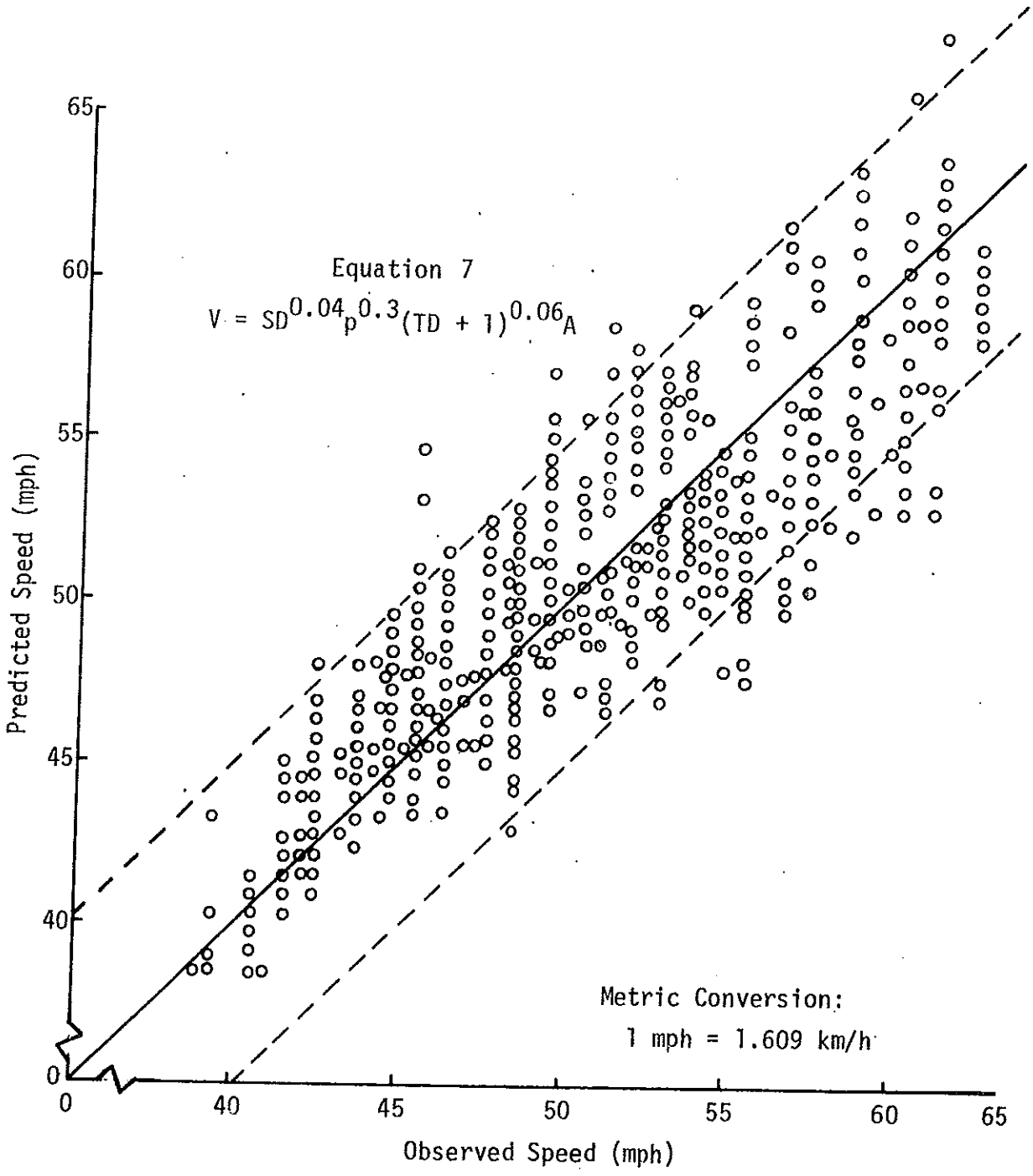

Figure 3. Data scatter for hydroplaning equation (data points at 10, 30 and 60% spindown)

Metric Conversion: 1 in = 25.4 mm, 1 mph = 1.609 km/h,
1 psi = 6.895 kPa

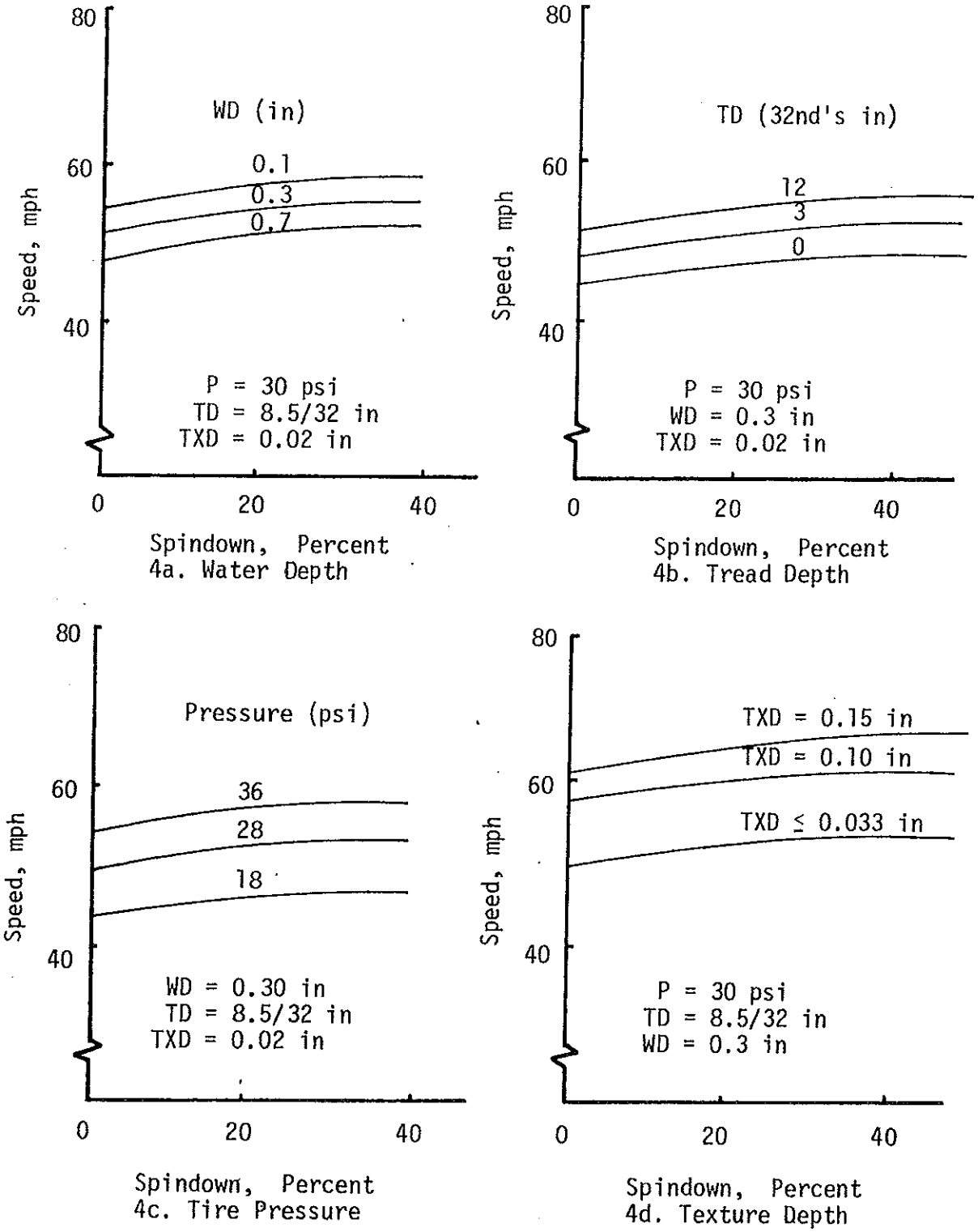

Figure 4. Influence of four parameters on hydroplaning speed

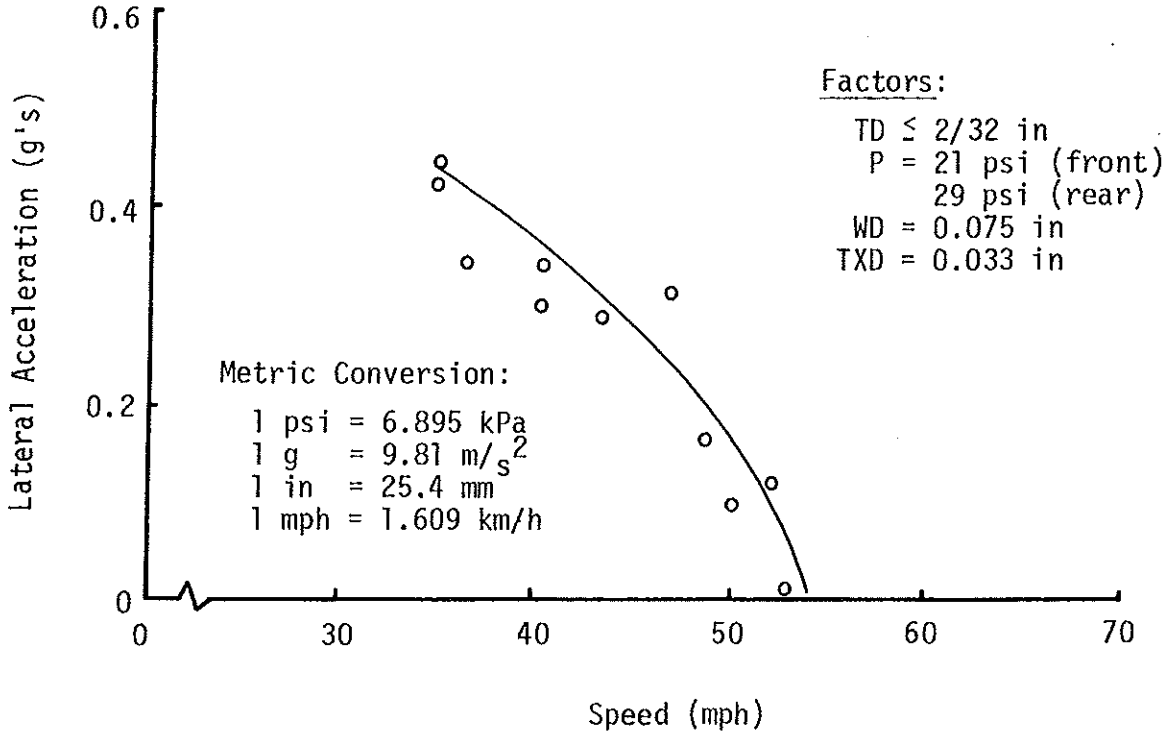

Figure 5a. Deterioration of available friction with speed

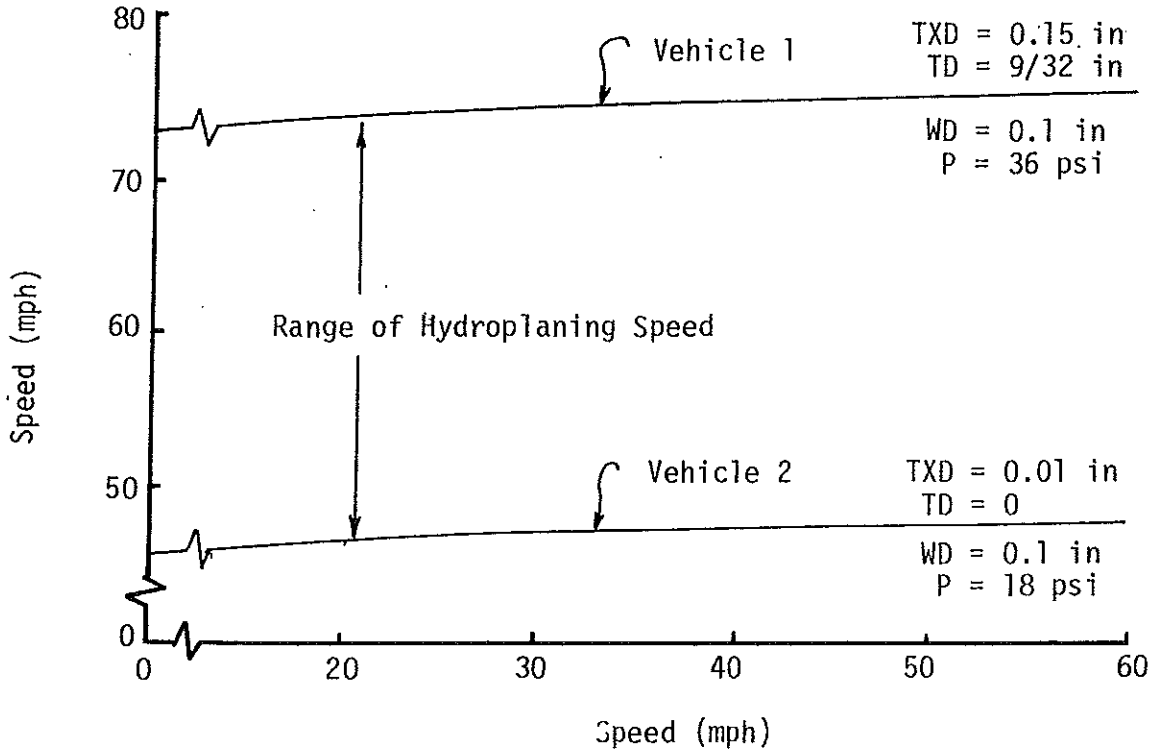

Figure 5b. Possible range of hydroplaning speeds

As shown in Figure 5b, Vehicle 1 may travel up to 28 mph (45 km/h) faster than Vehicle 2 without risking hydroplaning. One of the major problems in speed zoning lies in this wide variation of vehicle speed. If the zone is set for the worst case, drivers of better equipped vehicles recognize it as too slow for them, assume it is too slow for everyone, and thus lose respect for speed zones.

Now that an equation has been developed to predict the velocity for any degree of spindown for any situation where the other parameters may be specified, the point has been reached whereby a relationship between skid number and spindown may be developed. If, for example, the following equations were available for skid number at any velocity and velocity as a function of spindown,

$$SN = f_1(V, TXD, TD, WD, P) \qquad \text{Eq (8)}$$

and

$$V = f_2(SD, TXD, TD, WD, P), \qquad \text{Eq (9)}$$

it would be possible to substitute SD into Equation 9 giving V, then substituting V from Equation 9 into Equation 8, to predict SN. In this way a series of coincident values of SN and SD could be determined which could be used to ascertain the relationship between the two factors. Stated another way, the relationship for hydroplaning speed would be

$$SN = f_1[f_2(SD, TXD, TD, WD, P), TXD, TD, WD, P]. \qquad \text{Eq (10)}$$

Gallaway (9) has provided such an equation for random textured pavements.

$$SN = \frac{154}{V^{0.77}} \left[TD^{0.05} + \frac{4.71\ TXD^{0.09}}{(25.4\ WD + 2.5)^{0.09}} \right]^{*}. \qquad \text{Eq (11)}$$

This equation can be combined with Equation 7 by eliminating V to give SN as a function of spindown (SD) and the other pertinent variables, i.e.,

$$SN = \frac{154 \left[TD^{0.05} + \frac{4.71\ TXD^{0.09}}{(25.4\ WD + 2.5)^{0.09}} \right]}{[SD^{0.04}\ p^{0.30}(TD + 1)^{0.06} A]^{0.77}} \qquad \text{Eq (12)}$$

where A has been defined.

It is apparent that similar relationships can be developed from any of the SN equations given in Chapter IV. However, comparison of actual test values of SN might better illustrate the points that are pertinent to the current work.

---

*Equation developed from ASTM 14" tire @ 24 psi (165 kPa). (Intermediate-to-high random texture range, 0.020 to 0.150 in (0.508 to 3.81 mm).)

It might be assumed that at 100 percent spindown, values of SN would be the same on every pavement, that is, equal to that value of SN produced by hydrodynamic drag. However, both the data and the equations indicate this is not the case. For conditions which indicate 100 percent spindown by Equation 12, a rather wide range of SN values is indicated by tests.

The best fit lines of SN vs speed were used to calculate the correspondence of spindown at 2, 50 and 100 percent and SN. This resulted in the plot of SN vs SD shown in Figure 6 . Because of the heavy dependence on pavement texture, it can be concluded that full dynamic hydroplaning was not occurring when SN values were observed* even though the conditions reported would indicate that hydroplaning should occur. At first glance this would seem to represent a serious inconsistency between the SN and SD studies. However, the problem is not inconsistency in the data taken under the two studies but in significant differences in the test conditions predominating when the two data groups were developed. The main difference is found in the water depth. Spindown was observed in the presence of consistently positive water depths. Skid number values were observed in the presence of significantly lower average water depths which varied significantly about that average, the case more like actual highway conditions.

Figure 7 illustrates this variation with examples of water depth observations at 10 different points under the rainmaker during the SN determinations. Note the values of zero and negative water depths when in all examples the average water depth is positive. In this case periodic contact with the surface due to negative water depths on the significantly textured surfaces would drive the average value of SN up, as each SN value was determined over approximately 100 ft (30 m) of pavement length. Further, since even the higher water depths observed are rather low (less that 0.03 in (0.8 mm)), there may not be sufficient time for the tire to hydroplane between negative water depth areas. One obvious point is that it is less likely that full hydroplaning will occur on a nonuniform surface where water depth varies significantly. Thus, construction variations in the plane of the pavement surface may be working to prevent full hydroplaning.

In an effort to interpret the control forces available for vehicle maneuvers it would be valuable to estimate what part of the SN is due to friction between tire and pavement and what part is due to hydrodynamic drag as the tire moves across and through the water. An estimate of this hydrodynamic drag component may be developed by observing the skid numbers recorded at conditions which should obviously produce full hydroplaning.

Figure 8 shows average values of SN observed at 60 mph (97 km/h) for a number of different pavements. Again the relatively high SN is seen on the more highly textured pavements, indicating hydroplaning did not occur. On the low textured surfaces a lower boundary of about 7 SN is noticed. It seems probable that full hydroplaning was occurring at this time, thus the hydrodynamic drag, D, accounted for approximately 7 SN.

---

*Except perhaps in the case of surfaces 2 and 9 where very low and convergent values of SN were observed.

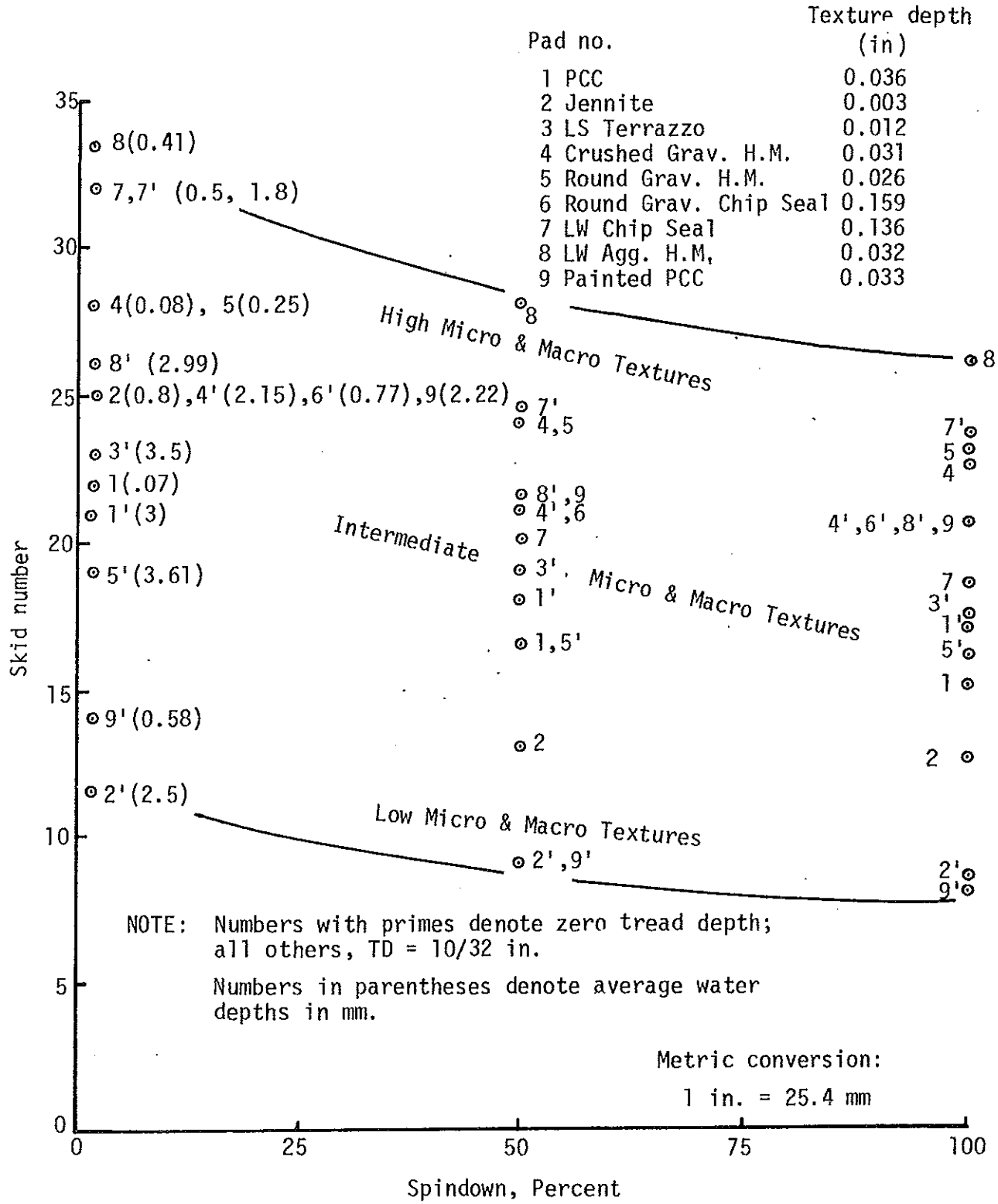

Figure 6. Observed values of skid numbers compared to calculated values of spindown

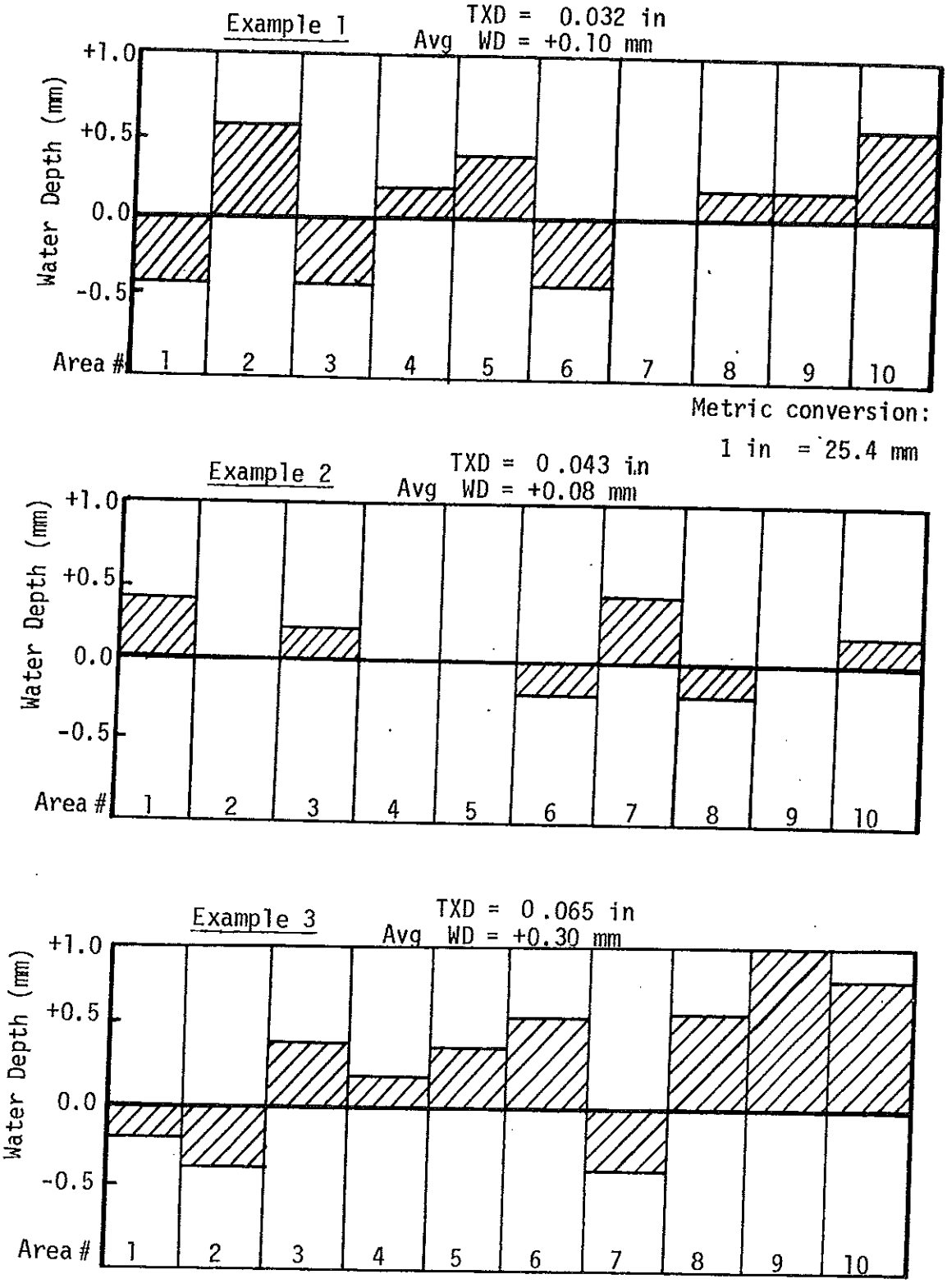

Figure 7. Variation of water depth during rainmaker SN tests

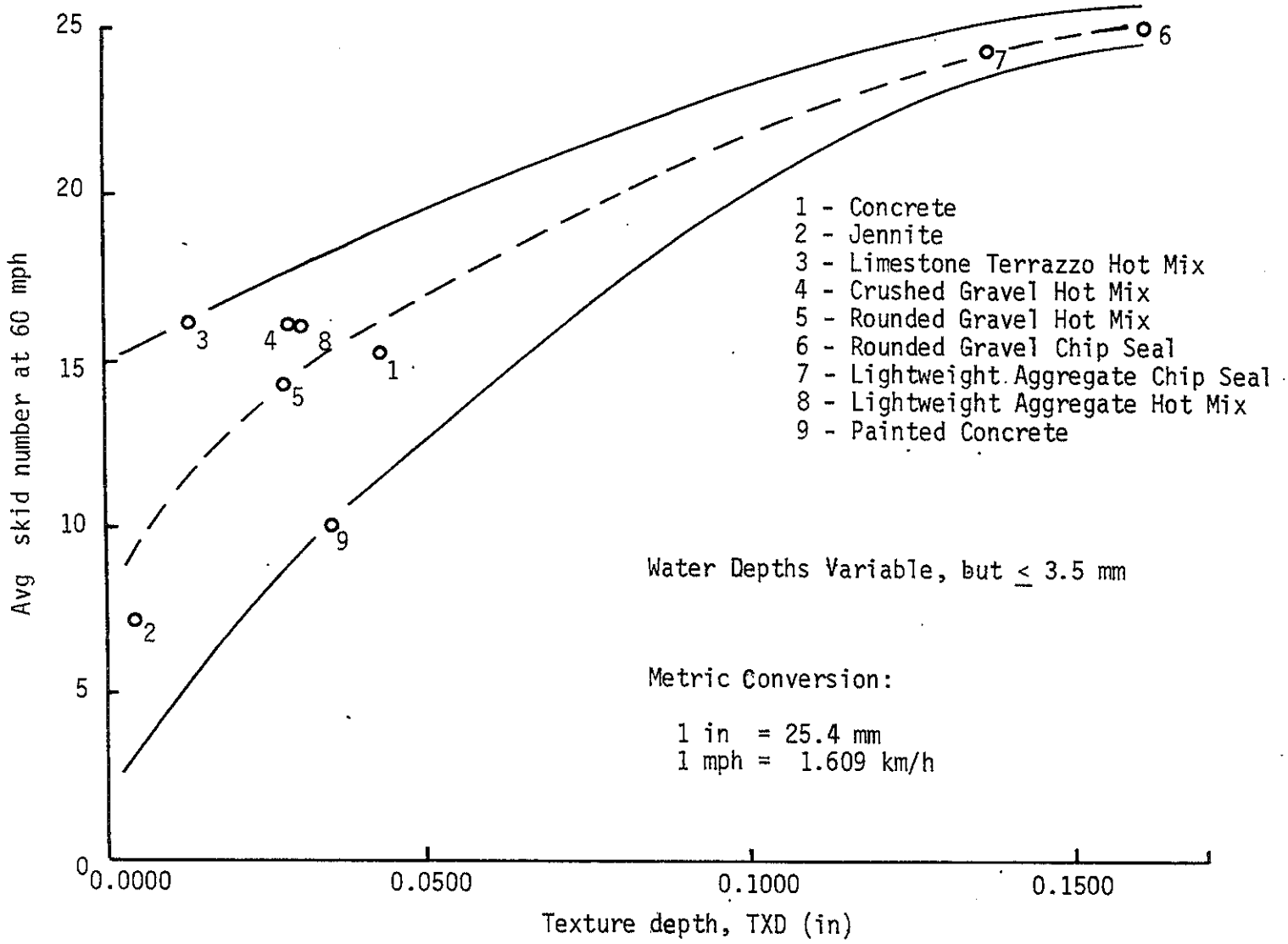

Figure 8. 60 mph skid numbers vs. texture depths

Another estimate of hydrodynamic drag is available from Gengenbach (4) as shown in Figure 9. At 0.08 in (2 mm) of water an apparent plateau is reached for hydrodynamic drag corresponding to about 22 lbf (98 N). Gengenbach states

> "...The depth of immersion of the hydroplaning tire adjusts itself according to the velocity and water depth in such a way that the resistance of the water against displacement remains nearly constant."

If this force is interpreted in terms of force per unit tire width and applied to the tires studied in the skid number and spindown experiments, it appears that hydrodynamic drag would amount to about three skid numbers. However, it is unclear from Gengenbach's presentation whether this is for a smooth or treaded tire.

Studies of both horizontal force at the tire pavement interface and torque on the test wheel are presented in detail in Chapter III. During full hydroplaning the hydrodynamic drag factor in fairly deep water (approximately 3/8 in (9.5 mm)) ranges from 5 to 8 skid numbers for a variety of tire tread conditions. The conclusion is that a significant part of a skid number observed when water depths are positive is not available for vehicle control. Only the difference between the observed value and that part due to hydrodynamic drag is available for vehicle control.

Observations concerning the effect of transverse and longitudinal texture patterns were made in the Phase I report (9). Several previous studies had shown that skid numbers were higher for transverse textures than for longitudinal textures. Although reasons for this were presented in detail it did not necessarily follow that transverse textures were better for vehicle control in highway curves. Beaton or Farnsworth (10) had shown a great reduction in accident rates where longitudinal grooves were provided in the highway. It was obvious that the longitudinal grooving was quite effective in reducing accidents but what was not shown was that it was more effective than transverse grooving. In an effort to gain a better understanding of relative control forces available due to longitudinal vs transverse grooves, cornering slip numbers were determined on both orientations. These tests are presented in Chapter IV. As might be expected, the transverse texture gave slightly higher cornering slip numbers (available friction for cornering) than the longitudinal texture. Perhaps the reasons are the same as the reasons presented in the Phase I report for higher skid numbers on transverse textures: i.e., 1) transverse textures, running in the direction of the cross slope, provide channels for better drainage of the pavement as a whole; 2) transverse pavement textures are more effective in draining the tire-pavement contact patch, just as cross grooves in the tire are more effective than circumferential grooves; and 3) transverse textures resist the forward motion of water necessary to produce the water wedge required for hydroplaning.

It should also be recognized that longitudinal grooving or texturing offers directional guidance to vehicles traversing curves when the cornering attack angles of tires are very small. It may be this difference in the attack angles, less than 2 degrees for most vehicles on highway curves compared to about 12 degrees for the cornering slip angles used in the tests reported here, that produces the difficulty in interpreting the test data. This difficulty may only be resolved when comprehensive accident studies are made in which the major variable is longitudinal vs transverse grooving and texturing.

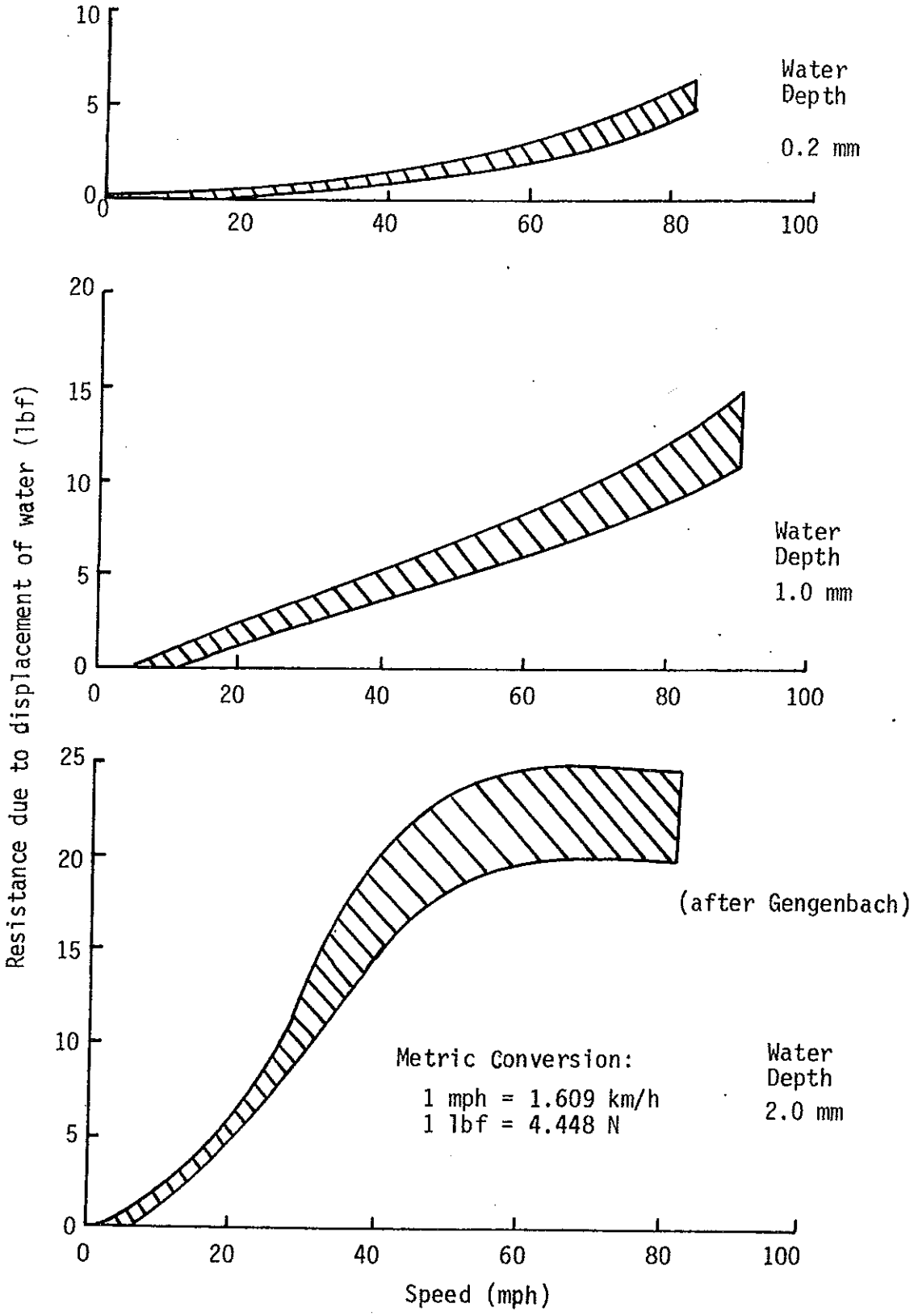

Figure 9. Resistance due to the displacement of water as a function of velocity for different water depths

CHAPTER II

DETERMINING THE PROBABILITY OF SELECTED RAINFALL INTENSITIES

General

The development of design criteria that will preclude hydroplaning under most wet-weather conditions necessitates an understanding of those factors related to hydroplaning, the interdependence of those factors and the occurrence probability of certain critical combinations of those factors. This probability is, in turn, a function of the probability of the existence of each individual factor. The purpose of this section is to develop guidelines that will determine the incident chance of influential environmental factors.

It has been shown by Gallaway (11), Yeager (3) and Horne (12) that the amount of water on the pavement (or water depth) is primarily a function of the rainfall intensity and wind velocity, neglecting transient conditions. It has also been shown that a significant positive water depth (above the asperities) is necessary before hydroplaning can occur. Therefore, the selection of highway surface characterisitics that would disallow positive water depths in all but the more extreme conditions of heavy rainfall would prevent most cases of hydroplaning. "Most" must be defined in probabilistic terms for particular rainfall intensities that occur in conjunction with specific wind velocities; but is wind velocity really needed to develop antihydroplaning criteria? Horne (12) has shown that as long as the water depth is not above the asperity tops there seems to be little wind effect on the flow path and speed of draining water. Therefore, if a criterion of zero water depth is preselected, the influence of wind becomes largely academic, although it is difficult to ignore some influence even on intra-asperity flow if the direction of the falling raindrops is not nearly vertical. The neglect of wind speed and direction seems sound when their effect on surface flow is so slight, although it may be argued that wind could make the difference in some cases between a water depth of height coincident with the tops of the pavement asperities and water depths that are very slightly higher than the asperities. The critical environmental factor, and possibly the only important one, is the intensity of rainfall. The remainder of this chapter will be dedicated to defining the probability of specific intensities.

It would be of little value to determine the average relationship between rainfall intensity and its probability for the U.S. as a whole as rainfall is so highly variable over this vast continent; a comparison between Yuma, Arizona, and New Orleans, Louisana shows great contrast. The other extreme would be to determine this relationship for every part of the proposed roadway with antihydroplaning surface characteristics changing from milepost to milepost, an extreme that is obviously not justified even if such extensive rainfall data were available.

The National Climatic Center in Asheville, North Carolina, the focal point for all climatic data developed by the National Oceanic and Atmospheric Administration (NOAA), has extensive data from over 300 weather stations throughout the country. In general, the number of weather stations is a

function of the geographic size of the state, although there are some exceptions. In many of the larger states wide intrastate variations in rainfall may indicate the need for several zones of rainfall intensity/probability; whereas, in many states a single statewide relationship may be quite sufficient.

The States of Alabama and Illinois were selected for the purposes of this study for several reasons. Extensive current and historical climatic data were available from a number of stations in each of these states. The State of Illinois was seen to be representative of the average moderate conditions across the continental United States. Alabama was chosen for study because the state is located in an area which experiences hurricanes and rainfall of very high intensity and was considered to be one of the most critical states with respect to the need for road surface design criteria to prevent flooding. Rainfall data from Texas stations in Austin and Fort Worth had been acquired on a previous study and published (13). The reduced data have been included later in this report for purposes of comparison. Isohyetal maps of Alabama, Illinois and Texas are shown in Figures 10, 11, and 12.

The outline shown in Table 3 gives the sequence of operations used to arrive at an appropriate relationship between rainfall intensity and the probability of the event for a specific state or geographic area. The paragraphs which follow detail the procedures used to derive the desired relationship for the State of Illinois.

Table 3. Sequence of Operations

I. Determination of Rainfall Data for a State

II. Selection of Representative Stations

III. Selection of Representative Years

IV. Confirmation of Availability and Acquisition of Detailed Rainfall Data

V. Analysis of Detailed Rainfall Data

Determination of Rainfall Characteristics

A listing from the U.S. Department of Commerce showed seven recording stations in Illinois. Figure 11 shows the variation in annual rainfall across the state is relatively small, leading to the conclusion that the state need not be subdivided into different regions for purposes of rainfall analysis.

A definite criterion for acceptable variation is given in Figure 13. This curve of acceptable percentage and absolute variation was developed from an understanding of different regional extremes in Texas. Study of the isohyetal map of Texas, Figure 12, indicated that the state should be divided into at least four zones to prevent the necessity of large data extrapolations. The variations of these four zones were plotted on Figure 13. The line of definition between acceptable and unacceptable variations was then placed to include these points in the acceptable zone. These points are

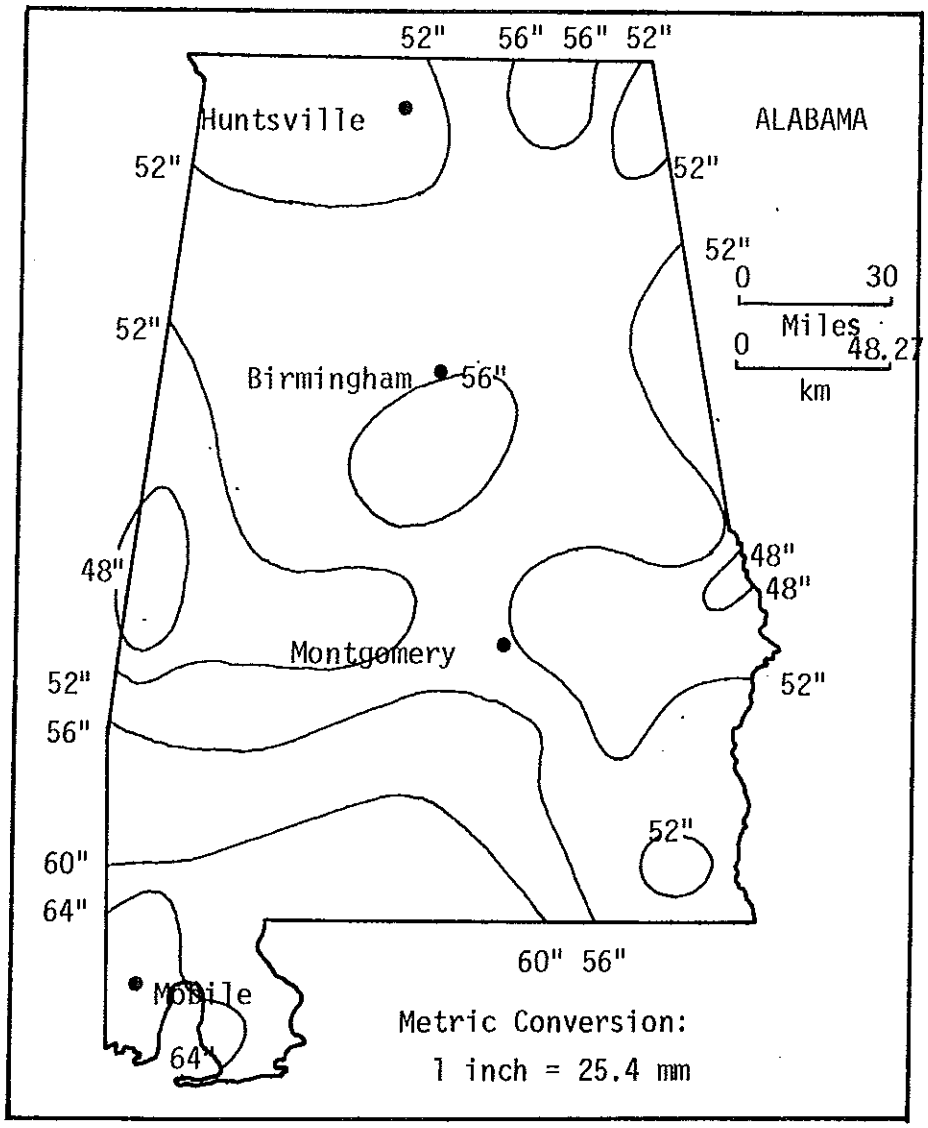

Figure 10. Isolines of mean annual precipitation (U.S. Dept. of Commerce, Environmental Sciences Services Administration, Environmental Data Services, Climatography of the U. S. No. 60-11, Climates of the States)

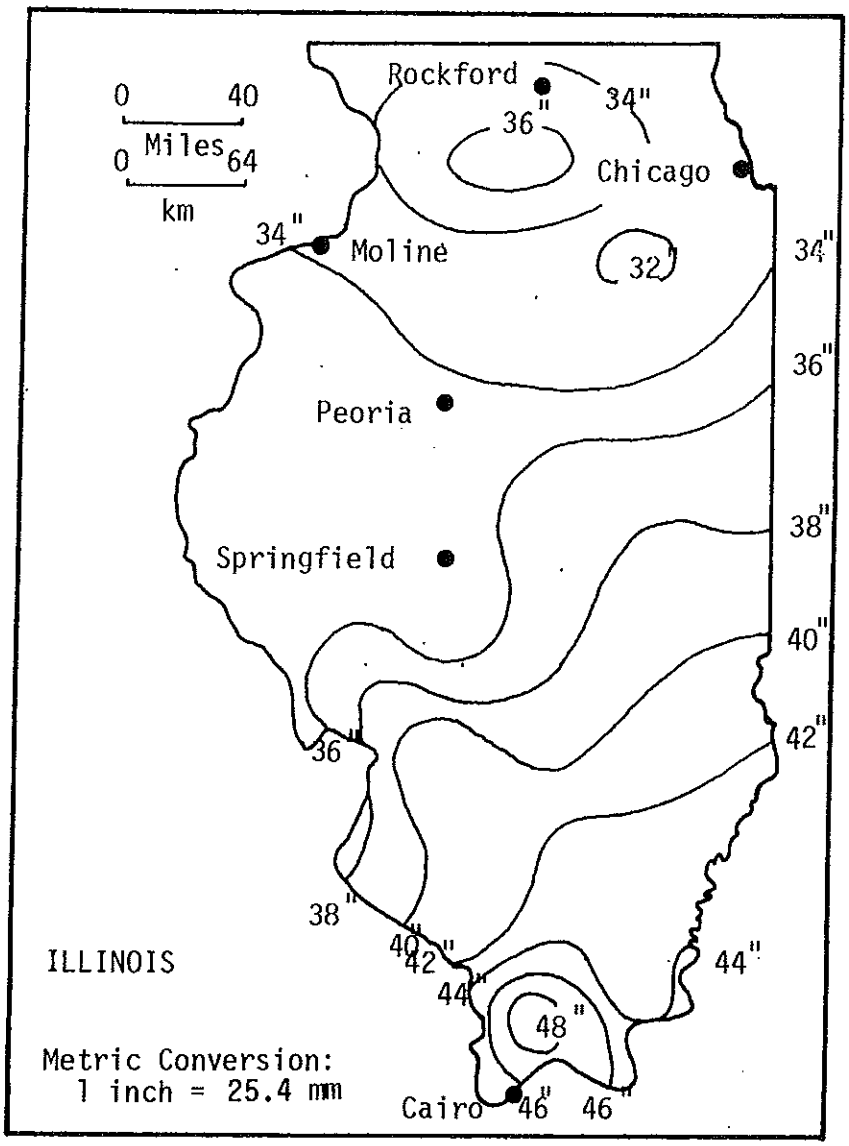

Figure 11. Isolines of mean annual precipitation (U.S. Dept. of Commerce, Environmental Sciences Services Administration, Environmental Data Services, Climatography of the U.S. No. 60-11, Climates of the States)

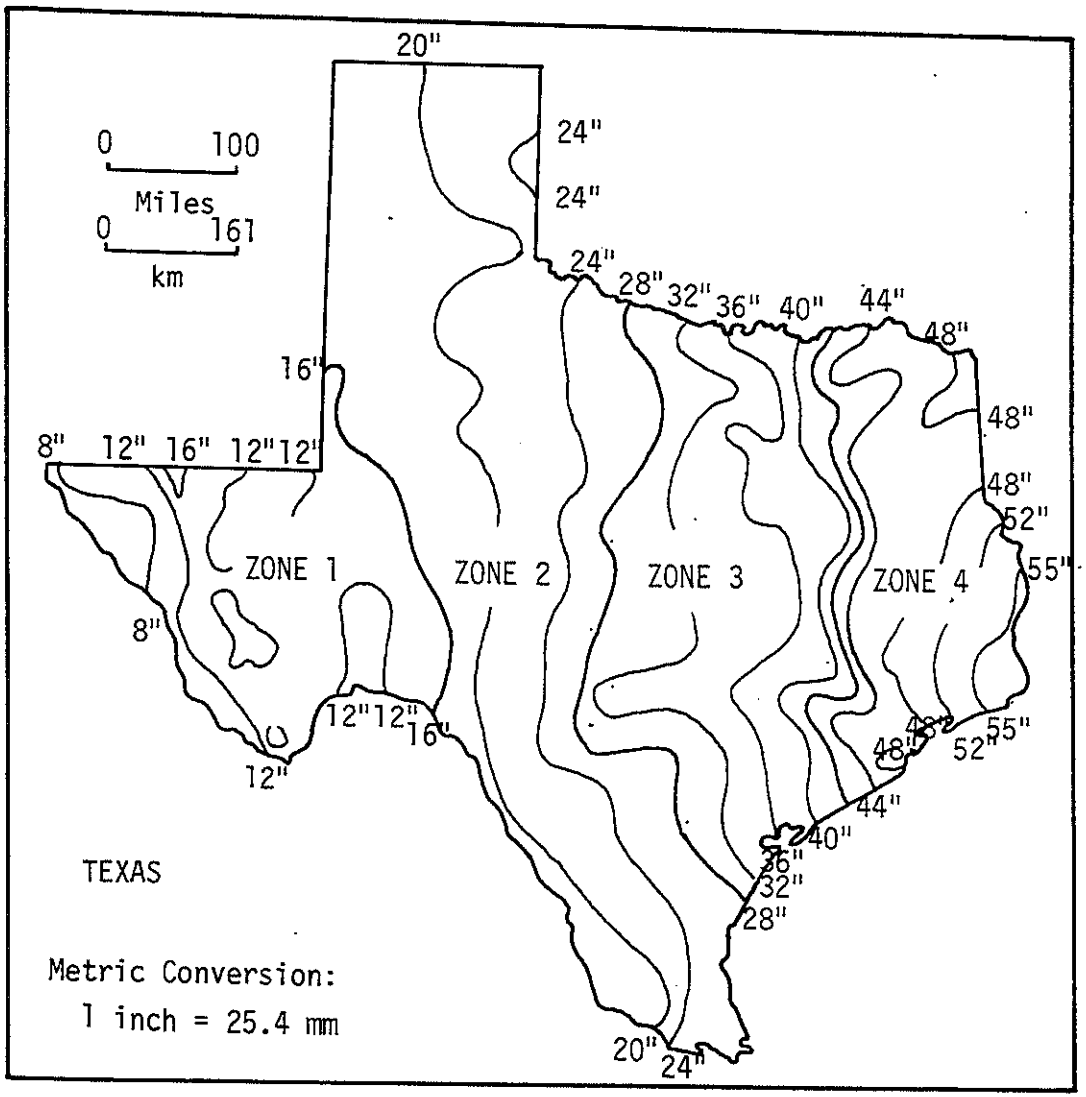

Figure 12. Isolines of mean annual precipitation (U. S. Dept. of Commerce, Environmental Sciences Services Administration, Environmental Data Services, Climatography of the U.S. No. 60-11, Climates of the States)

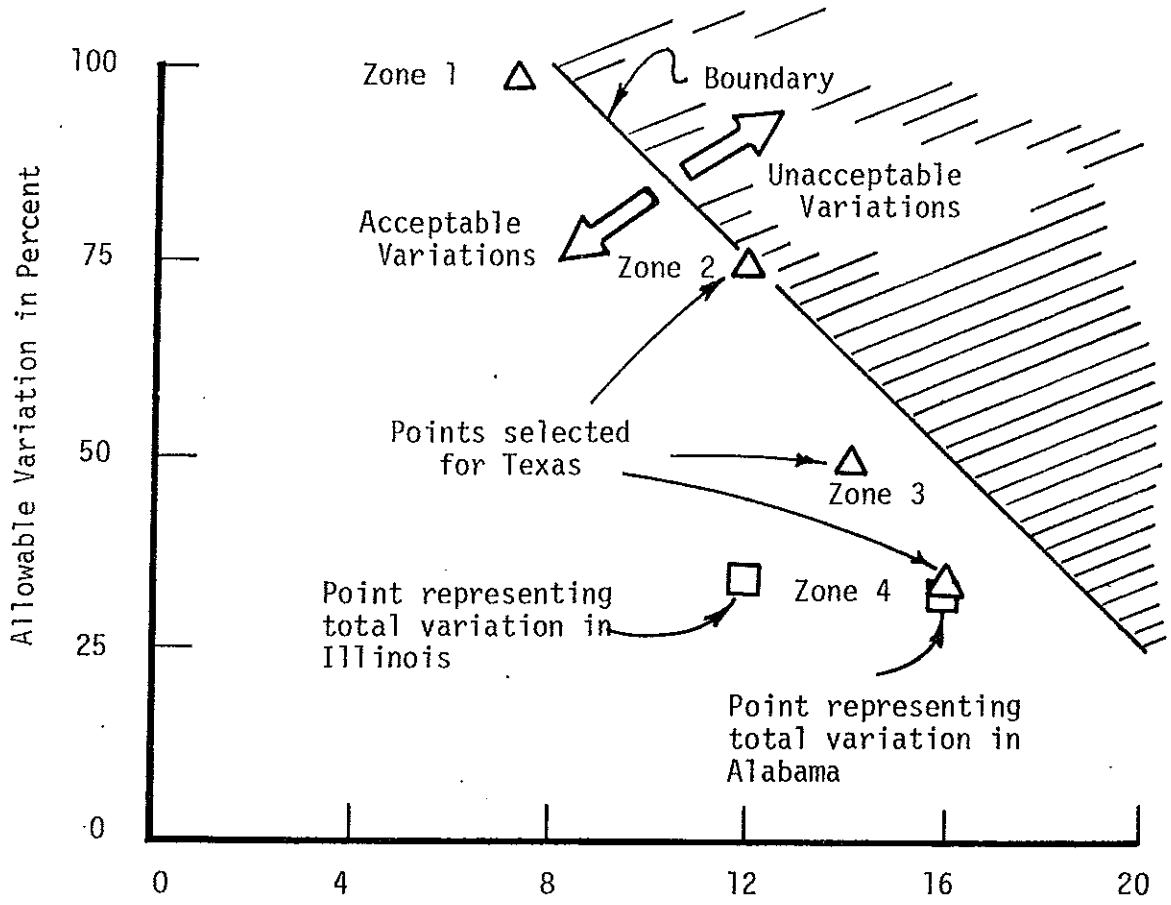

Metric Conversion: 1 inch = 25.4 mm

Figure 13. Tentative criterion for acceptable variation in annual precipitation (The major variation in Illinois is from 34 to 46 inches. The difference is 12 inches, which is absolute variation. The ratio of 12 to 34, times 100 is the percentage variation of 35.)

defined by determining from the isohyetal map the absolute variation in annual rainfall in a region and the percentage variation in annual rainfall in the same region, as can be seen in Figure 12. The variation in the entire State of Illinois does not represent as critical a variation as is seen in each of the four subdivisions of Texas.

Selection of Representative Stations

Once the operating weather stations have been shown on isohyetal maps it is possible to select the most representative stations for more detailed data analysis. Such geographic characteristics as mountain ranges, valleys or relatively large differences in elevations should be considered in selecting typical stations. The stations at Rockford, Springfield and Cairo were selected from the isohyetal map in Figure 11 to represent the high and low rainfall conditions that are geographically representative of the state. A similar process was used in selecting the Alabama stations of Birmingham, Mobile and Montgomery.

Selection of Representative Years for Rainfall Analysis

When specific weather stations were selected, a request was made to the Department of Commerce for complete rainfall records for years representative of the area conditions. These data were then reduced and extrapolated to predict rainfall characteristics during years of extreme precipitation. The method useful in selecting appropriate years for analysis involve the development of a frequency vs. annual rainfall plot as shown in Figure 14, based on data such as presented in Table 4. The data in Table 4 show an annual rainfall varying from 27.3 to 47.0 in (69.3 to 119 cm). It has been divided in eleven 2 in (5.1 cm) segments. The annual rainfall occurring most frequently, the mode, was between 34 and 36 in (86.4 to 91.4 cm) and occurred in five different years. In some cases as shown in Figure 14, the most frequently occurring division (34 to 36) will not necessarily include the mean. In order to determine this, the mean annual rainfall should be calculated. This computation for the data being considered yields a mean of 37.6 in (95.5 cm). It can be determined from Table 4 that the years having annual rainfalls in this range are 1948, 1958, 1959 and 1966. If one assumes that the population from which the sample was taken is a relatively normal distribution and that the mean and standard error, SE, of the sample approximate the mean and standard deviation of the population, then 95 percent of the data can be expected to fall within ±2 standard errors of the mean. The standard error calculated according to Equation 13, is 5.0 in (12.7 cm) so that the 95 percent confidence interval is 37.6 in ±2(5.0 in) = 27.6 in to 47.6 in (95.5 cm - (2) 12.7 cm = 70.1 to 120.9 cm).

$$SE = \sqrt{\frac{\sum_{i=1}^{n} (\bar{x} - x_i)^2}{n - 1}} = \sqrt{\frac{754.76}{30}} = 5.0 \text{ in } (127, \text{mm}) \qquad \text{Eq (13)}$$

where $\bar{x}$ = the mean value of n observations
x_i = individual observations of yearly annual rainfall
n = number of yearly annual rainfalls available.

Table 4. Average yearly rainfall for Illinois, 1942 through 1972

Year	State Average Rainfall (in)		*Average of Selected Station's Rainfall (in)	
1942	40.1		40.5	
1943	34.2		31.0	
1944	32.7		34.0	
1945	47.0		47.4	
1946	39.4		40.6	
1947	38.4		35.9	
1948	37.1		34.7	
1949	43.2		42.3	
1950	38.7		47.2	
1951	44.3		49.4	
1952	33.3		38.7	
1953	27.3	Average = 37.6	28.8	Average = 39.4
1954	35.2		36.9	
1955	35.9		34.4	
1956	29.5		32.9	
1957	45.4		49.2	
1958	36.7		32.7	
1959	37.2		43.0	
1960	34.5		41.6	
1961	44.1		46.3	
1962	33.0		37.1	
1963	28.5		29.8	
1964	32.8		38.0	
1965	41.3		45.9	
1966	36.6		38.3	
1967	42.0		42.4	
1968	38.0		39.9	
1969	42.7		40.0	
1970	41.6		42.3	
1971	34.5		32.2	
1972	41.8		49.1	

*These stations are Cairo, Springfield and Rockford, Illinois.

Metric Conversion: 1 inch = 25.4 mm

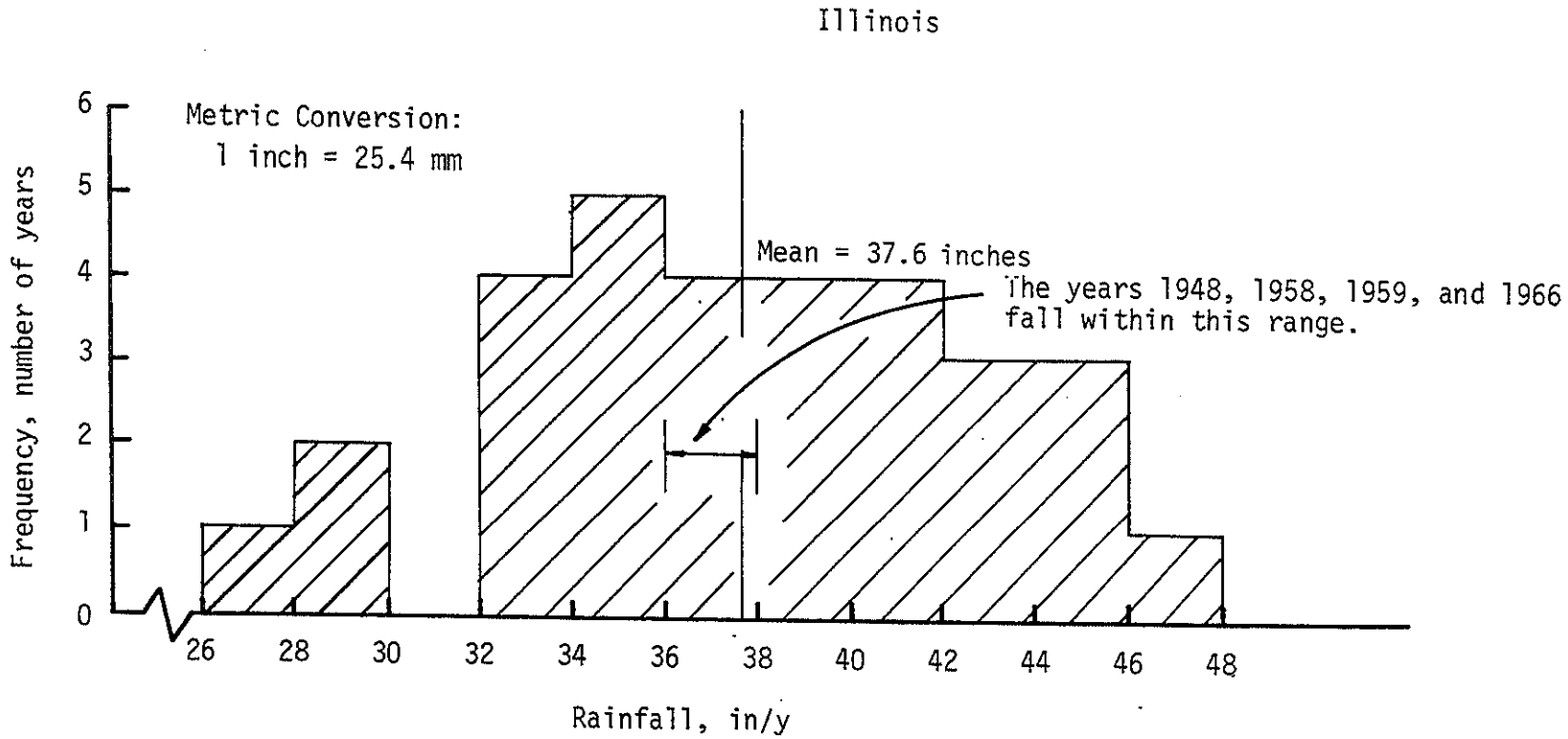

Figure 14. Statewide average annual rainfall frequency diagram

A 95 percent confidence interval can be determined for statewide data as shown in Figure 14, or for the selected stations (Figure 15) or finally for each selected station's data (Figure 16). The latter situations are illustrated by Figure 16 where the differences can be noted. The means vary from 34.4 to 47.9 in (87.4 to 121.7 cm).

In this case it was decided to use the mean from each station. It is obvious that from both Rockford and Cairo there was no year that had an annual rainfall that fell into the immediate range of the mean. In order to choose the specific years for analysis, selection rules were formulated that appear to give reasonable results.

1. Select three years whose annual rainfall occurs within the 95 percent confidence interval giving precedence to those years within the same frequency interval as the mean.
2. If data are not available for one or more years in that range
   a. Select, in the case of two needed stations, one year with annual rainfall above and one below the "mean" range, so that when the annual rainfall for the three stations is averaged, it approximates the mean.
   b. Select, in the case where one year is needed, the value closest to the mean, in either direction.
   c. Select, in the case where three are needed, two above and one below. This would be a slightly more conservative value than selecting one above and two below.
3. If more than the needed number of years are available, select the most recent years.

Table 5 lists the years for each of the Illinois stations as they fell into each range for the period used (1942-1972). The years selected were 1966, 1968 and 1970 for Rockford; 1955, 1959 and 1969 for Springfield; and 1965, 1968 and 1970 for Cairo. In some cases these years selections do not rigidly adhere to the rules for selection listed. This was due to consideration of the quality and/or availability of data in some years.

Analysis of Detailed Rainfall Records

The determination of periods of time during which specific intensities of rainfall occurred was then undertaken. Figure 17 is representative of the recordings supplied by NOAA. To determine the periods of time associated with specific intensities of rainfall, it was necessary to divide each rainfall period or shower into a number of short period elements. The number of elements was selected so that the average slope of the curve as shown in Figure 17 could be approximated by a straight line over each time segment interval. These segments are designated by "division numbers" in the figure. By determining the average slope of the curve, the slope of the straight line approximation of the curve over each segment, the average intensity of rainfall during that period was calculated. As an example, consider Division No. 2 in Figure 17. It is observed that the curve rises one division (0.01 in or 0.25 mm of rain) during an elapsed time of 4.8 divisions (72 minutes). Therefore, the rainfall intensity is the ratio of these two numbers (the slope of the curve), i.e.,

Table 5. The average rainfall of selected stations as grouped by rainfall ranges

Rainfall Range (in/y)	Station Years		
	Rockford	Springfield	Cairo
22.0-23.9		1953	
24.0-25.9	1946,'58		
26.0-27.9	1956,'62,'71	1954,'71	
28.0-29.9	1943,'44,'48,'53,'55	1963	1963
30.0-31.9	1949,'63	1948,'52,'56,'58,'62, '64,'66,'68	1943
32,0-33.9	1947,'57,'66	1943,'50,'72	1953
34.0-35.9		1944,'47,'55,'59,'69	
36.0-37.9	1945,'52	1949,'61,'67	1942
38.0-39.9	1950,'64,'67,'68,'70	1951,'60,'65,'70	1944,'47
40.0-41.9	1942,'54,'61	1957	1955,'56,'60,'71
42.0-43.9	1969	1942,'46	1954,'58,'64,'69
44.0-45.9	1960	1945	1948,'59
46.0-47.9	1959		
48.0-49.9	1965		1952,'65,'68,'70
50.0-51.9			1966,'67
52.0-53.9			1946,'62
54.0-55.9	1972		
56.0-57.9			
58.0-59.9			1949,'51,'72
60.0-61.9			1945,'61
62.0-63.9			
64.0-65.9			
66.0-67.9			
68.0-69.9			1950
70.0-71.9			1957
72.0-73.9			

Metric Conversion: 1 inch = 25.4 mm

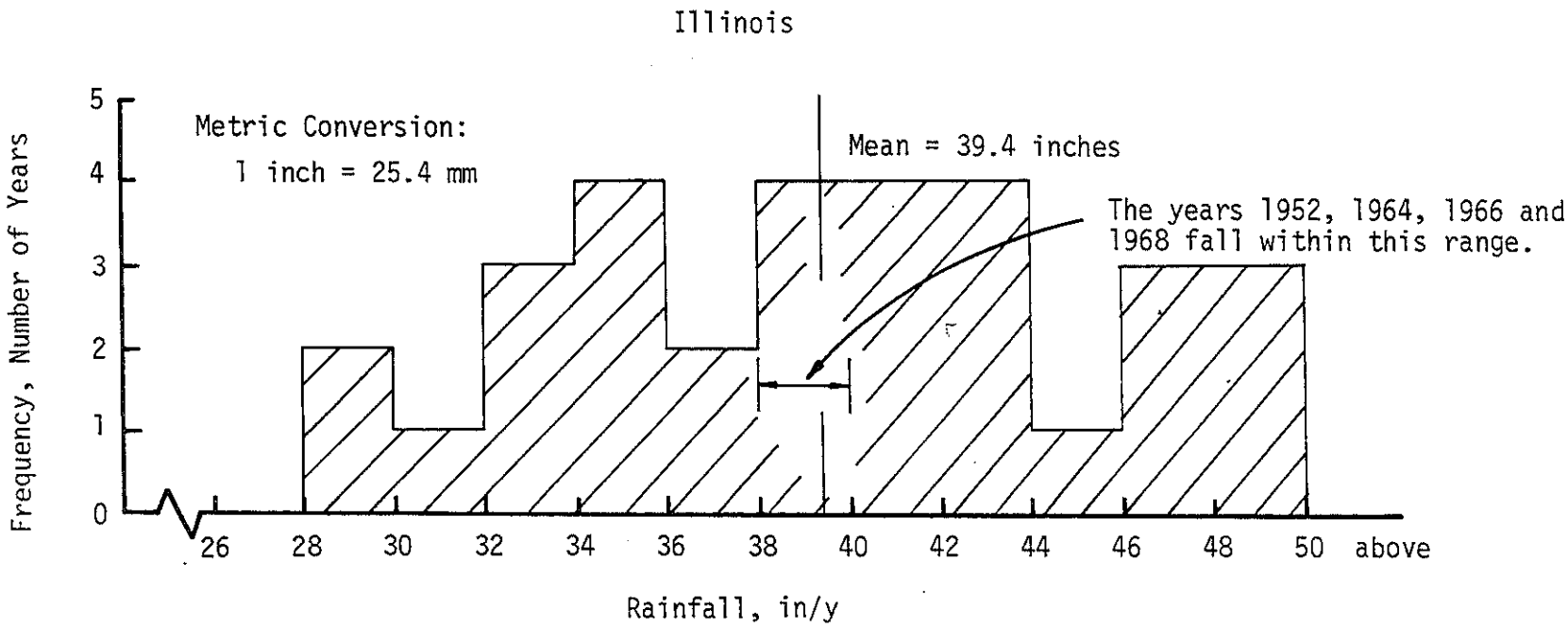

Figure 15. Average of selected stations annual rainfall frequency diagram

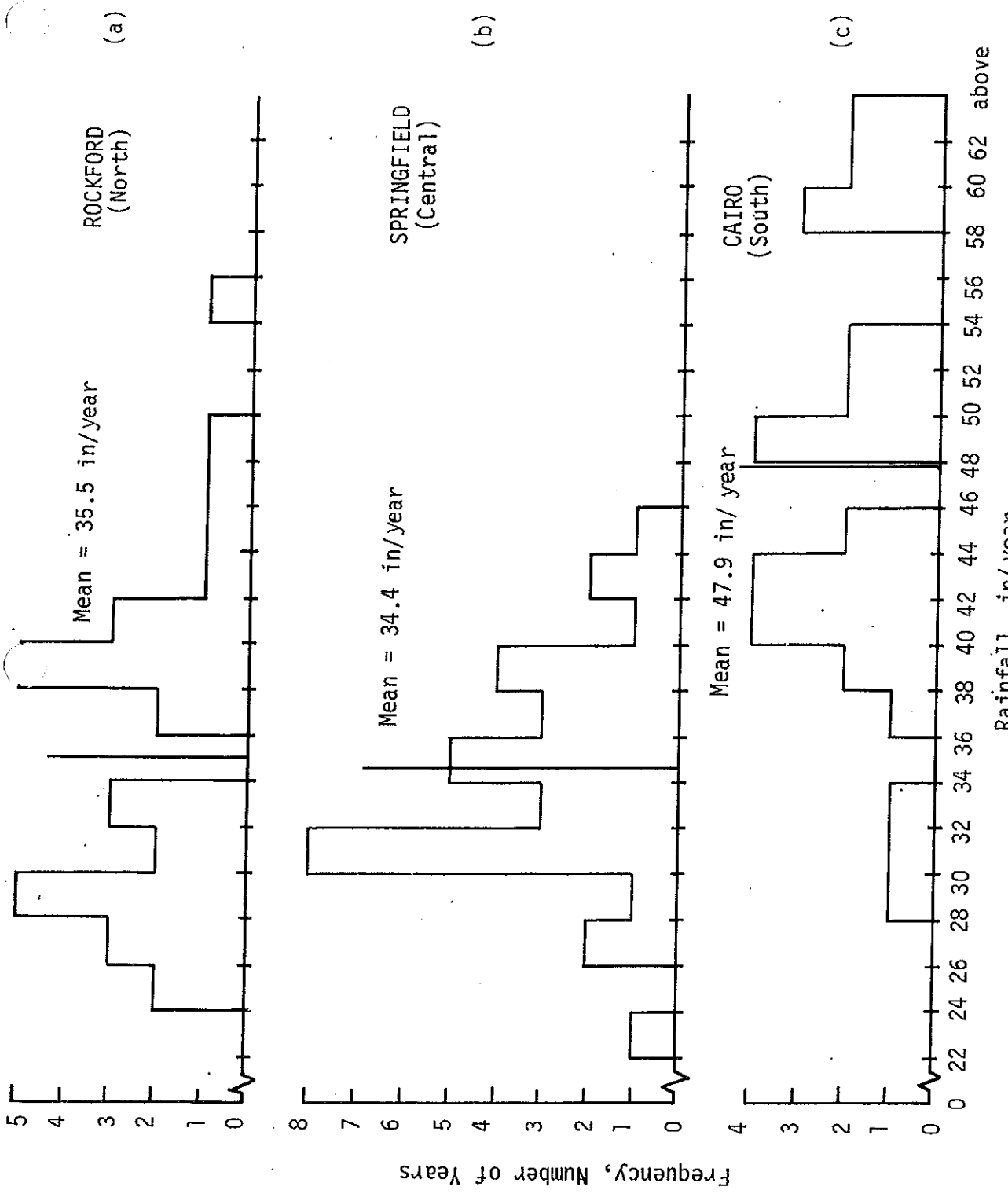

Figure 16. Frequency diagrams for selected stations

Metric Conversion: 1 inch = 25.4 mm

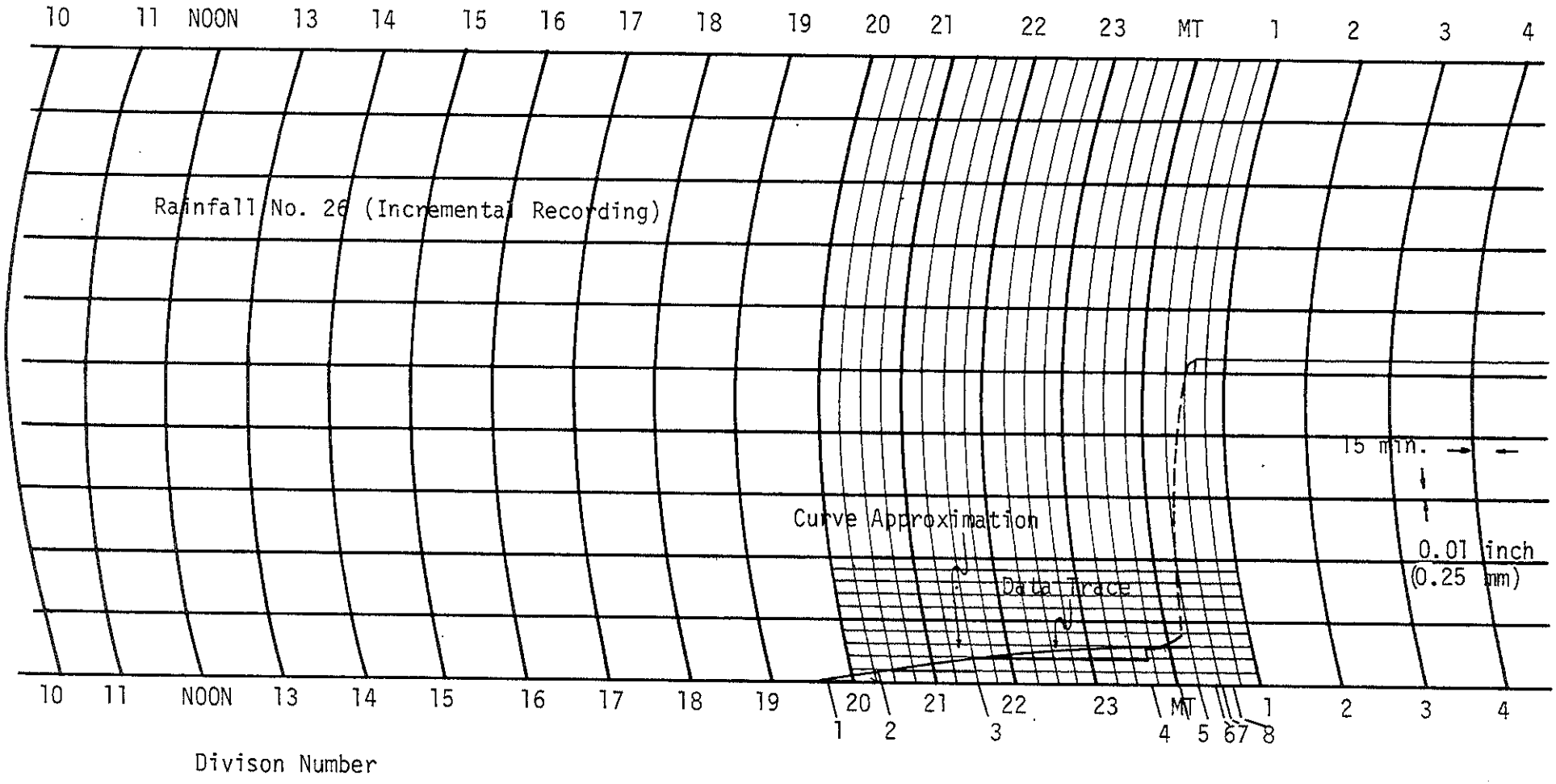

Figure 17. Incremental rainfall recording

$$I = \frac{0.01 \text{ in}}{72 \text{ min}} = 0.00014 \text{ in/min } (0.0035 \text{ mm/min})$$

or

$$I = \frac{0.01 \text{ in}}{72 \text{ min}} \times 60 \text{ min/h} = 0.0083 \text{ in/h } (0.21 \text{ mm/h}).$$

This computation was performed for every division resulting in the data presented in Table 6.

Judgment was exercised when selecting segment lengths in order to represent the curve with reasonable accuracy. When curve segments were nearly linear, time segments over one hour were occasionally used, as shown for Division No. 3 of Table 6. When rapid changes in curvature occurred, smaller divisions were used.

Once all rainfalls had been analyzed during the three years for the three data stations (i.e., 9-data station-years)*, the resulting data were placed in intensity brackets as shown in Table 7. With the foreknowledge that a great majority of rainfalls lie in the range of intensities less than 1 in/h (25.4 mm/h), the brackets were selected to carefully subdivide this range in steps of 0.1 in/h (2.54 mm/h) to 0.5 in/h (12.7 mm/h), in steps of 0.25 in/h (6.35 mm/h) to 1.0 in/h (25.4 mm/h) and then in steps of 1.0 in/h (25.4 mm/h) up to 6 in/h (152.4 mm/h).

Rainfalls of less than 0.01 in/h (0.25 mm/h) were considered trace rainfalls and ignored when tabulating the Illinois data. However, trace durations were included in the reduction of the Alabama data in order to estimate the possible significance of this factor. The time in each of the intensity brackets was tabulated as shown for the Alabama data in Table 8 for the 9-data station-years analyzed. The average for the 9-data station-years in each of the brackets was calculated and presented in the third column of Table 8. The fourth column is a cumulative total of the rainfall at intensities equal to or greater than the lower limit of the corresponding intensity bracket. (The durations in each bracket were totaled from the most intensive to the least.) This cumulative total at each bracket limit, when divided by the total yearly time of rainfall, is the probability that a given rainfall period will be of the corresponding intensity or greater. The cumulative total can also be expressed as a percentage of the calendar year by using the conversion factor of one year equal to 525,600 minutes.

Determining the Probability of Specific Rainfall Intensities

The values used to construct Figure 18 are the probabilities that the intensity at any given time during a rainfall will be of certain intensity or greater. These figures were based on the assumption that trace rainfalls (I is less than 0.01 in/h (0.25 mm/h)) would be considered negligible. Precedent for this assumption exists. Farnsworth (10) has concluded previously that trace rainfalls are not sufficient to "wet" the pavement surface. Trace rainfalls accompanied with high humidity for long periods of time may be exceptions. The influence of trace durations can be clearly seen in Figure 19 where the probabilities from the Alabama data using both assumptions are compared graphically. It can be seen that the addition of trace durations lowers the probability curve; so, assuming the trace durations to be negligible

*Several thousand individual rainfalls

Table 6. Data from Figure 17

Division Number	Time Increment, T Minutes	Rainfall, R Inches	Intensity T/R in/min x 10^{-3}	in/h
1	38	0.01	0.26	0.02
2	72	0.01	0.14	0.01
3	130	0.01	0.08	0.01
4	20	0.03	1.50	0.09
5	15	0.07	4.67	0.28
6	12	0.21	17.5	1.05
7	3	0.01	3.33	0.20
8	6	0.01	1.67	0.10

Metric Conversion: 1 inch = 25.4 mm

Table 7. Summary of individual rainfall analyses from nine data stations in Illinois

Rainfall Intensity Range, in/h		Total Number of Minutes, N	Average Number of Minutes N/9	Total Average Number of Minutes With I > Value Shown Below		Percent of Rainfall Time Greater Than I, (Assume Trace = 0)
from	to			I	Min	
0.01	0.09	113,319	12,591	0.01	18,521	100.00
0.10	0.19	24,259	2,695	0.10	5,930	32.02
0.20	0.29	13,355	1,484	0.20	3,235	17.47
0.30	0.39	5,271	586	0.30	1,751	9.45
0.40	0.49	3,311	368	0.40	1,165	6.29
0.50	0.74	3,167	352	0.50	797	4.30
0.75	0.99	1,136	126	0.75	445	2.40
1.00	1.49	1,215	135	1.00	319	1.72
1.50	1.99	689	77	1.50	184	0.99
2.00	2.99	661	73	2.00	107	0.58
3.00	3.99	198	22	3.00	34	0.18
4.00	4.99	60	7	4.00	12	0.06
5.00	5.99	25	3	5.00	5	0.03
6.00	UP	15	2	6.00	2	0.01

Metric Conversion: 1 inch = 25.4 mm

Table 8. Summary of individual rainfall analyses from nine data stations in Alabama

Rainfall Intensity Range, in/h from	to	Total Number of Minutes, N	Average Number of Minutes N/9	Total Average Number of Minutes with Intensity ≥ I I	Min	Percent of Rainfall Time Greater Than I, (Assume Trace = 0)	(Assume Trace > 0)
0	0.009*	———	10,610	0	31,877	100	100
0.01	0.09	131,250	14,583	0.01	21,267	100	66.7
0.10	0.19	27,294	3,033	0.10	6,684	31.43	21.7
0.20	0.29	11,531	1,281	0.20	3,651	17.17	11.5
0.30	0.39	5,884	654	0.30	2,370	11.14	7.4
0.40	0.49	2,766	307	0.40	1,716	8.07	5.4
0.50	0.59	5,312	590	0.50	1,409	6.63	4.4
0.75	0.74	1,726	192	0.75	819	3.85	2.6
1.00	0.99	2,455	273	1.00	627	2.95	2.0
1.50	1.49	1,380	153	1.50	354	1.66	1.1
2.00	1.99	999	111	2.00	201	0.95	0.6
3.00	2.99	569	63	3.00	90	0.42	0.3
4.00	4.99	174	19	4.00	27	0.13	0.08
5.00	5.99	0	0	5.00	8	0.04	0.025
6.00	UP	70	8	6.00	8	0.04	0.025

Metric Conversion: 1 inch = 25.4 mm

* Trace Category

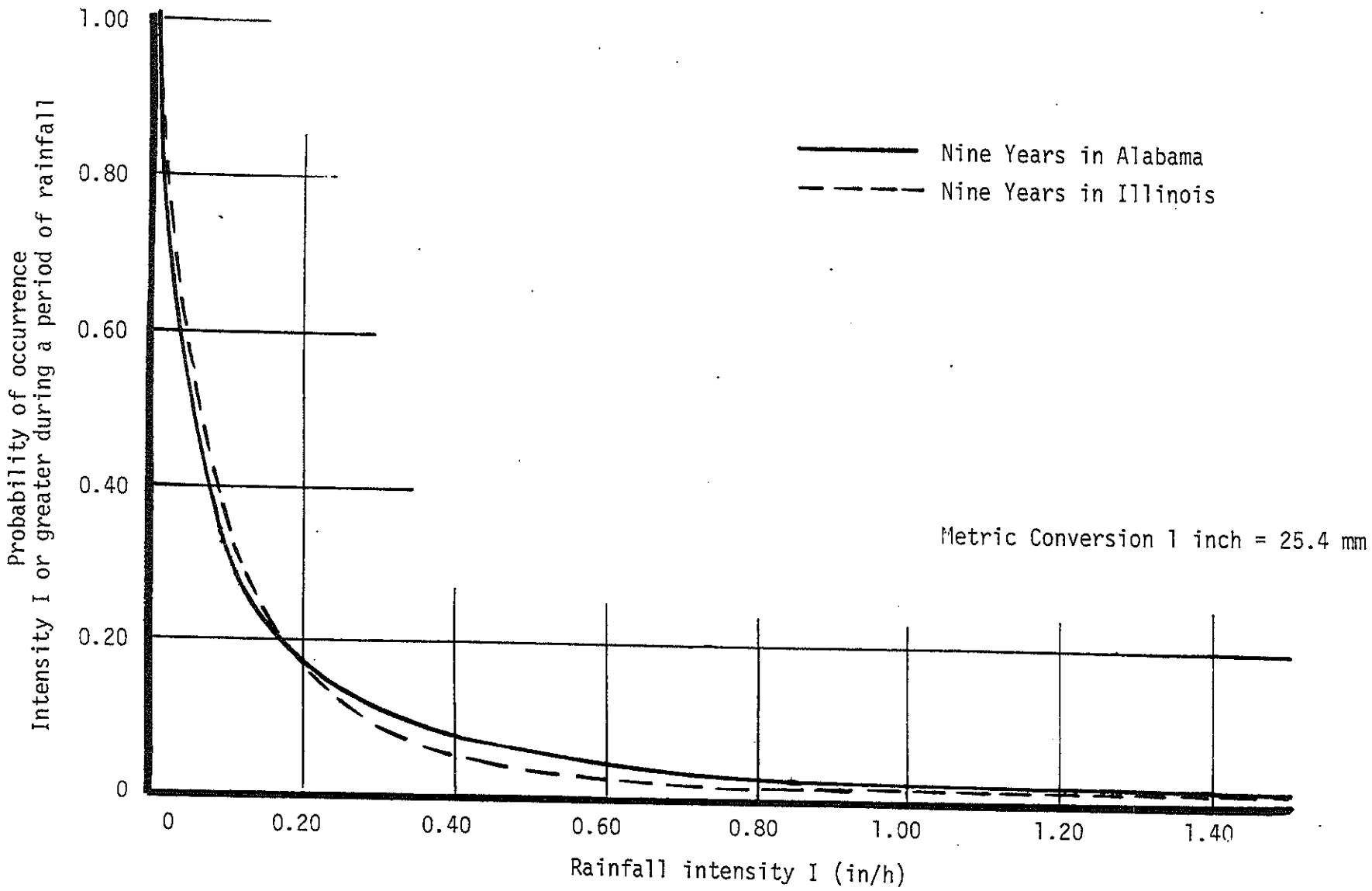

Figure 18. Probability of a given rainfall intensity I or greater vs rainfall intensity I (trace rainfall neglected)

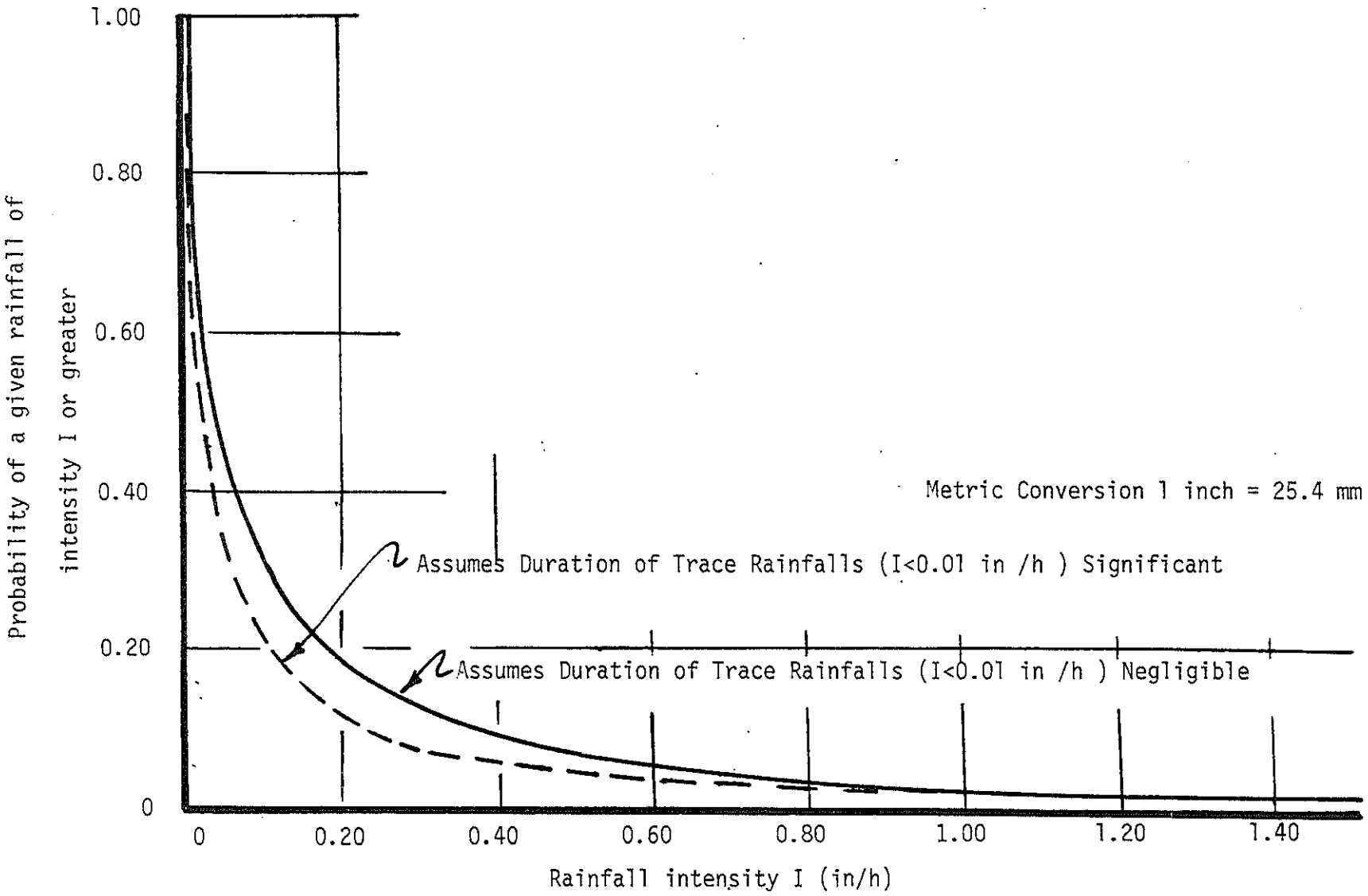

Figure 19. Influence of trace rainfall duration on probability curves, Alabama data

causes a rainfall intensity at a given probability to be slightly overestimated. A roadway surface designed using such an assumption will merely result in the inclusion of a small additional safety factor. This may be appropriate since the available friction of a surface is certainly reduced during trace rainfalls, though hydroplaning is not a problem.

Returning to Figure 18, the probability curves of Illinois and Alabama appear similar, but this graph may be somewhat misleading, since it is a normalized curve which does not account for the total amount of rainfall or for the total amount of exposure time. Figure 18 contrasts two states which are quite different in terms of annual rainfall. The nine station-years analyzed for Alabama average 57.3 in/y (145.5 cm/y), one of the highest rainfall areas on a statewide basis in the U.S., and one where tropical storms, and their associated high intensities, play an important part in the rainfall environment. In contrast Illinois has an annual rainfall of slightly less than 40 in (101.6 cm) with a fairly low variation across the state, thus more closely representing the national average.

It is seen that the curves cross at the 0.20 in/h (5 mm/h) intensity level. For any intensity greater than 0.20 in/h (5 mm/h) the probability of its occurrence is higher in Alabama than in Illinois, perhaps a somewhat less than startling conclusion to Mobile residents. The converse is also true. The probability is higher that intensities less than 0.20 in/h (5 mm/h) will occur during a given rainfall period in Illinois than in Alabama.

Figure 20 places these probability levels in a different perspective. Here the ordinate is the percentage of total time (both dry and wet) that a rainfall of a given intensity or greater is falling. The curves are positioned, with Texas included, in the order of their average annual rainfalls. Table 9 gives the data from which these curves are plotted. Of some importance is the fact that all three states are subjected to rainfall intensities of 0.5 in/h (12.7 mm/h) or more for approximately 1/4 of 1 percent of the time. This is approximately 24 hours per year. Intensities greater than 1 in/h (25.4 mm/h) occur more on the order of 10 hours per year.

Table 10 summarizes the exposure percentages for four regions of the country, varying from the extremely arid climate of the southern Arizona desert to the subtropical conditions of Alabama. It should be noted that the detailed data used to arrive at the Illinois and Alabama exposure times were not used for Central Texas (13), and that the southern Arizona desert data point of approximately 1 percent exposure was adjusted up by a 1 hour drying time for most rainfall events. The exposure time for the Arizona desert directly comparable to the Illinois and Alabama data would be less than the 1 percent presented by Burns (14). These data are plotted in Figure 21. Although four data points must not be considered definitive, they do appear to follow the same trend, a curve with decreasing positive slope, as do the data shown in Figure 22. Figure 22 is a plot of the percentage of wet-weather accidents in 19 states versus the annual state rainfall. The similarity in curvature may be significant.

It is demonstrated that analysis of NOAA rainfall data can yield both the total exposure time and the occurrence probability of any specific intensity level. Although these two factors are highly pertinent to the determination of whether a specific pavement surface will be flooded, they do not constitute enough information to specify the exact probability of flooding. To do this it would be necessary to determine the short-term (a matter of

Table 9. Duration of threshold intensities for one year

Minutes of Rainfall of Intensity ≥ I

Total Minutes in One Year

Intensity I (in/h)	Texas* Average of 2 Stations 1 Year at Each		Illinois Average of 3 Stations 3 Years at Each		Alabama Average of 3 Stations 3 Years at Each	
	Minutes	Percent of Calendar Year	Minutes	Percent of Calendar Year	Minutes	Percent of Calendar Year
≥ 0	32,750	6.25			31,877	6.1
≥ 0.01	18,650	3.54	18,521	3.52	21,267	4.1
≥ 0.25	2,089	0.40	2,493	0.47	3,011	0.57
≥ 0.50	869	0.165	757	0.15	1,409	0.27
≥ 1.00	304	0.06	319	0.16	627	0.12
≥ 2.00	82.5	0.015	107	0.02	201	0.04
≥ 4.00	14	0.0025	12	0.0023	27	0.005

Metric Conversion: 1 inch = 25.4 mm.

*From: "Rainfall and Visibility - The View From Behind the Wheel"; Ivey, et.al., Journal of Safety Research, A National Safety Council Publication, December 1975, Volume 7, Number 4.

Table 10. Summary of rainfall exposure time in four states

Geographic Area	Annual Rainfall (Inches)	Total Time of Rainfall* (Minutes)	Total Time of Significant** Rainfall (Minutes)	% of Exposure Time	
				Including Trace	> 0.01 in/h
Alabama	57.3	31,877	21,267	6.1	4.1
Illinois	39.4	--	18,521	--	3.5
Central Texas	35.2	32,750	18,650	6.2	3.5
Southern Arizona Desert	<5	--	--	1***	--

*Includes Trace

**Intensities > 0.01 in/h

***Arizona correction

Metric Conversion: 1 inch = 25.4 mm

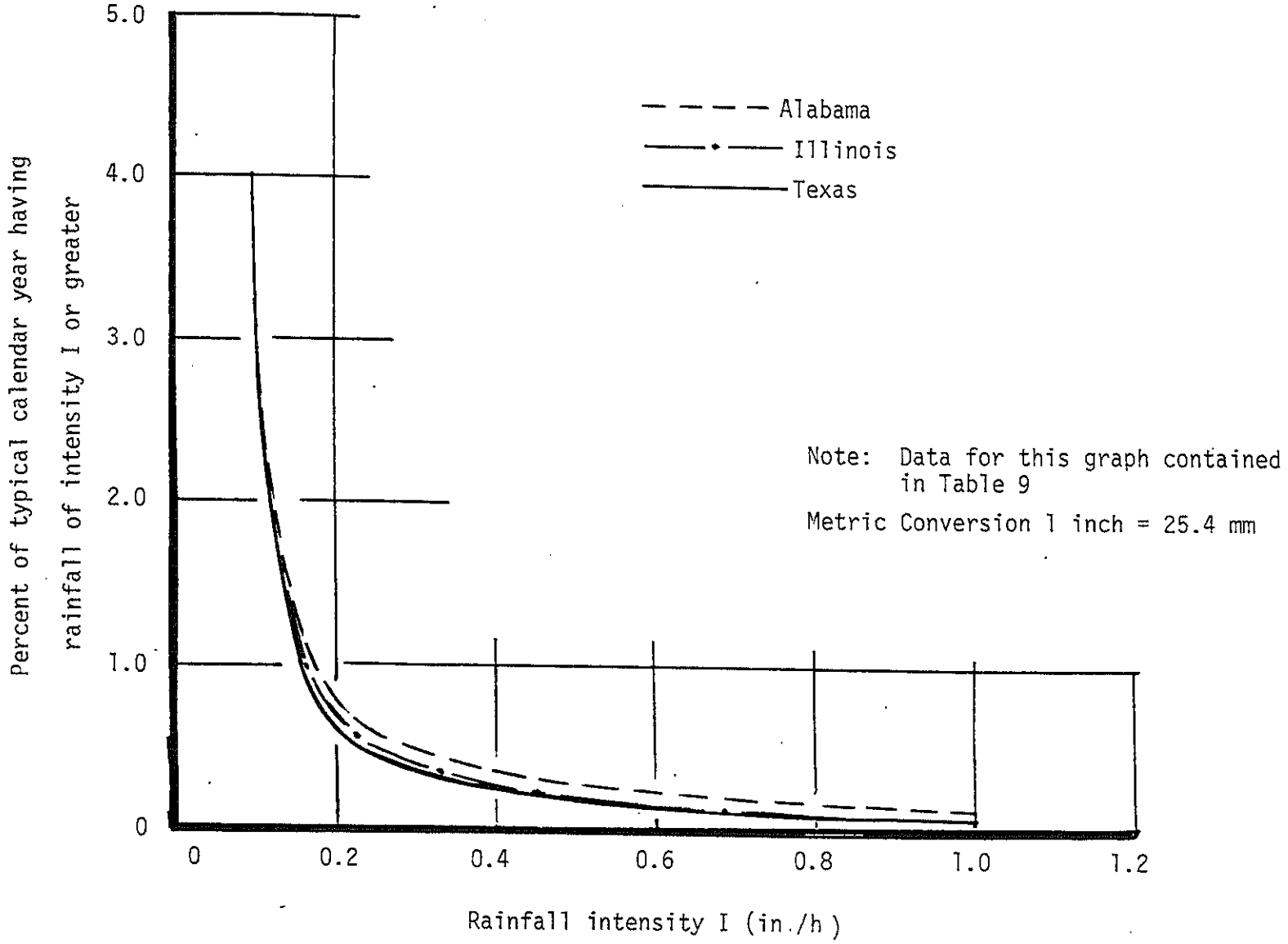

Figure 20. Percent of typical calendar year having rainfall of intensity I or greater

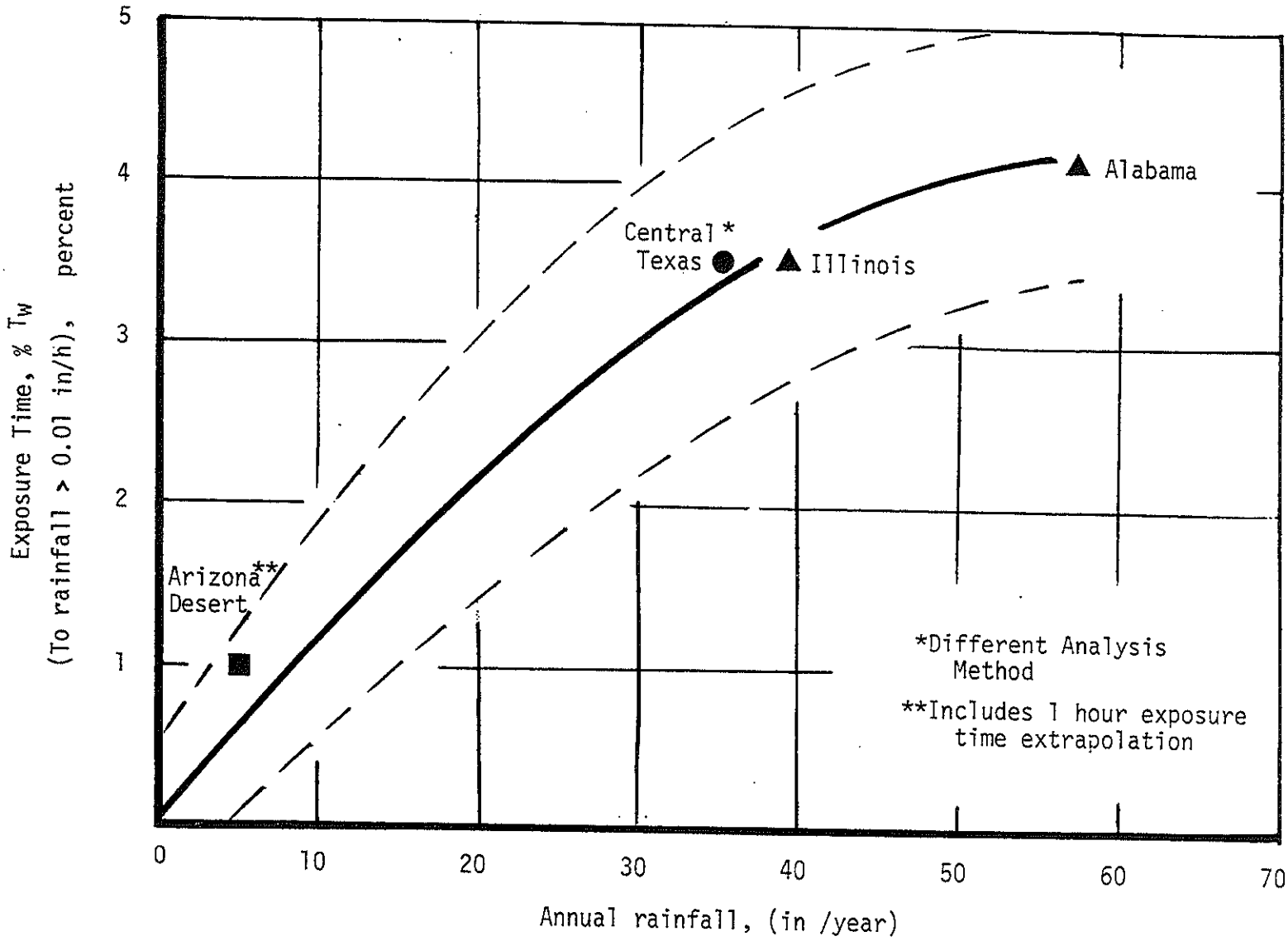

Figure 21. Determination of percent time of exposure to > 0.01 in./h rain

Metric Conversion
1 inch = 25.4 mm

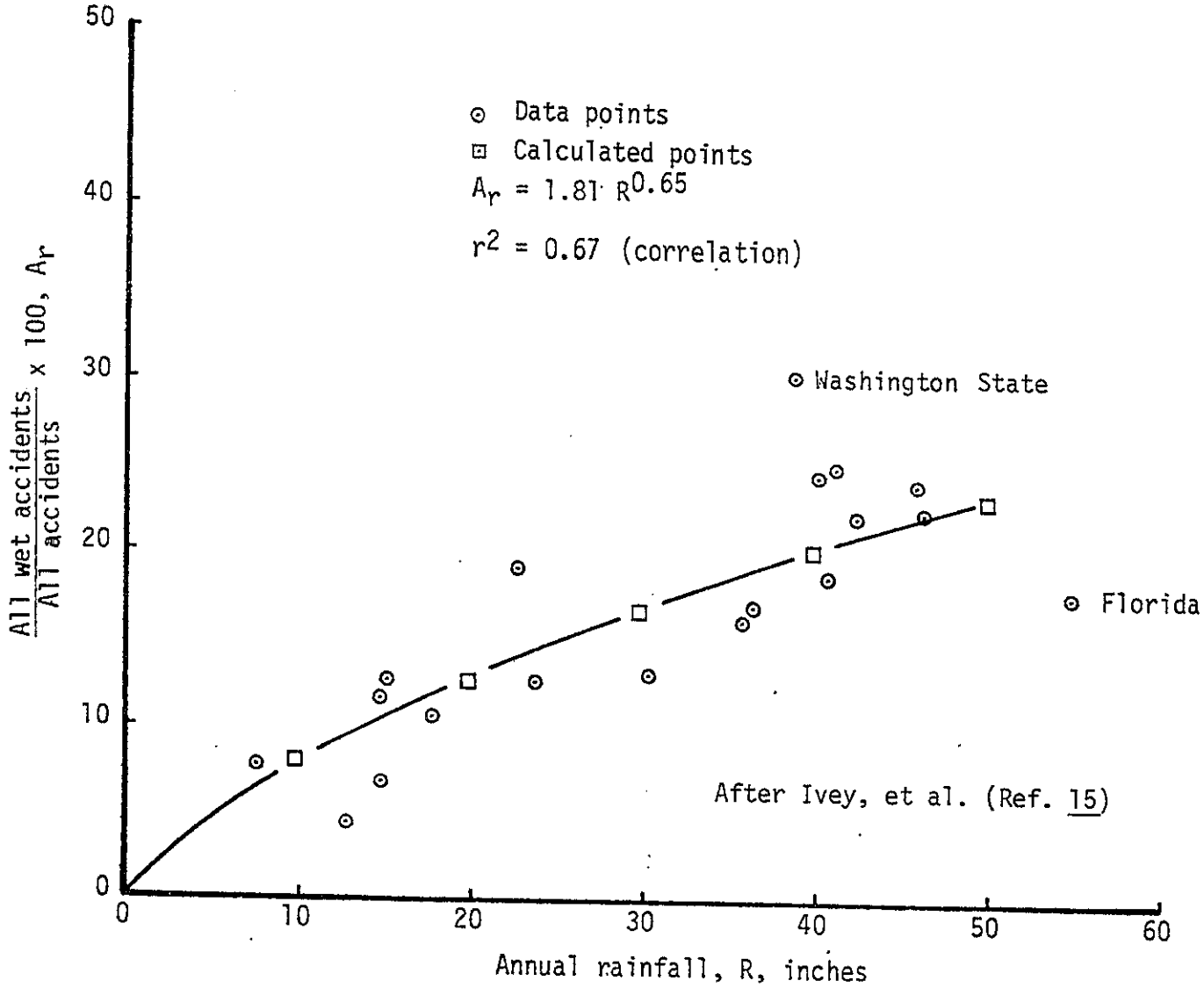

Figure 22. Percent of all accidents occurring during wet weather vs. annual rainfall

minutes) intraevent history probability of rainfall intensities. As an illustration, consider the fact that an intensity of 1/2 in/h (12.7 mm/h) will flood a given pavement if it lasts for 6 minutes; but it will not flood the pavement if the intensity lasts for only 2 minutes or even 5 minutes. In contrast if the 1/2 in/h (12.7 mm/h) intensity lasts for only 1 minute it may flood the pavement if the intensities leading up to the 1/2 in/h (12.7 mm/h) level have gradually varied from trace up to 0.49 in/h (12.4 mm/h) over a period of 15 minutes. It should be recognized that the determination of precise probability levels for intraevent short-term intensity histories is complex, a degree of sophistication not attempted in this study. As an indicator of the likely duration of a specific intensity, Figure 23 was prepared. It is a frequency diagram of rainfall intensities between 0.41 and 0.61 in/h (10.4 and 15.5 mm/h). This bracket may be considered nominally 0.5 in/h (12.7 mm/h). The information was taken from the years 1967 and 1974 in Montgomery, Alabama. These years were selected because the data were recorded on paper with time definition lines of 2 minutes compared to other data recorded on paper having time definitions of only 5 minutes or in some cases 15 minutes. The figure shows the average frequency of selected durations for the two station-years. The 1/2 in/h (12.7 mm/h) rainfall event occurred 36 times for periods equal to or less than 2 minutes. It occurred only one time for a period between 30 minutes and 1 hour.

The average duration of the 1/2 in/h (12.7 mm/h) rainfall event is about 4 minutes, a duration that would not flood* most pavements having cross slopes of 2 percent and a texture of at least 0.04 in (1 mm). The question is still unanswered, however, concerning the intraevent, or transient history.

The resulting position is that an assumption must be made regarding this intraevent history or its effect must be ignored. Ignoring this history could lead to nonconservative conclusions that specific intensities of fairly short duration would not cause pavement flooding, when in fact the opposite might generally be true.

A conservative assumption would likely be a much better choice to use in setting design criteria to eliminate pavement flooding. Consider the result of assuming that the steady-state water depth condition would be reached for a given rainfall intensity no matter what the duration of that intensity. This might result in some exposure time at that intensity when the steady-state water depth actually would not be reached but for which time it would be assumed to occur (see Figure 24a). In many cases even a very short exposure to the given intensity might cause the steady-state level to be achieved due to the intraevent history as shown in Figure 24b. The fact that some of the given intensity rainfall periods will occur after a higher intensity intraevent history reduces the conservative magnitude of the assumption to some degree. This is illustrated by Figure 24c. In summary, it is suggested that this assumption be used, i.e.,

> During all times of actual exposure to a given rainfall intensity the water depth is assumed to have reached its steady-state condition.

*In this case the term "flooding" means the development of water depths that completely immerse the pavement asperities.

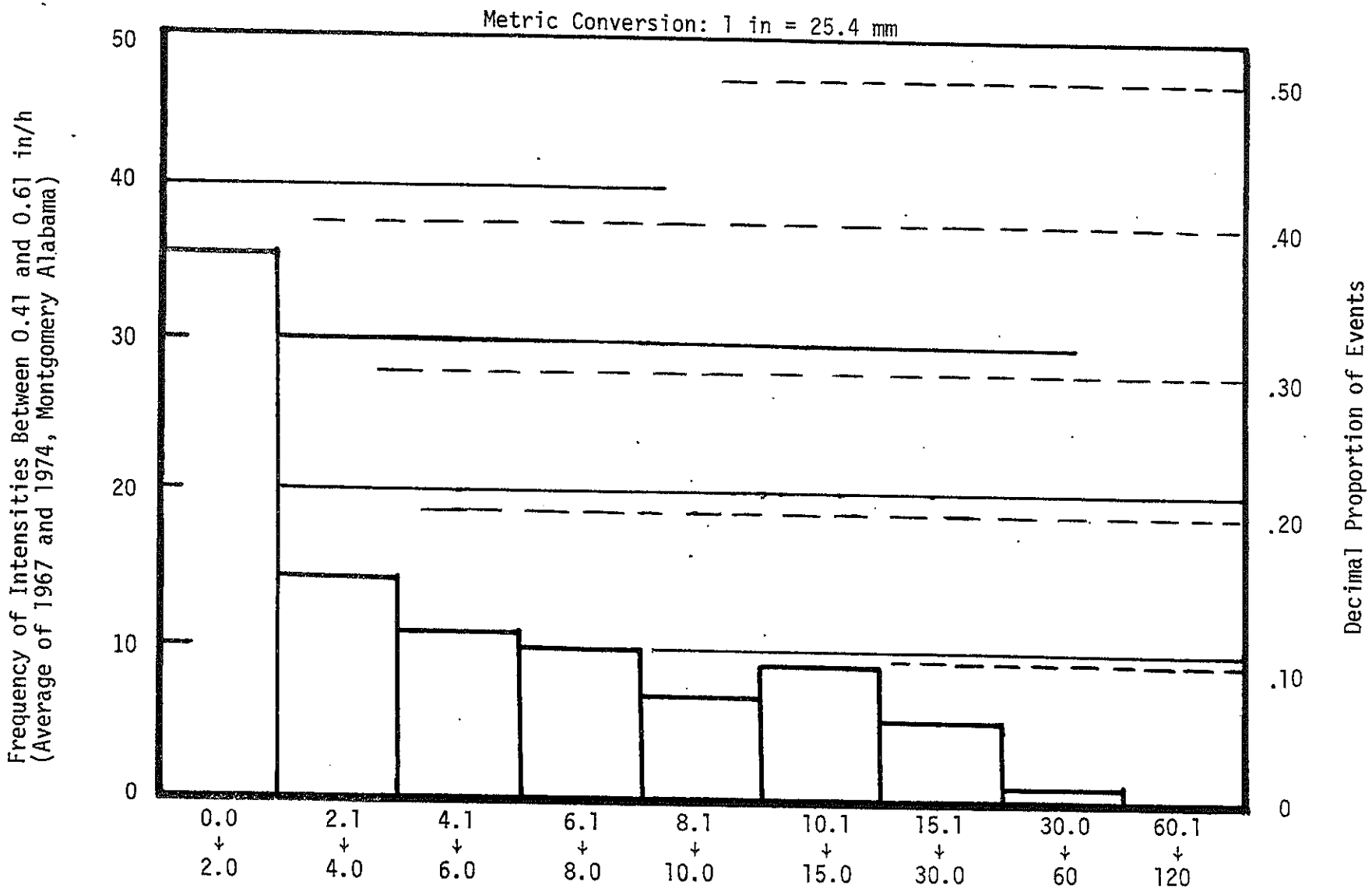

Figure 23. Duration of rainfall events of nominally 1/2 in/h intensity

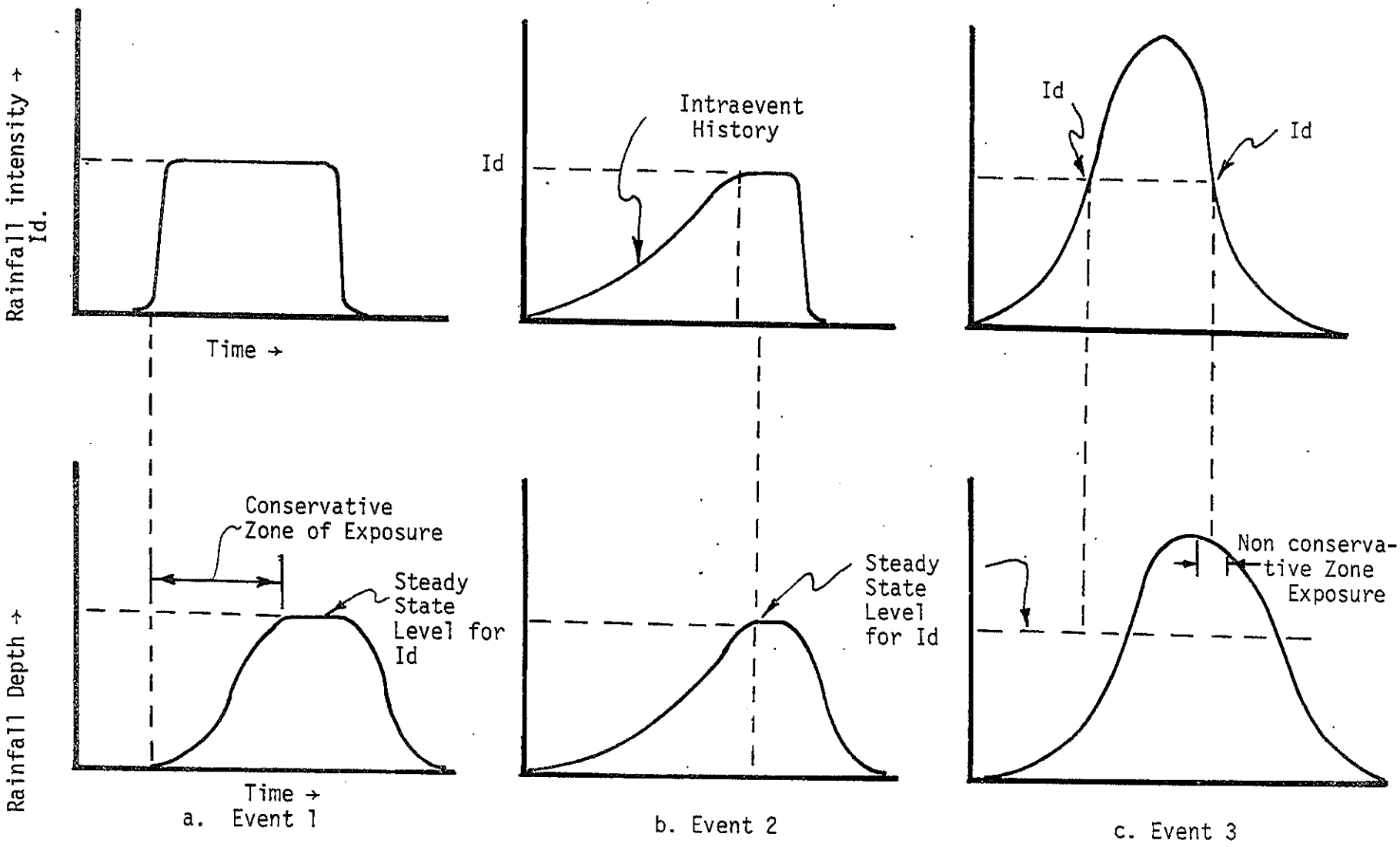

Figure 24. Influence of different theoretical rainfall patterns on the simplifying assumption (I_d is the assumed "design" rainfall intensity)

It is now possible to conservatively estimate the probability of driving in a specific intensity rainfall or greater and/or on the steady-state water depths produced by that variety of intensity, i.e.,

$$P_{ri} = T_W(P_i) \qquad \text{Eq (14)}$$

where P_{ri} = the resultant probability of driving in a specific intensity rainfall or greater as designated by the subscript i.

T_W = the decimal portion of time that rainfalls of intensity greater than 0.01 in/h (0.254 mm/h) are falling.

P_i = the probability of an intensity equal to or greater than i occurring during any period of rainfall.

A state may determine T_W and P_i in the way presented in this chapter, or reasonable estimates can be made based on Figure 21 (to determine T_W) and Figure 18 (to determine P_i). The latter approach should be used with caution, especially in those areas of the country where rainfall patterns are atypical, such as in some mountainous regions.

CHAPTER III

HYDROPLANING AND TRACTION TESTS UNDER CONTROLLED CONDITIONS

A series of tests were performed under relatively controlled conditions in the "hydroplaning trough". This facility consists of a pair of rails 2.5 ft (0.76 m) apart and 800 ft (244 m) long. The underlying surface has a longitudinal slope of about 1 percent, and water can be injected at the upper end and allowed to slowly flow over the surface contained by the rails. Various flow rates permit the water depth throughout the trough to be varied, and different surfaces can be installed within the trough. The trough has been used for other hydroplaning studies and has been described more fully by Stocker, et al. (16). Figure 25 shows the trough, and Figure 26 shows a run being made with the offset test wheel in the trough.

The tests were performed with the TTI research trailer which, in addition to the capability of measuring ASTM E274 locked-wheel skid numbers, can measure test wheel rotational speed referenced to a fifth wheel which measures forward speed. Horizontal force, vertical force and torque can be measured with the test wheel locked or freewheeling.

Test Conditions

The primary test matrix was as follows:

SURFACES: Open-graded hot mix and lightweight aggregate slurry seal.
TIRES: ASTM E501 and B. F. Goodrich FR 78-14 steel-belted radial.
TIRE PRESSURE: 24 and 18 psi (165 and 124 kPa).
TREAD DEPTHS: 11/32 and 2/32 in (8.7 and 1.6 mm).
WATER DEPTHS: 3/32 and 8/32 in (2.4 and 6.4 mm).
NOTE: All combinations of tire, tread depth, tire pressure and water depth were used on each surface.

A longitudinally grooved portland cement concrete (PCC) surface was in the trough at the time testing began. Preliminary tests were conducted on this surface. This was followed by overlaying a coarse open-graded surface, and the full test matrix was performed. This surface was then overlaid with a uniform lightweight aggregate slurry seal of medium texture, and the tests were repeated.

Locked-wheel "skid numbers" were determined both in the external water conditions and using internal water (ASTM E274 procedure) on this dense medium textured surface.

As an adjunct, freewheeling spindown and horizontal drag forces were measured while traversing "puddles" of various lengths and depths.

Preliminary Tests on Grooved PCC

The TTI research skid measurement system was adjusted and calibrated, and an exploratory test program was conducted on the existing surface. These tests were run in 3/8 in (9.5 mm) (average) water depths using an ASTM E501 tire with 2/32 in (1.6 mm) tread depth and 24 psi (165 kPa) (cold) inflation pressure. The runs were conducted in the following three-speed conditions: while accelerating, during deceleration, and at incremented constant speeds. Both

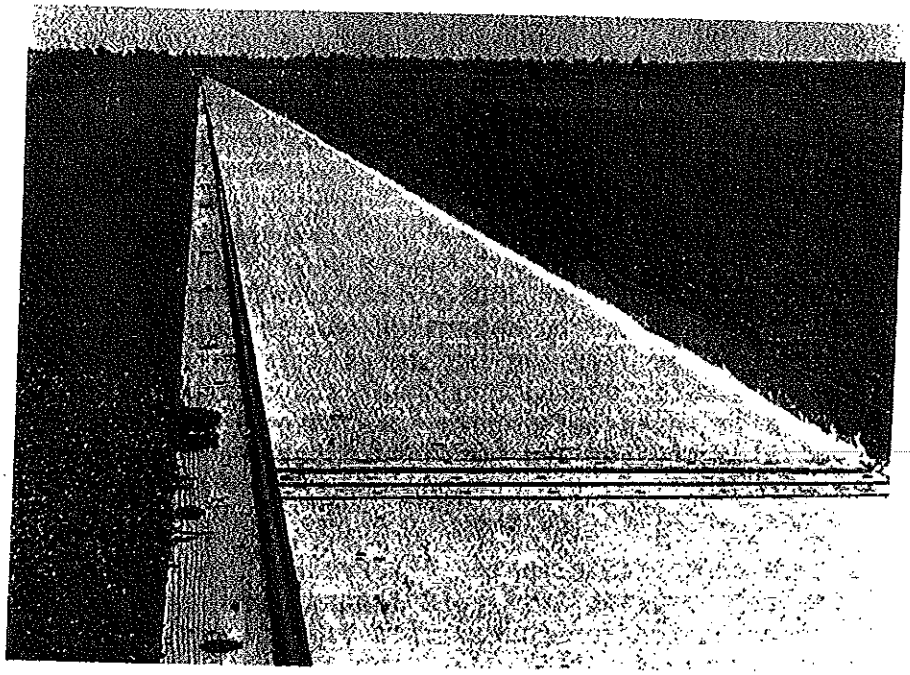

Figure 25. Hydroplaning trough
(Water is injected through the slit in the foreground and slowly flows down between the rails.)

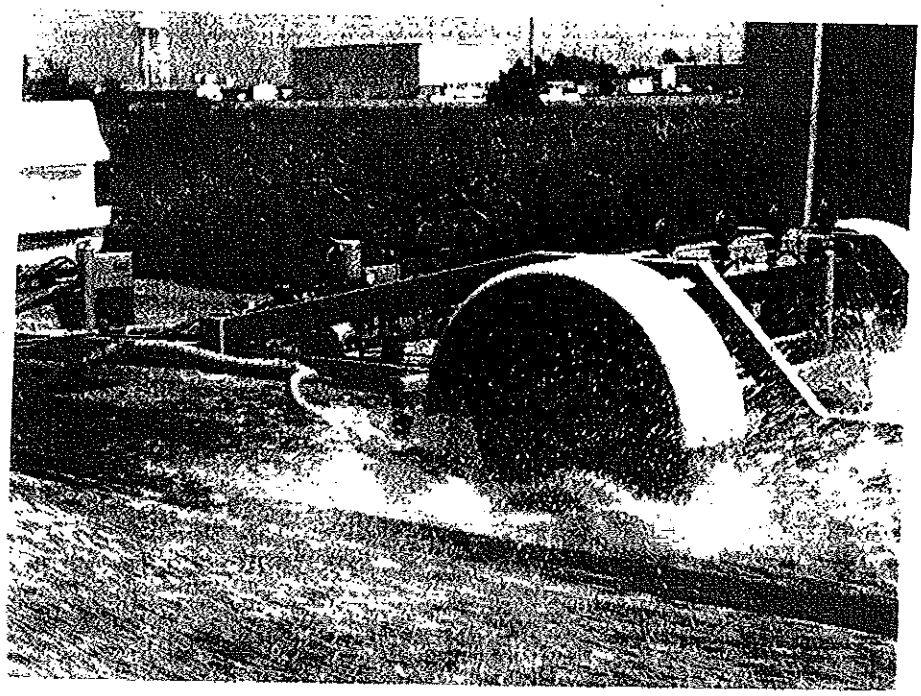

Figure 26. Test run in the hydroplaning trough
(The test wheel is offset to allow tow vehicle to straddle the trough.)

freewheeling and locked-wheel data were obtained from the horizontal force and torque transducers. In addition, standard ASTM E274 skid numbers (and traction forces) were obtained in the trough using the internal watering system and a fully treaded but broken-in ASTM E501 tire.

With external watering, there was a smooth, though not necessarily linear, loss of traction with increased speed until the tire lost contact with the pavement, at which time the horizontal force leveled out to that produced by hydrodynamic drag (see Figure 27). In addition, it appears that horizontal force, F_H, for a given speed is not dependent on whether the vehicle is accelerating or decelerating through the speed, or traveling at a constant speed. This fact allows data points to be obtained at several speeds during one run. In general, a speed change of about 10 mph (16 km/h) was used in succeeding tests. It takes about 15 minutes between runs for the water depth to restabilize, so this technique results in considerable time saved. At speeds above "full hydroplaning", the horizontal force under these conditions is about the same (~90 lbf) (~400 N) whether locked-wheel or freewheeling.

Figure 28 shows that the horizontal force measured on the torque transducer, F_T, exhibits the same trend but is consistently about 70 lbf (311 N) lower than that measured on the horizontal force transducer. These transducers read the same under static (force plate) calibration. A simple analysis of the force and torque mechanisms indicates that the lower torque force can be explained by a 0.8 in (20.0 mm) dynamic forward shift at the "center of effort" as opposed to the force plate condition. The wedge of water in front of the tire in the dynamic test condition could very well cause this degree of shift.

It is also interesting to note that the resistance to movement, or drag on the vehicle at the tire/surface interface, both dry and with internal watering, is about 20 lbf (89 N) while the drag in 3/8 in (9.5 mm) of water is about 90 lbf (400 N), a difference of 70 lbf (311 N). In addition, the freewheeling drag forces above are relatively speed-independent except at low speeds in the external water condition (see Figures 29 and 30). Again, accelerating, decelerating or constant speed seems to make no difference within the band of precision.

Figure 31 compares the locked-wheel "coefficients" using ASTM E274 procedure (full tread tire and internal watering producing a computed value of water depth of 0.02 in (0.5 mm)) with a similar procedure for a 2/32 in (1.6 mm) thin tread and 3/8 in (9.5 mm) water depth. The "traction coefficients" are equivalent at about 35 mph (56 km/h).

Figure 32 indicates the percent spindown as a function of vehicle speed. The spindown starts to occur at about 46 mph (74 km/h), the speed at which the horizontal force becomes constant and equal to the freewheeling drag force. The curves for accelerating, decelerating and incremented constant speeds cannot be significantly resolved. Apparently, when spindown is detected, the tire has lost contact with the pavement; and only hydrodynamic forces, which seem to be speed-independent in the test conditions, are present.

Figure 33 shows the time as a function of speed for the wheel to reach zero spindown after unlocking the brake. Obviously it takes a finite time for this to occur even on dry pavement. However, the rather sharp divergence of spinup time near 46 mph (74 km/h) indicates that this may be a more sensitive indicator of "full hydroplaning" speed, or the speed at which essentially all pavement contact is lost, than is spindown.

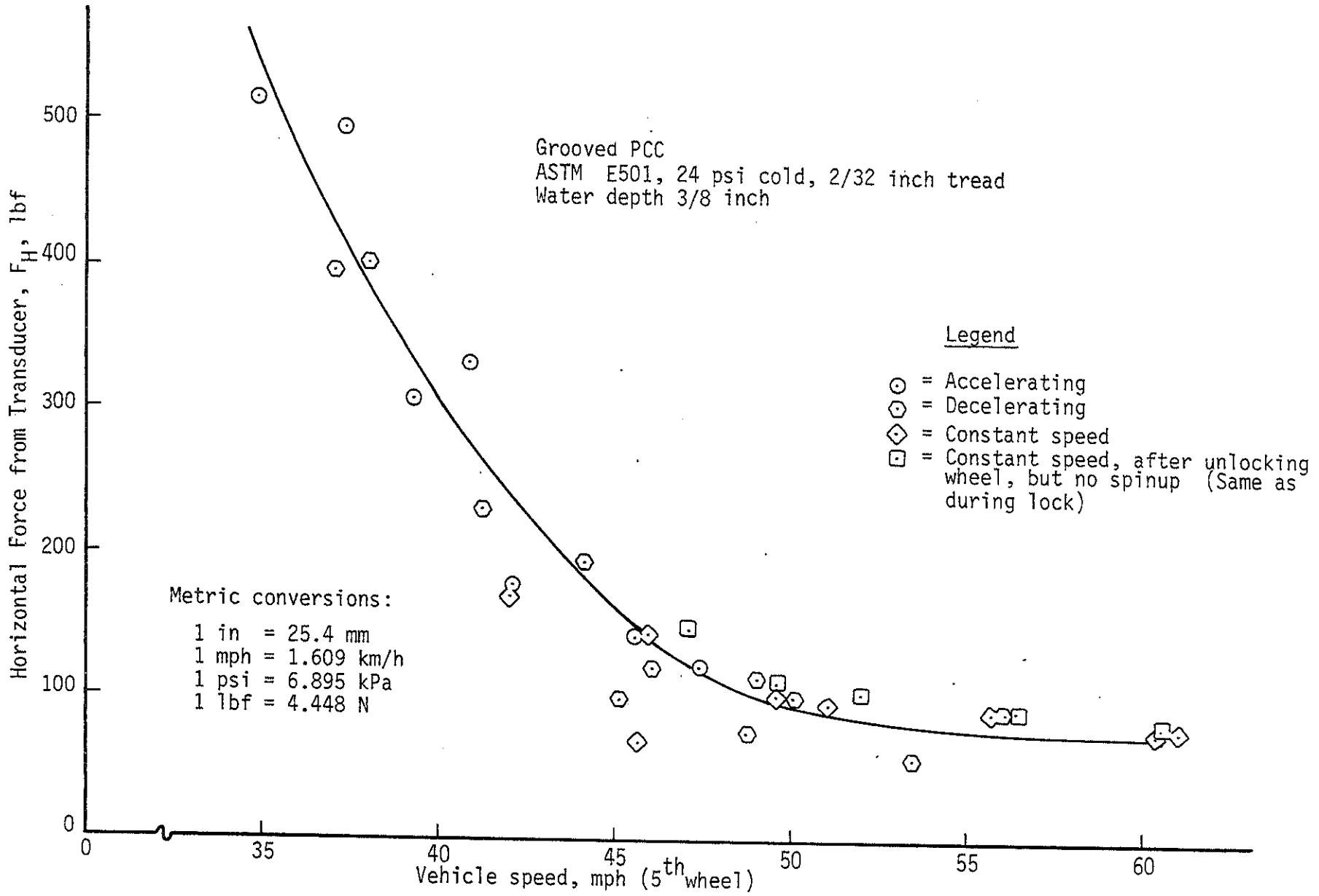

Figure 27. Locked-wheel horizontal force from force transducer vs. 5^{th} wheel vehicle speed

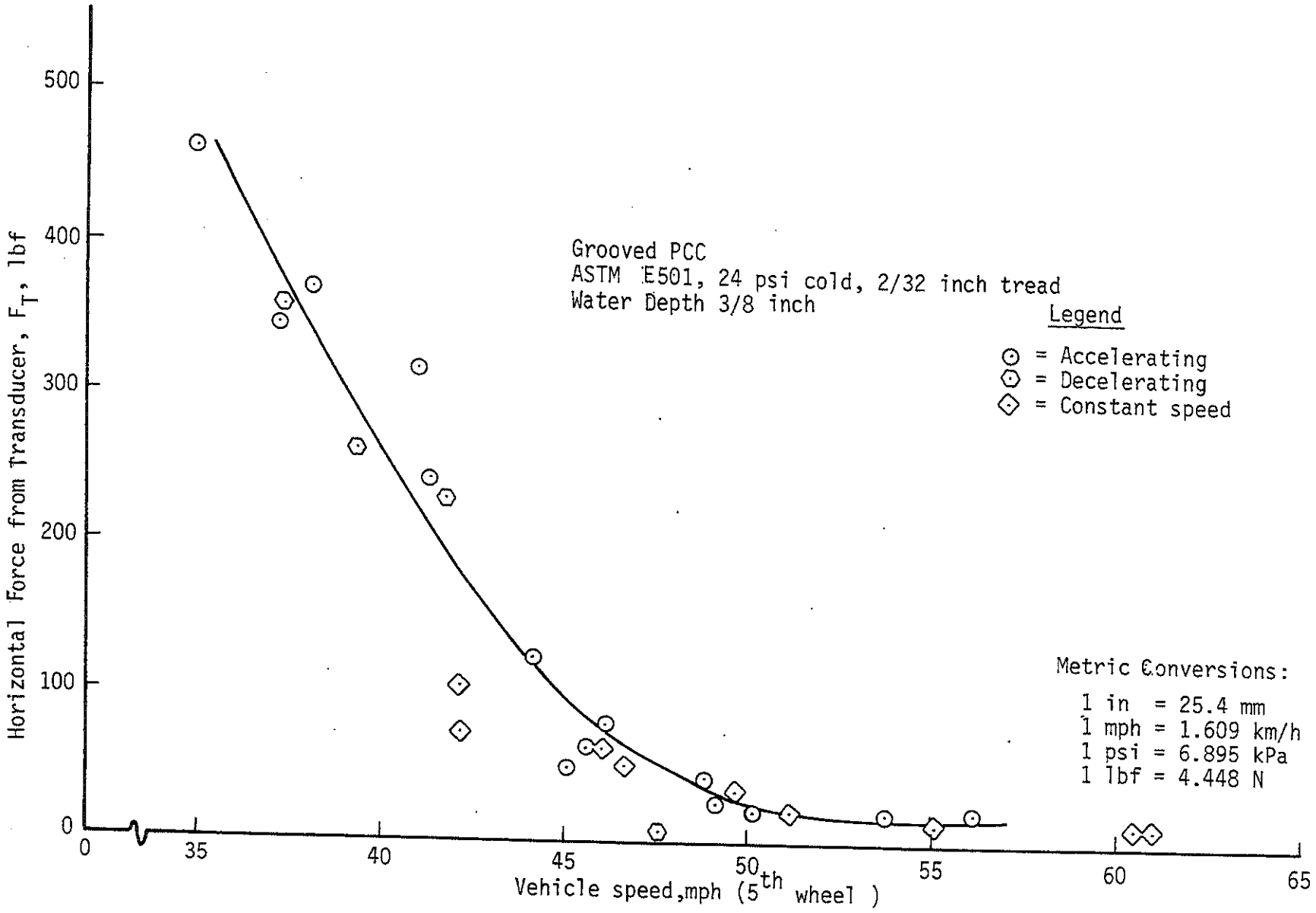

Figure 28. Horizontal force from torque transducer vs. 5th wheel vehicle speed

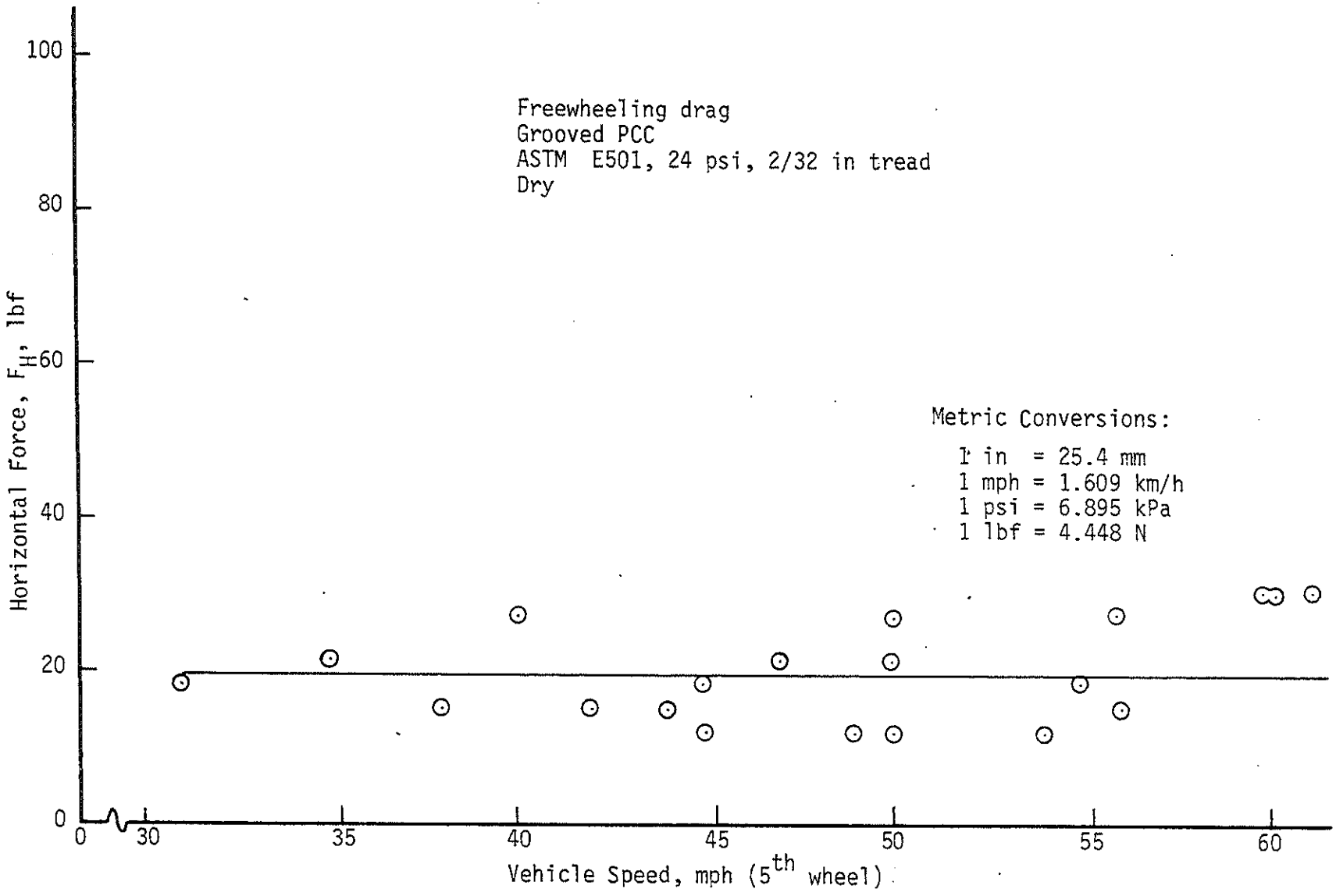

Figure 29. Freewheeling horizontal force vs. 5th wheel speed

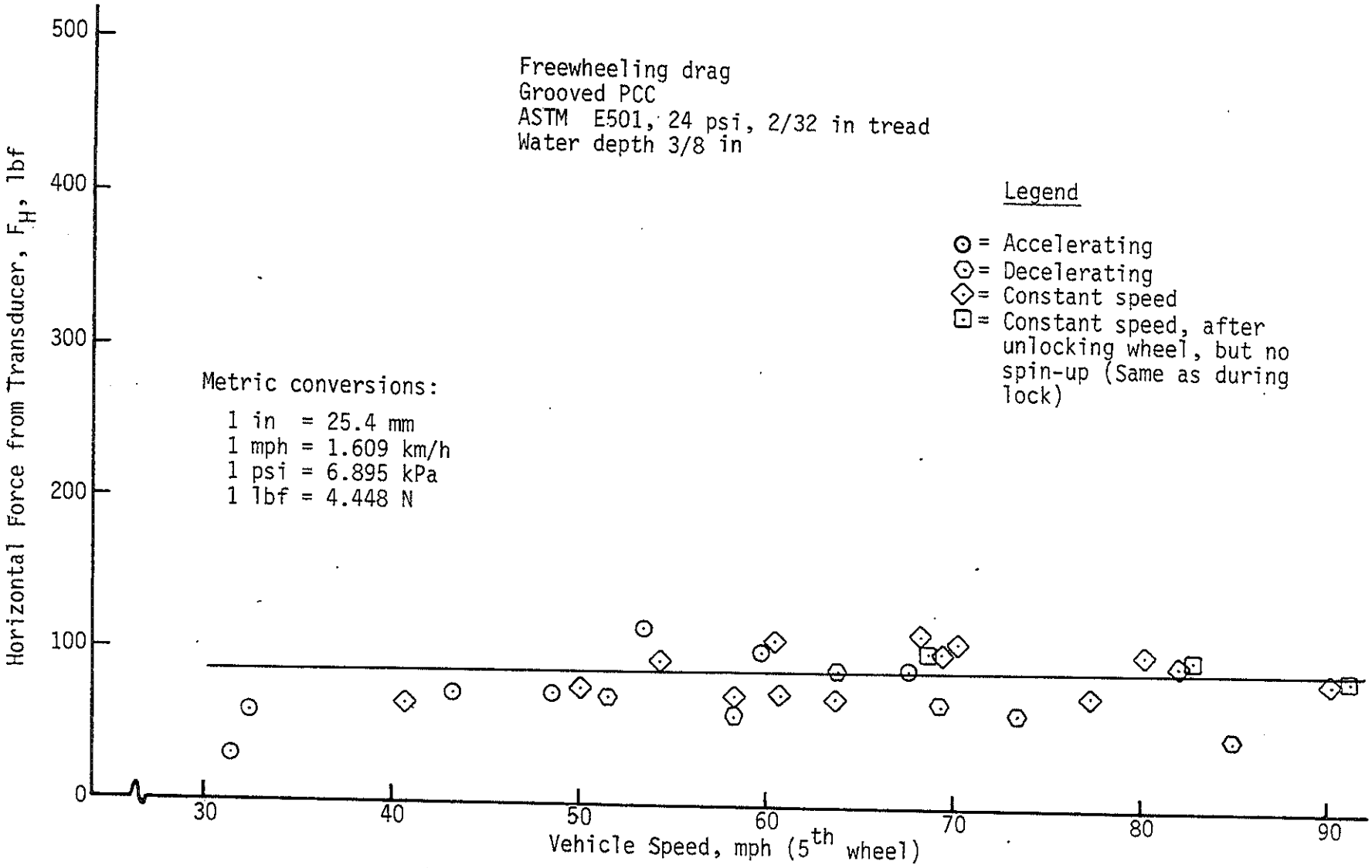

Figure 30. Freewheeling horizontal force vs. 5th wheel speed

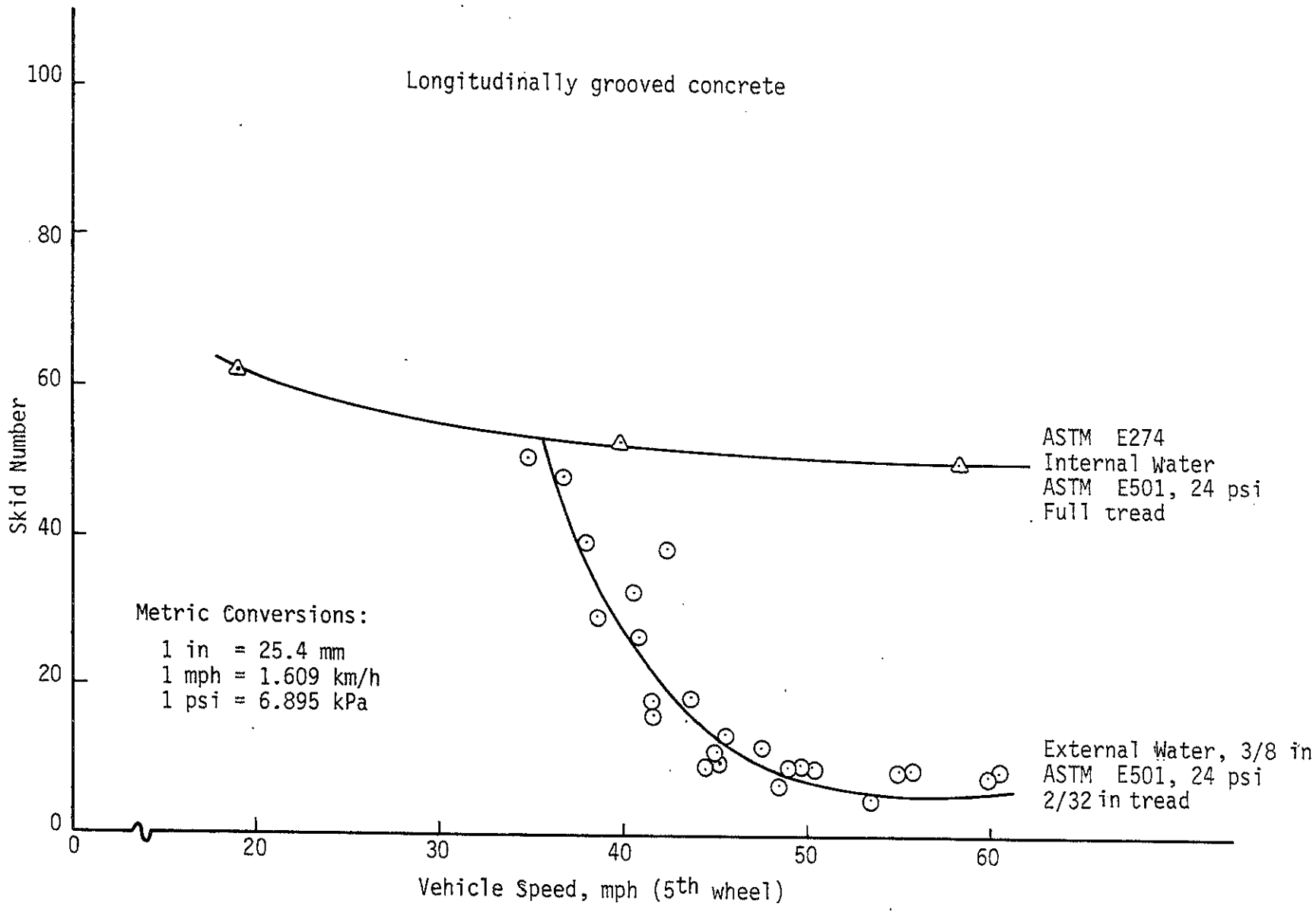

Figure 31. Locked-wheel skid number vs. speed

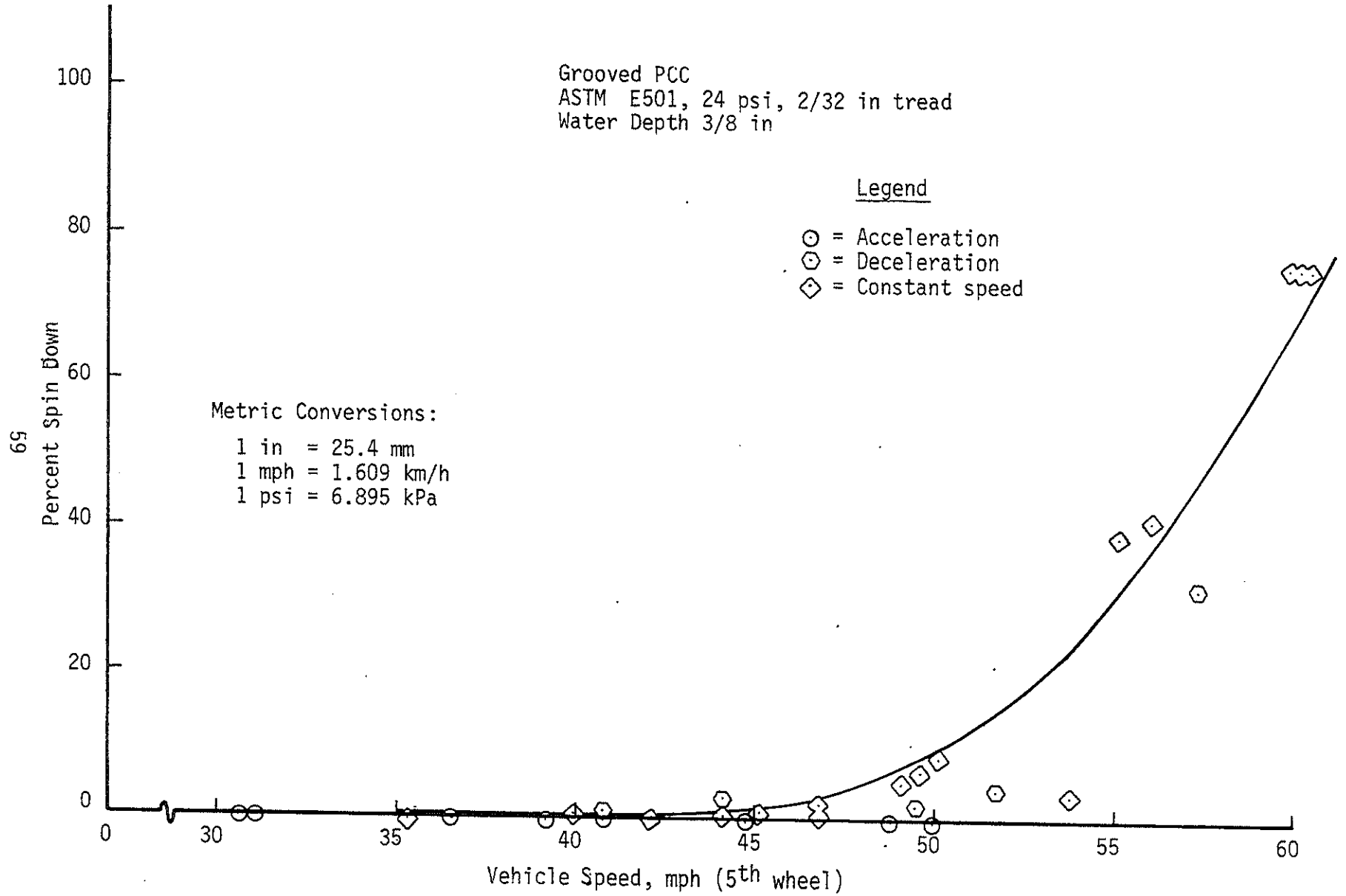

Figure 32. Percent spin down vs. vehicle speed

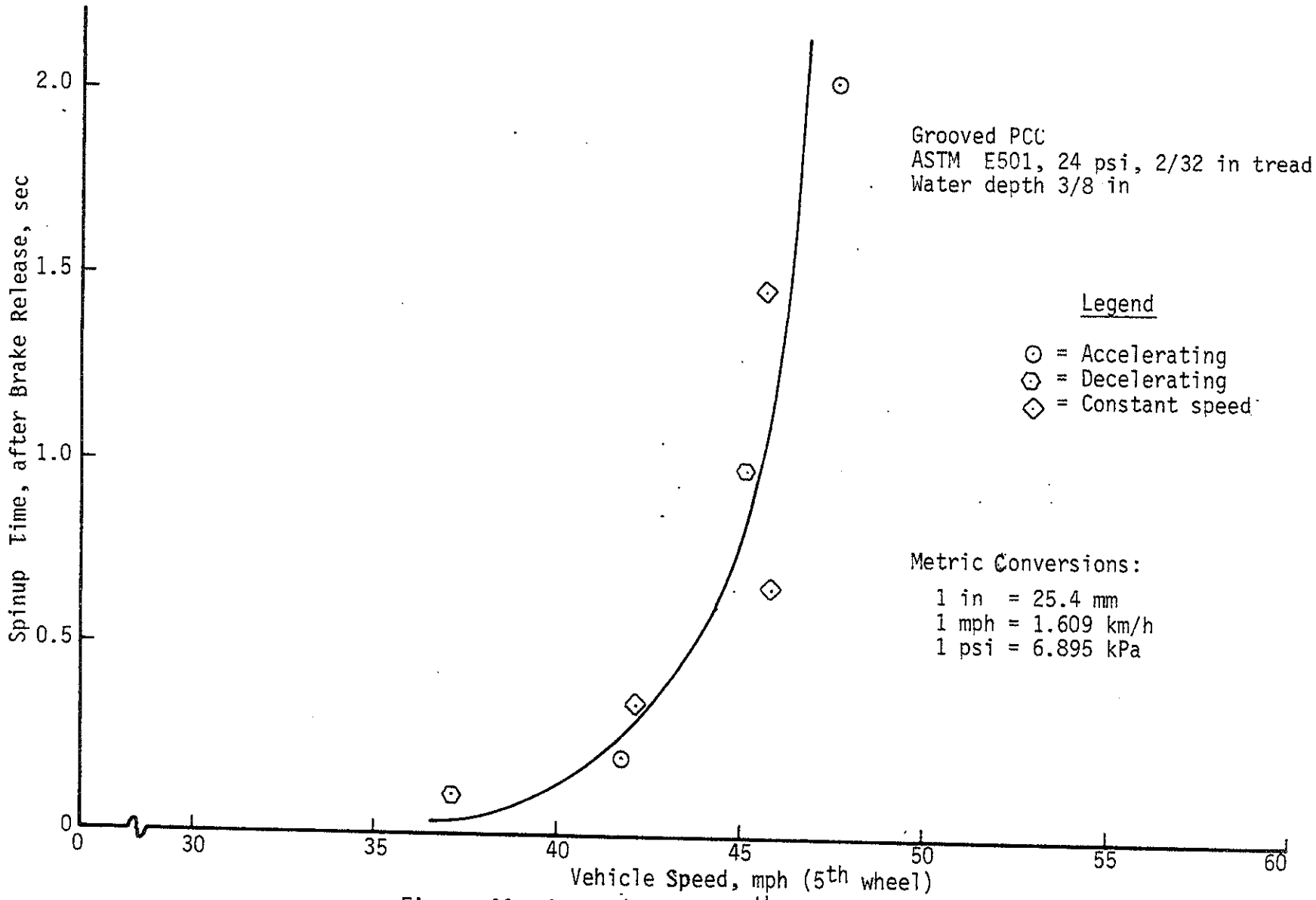

Figure 33. Spinup time vs. 5th wheel vehicle speed

To illustrate the order of magnitude of the hazard potential due to such water and tread depth, simple computations of stopping distance were made using the internal and external skid number curves of Figure 31. It is not justifiable to assume that a vehicle would have corresponding frictional forces available. However, as a first approximation it is instructive. Figure 34 is a plot of the theoretical increase in stopping distance (as a function of speed) that would result with 3/8 in (9.5 mm) water and 2/32 in (1.6 mm) tread depth as opposed to 0.02 in (0.5 mm) pavement wetting a full tread depth tire. Above the "full hydroplaning" point, the stopping distance increases dramatically with increased speed.

Summary of Observations from Preliminary Tests on Grooved PCC

1. Under the stated test conditions, the freewheeling drag force is approximately constant at 90 lbf (400 N), and is the same as the locked-wheel horizontal force above the apparent "full hydroplaning" speed of 46 mph (74 km/h). If asymmetrically distributed, this could cause unstabilizing yaw forces on a vehicle. (See Figure 30.)
2. Except for hydrodynamic drag, the locked-wheel horizontal force is the same as the internal water horizontal force at about 35 mph (56 km/h) and below, but it decreases smoothly to a minimum at "loss of contact" where it equals the freewheeling drag at 46 mph (74 km/h) and above. (See Figure 31.)
3. Performance spindown and spinup times as functions of speed diverge from the horizontal at about 46 mph (74 km/h), but spinup time does so more dramatically and may be a more sensitive indicator of full loss of physical contact.
4. In 3/8 in (9.5 mm) water, the force from the torque transducer is consistently about 70 lbf (311 N) lower than the force from the horizontal force transducer when calibrated to read the same statically on the force plate. This can be accounted for by a shift of the "center of effort" forward about 4/5 in (20 mm) when in the 3/8 in (9.5 mm) deep water.
5. No significant difference was apparent in any case if the data were taken at different speeds while accelerating or decelerating, or at different speeds using discrete constant-speed runs. This allows a significant saving in number of individual runs and time consumed.
6. The freewheeling drag force is about 20 lbf (89 N) dry or with internal water, about 90 lbf (400 N) in 3/8 in (9.5 mm) water and about 90 lbf (400 N) either locked or freewheeling above full hydroplaning speed.
7. No quantitative estimate of the effect on cornering was made, but one can assume that at full hydroplaning the directional control would be inadequate or nil.

Tests on Asphalt Surfaces

Figures 35 through 42 compare the results on the two surfaces with the various combinations of tire inflation pressure and water depth. The ordinate is labeled "Skid Number", but technically the lower pair of curves are the

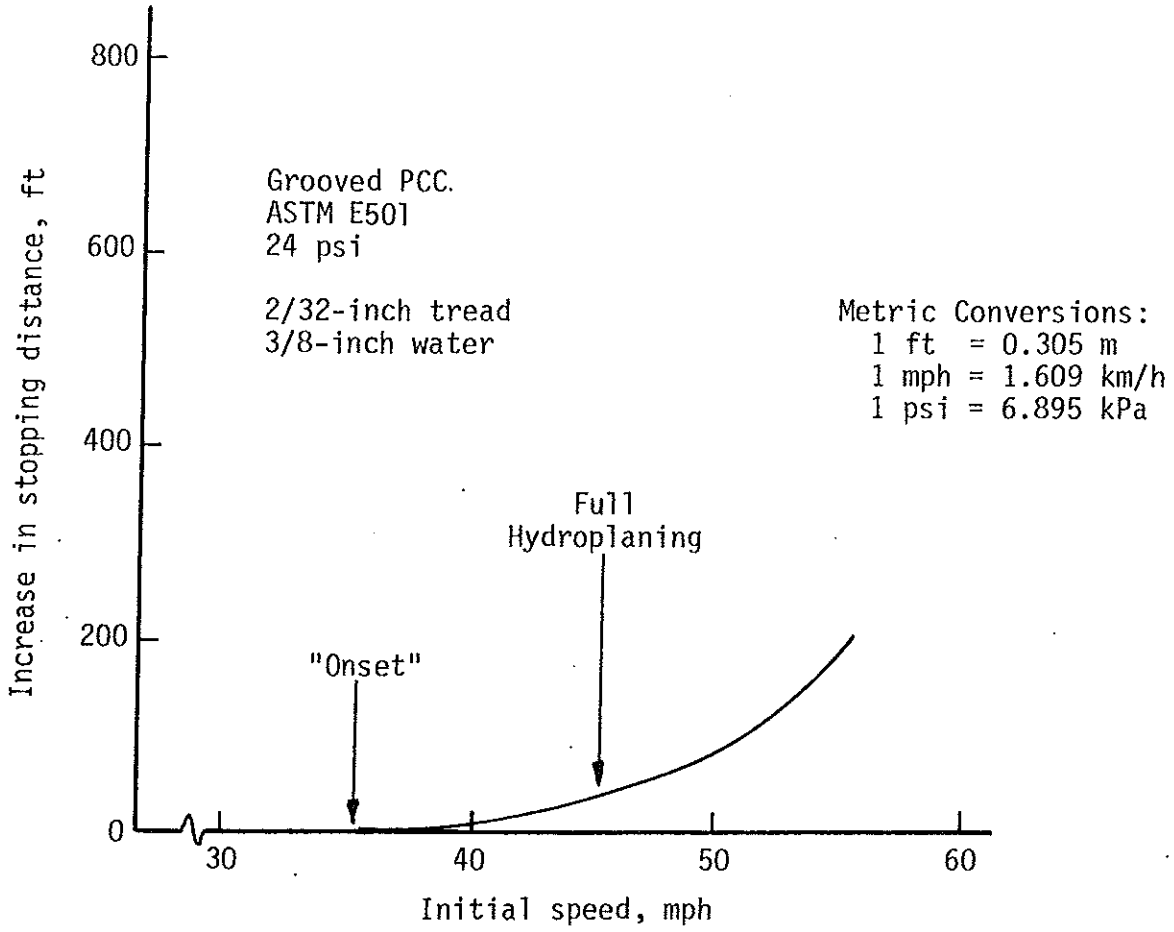

Figure 34. Increase in stopping distance due to hydroplaning

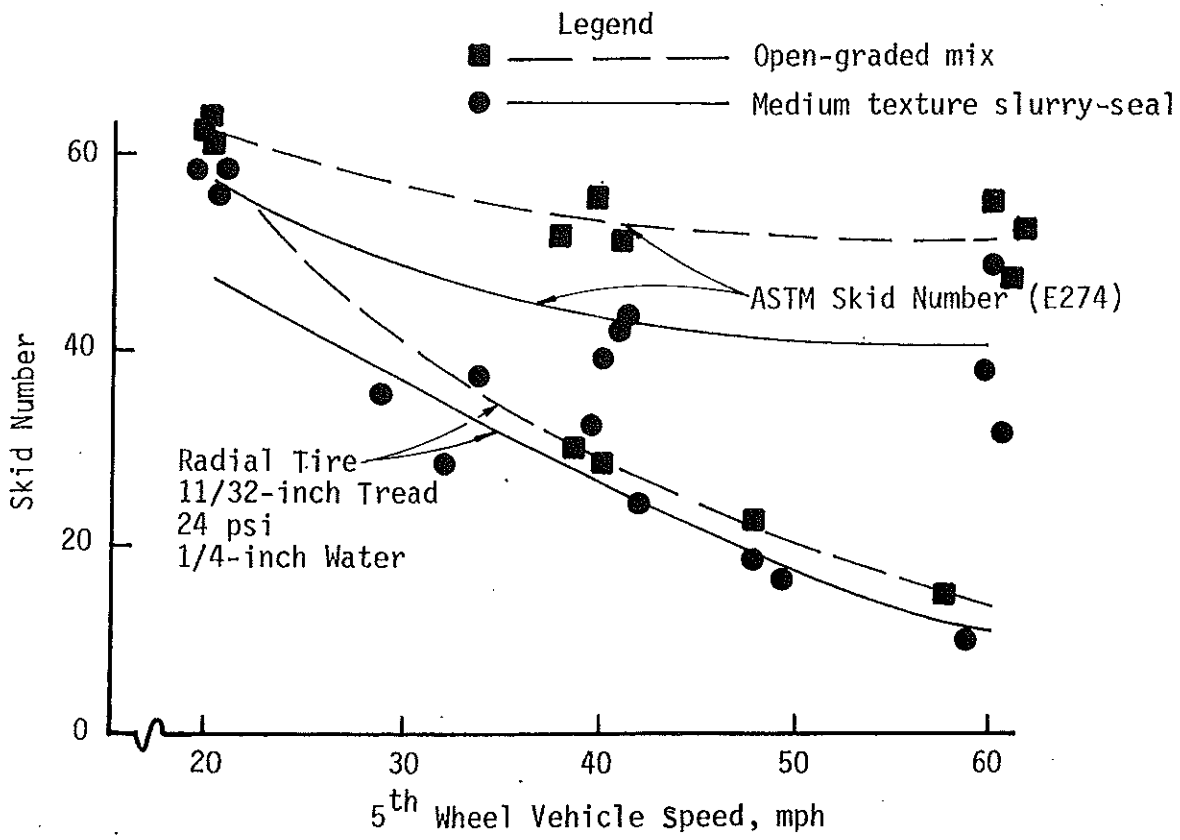

Figure 35. Comparison of open-graded and slurry-seal surfaces

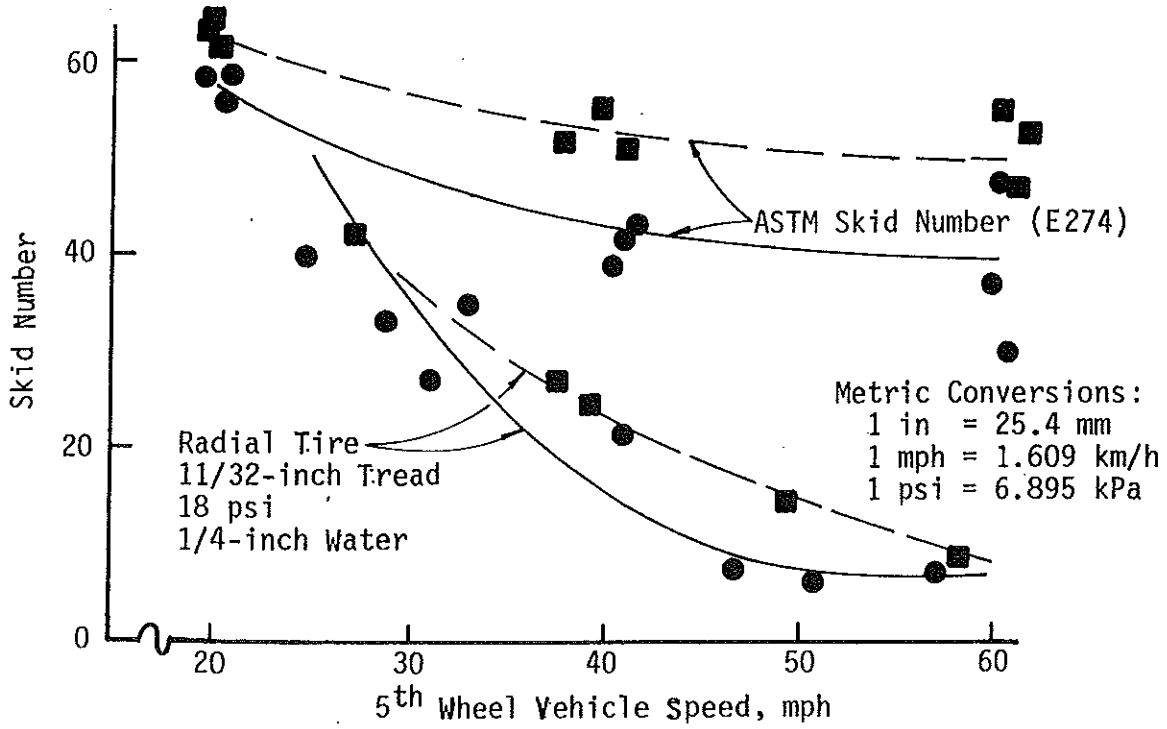

Figure 36. Comparison of open-graded and slurry-seal surfaces

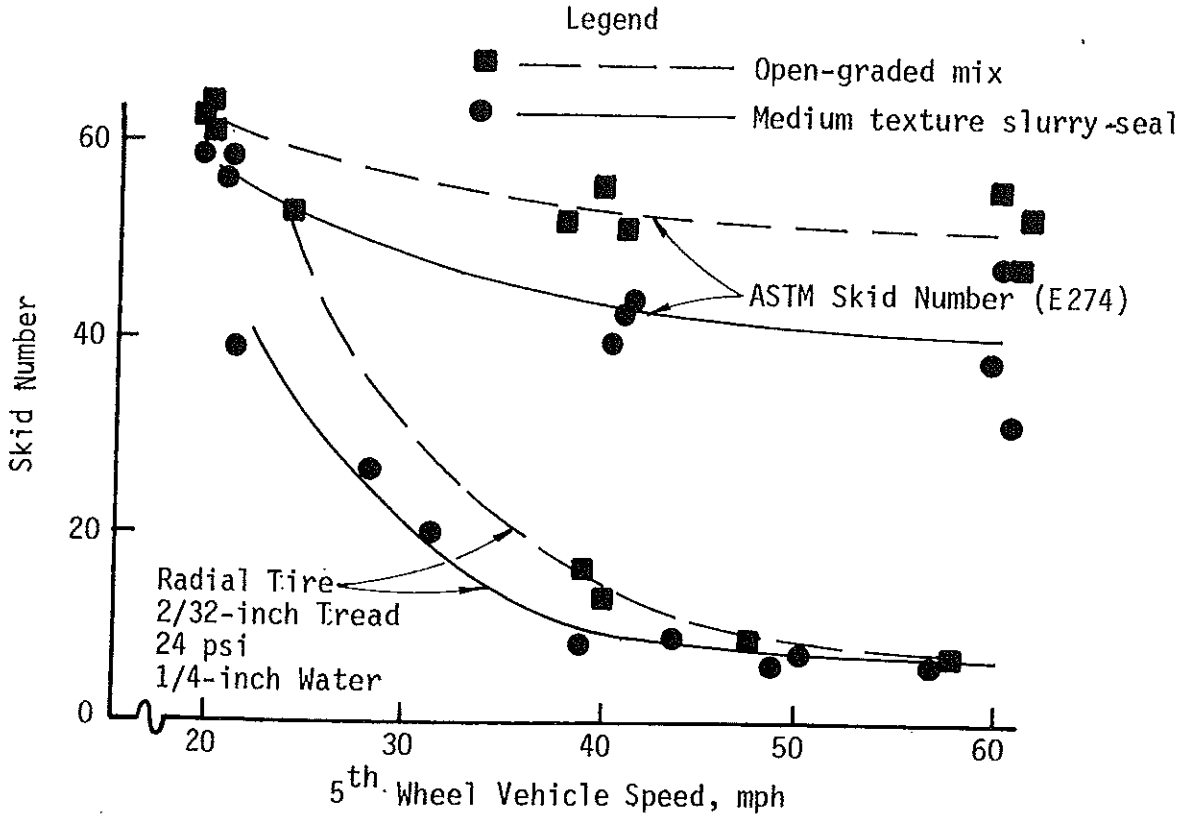

Figure 37. Comparison of open-graded and slurry-seal surfaces

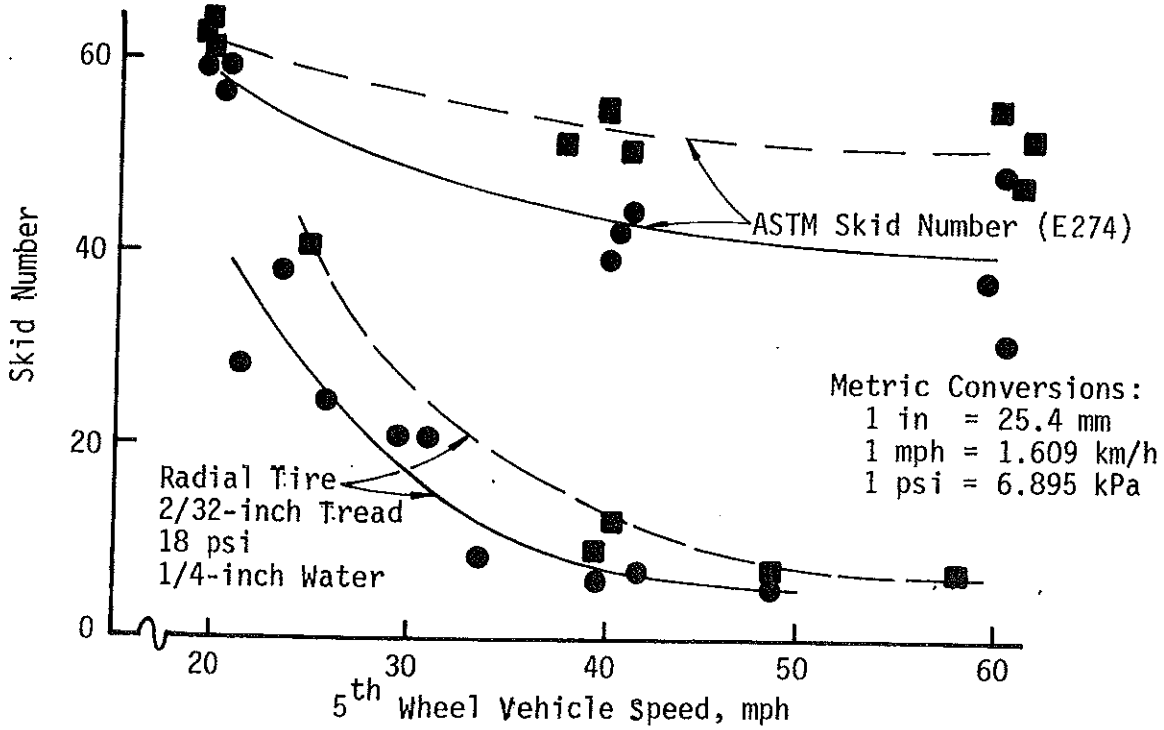

Figure 38. Comparison of open-graded and slurry-seal surfaces

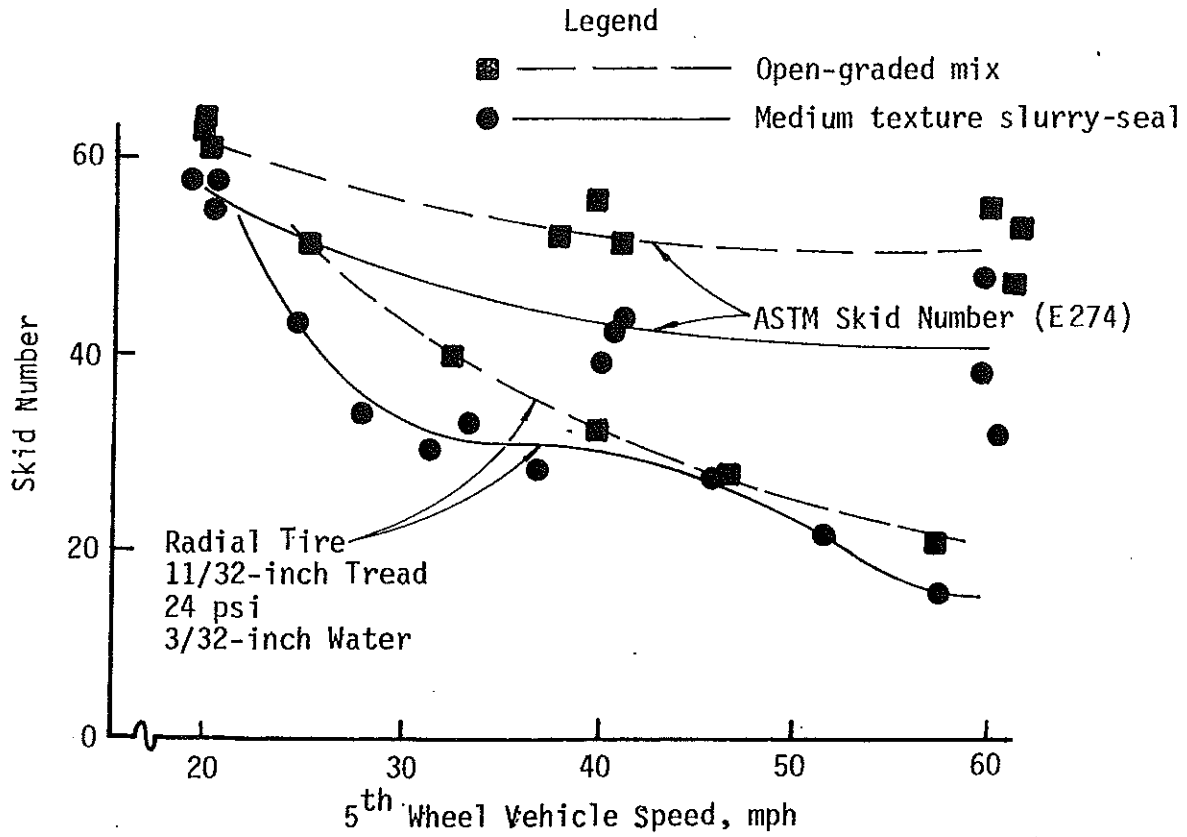

Figure 39. Comparison of open-graded and slurry-seal surfaces

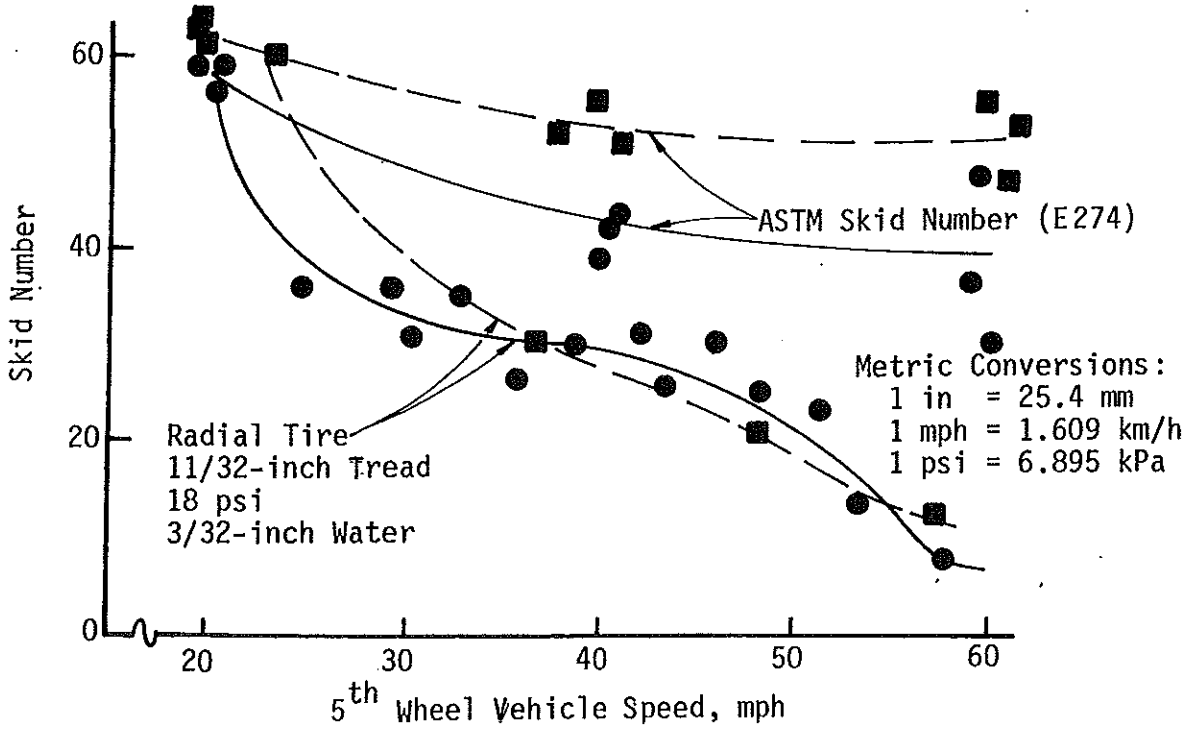

Figure 40. Comparison of open-graded and slurry-seal surfaces

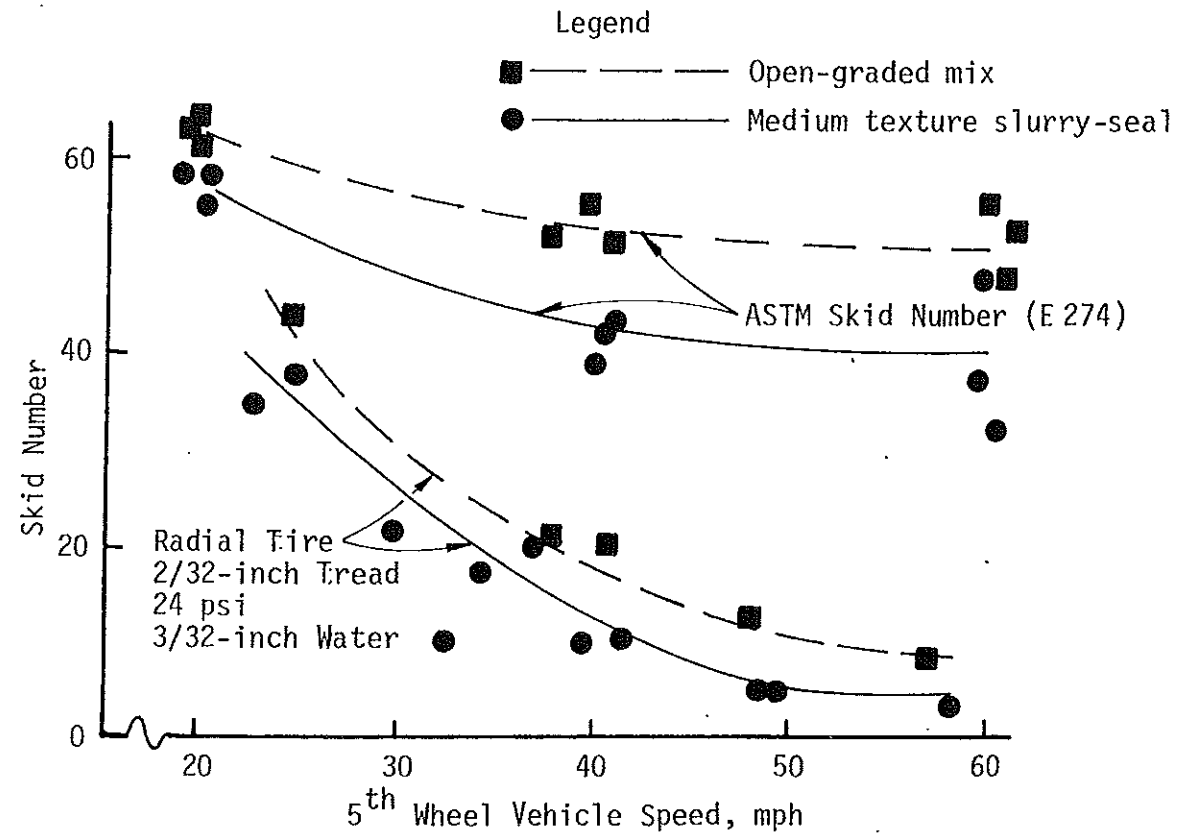

Figure 41. Comparison of open-graded and slurry-seal surfaces

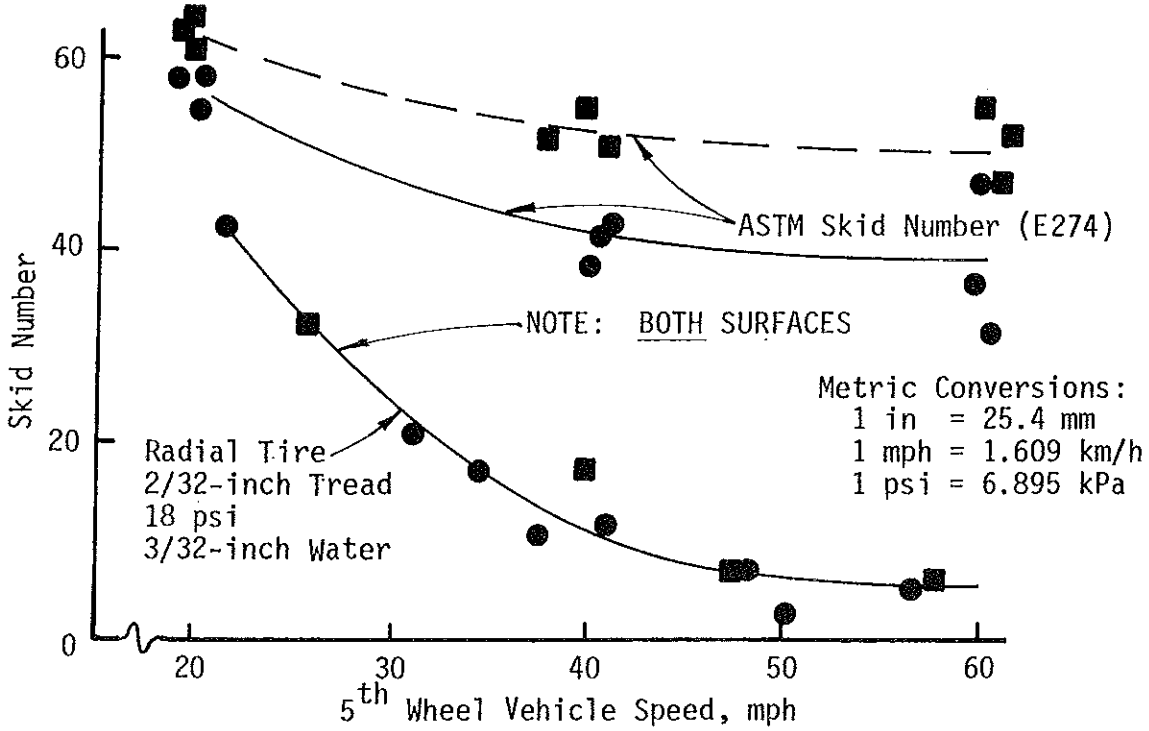

Figure 42. Comparison of open-graded and slurry-seal surfaces

results under the stated conditions using the FR 78-14 steel-belted radial tire which is an example of the current real-world tire population.

Again, we see that with water covering the asperities, loss of traction begins to occur as low as 20 mph (32 km/h). The open-graded surface has a higher skid number and in general provides more traction under "partial hydroplaning" conditions. Usually, as would be expected, the curves tend to converge at higher speeds where loss of pavement contact occurs.

On the slurry-seal surface, spindown is first detected at the point where the "SN" curve flattens out. The spindown on the open-graded mix was only detected in two cases, and then only briefly. This surface was not as smooth as the slurry seal, and the tire may have been contacting enough high points to prevent spindown in the freewheeling condition but not in contact firmly enough to generate higher traction at the higher speeds.

It is noted that on the slurry-seal surface with low water depth, full tread and both tire pressures, there is a "plateau" in the available friction in the speed midrange; and then at higher speeds it continues to drop (see Figures 39 and 40). The two graphs are from data taken on different days, and the phenomenon only occurred under these specific conditions for both water depths. Other combinations of conditions were used on those days without this behavior being observed. This effect cannot be fully explained from the data gathered, but it is suspected that under these specific test conditions an unusual hydrodynamic situation is created at certain speeds.

On the slurry-seal surface which usually produced a definite spindown, comparisons were made of the speeds at which some spindown began to appear. With both water depths, the lowest speed at which spindown began was, expectedly, with low tire pressure and low tread depth; and the highest initial spindown speed occurred with high tread and high pressure.

Although the differences are not always pronounced, within the range of test conditions used, the speed at which spindown began to occur decreased with increasing water depth; and the largest decrease due to increasing water depth occurred with the combination of higher tire pressure and lower tread depth. Similarly, the largest change in "onset" speed due to changing tire pressure occurred with low tread depth and low water depth. Finally, the largest change due to decreasing tread depth occurred with the combination of higher tire pressure and greater water depth.

Comparing the effects of changing tire pressure alone and water depth alone showed no clear-cut and consistent variation in traction. However, the higher tire tread depth seemed to consistently improve traction, at least at some speed, under all conditions.

Figures 43 through 50 represent data using the ASTM E501 tire only. Again, the upper curves represent ASTM E274 skid numbers on the two surfaces. The lower pair of curves compare results on the two pavements using various combinations of tire pressure, tread depth and average water depth.

The results using external water were much more consistent with the ASTM tire in all combinations of conditions. Usually, the open-graded surface provides significantly more traction at lower speeds, with the traction converging at hydroplaning speeds. (Actually, at these speeds the "traction" is primarily hydrodynamic drag.)

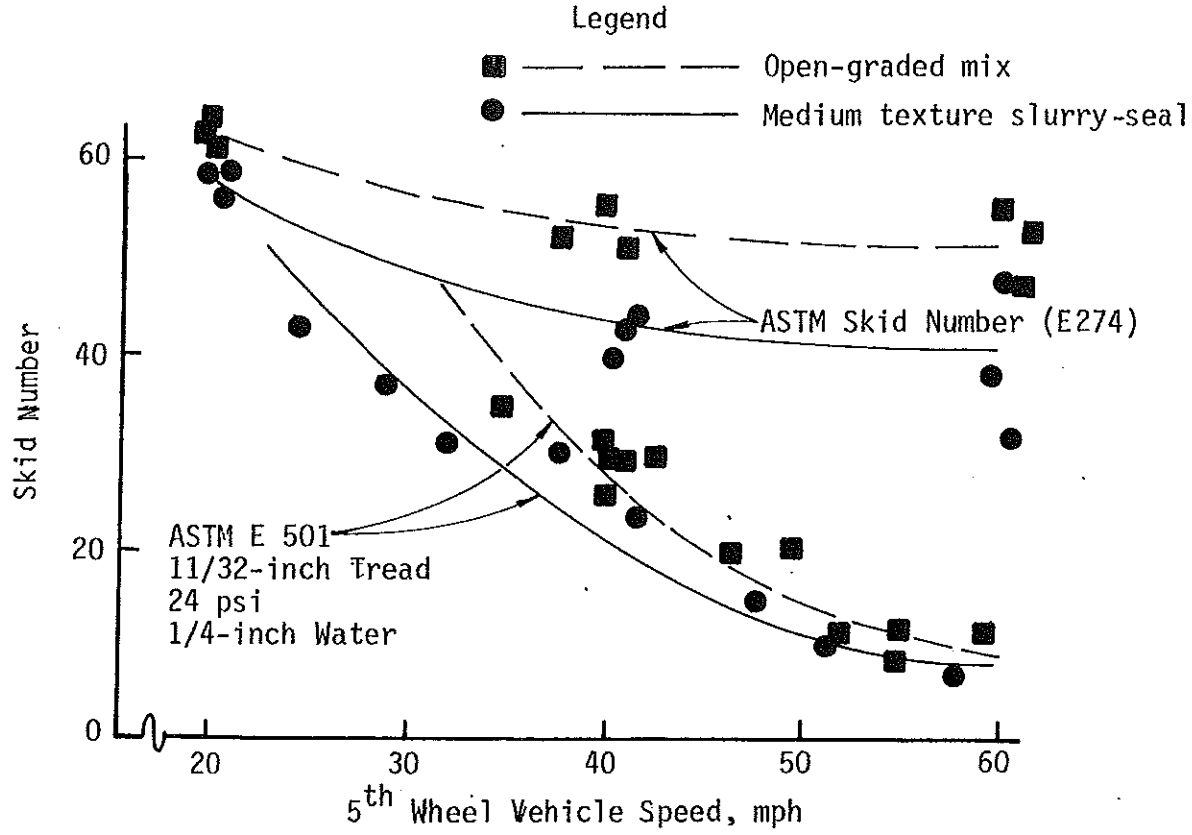

Figure 43. Comparison of open-graded and slurry-seal surfaces

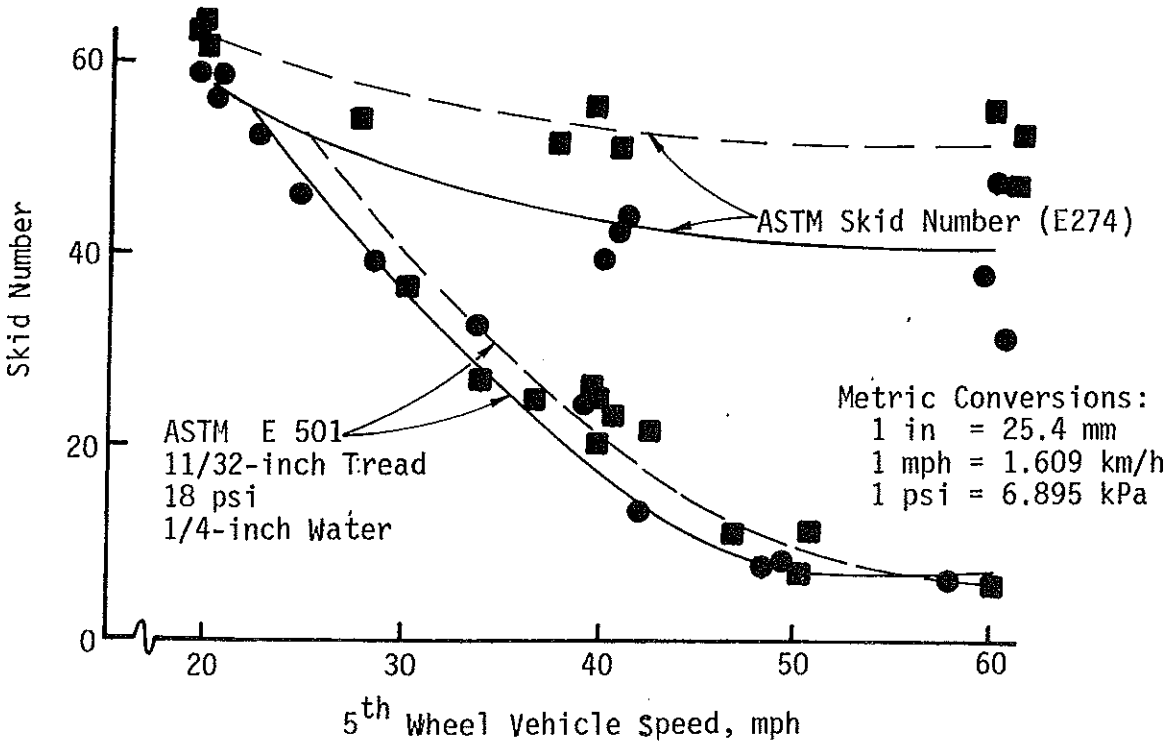

Figure 44. Comparison of open-graded and slurry-seal surfaces

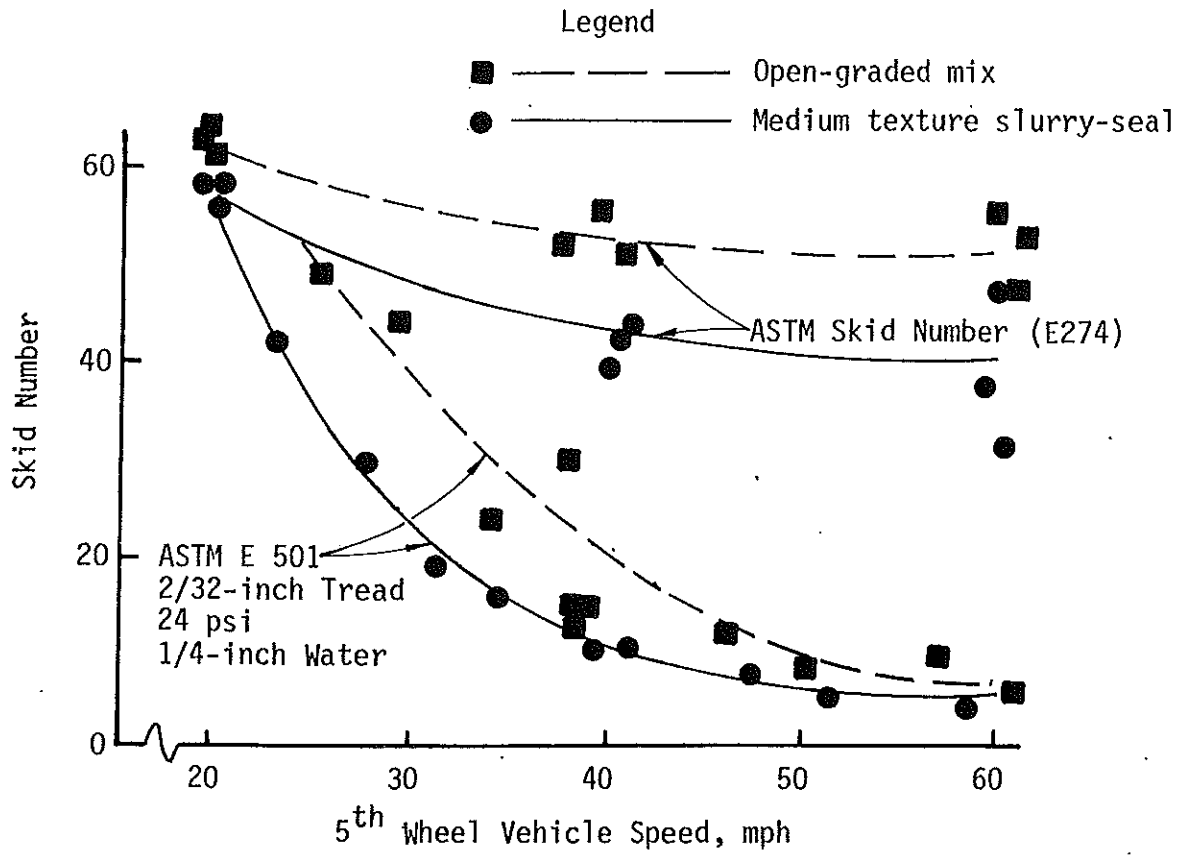

Figure 45. Comparison of open-graded and slurry-seal surfaces

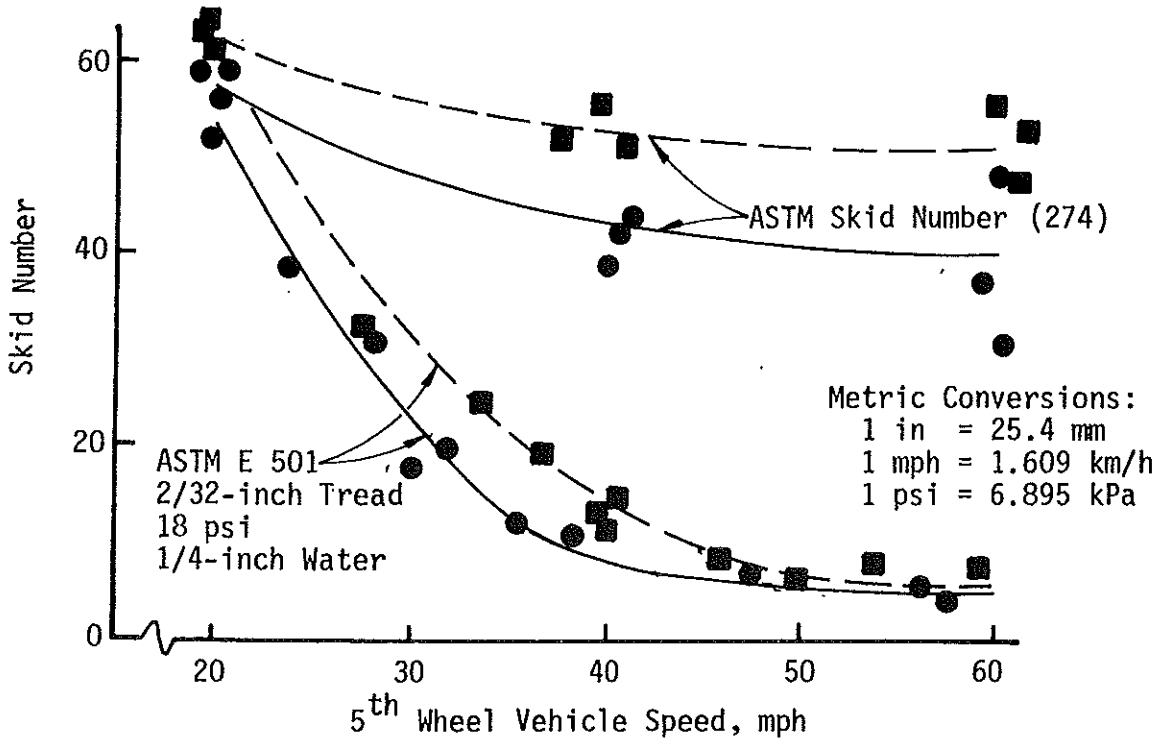

Figure 46. Comparison of open-graded and slurry-seal surfaces

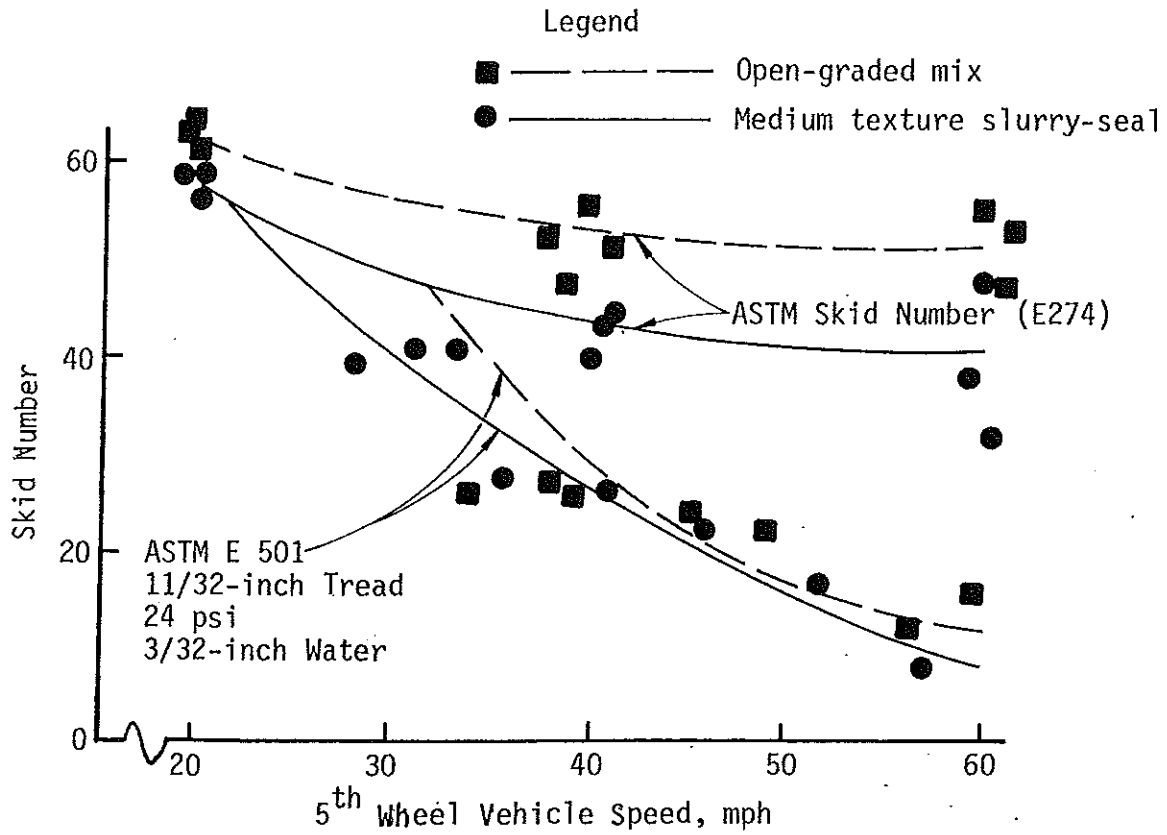

Figure 47. Comparison of open-graded and slurry-seal surfaces

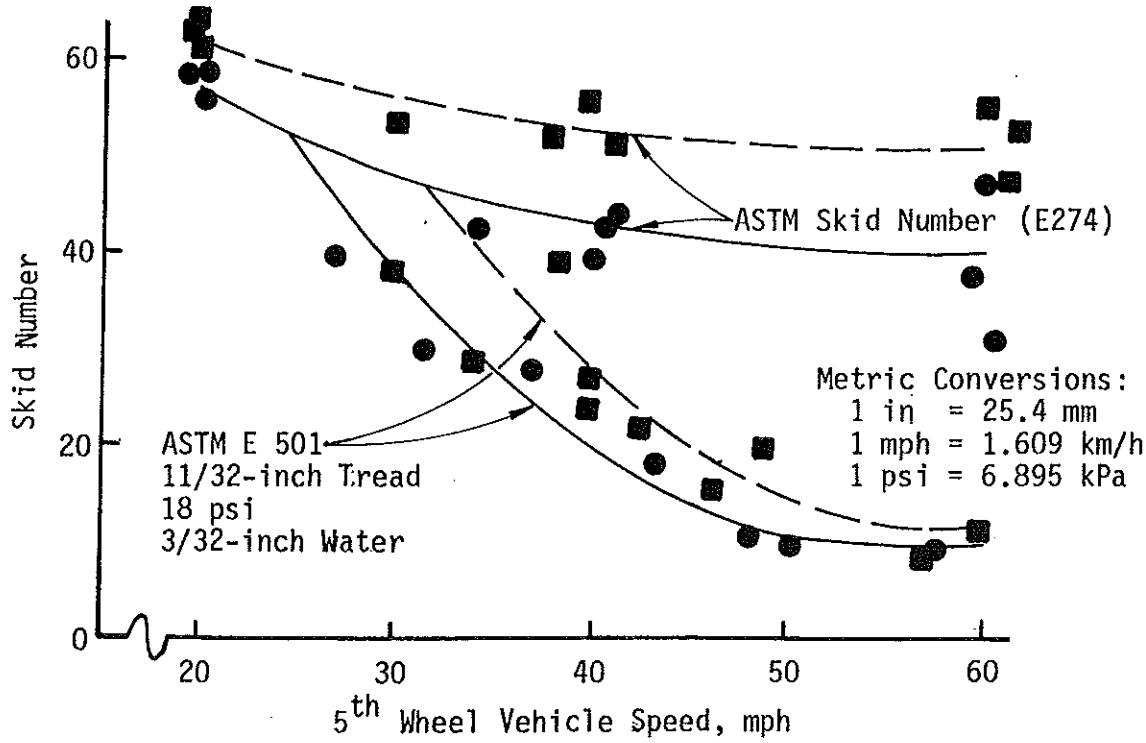

Figure 48. Comparison of open-graded and slurry-seal surfaces

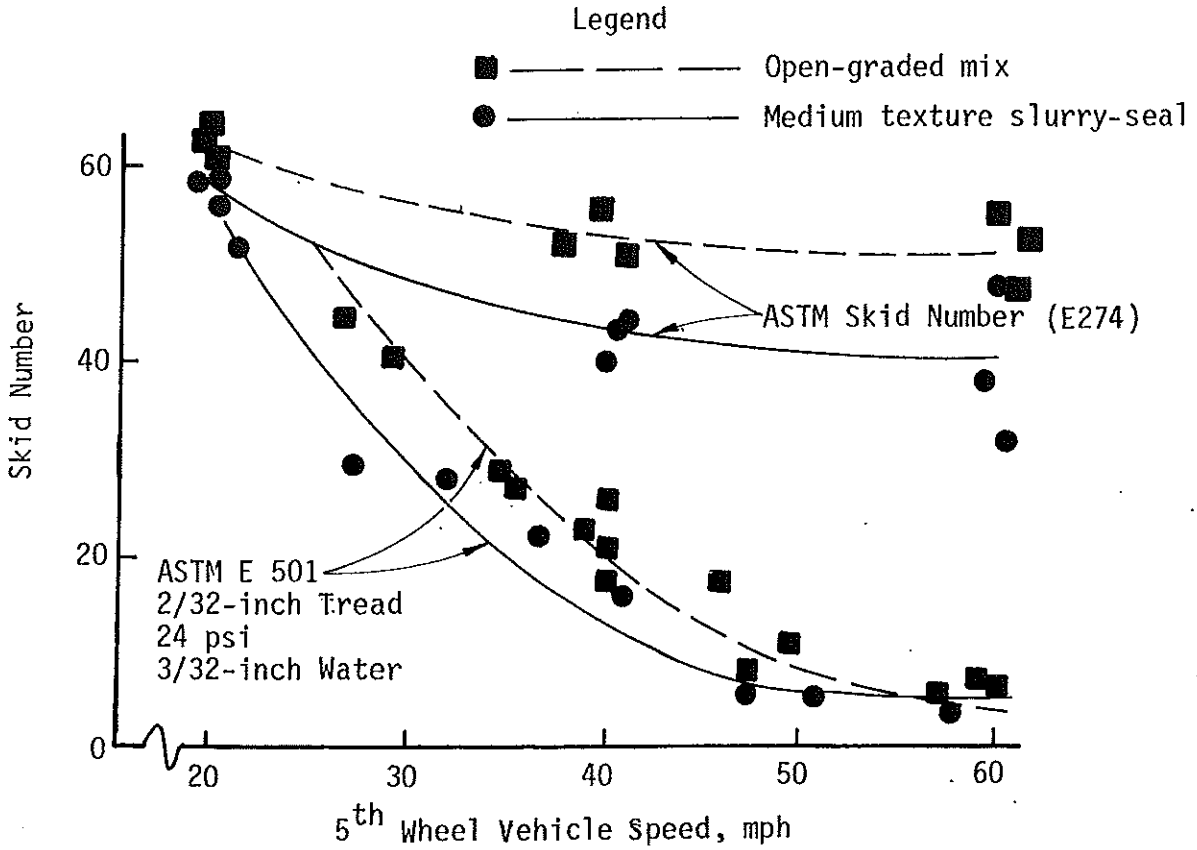

Figure 49. Comparison of open-graded and slurry-seal surfaces

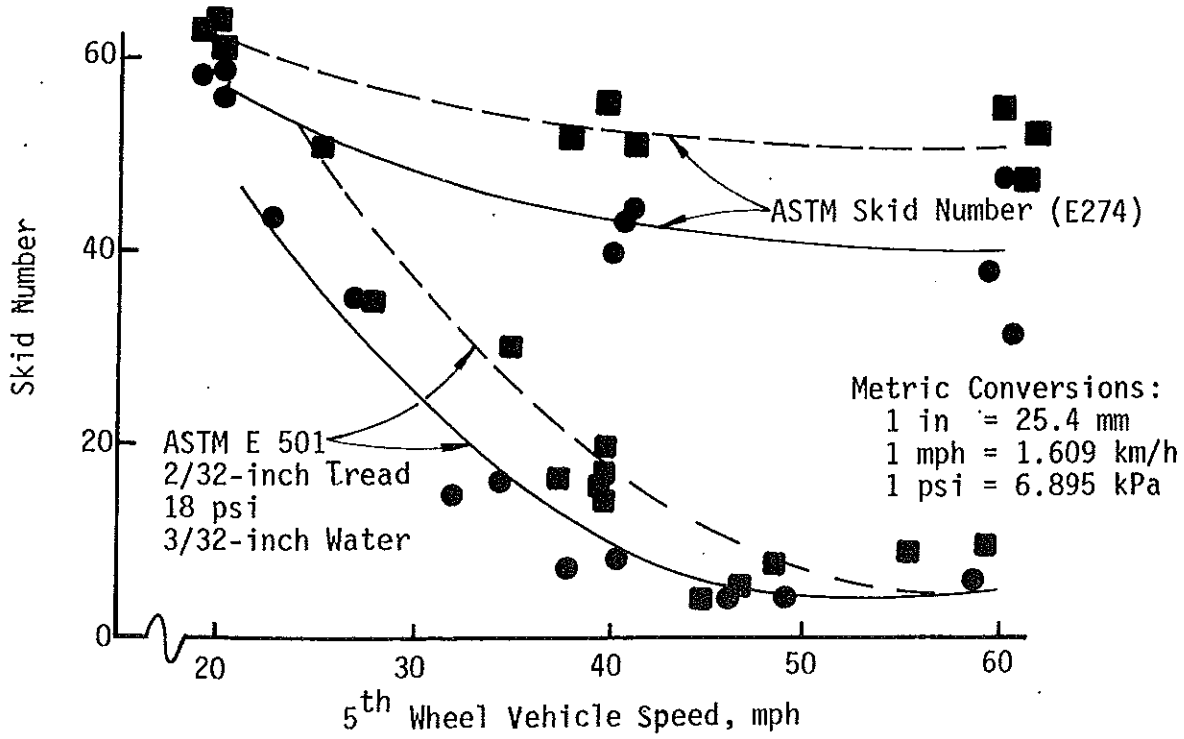

Figure 50. Comparison of open-graded and slurry-seal surfaces

The effect of tire inflation pressure with other parameters constant is not consistent, and only in some cases does increased pressure significantly improve the traction on one or the other of the surfaces. The same can be said of the effect of water depth in the range used. However, increased tread depth, for a given inflation and water depth, causes a significant improvement on both surfaces except at higher speeds where full hydroplaning occurs.

Tests in Free-Standing Pools ("Puddles")

A limited number of freewheeling runs was made on the PCC surface through puddles of standing water following a rain. The puddles ranged from 30 to 50 ft (9 to 15 m) in length and 1/4 to 1-3/4 in (6 to 44 mm) in depth. Figures 51 through 53 indicate the water depths in the three puddles used (note lane designations). Figure 54 is a photograph looking down lane 2 in the direction the runs were made with puddle "A" in the foreground.

The test wheel was centered between the two vehicle tracks. The effect of tow vehicle wake on the water condition at the test wheel is unknown, so these tests can only be interpreted qualitatively in regard to water depths. Figure 55 shows the system entering a puddle while Figure 56 indicates a "worst case" condition in which the trailer is virtually obscured by spray from the tow vehicle and that generated by the trailer itself.

The data were not highly reproducible because of some water loss or redistribution following a run, and possibly because of the short duration of the interaction. Table 11 shows the peak forces and percentage spindowns with speed. The tire used was the FR 78-14 radial, with 2/32 and 11/32 in (1.6 and 8.7 mm) tread depths and 24 psi (165 kPa) inflation pressure.

Some spindown began between 40 and 45 mph (64 and 72 km/h) in all cases except puddle C, lane 2, with 11/32 in (8.7 mm) tread depth. In this case it occurs between 45 and 49 mph (72 and 79 km/h).

Peak longitudinal drag forces were as high as 300 lbf (1.3 kN) on the test wheel. If this force were applied to one vehicle front wheel only, it could have a significant vehicle destabilizing effect. Such an event might occur in a situation in which water collects along a curb due to cross slope and/or poor drainage.

To obtain a rough estimate of the potential real-world effect, some simple computations were made using a hypothetical vehicle weighing about 3400 lbs (1544 kg), with a wheel base of 112 in (2.84 m) and track width of 60 in (1.52 m). A conventional American automobile of this size would have a vertical load on each front wheel of about 1000 lbf (4448 N). If we neglect inertial effects and compute the produced torque about the center of gravity (not necessarily where it should be computed), then it would take a corresponding opposing torque to counteract it to maintain directional stability.

Now, if we assume that the opposite front wheel were on pavement that is only wetted, with no standing water, this opposing torque could be applied by developing a cornering slip angle by steering. Data for a typical tire on wetted pavement indicate that a front wheel slip angle of about 2 degrees would be required. For a typical steer ratio of about twenty-to-one, this would require a steering wheel correction of about 40 degrees. If such a correction

Table 11. Peak forces and percent spindown traversing "puddles" shown in Figures 51 through 56

Puddle	Lane	Tread Depth(in)	Speed (mph)	Peak Force (lbf)	Spindown Peak %
A	2	2/32	45	160	11
	2	"	45	110	7
	2	"	45	140	8
	2	"	40	110	0
	2	11/32	50	140	8
	2	"	45	100	0
B	1	2/32	50	330	22
	2	"	48	150	10
	2	"	40	150	0
	2	"	45	180	5
	2	"	40	150	0
	2	11/32	50	150	6
	2	"	45	200	4
	2	"	39	240	0
	2	"	44	250	0
	2	"	49	300	7
C	1	2/32	48	290	17
	2	"	48	70	4
	2	"	40	160	0
	2	"	45	180	5
	2	"	40	150	0
	2	11/32	49	70	5
	2	"	45	140	0
	1	"	39	180	0
	1	"	43	210	0
	1	"	49	290	5

Metric conversion: 1 in = 25.4 mm 1 mph = 1.609 km/h
1 lbf = 4.448 N

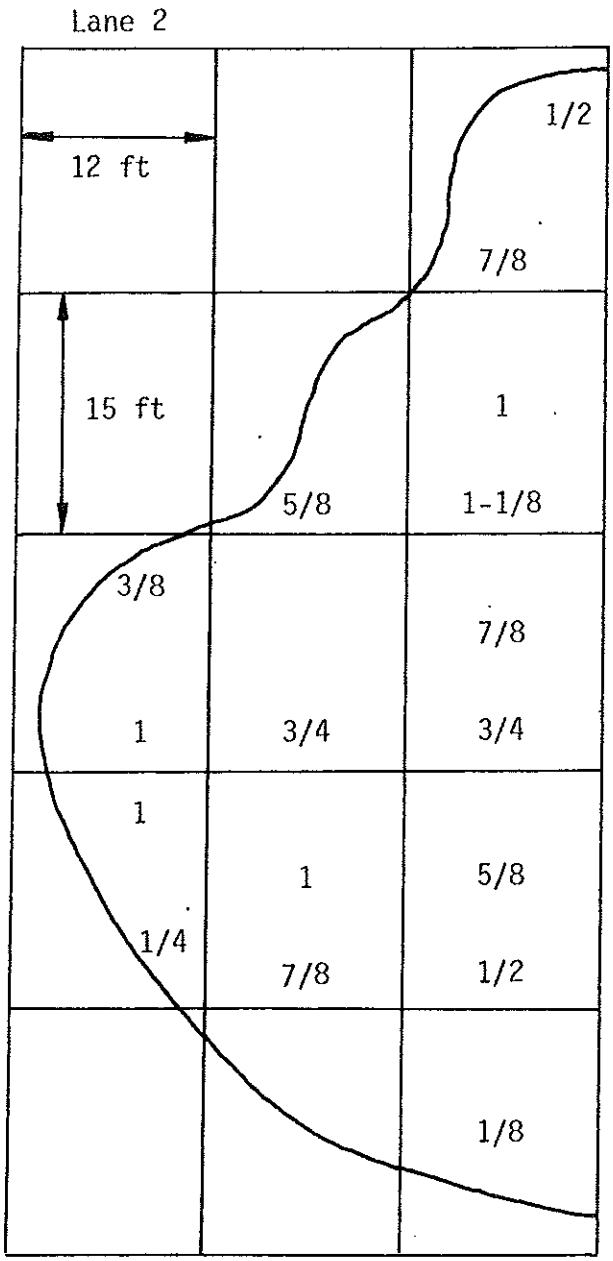

Figure 51. Puddle "A" (Water depths in inches)

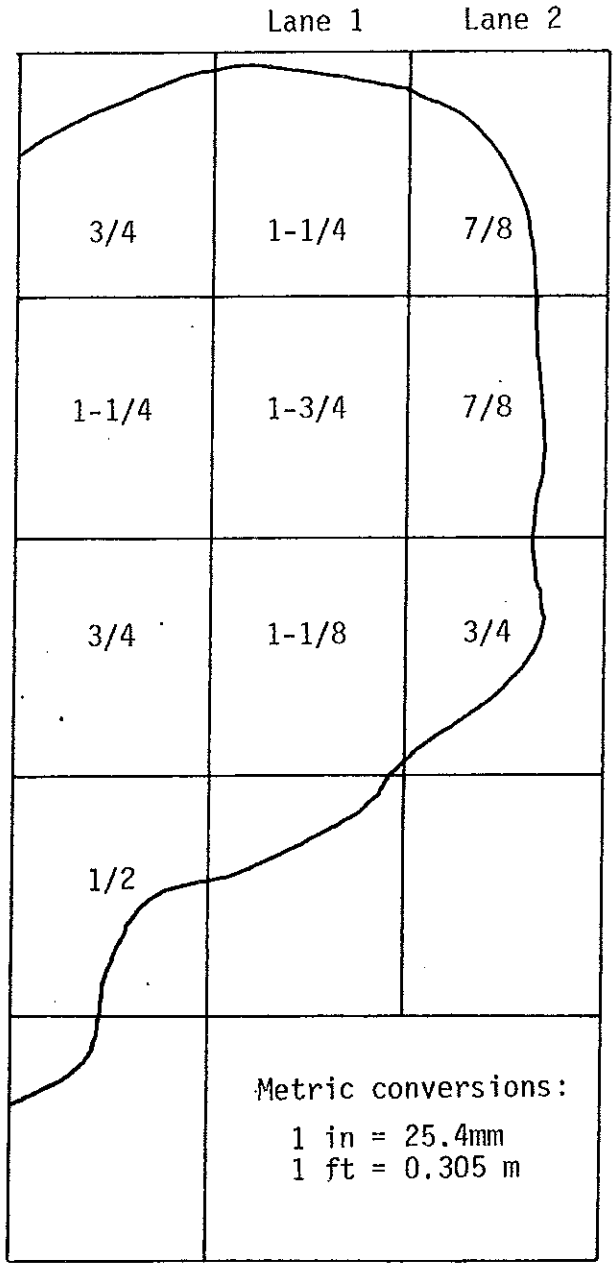

Figure 52. Puddle "B" (Water depths in inches)

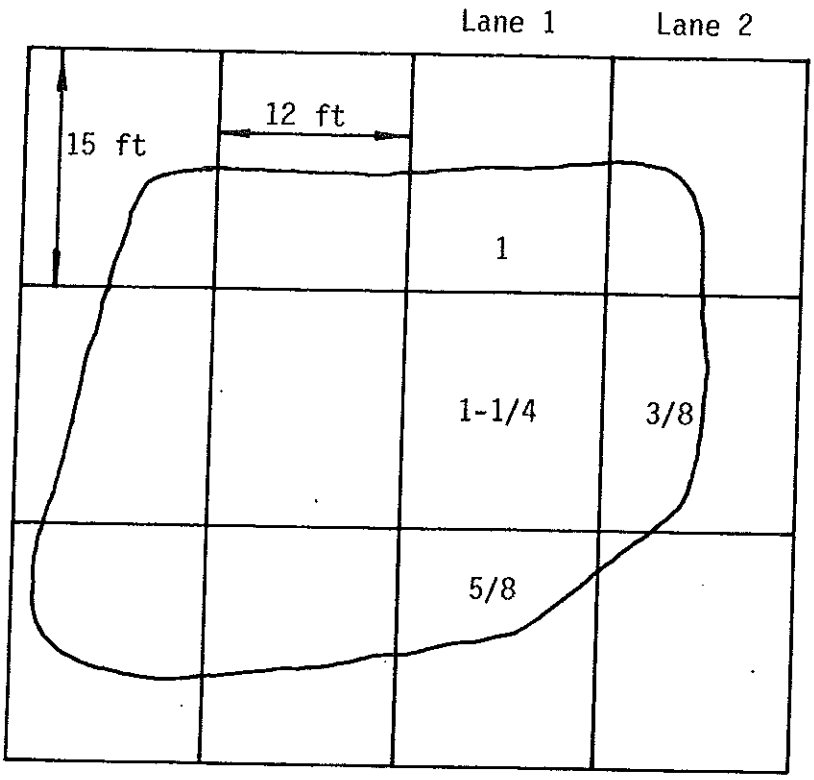

Metric Conversions:
1 in = 25.4 mm
1 ft = 0.305 m

Figure 53. Puddle "C" (Water depths in inches)

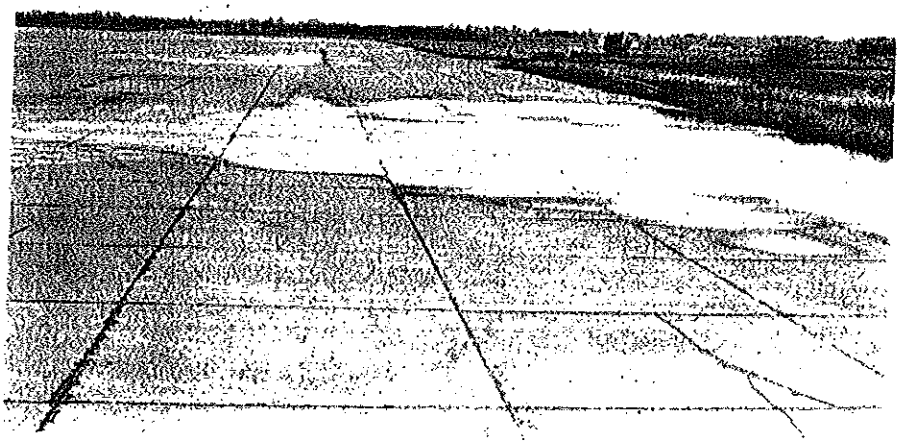

Figure 54. "Puddles" used in short-duration hydroplaning tests

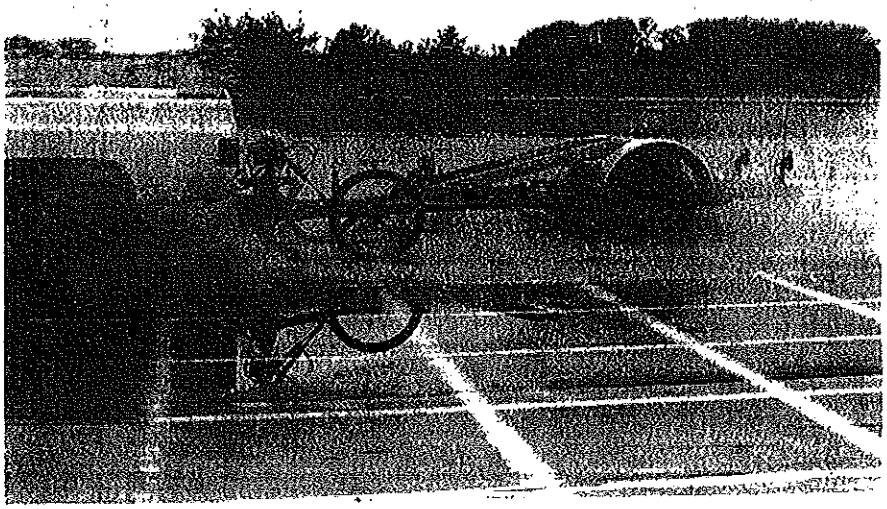

Figure 55. Tow-vehicle splash and wake entering puddle "B"

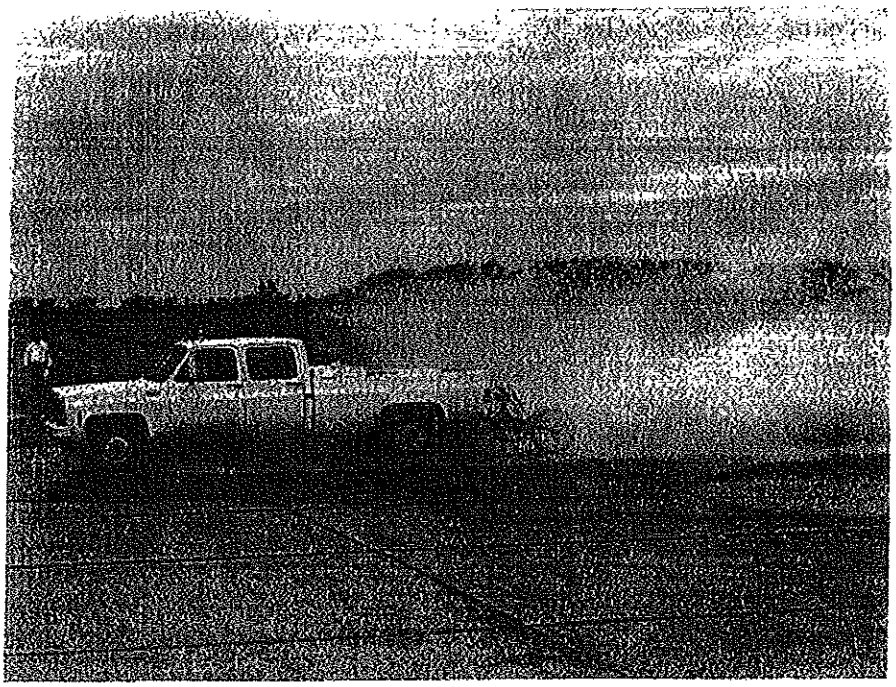

Figure 56. Severe splash and spray (some self-generated) obscuring test trailer

were made, and full pavement contact were suddenly regained, it could cause a divergence toward the opposing traffic lane before appropriate steering recorrection is possible.

In the case in which both front wheels are fully hydroplaning, but unequal water depths exist laterally, the unequal drag forces would cause yaw instability with little or no corrective steering capability available to the driver.

Irrespective of the accuracy or validity of the example computation, there is little doubt that the kind of drag forces generated by the positive water depths distributed unevenly could pose a hazard to unwary drivers.

General Observations

The following observations are based on results of the tests described in this chapter. Obviously, sweeping generalizations cannot be made based on a small fraction of the possible real-world conditions. However, valuable insights can be obtained, and areas that seem to be worthy of further consideration can be identified from tests under controlled conditions.

1. Under all test conditions, the open-graded pavement provided as much, and usually more, traction than the asphalt slurry seal except at full hydroplaning where they are about equal. The open-graded surface has the added advantage of reducing the probability of positive water depths in the field.
2. With the externally applied water, the difference in traction between the two pavements was more dependent on test conditions (water depth, tire pressure and tread depth) for the radial tire than for the ASTM E501 tire. That is, the ASTM tire produced a more consistent "ranking" of the pavements with various combinations of tire parameters and water depths.
3. With positive water depths, traction becomes less than that for ASTM E274 skid numbers as low as 20 mph (32 km/h). It continued to decrease, usually smoothly, until full loss of contact with the pavement occurs at which speed it becomes equal to the freewheeling hydrodynamic drag.
4. Within the boundaries of the test matrix, tread depth usually has a greater influence on traction and hydroplaning speed than either tire inflation pressure or positive water depth with all other factors equal.
5. Spinup, after unlocking the test wheel, may be a more positive and precise indicator of full hydroplaning speed than spindown. Complex hydrodynamic forces are involved, with subtle interactions of tire, tread, inflation pressure, water depth, pavement and speed.
6. No consistent difference in skid numbers was observed whether accelerating slowly, decelerating slowly or at constant speed. This permits data points to be taken at several speeds during one variable-speed run, which in turn results in savings of time and cost.
7. Loss of contact can occur between 40 and 45 mph (64 and 72 km/h) in "puddles" of about 1 in (25 mm) maximum depth and about 30 ft (9 m)

in length. In addition, horizontal drag forces up to 300 lbf (1.3 kN) were observed. Three-eighths in (9.5 mm) of water can produce about 90 lbf (400 N) of drag. If unevenly distributed laterally by pooling against a curb or raised shoulder on a cross slope, these forces could cause hazardous directional instability.

CHAPTER IV

MINIMIZING HYDROPLANING CONDITIONS ON PORTLAND CEMENT CONCRETE SURFACES

Introduction

The parameters involved in this study that influence hydroplaning of portland cement concrete (PCC) surfaces fall into two groups: those associated with the pavement surface and those associated with the vehicle.

This phase of the study involved two separate investigations. The first was to determine the validity of the predicted water depth for drainage lengths to 48 ft (14.6 m) (simulating multilane facilities now in use), and the other was to examine skid resistance and cornering slip on textured PCC surfaces. In the following sections, the results from each investigation are presented.

Water Depth Prediction on PCC Surfaces for Multilane Roadways

To determine the applicability of predictive equations for water depth as a function of relatively long drainage lengths, water depths were determined for drainage lengths, L, up to 48 ft (14.6 m) under rainfall intensities up to 2 in/h (5 mm/h) and slopes up to 8 percent. Textures included the longitudinal burlap drag (TXD = 0.035 in (0.9 mm)), the longitudinal tines (1/4 in (6 mm)) clear distance - TXD = 0.068 in (1.7 mm), and the transverse tines (1/4 in (6 mm)) clear distance - TXD = 0.059 in (1.5 mm). A total of 117 water depth measurements was taken, and subsequently added to 218 measurements taken some five years ago (11). All measurements were statistically analyzed in the computer using a two-step regression technique to develop the best fit equations for the data. Neglecting texture type and texture direction, the resulting overall equation for concrete surfaces is

$$WD = [0.2031\ (TXD)^{1.325}(L)^{0.443}(I)^{0.598}(1/S)^{0.355}] - TXD \qquad \text{Eq (15)*}$$

Correlation coefficient squared, $R^2 = 0.68$

WD = water depth from the top of the asperities - in (1 in = 25.4 mm)
I = rainfall intensity - in/h (1 in/h = 25 mm/h)
S = slope of pavement - ft/ft (m/m) or percent
TXD = texture depth (sand patch) - in (1 in = 25.4 mm)
L = drainage length - ft (1 ft = 0.305 mm)

To compare this overall equation with the previously developed equation for water depth which was presented in the first report on this study (9); i.e.,

$$WD = [0.00338\ (TXD)^{0.11}(L)^{0.43}(I)^{0.59}(1/S)^{0.42}] - TXD \qquad \text{Eq (16)}$$

$R^2 = 0.81$

a hypothetical example was selected (I = 3.00 in/h) (76.2 mm/h), slope = 0.5 percent, and TXD = 0.045 in (1.1 mm). Figure 57 shows the relationship between the equation and the old equation reported in the interim report (9).

---

*Equation 15 is an independent derivation of Equation 16 with new coefficients. Differences between the two are not significant; therefore, Equation 16 is recommended for all computations of water depth.

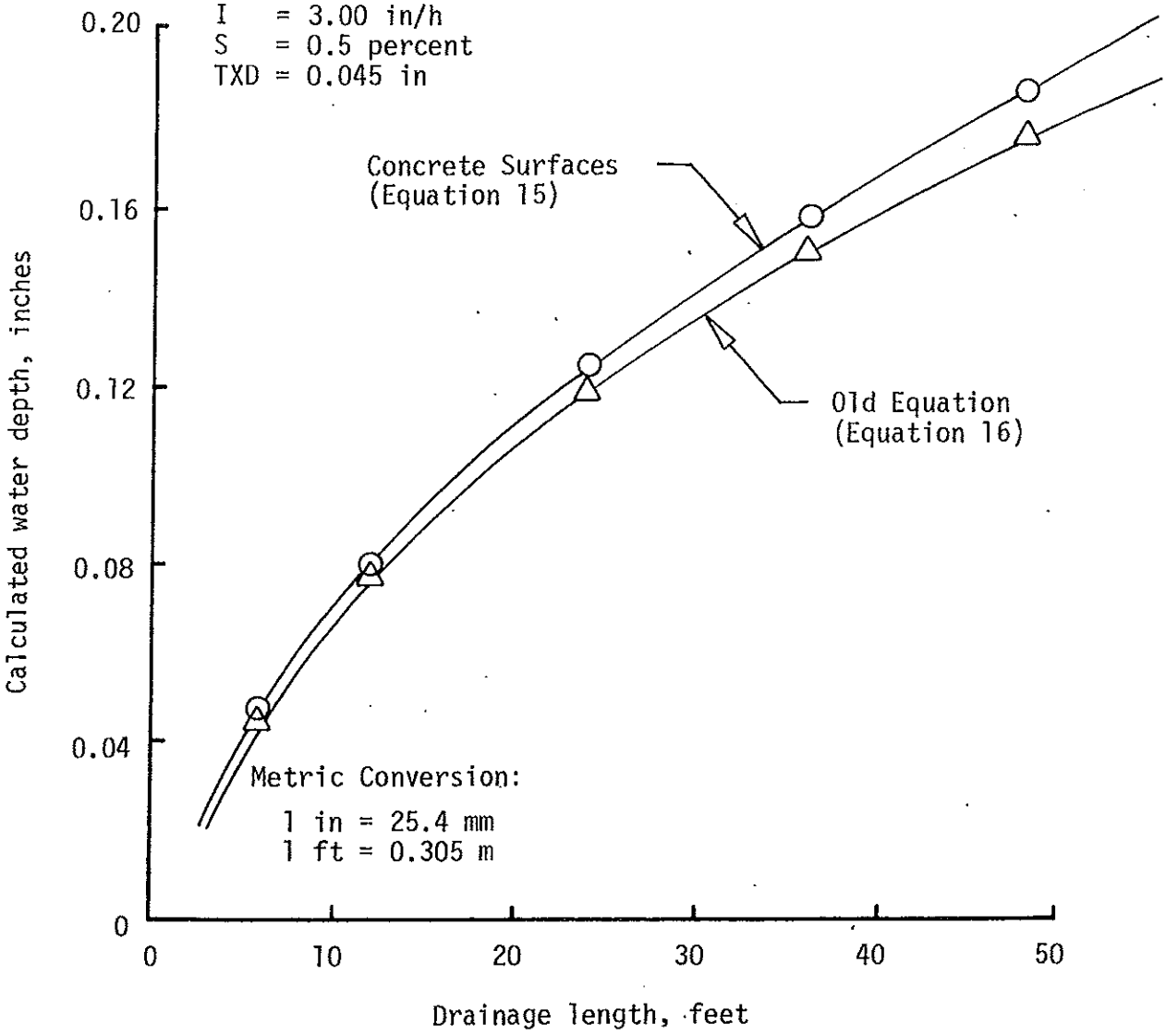

Figure 57. Water depth vs. drainage length for concrete surfaces and old equation

The conclusion here is that water depths for drainage lengths to 48 ft (14.6 m) (and probably considerably beyond) can be predicted with confidence from either equation. Furthermore, the data showed that texture type (brush, tines, burlap, etc.) did not appreciably influence water depth.

To assess the differences between longitudinal and transverse texture directions, the data were statistically analyzed for each condition. The resulting equations are

A. Longitudinal Concrete Textures

$$WD = [0.3581\ (TXD)^{1.544}(L)^{0.457}(I)^{0.609}(1/S)^{0.362}] - TXD \qquad \text{Eq (17)}$$

$$R^2 = 0.49$$

B. Transverse Concrete Textures

$$WD = [0.09858\ (TXD)^{1.002}(L)^{0.421}(I)^{0.574}(1/S)^{0.314}] - TXD \qquad \text{Eq (18)}$$

$$R^2 = 0.90$$

A plot of these two equations (Nos. 17 and 18) for the same assumed conditions reveals no significant difference in water depth as a function of texture direction (Figure 58).

By combining all previously obtained data (11) with the data gathered on this study, the following equation was developed (using 1059 data values):

$$WD = [0.003726\ (TXD)^{0.125}(L)^{0.519}(I)^{0.562}(1/S)^{0.364}] - TXD \qquad \text{Eq (19)}$$

$$R^2 = 0.83$$

Using the same hypothetical example, the results of this equation are compared with the old equation (No. 16) in Figure 59.

One additional set of data was gathered during this experimental investigation: the runoff from the surface as a function of time after cessation of rainfall. From these data the water depth at the outer edge of the beam (which represented a drainage length of 54 ft (16.5 m)) could be accurately determined as a function of time after rainfall cessation. Using these data, a best fit equation was developed using the two-step linear regression computer technique. The resulting equation is

For L = 54 ft (16.5 m) only:

$$BWD = 1.283 \times 10^{-3}\ (TXD)^{-0.044}\ (I)^{-0.026}(1/S)^{0.815}e^{-0.328t} \qquad \text{Eq (20)}$$

$$R^2 = 0.49$$

where BWD = average water depth from the bottom of the asperities, in (1 in = 25.4 mm)
t = time after rainfall cessation, min.

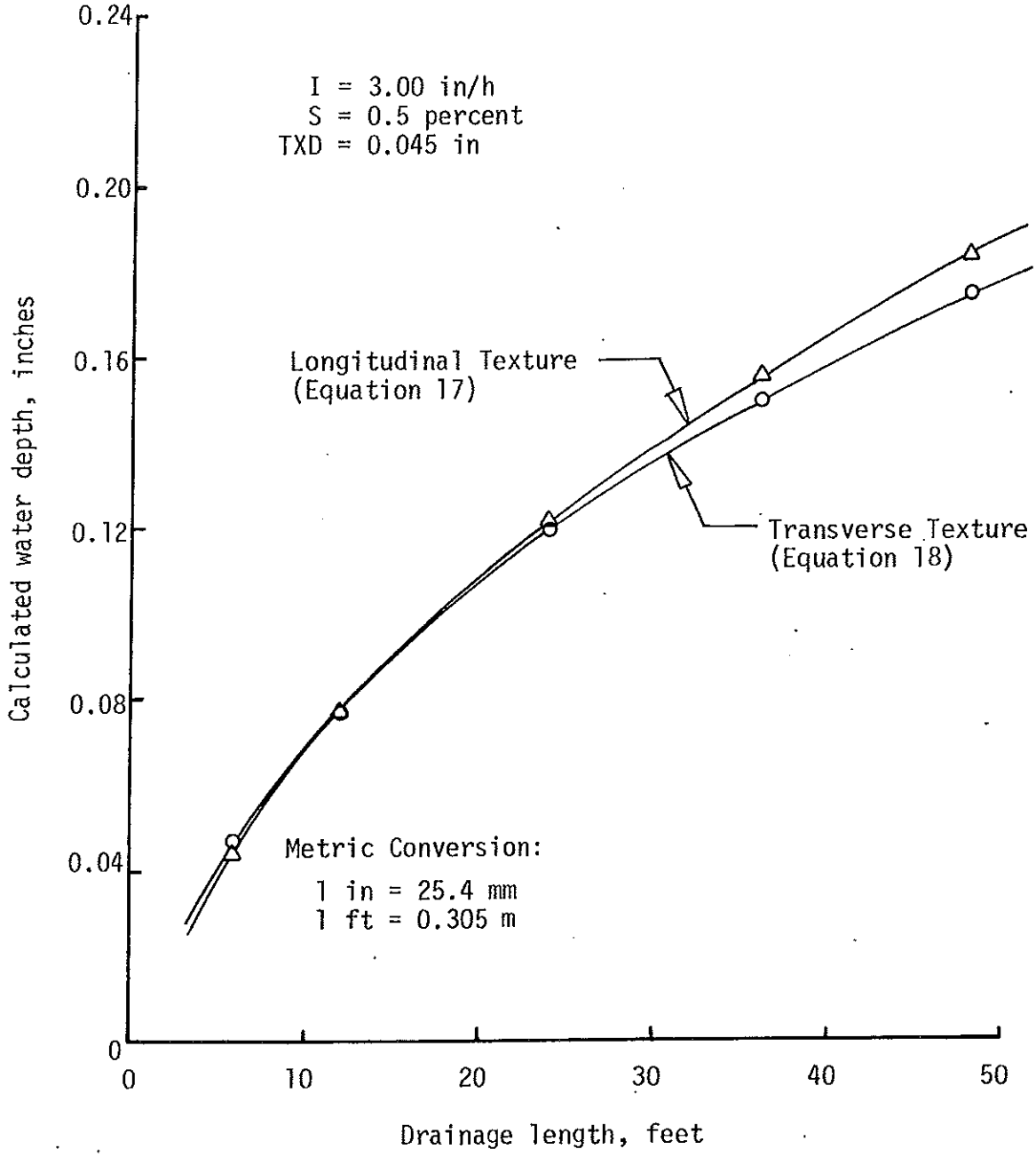

Figure 58. Water depth vs drainage length for longitudinal and transverse textures

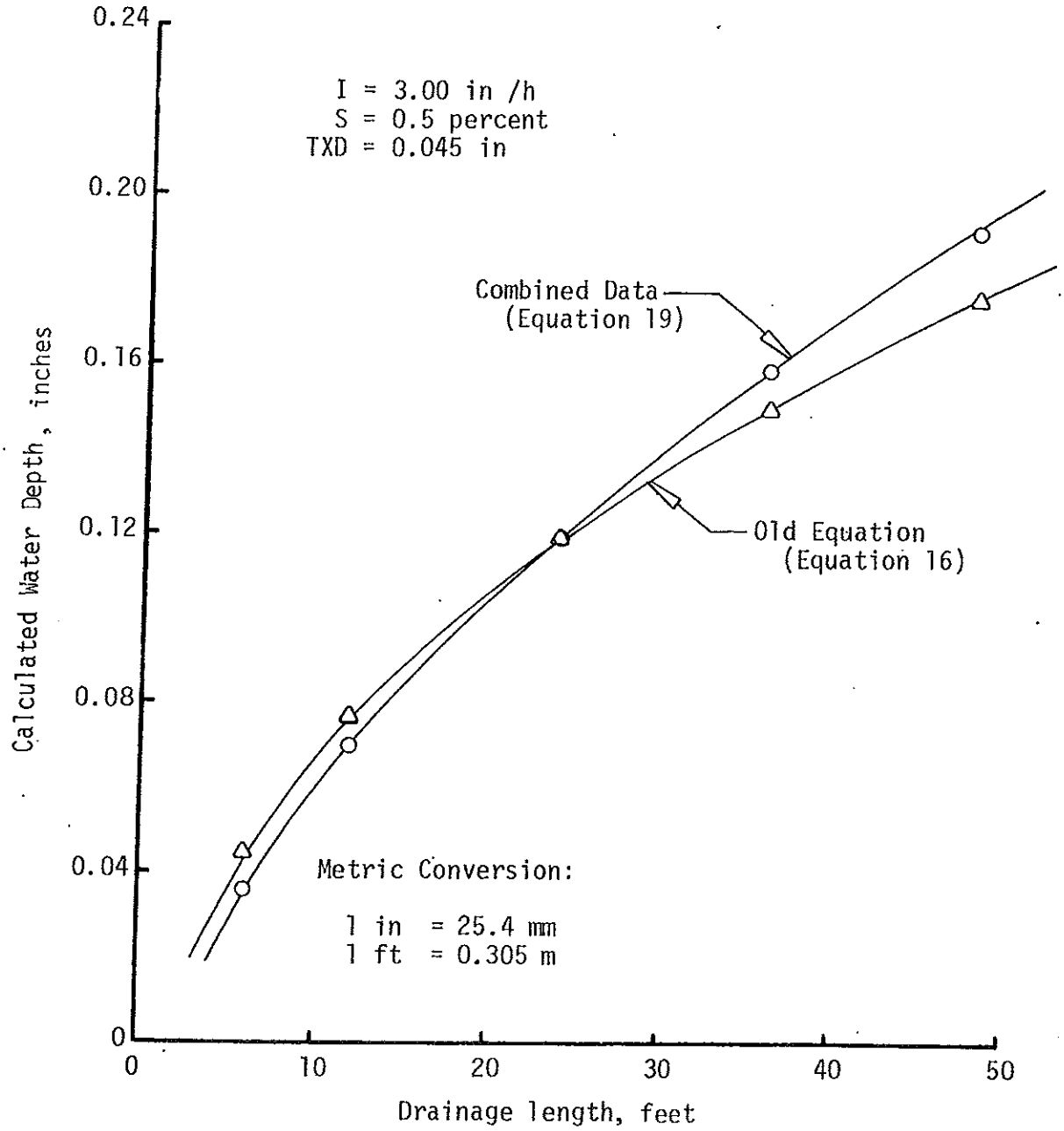

Figure 59. Water depth vs. drainage length for combined data and old equation

A graph of this equation for a hypothetical situation with two texture depths is given in Figure 60. Note that bottom water depth is almost independent of texture depth. These curves indicate the time the pavement surface (at an L = 54 ft (16.5 m)) would contain water after cessation of rainfall. For a 0.025 in (0.6 mm) texture, the pavement would have positive water depths for approximately 4-1/2 min after the rainfall stopped. While these data are very limited, they emphasize the important fact that pavements do remain wet for relatively long periods of time after appreciable rainfall; especially when one considers that rainfalls do not suddenly cease, rather are sporadic in intensity and trace amounts of rainfall often occur for some time (9). Thus, wet pavement conditions may exist for significant periods of time even though water depth predictions may not indicate the presence of positive water depths.

Skid Resistance and Cornering Slip on Textured PCC Surfaces

No analysis of hydroplaning would be complete without investigating both skid resistance and cornering slip of wetted pavements. To accomplish this, the standard ASTM skid trailer was used to measure skid resistance, and the HSRI Mobile Tire Tester was utilized with a number of tires to measure cornering slip at various vehicle speeds and tire slip angles.

Results from a previous study (17) in which 17 test sections were subjected to standard skid testing under simulated rainfall are fully reported in the earlier hydroplaning report (9). For completeness these results are summarized here. All of these data were statistically analyzed using a two-step select regression analysis technique where best fit models were developed. They are

A. For Transverse Textures

$$SN = \frac{239}{V^{1.15}} \; 26.65 \; (TD + 1)^{0.18} \; TXD^{0.49} + \frac{1}{(WD + 0.1)^{0.53}} \qquad \text{Eq (21)}$$

$$R^2 = 0.78$$

B. For Longitudinal Textures

$$SN = \frac{909}{V^{1.37}} \; 3.32 \; (TD + 1)^{0.14} \; TXD^{0.06} + \frac{1}{(WD + 0.1)^{0.31}} \qquad \text{Eq (22)}$$

where:

SN = calculated skid number
V = vehicle speed in mph((km/h)/1.609)
TD = skid tire tread depth in 32nds in (mm x 32/25.4)
TXD = pavement texture depth in inches (mm/25.4) based on putty impression values

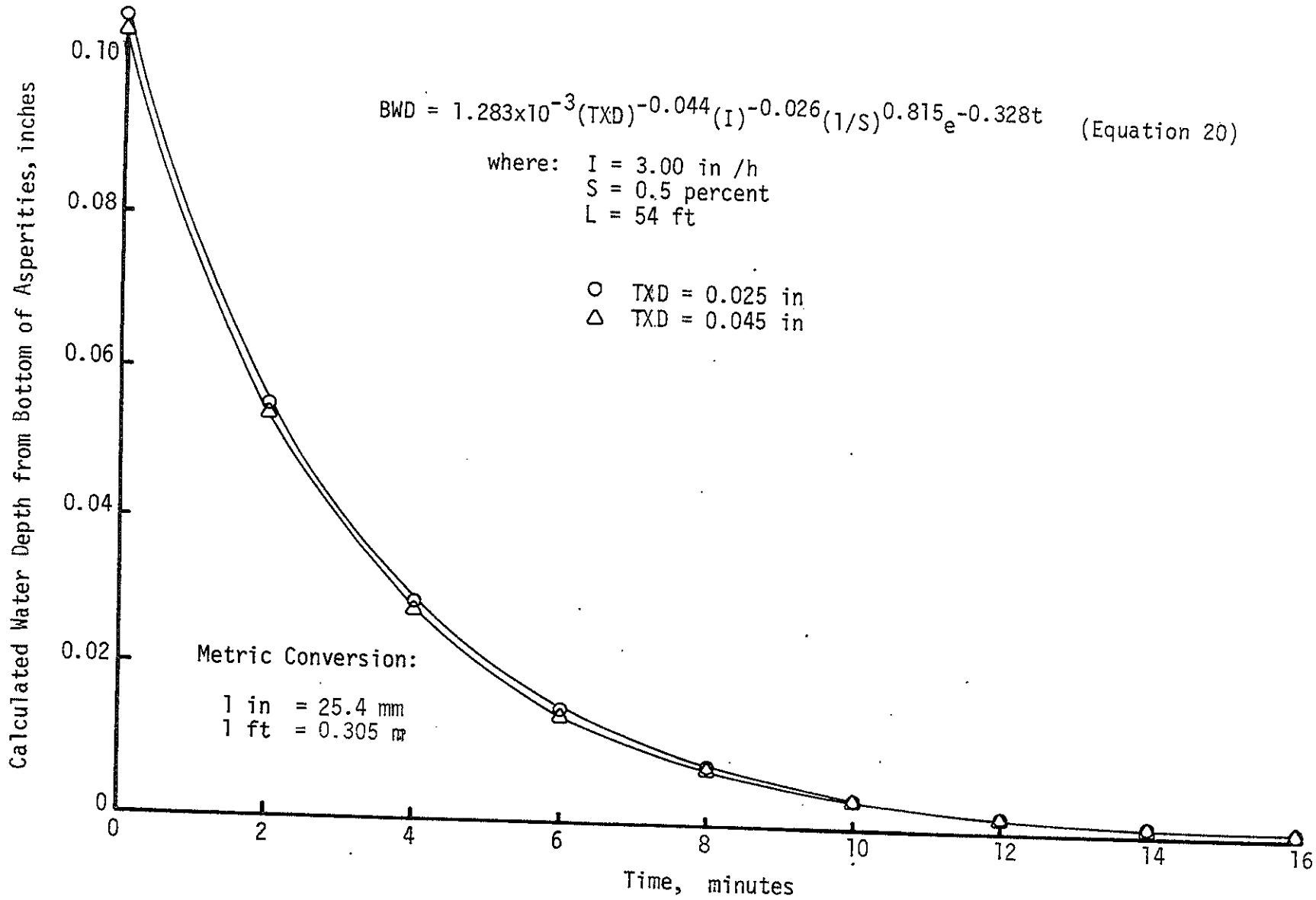

Figure 60. Water depth vs. time after cessation of rainfall

WD = water depth on the pavement surface in inches (mm/25.4) measured from the top of the pavement asperities.

The effect of speed on skid values as a function of texture direction and water depth is shown in Figure 61. Here the influence of texture direction is shown. At higher speeds (greater than 40 mph (64 km/h)) transverse texturing results in significantly higher values of skid numbers than longitudinal texturing. The effect of vehicle speed on skid values as a function of texture direction and texture depth is shown in Figure 62. Here again, even for the very deep texture pavement (0.060 in (1.5 mm)) in this example, transverse texturing results in significantly higher skid numbers at higher speeds where hydroplaning is most likely. Furthermore, deeper tranverse textures do result in higher skid values at every speed.

The obvious question is, do these findings hold true for cornering slip? To answer this question a total of 504 observations were made on seven PCC test sections on SH-6 in College Station, Texas (see Appendix for data). As these test sections were fully described in the previous hydroplaning report (9), only their textures are summarized (Table 12). These measurements were made with the HSRI Mobile Tire Tester, which consists of a retractable test wheel mounted on the rear of a modified tandem-axle commercial tractor (Figure 63) which serves as the test bed. The test wheel accommodates tires in a size range 6.45-14 to 9.15-15. A dead-weight vertical tire load (independent of the test bed) in the range 600 to 2000 lbf (2670 to 8900 N) may be used. The test wheel is attached to the test bed through a transducer sensitive to longitudinal and lateral tire forces and aligning moment. Calibration tests show transducer accuracy to be approximately $\pm$1.5 percent of full scale as calibrated "on truck" under all conditions of loading.

The on-board data acquisition system, consisting of an FM magnetic tape recorder and a light-beam oscillograph, is mounted in the sleeper portion of the tractor cab along with test wheel control instrumentation. Electrical power for the instrumentation is supplied by an on-board gasoline-fueled 6.4 kW AC generator. Other test data recorded are tread surface temperature (from an infrared radiometer mounted above the test tire), test wheel angular velocity, and test bed velocity. These last two quantities yield a precise measure of test tire longitudinal slip.

The test wheel is driven by a hydraulic motor which allows test wheel speed to be varied independently of test bed speed. The hydraulic motor is controlled from the cab and operated in three modes: steady-state (constant) slip, slip varying linearly with time and sinusoidal slip variation with time. The last two modes are controlled by automobile programs to cycle the longitudinal slip between adjustable limits in an adjustable time span.

Either braking or driving torque is developed by driving the test wheel at a rotational rate corresponding to a linear velocity less than or greater than the road speed, and has several advantages over braking by a conventional mechanical brake (drum or disk). A tire controlled by a mechanical brake exhibits extremely rapid lock-up after developing its peak braking force and the data are prone to spurious transients. The mobile tire tester is able to precisely control test wheel acceleration and deceleration over the entire longitudinal slip range of tire operation (driving to free-rolling to locked wheel).

Table 12. Concrete test section texture depths

Test Section	Date	Texture Depth (in)
F-1	Jan 73	0.042
Transverse	Mar 73	0.032
Broom	June 74	0.030
	Jan 76	0.027
F-2	Jan 73	0.060
Transverse	Mar 73	0.051
Tines (1/8 in)	June 74	0.050
	Jan 76	0.034
F-3	Jan 73	0.027
Longitudinal	Mar 73	0.023
Broom	June 74	0.018
	Jan 76	0.029
F-4	Jan 73	0.059
Longitudinal	Mar 73	0.056
Tines (1/8 in)	June 74	0.051
	Jan 76	0.056
F-5	Jan 73	0.074
Burlap + Longitudinal	Mar 73	0.072
Tines (1/8 in)	June 74	0.062
	Jan 76	0.064
F-6	Jan 73	0.024
Burlap Drag	Mar 73	0.021
(Control)	June 74	0.023
	Jan 76	0.027
F-7	Jan 73	0.026
Transverse Natural	Mar 73	0.024
Brush	June 74	0.026
	Jan 76	0.031

1 in = 25.4 mm

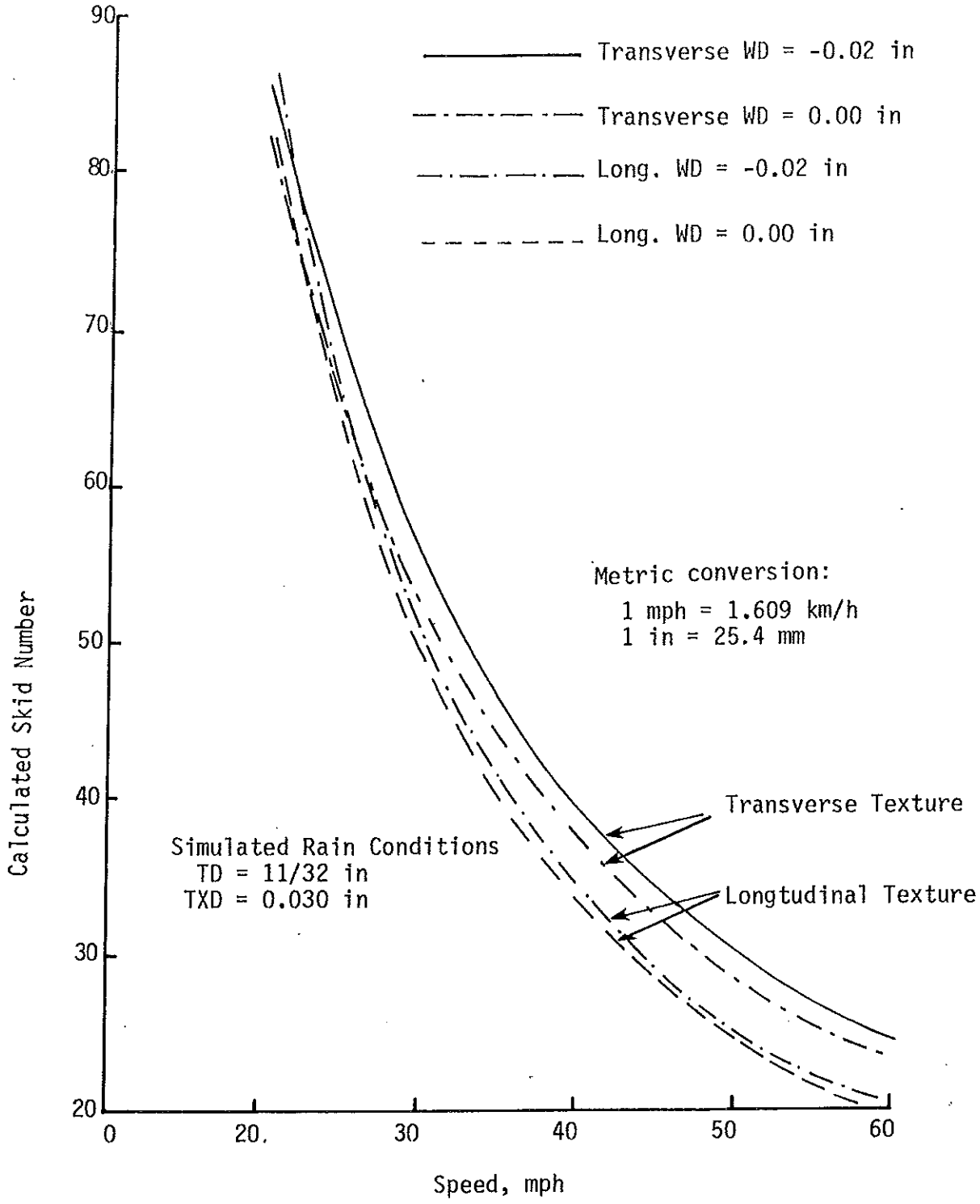

Figure 61. Effect of vehicle speed on skid number for tread depth of 11/32 in and texture depth of 0.030 in (curves calculated from equations)

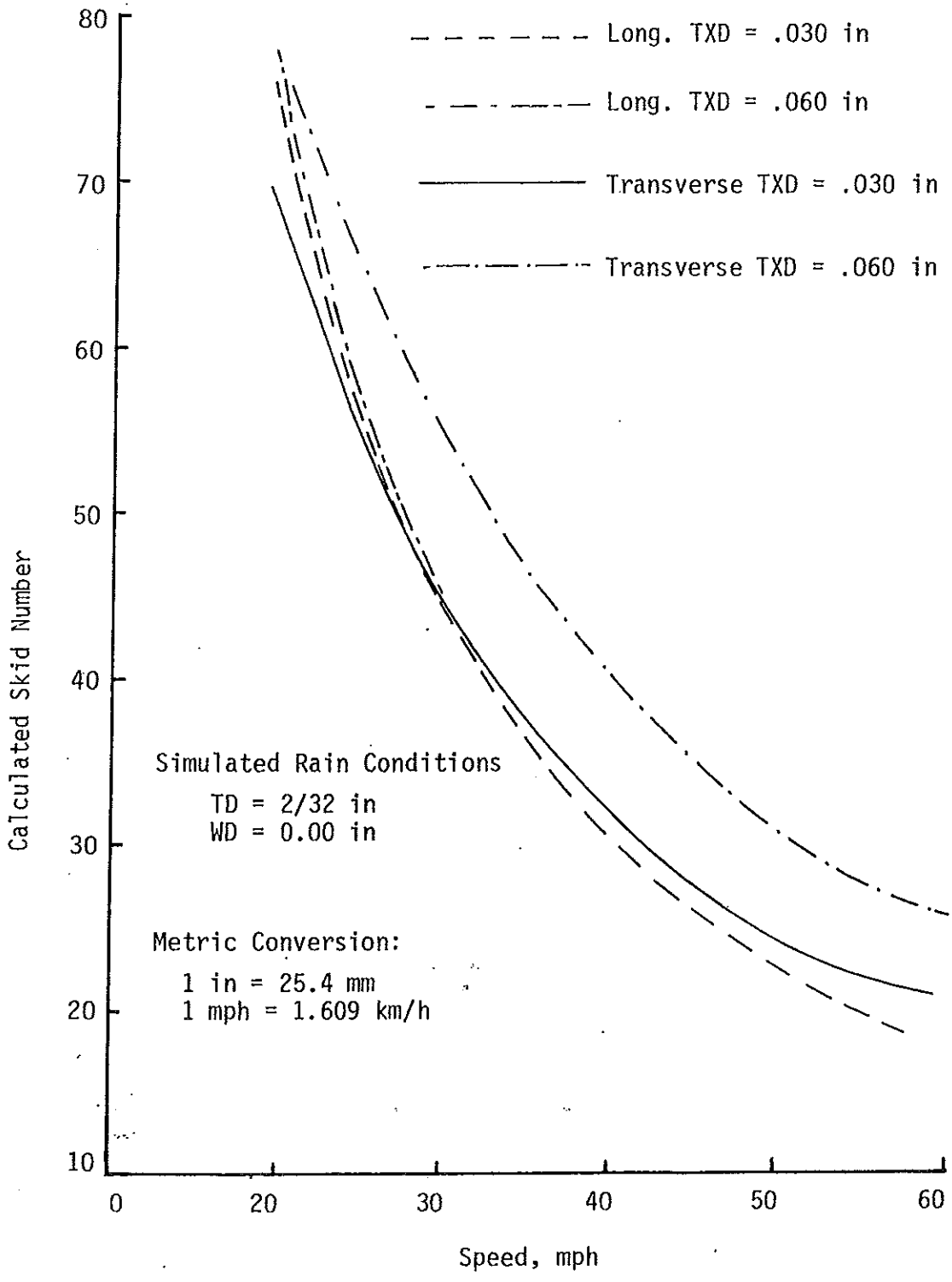

Figure 62. Effect of vehicle speed on skid number for tread depth of 2/32 in and water depth of 0.00 in (curves calculated from equations)

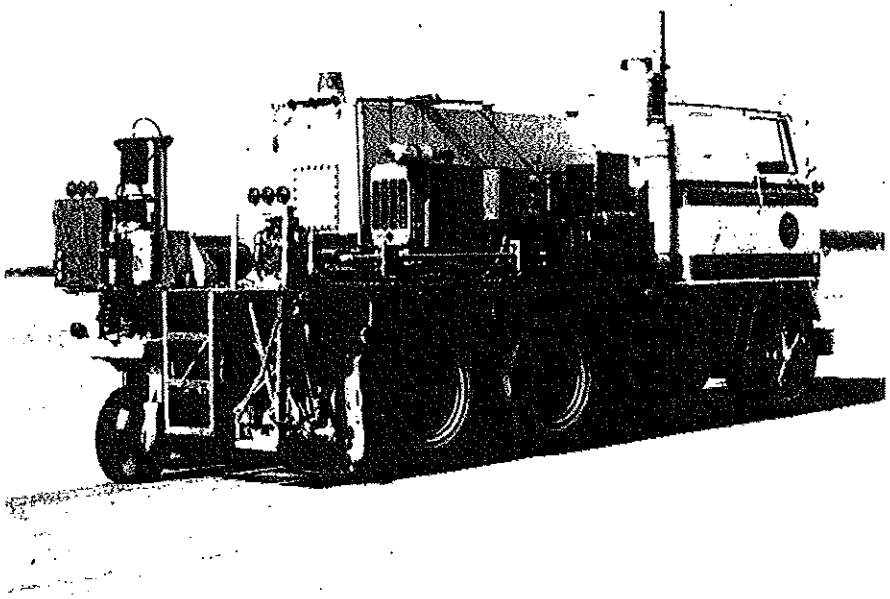

Figure 63. Michigan's tire-pavement friction tester (HSRI Mobil Tire Tester)

The data summarized in Appendix A represent the attempts to measure cornering slip under conditions in which positive water depths were present. To accomplish this a number of test runs was made during actual rainfall. Unfortunately, the weather chose to be uncooperative and during the time the Michigan tire tester was available for use on this project (five months) no heavy, sustained rainfalls occurred. Toward the end of this period, in an attempt to gather additional data on cornering slip, the test sections were wetted using a 4000 gal ($15m^3$) water truck. For safety reasons the water truck traveled at 40 mph (64 km/h) with the Michigan tire tester following part of the time at the same speed and part of the time at 55 mph (88 km/h). This system was only partially successful in that, while positive water depths were not obtained, the pavement was wetted.

In one final effort to obtain cornering slip under conditions approaching hydroplaning, on each of three test sections, the water truck passed over at 5 mph (8 km/h) and was followed by the Michigan tire tester at 55 mph (88 km/h) with a 4 degree slip angle using the ASTM tire at 24 psi (165 kPa) and 2/32 in (1.6 mm) tread depth. The results of these tests are

Test Section	Cornering Slip
F2 Transverse Tines	58
F4 Longitudinal Tines	55
F6 Burlap (Control)	35

The data reported in Appendix A represent more than 1000 combinations of the variables involved. To analyze the data, statistical regression computations were performed with the aid of the computer, and the following variables were found to insignificantly influence cornering slip (CS):

Cross slope (S) (between 1.7 and 2.4 percent)

Tire inflation pressure (P) (between 18 and 24 psi (124 and 165 kPa)),

While the other values overshadowed the influence of these two variables, it should not be construed that these variables are not important in hydroplaning. Rather, it means that only under the conditions of the experiment reported were these variations undefined.

Table 13 summarizes those predictive equations with the best correlation coefficients. For completeness, one of the insignificant variables, tire pressure, has been included in some of the equations. But for pressures from 18 to 32 psi (124 to 221 kPa) the resulting CS values are almost the same. Note that some of the equations (Nos 26 through 31) are good for only a 40 mph (64 km/h) vehicle speed. Although data were gathered at 55 mph (88 km/h),

Table 13. Cornering slip equations

Condition	Equation	R^2	Eq. No.
1. Natural Rainfall - ASTM Tire with 11/32 in TD @ 24 psi			
a) Trans. Textures	$CS = 123.7\ TXD^{0.162}SA^{0.242}V^{-.144}$	0.78	23
b) Long. Textures	$CS = 194.5\ TXD^{0.181}SA^{0.231}V^{-.248}$	0.66	24
c) All Surfaces	$CS = 152.5\ TXD^{0.158}SA^{0.236}V^{-.203}$	0.69	25
2. Truck Water, Trans. Textures, 2/32 in TD @ 24 psi, V = 40 mph			
a) ASTM Tire	$CS = 299.8\ TXD^{0.682}SA^{0.240}P^{.108}$	0.62	26
b) Wide Oval Tire	$CS = 780.3\ TXD^{0.553}SA^{0.111}P^{-.232}$	0.54	27
c) Radial Tire	$CS = 33.9\ TXD^{0.258}SA^{0.357}P^{.268}$	0.70	28
d) Bias-Belted Tire	$CS = 145.6\ TXD^{0.256}SA^{0.236}P^{-.118}$	0.81	29
3. Truck Water, Long. Textures, 2/32 in TD @ 24 psi, V = 40 mph			
a) Radial Tire	$CS = 47.1\ TXD^{0.249}SA^{0.385}P^{.122}$	0.70	30
b) Bias-Belted Tire	$CS = 106.1\ TXD^{0.323}SA^{0.249}P^{.035}$	0.77	31
4. Overall Equation for All Conditions	$CS = 267.3\ TXD^{0.304}SA^{0.206}P^{-.0218}V^{-.194}$	0.63	32

CS - Cornering Slip Number
TXD - Texture Depth-in (mm/25.4)
SA - Slip Angle - degrees
P - Tire Pressure, psi (kPa/6.895)
V - Vehicle Speed, mph (km/h /1.609)

the data scatter was such that too low a correlation coefficient was obtained for the equations to be meaningful. The reason for this scatter was due to the different speeds of the water truck and the Michigan tire tester resulting in differing degrees of pavement wetness.

Unfortunately, the data obtained were not sufficient to reflect the relationship between CS and tread depth. Initially, data were gathered using the standard ASTM tire with full tread to relate the results to standard SN values. When the weather chose to be uncooperative, the final series of tests was made utilizing minimum tread depths. Thus, Equations 23, 24, and 25 are not directly comparable to Equations 26 through 31 (Table 13) because of the different tread depths.

To illustrate the meaning and import of these equations in Table 13, certain assumed conditions were taken and the cornering slip (CS) numbers were calculated from the equations. Under natural rainfall conditions with full ASTM tire tread depth, cornering slip at 4 degrees, as a function of vehicle speed and texture direction, is portrayed in Figure 64. For these conditions (0.030 in (0.76 mm)), the effects of texture direction are minimal. The higher the vehicle speed the lower the cornering slip, as expected. At speeds above 40 mph (64 km/h) the transverse textures result in somewhat higher CS numbers than the longitudinal textures. This is the same result, as obtained with standard SN values (Figures 61 and 62). The effects of texture depth and texture direction under the same conditions (Figure 65) indicates that doubling the texture depth from 0.030 to 0.060 in (0.8 to 1.5 mm) increases CS approximately 15 percent for slip angles from 2 to 16 degrees. Note also the higher CS number for transverse textures at this speed.

Figure 66 illustrates the effects of the various tire types (with reduced tread depth) on CS at various slip angles. For this case four of the five tires contained only 2/32 in (1.6 mm) tread depth. (The fifth tire was standard ASTM and is shown for comparison purposes.) Examination of this figure reveals some interesting results. First, at low slip angles the wide oval tire exhibited the greatest CS, but at higher slip angles this same tire exhibited the lowest CS. The reverse situation occurred with the radial tire. At first glance this may appear confusing, but it must be remembered that although the pavement sections were wetted, in no cases were positive water depths present. Thus these results represent conditions in which significant portions of the tire are in contact with the pavement surface, especially at the lower slip angles. For the higher slip angles, some partial hydroplaning may be occurring, so the results are more nearly as expected. By comparing the two ASTM tires, the beneficial effects of tread depth may be observed. The full tread resulted in a three to five number increase in CS for slip angles from 2 to 16 degrees. This increased CS can become extremely important in a partial hydroplaning condition and thus the importance of deep treads on all tires cannot be overemphasized.

The combined effects of water depth and texture direction are shown in Figure 67. Here for the 16 degree slip angle, the calculated CS numbers for longitudinal and transverse textures as a function of texture depth are compared with the three data points of Figure 67 obtained under more nearly

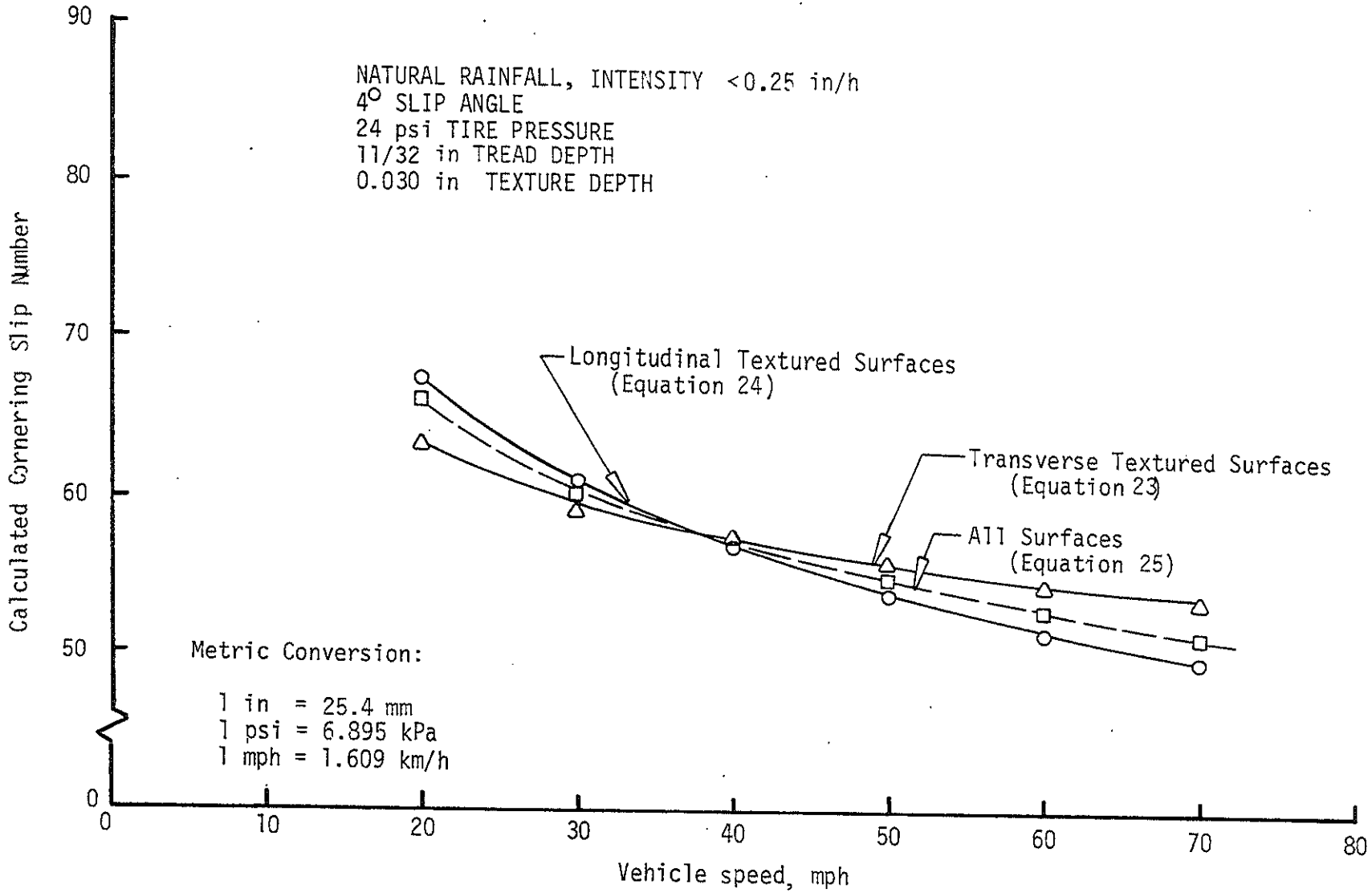

Figure 64. Cornering slip number vs. vehicle speed for ASTM tire E501 at a 4° slip angle

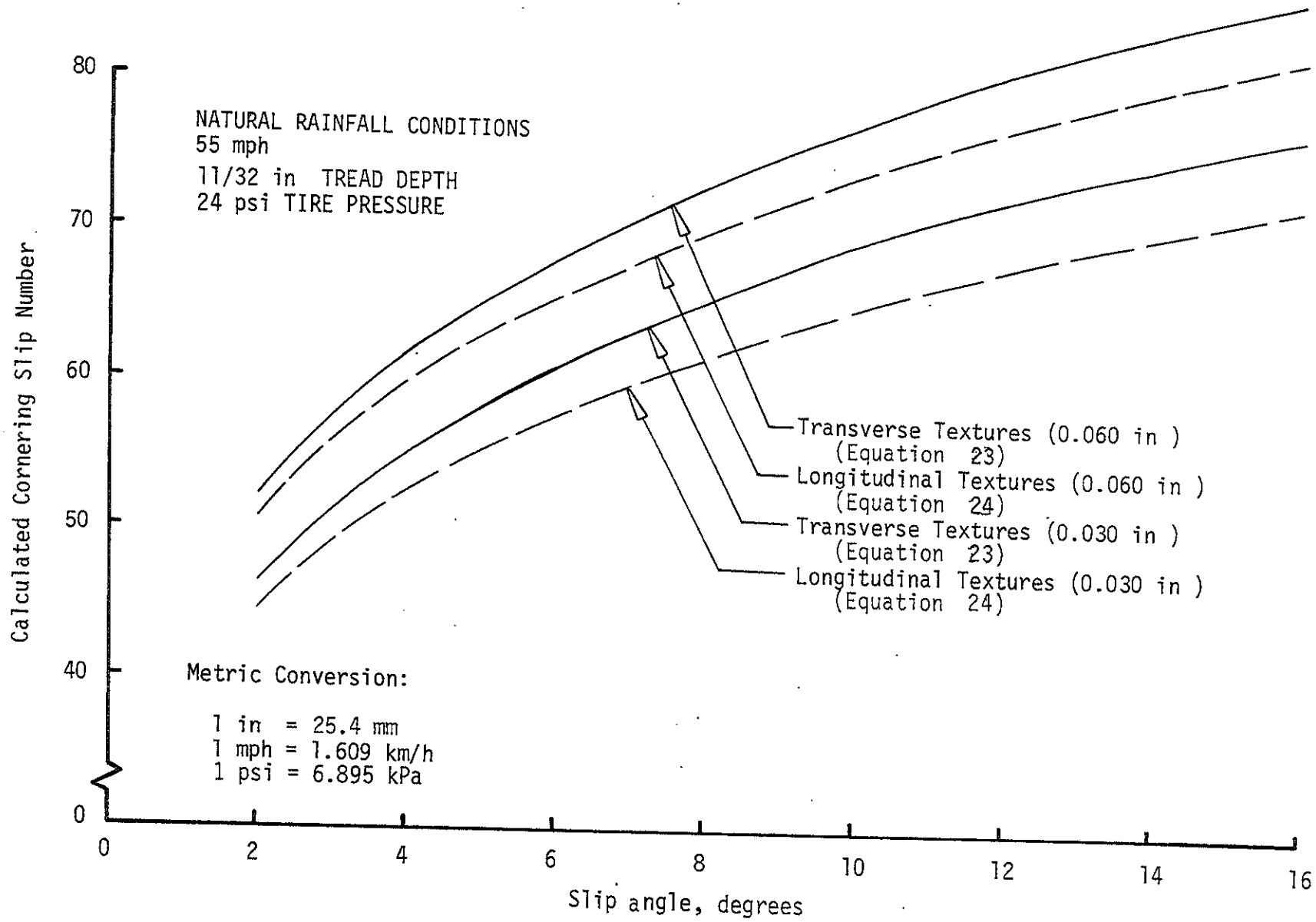

Figure 65. Cornering slip number vs. slip angle for ASTM tire E501 at 55 mph

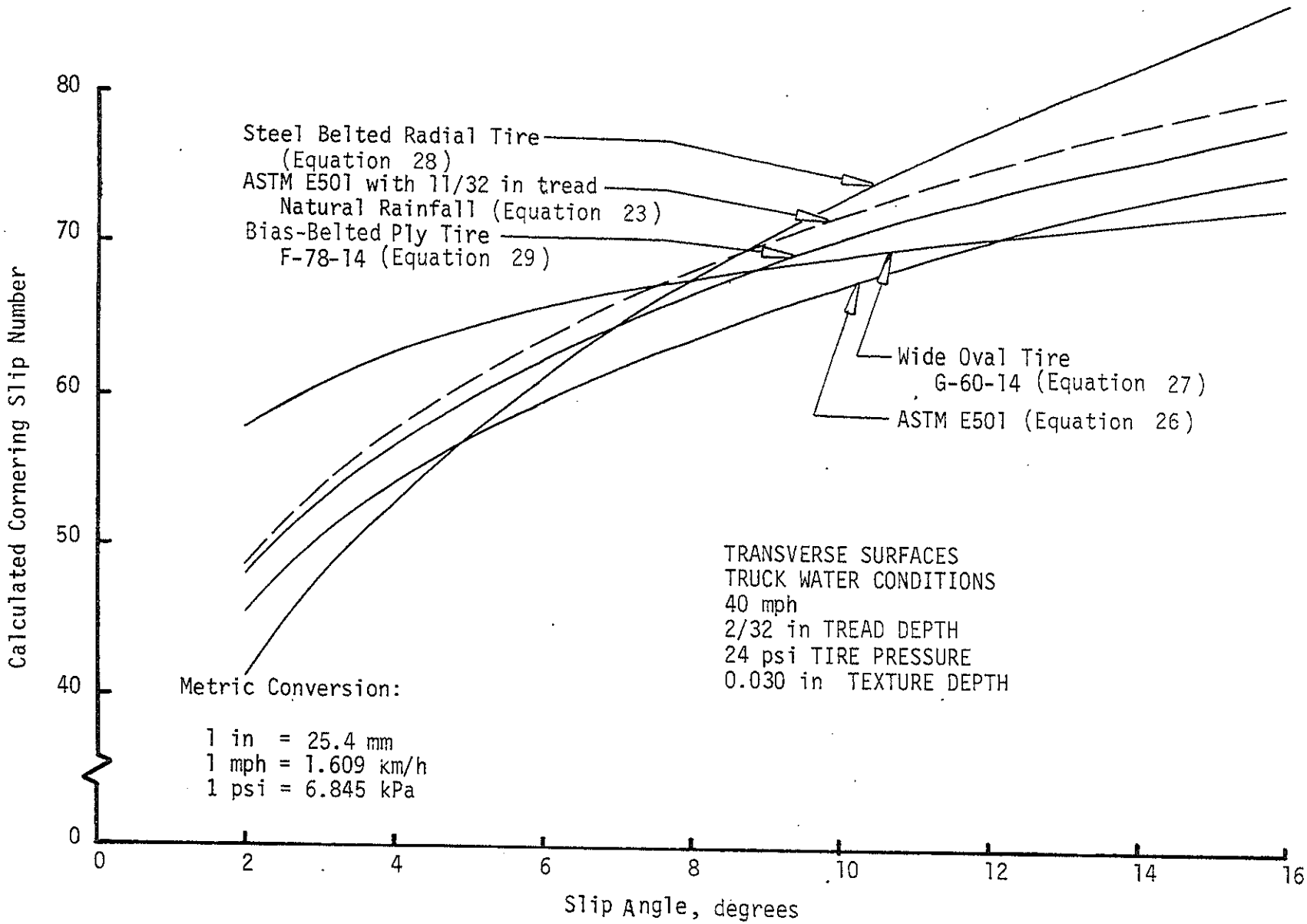

Figure 66. Cornering slip number vs. slip angle for various tire types

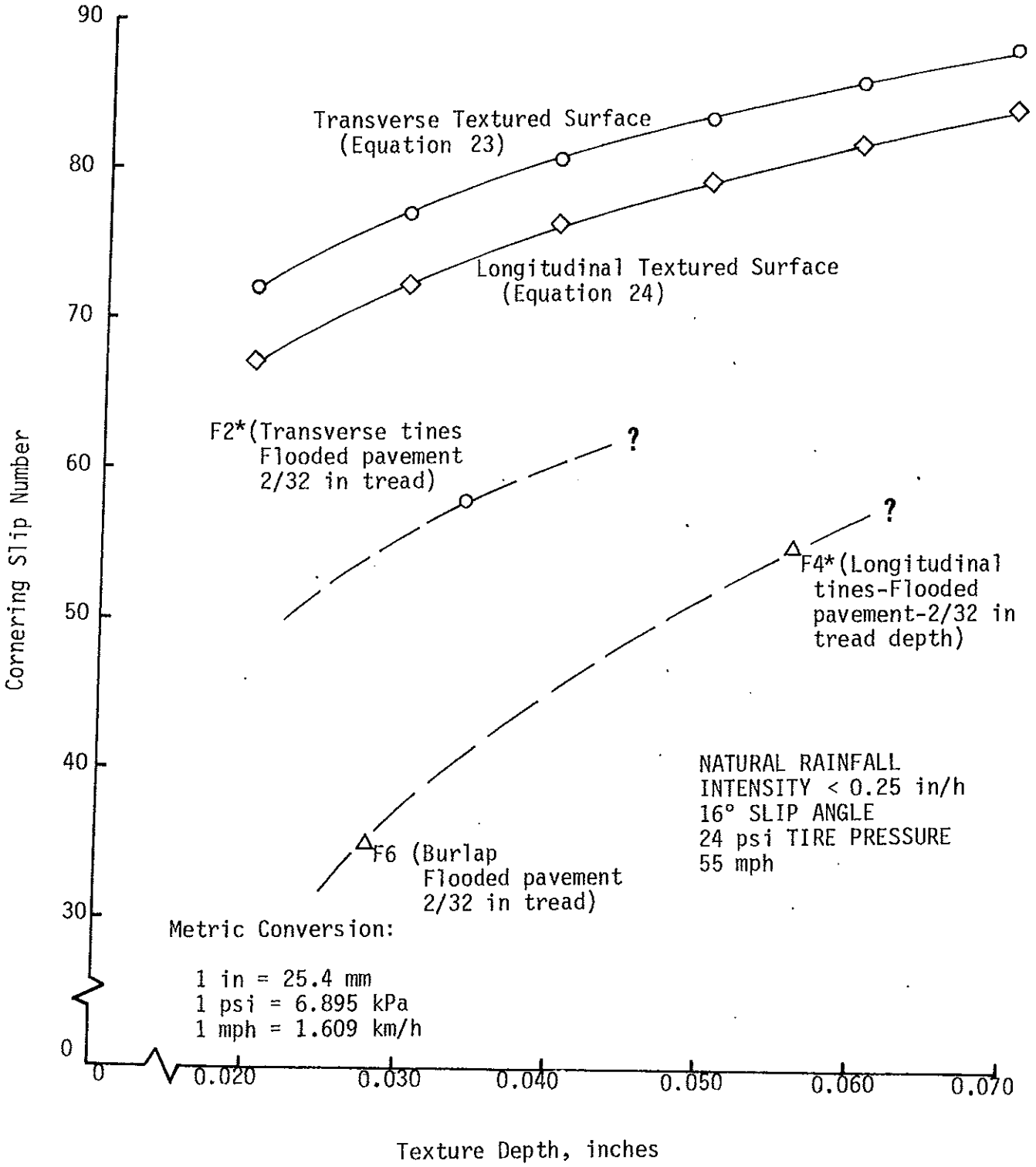

Figure 67. Cornering slip number vs. texture depth for ASTM standard tire E501 with full (11/32 in) and low (2/32 in) tread depth at hydroplaning conditions.

*See page 87.

hydroplaning conditions. The data under the more nearly hydroplaning conditions (flooded pavement with shallow tread depths) are frighteningly lower than the calculated values from data obtained under natural rainfall conditions in which the pavement did not have positive water depths and using deeper tread depths. Note that the transverse texture, under both conditions, exhibited higher CS numbers. This is in agreement with the ASTM E274 SN_{40} numbers obtained under simulated rainfall (Figures 61 and 62) and the other CS data. The dotted curves through the three data points (Figure 67) obtained for positive water depths are only suggestive of what might be the shapes of the curves based on all the other data obtained. But, due to the paucity of these data, no firm relationships could be established and hence the question marks by the curves. Once again, however, the extremely reduced CS values on flooded pavements using reduced tread depths point up the dangers of hydroplaning under these conditions.

Table 13 contains one equation (No. 32) which represents the regression analysis of all data gathered. Here again the variable of tread depth was indicated to be insignificant as it did not appear in the equation (which is obviously in error). A plot of this equation from all the data is compared to Equation 25 (which was calculated using a full treaded ASTM tire) in Figure 68. The difference in the two curves can be attributed to the deeper tread utilized in the natural rainfall conditions. Thus the influence of tread depth can be partially seen in this figure. Equation 32 should not be used to predict CS because of the wide data scatter and omission of such important parameters as tread depth and texture direction.

Discussion and Conclusions

A large amount of data was gathered and analyzed in this phase of the investigation. The phenomenon of hydroplaning on highway surfaces is exceedingly complex and involves many, many variables. Although most of the data obtained were for conditions which did not approach full dynamic hydroplaning, the findings are extremely important because they relate to frequently occurring conditions in which the pavement is completely wetted and thus potentially hazardous to the motorist. These data obtained under hydroplaning conditions verify the types of relationships developed between CS, speed, tread depth, and texture direction.

From the data the following conclusions have been drawn

1. Water depth as a function of cross slope, texture depth and rainfall intensity can be reliably predicted for drainage lengths up to 48 ft (14.6 m), and probably considerably beyond. The direction of the texturing does not significantly influence the resulting water depths.
2. Potentially hazardous positive water depths exist for several minutes beyond the cessation of an appreciable rainfall, and a wetted surface exists for many minutes beyond cessation of rainfall. A predictive equation of the time a pavement will remain either with positive water depth or wetter to any desired degree was developed (Eq. 20).

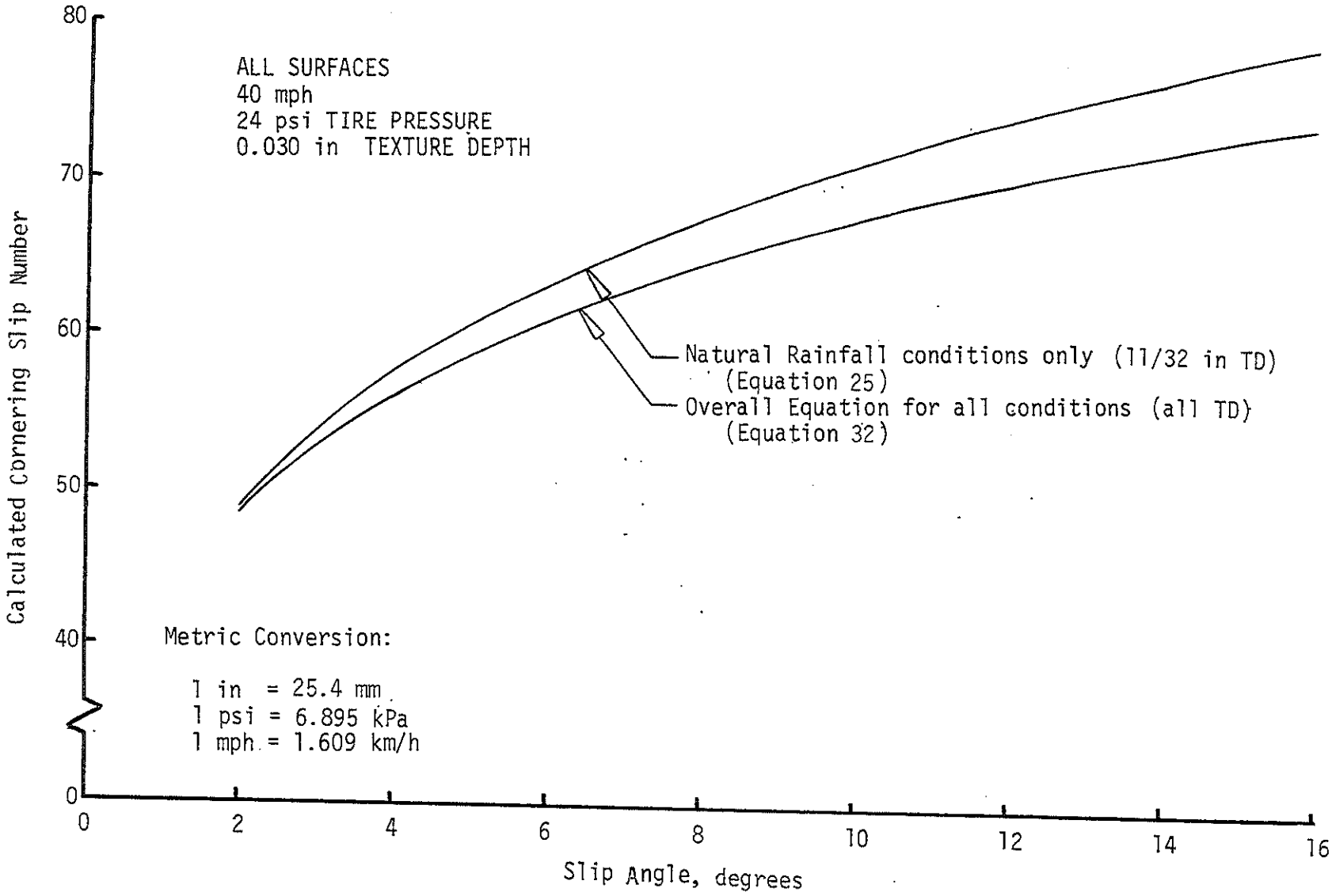

Figure 68. Cornering slip number vs. slip angle for all surfaces (Neglecting tire types and texture direction)

3. Under both SN measurements and CS measurements on wetted surfaces, transverse textures yield higher values than do longitudinal textures. Thus the logical recommendation would seem to be to require transverse textures for both tangent and horizontally curved sections of the roadway. But, it should be pointed out that this research, as detailed as it was, did not investigate the potentially hazardous maneuver of full dynamic hydroplaning of an automobile around a horizontal curve! Here the conditions are not approximated by either skid numbers or cornering slip numbers. Logic would strongly suggest that vehicle tracking could be very influential in keeping the vehicle in its respective lane. This tracking could best be obtained by providing longitudinal texturing, rather than transverse, throughout the horizontal curves. Certainly the dramatic decreases in accident rates documented (18) in California (and elsewhere) after longitudinal grooving attest to the validity of this approach. What is not known is whether or not transverse grooving would have been as good as, worse or better than longitudinal grooving in terms of accident reduction.

   California DOT (18) uses longitudinal grooves on horizontal curves and they report 90 to 95 percent reduction of spinout type of accidents. California has one installation which utilizes transverse grooves on horizontal curves and one installation with "diamond" grooves. Accident records are currently unavailable on these.

   Recently California DOT has used transverse texturing of plastic concrete. Accident data on these installations are being collected but a conclusion at this time is premature.

   Skid number and cornering slip data clearly establish the validity of requiring transverse textures on tangent sections, but on horizontal curves the jury is still out!

4. Increasing texture depth provides the greatest increase in either SN or CS values. Thus deep textures should be constructed; however, noise and tire wear must be considered. From a construction viewpoint, texture depths of 0.06 in (1.5 mm) can be easily constructed utilizing tines spaced 1/4 in (6 mm) clear distance (9). Therefore, initial texture depths of 0.06 in (1.5 mm) should be required as an average minimum and in no case should the construction of texture depths below 0.05 in (1.3 mm) be permitted.

5. The type of tire and tread depth significantly influence CS values. At elevated speeds and relatively high slip angles the wide oval tire developed the lowest CS values while the radial developed the highest CS values. Shallow tread depths produced significantly lower CS values than did deeper tread depths.

CHAPTER V

TIRE-PAVEMENT INTERACTIONS ON OPEN-GRADED FRICTION COURSES IN SIMULATED AND NATURAL RAINFALL

Introduction

The interrelation between skid resistance, road surface texture and water film thickness has been under serious and intensive study for the past decade or more. The danger potential of inadequate friction at the tire-pavement interface during wet-weather conditions has been magnified by ever increasing traffic volumes and steadily rising numbers of heavy trucks.

Inflation continues to reduce the effectiveness of available funds for highway construction and maintenance. These forces acting together with a continuing reduction in the economic availability of aggregates with long-lasting skid-resistance properties place heavy demands on responsible highway personnel all across the United States.

An introduction to a problem as complex as tire-pavement interactions during wet weather demands a nominal review of past studies, known basic information, current approaches now being utilized to minimize the problems and possibly futuristic thinking regarding idealized practices that would eliminate the slippery pavement problem.

Review of Recent Literature

During the past approximately five years, three symposiums on skid resistance have been conducted with each of these conferences including contributions from leading researchers from throughout the United States and Europe. A review of the findings presented, as these may be considered to apply to the subject report, seems appropriate and will therefore be included. The symposiums cover one developed and presented in 1973 by the Association of Asphalt Paving Technologists (AAPT) in Houston, Texas; one developed and presented by the Study Center for Road Construction in 1976 in Amsterdam, Holland; and one conducted by the Transportation Research Board, National Academy of Sciences, in 1977.

The first and third of these conferences were general in scope; whereas, the second one dealt entirely with porous pavements, the specific subject of this segment of this report. As the author sees them, the applicable aspects of these conferences will be reviewed and related to the current study as seems appropriate.

Goodwin (19) has reiterated the interdependence of the driver, the vehicle and the driving environment as key elements in highway accident picture, detailing the driving environments subelements as:

1. Roadway geometric and hardware,
2. Road surface design,
3. Road surface construction,

4. Traffic volume and character and

5. Wet weather

In his concluding remarks Goodwin stated:

> "...There are still many unknowns, but the state-of-the-art is such that important contributions can now be made by the roadway designer, the automobile and tire manufacturer, and those responsible for driver education. There remains only the task of bringing these groups together in a systematic approach to seeking total solutions to providing adequate skid-safe facilities depending on the type and driving requirements. The most promising improvements seem to be in the area of improved geometrics and surface characteristics on the part of the highway designer, a greater attention to tire type and conditions by the tire manufacturer, concern with tire condition by the public, improved handling characteristics and braking by automobile manufacturers, and the education of drivers in handling of emergency situations...."

The current study touches on several elements of the total wet-weather accident picture described in part by Goodwin but omits from consideration such critical elements as driver input, vehicle handling and braking operations. Tire type and tire tread depth are considered only in modest detail.

Nakkel's (20) review of early European developments brings home several points common to Europe and the United States and at the same time he reveals stark differences in pavement mixture design and traffic demands, particularly the heavier loads and higher tire pressures of trucks. Nakkel further reports that:

> "...By means of basic research efforts most (European) countries are attempting to better understand relationship between surface texture, materials properties, properties of binders, and the evaluation of the properties with time and/or traffic load vs skid resistance...."

In general, suitable microtexture and macrotexture of road surface provide acceptable anti-skid properties for both low- and high-speed conditions. The surface texture affects skid resistance directly, owing to the effects on the thickness of water film on pavements under wet condition and/or quicker removal of water from the surface.

Nakkel has systematically classified road surfaces into seven groups shown in Figure 69 and it is apparent that, in general at least, surface types 1 and 7 would not be desirable; whereas, surface types 3 and 5 would have merit. The speed sensitivity of types 2 and 4 would limit these to lower speeds.

Nakkel further reports on the extensive skid measurements made in Germany for the more than two past decades. The frequency distribution diagram of Figure 70 gives the limits of the spectrum for locked wheel coefficients. These data are based on more than 700 highway control stations and include

TYPE OF SURFACE	REPRESENTATION	DESCRIPTION
1		NEITHER MACROTEXTURE NOR MICROTEXTURE
2		ONLY MICROTEXTURE
3		MACROTEXTURE AND MICROTEXTURE
4		MACROTEXTURE AND MICROTEXTURE AS UNDER 3. (SLIGHT DENSITY OF MACROTEXTURE)
5		MACROTEXTURE (DUE TO GAPS BETWEEN COARSE AGGREGATES) AND MICROTEXTURE (DUE TO SHARP-EDGED COARSE AGGREGATES)
6		MACROTEXTURE (DUE TO GAPS BETWEEN COARSE AGGREGATES), NO MICROTEXTURE
7		MACROTEXTURE (FISSURES AND HOLES), NO MICROTEXTURE

(After Nakkel (20))

Figure 69. Classification of surface types

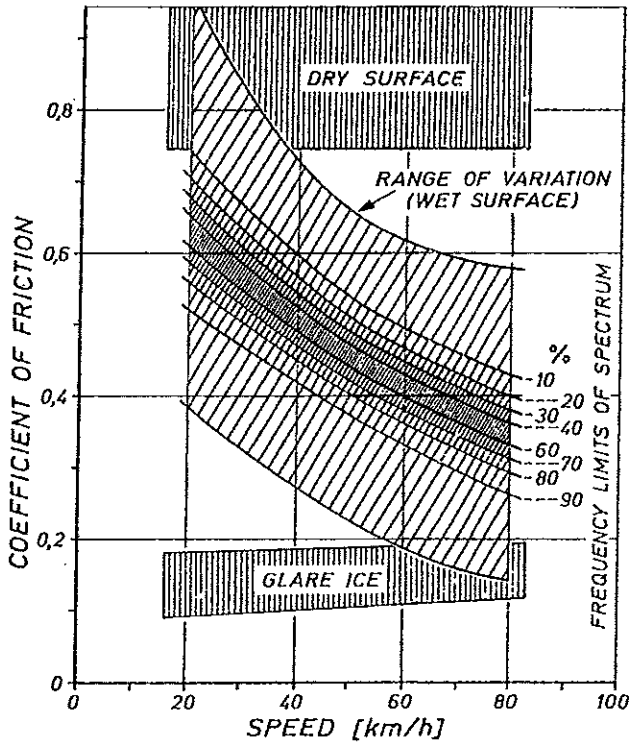

(After Nakkel (20))

Figure 70. Frequency distribution of the friction coefficients on German highways and motorways

gussasphalt, asphalt concrete and portland cement concrete. From this frequency distribution guide values for adequate skid resistance were set to correspond to the 90 percent curve. Similar but slightly higher values prevail in Holland. In Great Britain no mandatory skid requirements are in force; however, mandatory requirements do prevail on the properties of paving mixtures and their individual constituents. Limits are placed on the polish susceptibility and the abrasion resistance of the stone used in the paving mixture. Blending of petroleum asphalt and tar is practiced in selected situations to effect controlled oxidation of the binder.

Based on Nakkel's review of the European situation, adequate skid measurements must be made to determine skid values that can be produced and preserved within economic engineering practice. The burden is being shifted to the contractor who, in many instances, must furnish a surface coefficient guarantee for periods up to three or more years. This would seem unfair unless the mandatory limits were set rather loosely, in which case they would be of minimal value.

The European approach to obtaining adequate initial anti-skid values includes

"(a) mixes with a high content of matrix and no gritting: use of very high amounts of extremely hard crushed sand providing the bituminous material with a very high degree of surface texture sharpness;

"(b) mixes with a high matrix content without adequate amounts of hard crushed sand: gritting of hot surfaces with crushed sand or crushed stone of 2 to 5 mm and rolling-in on the surface;

"(c) hot rolled asphalt: use of sufficiently large quantities of gritting material (crushed stone); with distribution as uniform as possible. Further tests are needed to determine the quantities of gritting materials required to obtain adequate initial anti-skid values."

Inherent in all practical situations (neglecting the heavy use of studded tires) has been the reduction of skid resistance under the action of time and in high volumes of traffic; reduction being brought about mainly by polishing of the key fraction of the aggregate and (in the case of bituminous pavements) closing up of the surface mat. It would therefore seem that successful aggregate systems would be those that form a paving mixture with a fixed drainage capability (surface and/or internal) and a built-in capacity to maintain adequate microtexture by a differential-rate-of-wear property or a continuing renewal ability.

The preceding conclusion has been voiced by others over the past several years and was reiterated by Gallaway (21) at the AAPT 1973 Annual Meeting.

The special treatment of transitions to horizontal curves has been emphasized in the past, and this problem persists. A suggested solution to this problem was presented by Gallaway (21) and is shown skematically in

Figure 71. In this concept the needed pavement cross slope is built into the system as if the curve did not exist and then the design cross section with an open-graded friction course is placed as the surface. A capability for free drainage at the edge of the pavement must be included for this concept to be advantageously effective.

The International Symposium on Porous Pavements held in Amsterdam in 1976 included contributions from eight different countries who are trying or actively using open-graded bituminous surface courses for various reasons. In Europe and South Africa the primary objectives of this type surface are essentially the same as those in the United States; namely, improved friction during wet conditions and the reduction of splash and spray. In Japan, porous pavements are utilized to assist in replenishing ground water, lowering underground soil temperature, supplying water and oxygen to tree roots and reducing glare of vehicle headlights, these in addition to the conventional attributes.

A review of some of the detailed findings presented at the Amsterdam Symposium seems appropriate and it therefore follows.

Huschek (22) reported the relationship shown in Figures (72a) and (72b) for hydroplaning speeds for surfaces A and B and water depths of 0.5, 2 and greater than 5 mm with a minimum tread depth of 7 mm. The advantage of the large scale roughness (macrotexture) is evident. The macrotexture of 0.3 mm and 0.7 mm for surfaces A and B, respectively, do not compare with current recommendations in the United States; however, the 7 mm tread depth is roughly four times the generally accepted U.S. minimum of 1.6 mm.

Furthermore, Huschek compared a porous pavement surface, C, in Figure 73 with surfaces A and B above with locked-wheel force coefficient frequency distribution of some 220 road surfaces in Switzerland. The format is fairly typical of similar measurements made in Texas; however, the fifty percent line at 40 mph (64 km/h) is considerably higher, 0.47 for Switzerland vs about 0.40 for Texas. In summary Huschek concluded that:

> "...Porous asphalt may be considered as a surfacing with a high degree of macrotexture. An additional advantage is that evacuation of water through the layer is possible. Porous asphalt is undoubtedly a quite ideal solution as far as skid resistance on wet surface at high speed is considered. On the other hand important requirements such as durability at low temperature, wear and stability at high temperature may cause problems."

The Swiss recommendations for classifications of road surfaces by texture depths (sand patch method) are presented in Table 14.

Based on previous and current recommendations of the authors of this report these values are low. Indeed, the "very coarse" classification "suitable for special conditions only" corresponds to previous values outlined in the Phase I report for high-speed rural highways.

Careful laboratory tests by Welleman (23) indicated that only about 70 percent of the measured voids in porous paving mixtures made in his laboratory were permeable to water. This is shown more clearly in Figure 74.

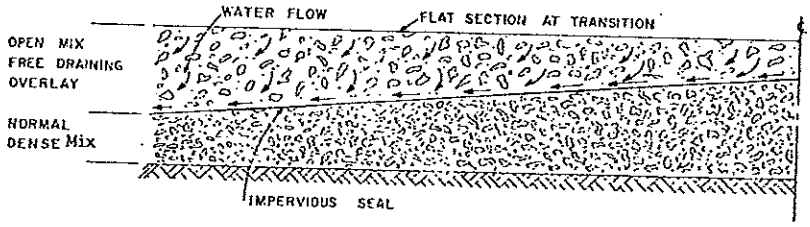

(After Gallaway (21))

Figure 71. Pavement cross section at transition from tangent to superelevated curve (flat section--no surface cross slope)

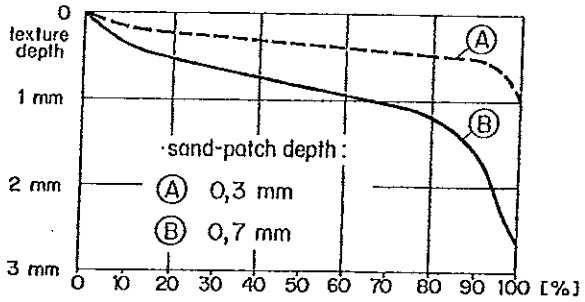

(After Huschek (22))

Figure 72a. Summation curve of the texture depth resulting from profile measuring device

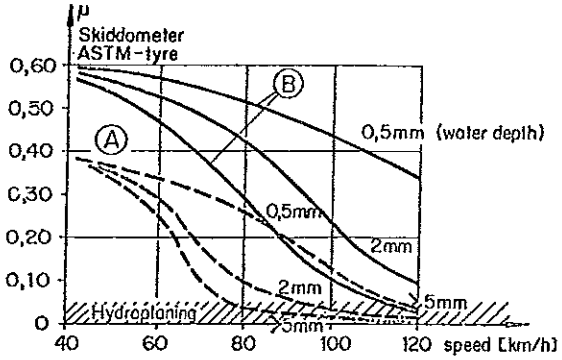

(After Huschek (22))

Figure 72b. Coefficient of friction in relation to speed for different water depths

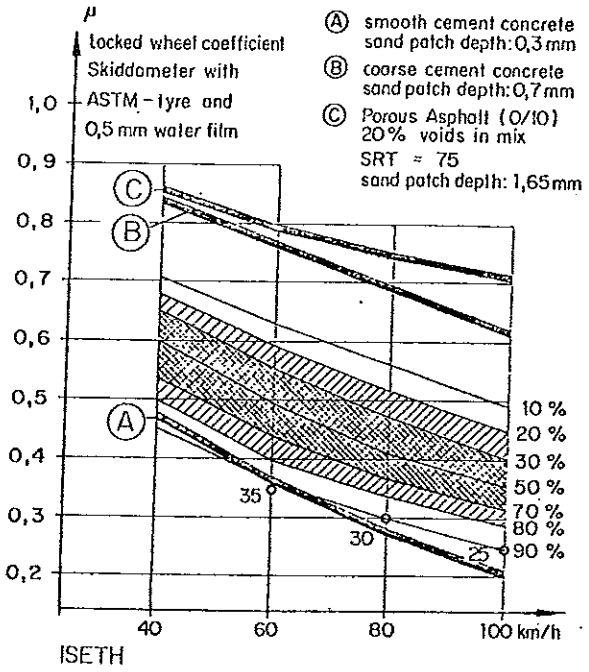

(After Huschek (22))

Figure 73. Frequency distribution of locked-wheel braking-force coefficients of 200± road surfacing

Table 14. Swiss classification of road surfaces

Sand-Patch Depth (mm)	Classification	
<0.2	Very fine	To be avoided every where
0.2 - 0.4	Fine	Surfacings to be limited to urban areas (speed limit 80 km/h)
0.4 - 0.6	Medium	0.4 is necessary for all roads with no limitation of speed
0.6 - 1.0	Coarse	Suitable for highways with traffic at very high speeds
>1.0	Very coarse	Suitable for special conditions only

(After Huschek (22))

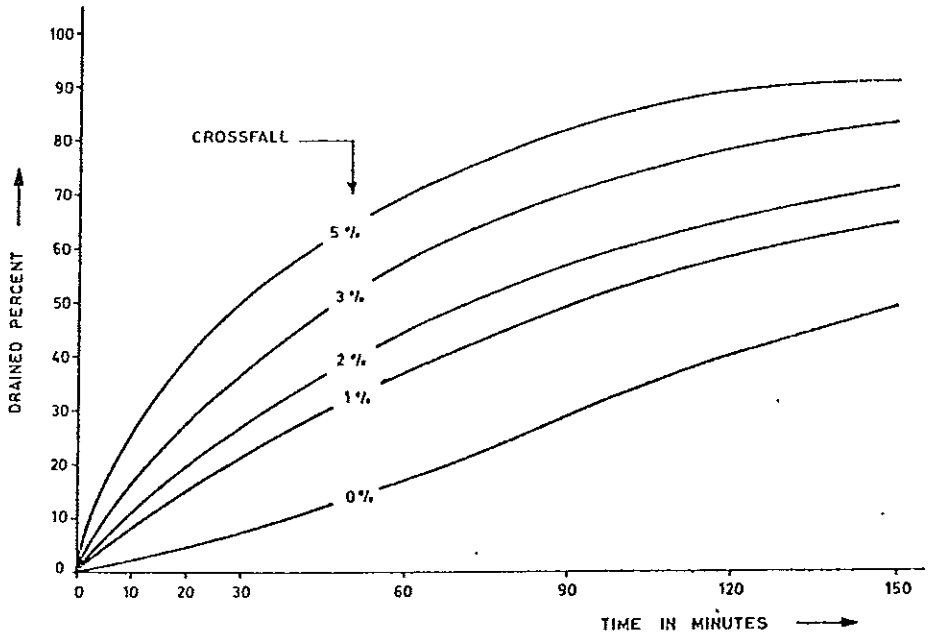

(After Welleman (23))

Figure 74. Percentage draining as a function of crossfall

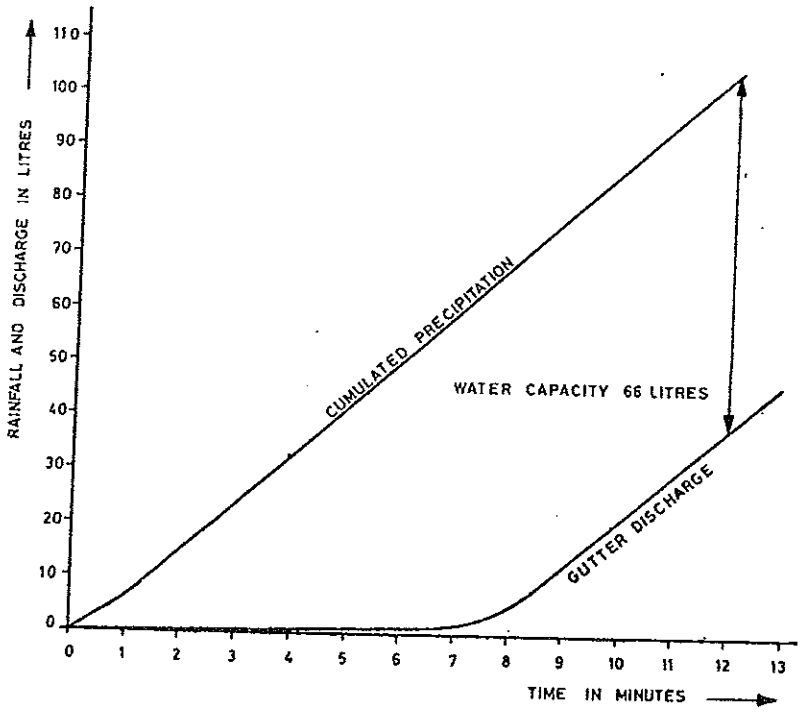

(After Welleman (23))

Figure 75. Rainfall and discharge as function of time

Welleman further postulated that the remaining permeable voids would be further reduced by traffic compaction and infiltration of debris -- and to this should be added aggregate breakdown and the effects of thermal cycling. In Holland where the porous surface was extended from the travelled roadway across the shoulder, certain areas of the shoulder were completely filled with debris thus reducing the total effectiveness of the porous surface subject to traffic.

Welleman, from a study of the weather in Holland, concluded that for 40 mm thick porous pavements with 12 to 13 percent permeable voids, 5 mm of rainfall can be stored in the mat. If this fact is combined with discharge rates shown in Figure 75, it may be deduced that splash and spray would be a problem only about 15 percent of the time during which rainfall occurs.

Wellemen also cited the advantage of using porous pavement surfaces as transitions to horizontal curves, and his photograph shown in Figure 76 clearly shows the long flow lines and flat area at the entry to such curves. He makes no mention of substrate cross slope for water removal, and he further emphasizes that controlled macrotexture be regarded as the most important favorable property of highly pervious asphaltic concrete.

Szatkowski and Brown (24) drew the following general conclusions regarding pervious surfacing used on British roads.

"(a) The 20 mm nominal size pervious macadam has a longer effective life under heavy traffic than the 10 mm friction course.

"(b) Useful spray reduction can be achieved under the heaviest motorway traffic (over 7000 commercial vehicles in nearside lane per day) for at least 3 years and under medium traffic (2500 CV/lane/day) for about 6 years.

"(c) Bitumen of lower viscosity than 100 pen should not be used as otherwise the spray-reducing life is shortened due to early compaction.

"(d) There is evidence that the type of bitumen may be important. The use of those bitumens which show a higher miscibility with oil is liable to lead to early compaction and should therefore be avoided."

Szatkowski and Brown rated chip seals, pervious macadam (open-graded friction courses) and rolled asphalt (dense-graded asphalt concrete) for their various merits and clearly placed pervious macadam surface first choice for friction, low noise and low spray at a cost of half that for rolled asphalt based on area covered. Noise values on pervious macadam were 6-8 dBA below the corresponding values for rolled asphalt.

Hutson (25) reported on the highly successful use of open-graded macadam for British airfield surfaces, the material for such surfaces being reported superior in performance to other common treatments including grooving and milling. The material as specified by the Air Ministry is described in the following quotation from Hutson's paper.

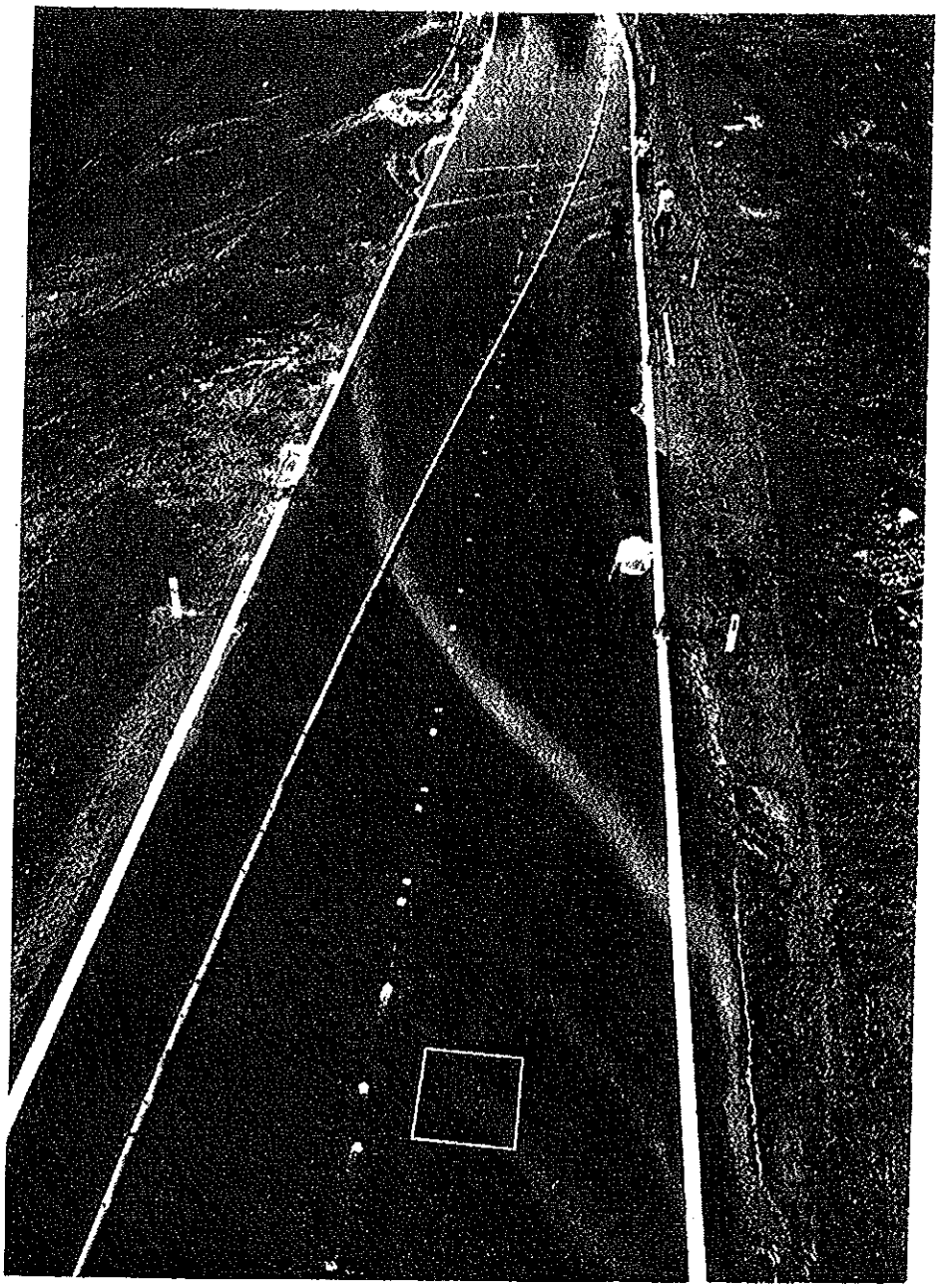

(After Welleman (23))

Figure 76. Lines of flow at a transition curve

"The aggregates shall be crushed rock of the following groups as classified in BS* 812: Granite, Basalt, Gabbro, Hornfels or Porphyry. When tested in accordance with BS 812 its flakiness index shall not exceed 25 percent, crushing value 16 percent and water absorption 1.5 percent. It shall also be subjected to test for soundness and stripping of binder. The grading of the aggregates shall be in accordance with the following table:

BS 410 Sieve mm	Percentage by Weight Passing
14 mm	100
10 mm	100 + 0 - 10
6.3 mm	48 ± 8
3.35 mm	25 ± 3
75 microns	4 ± 1

"Of the percentage of fines passing the 75 micron sieve 1.5 percent of the combined aggregate filler specified shall be hydrated lime. Should additional material of this grading be required it shall be supplied as crushed limestone.

"A 200 grade petroleum bitumen is used and the minimum binder content is laid down as 5 percent by weight. Mixing should take not less than 1 1/2 minutes at a temperature in the region of 100°C.

"The minimum thickness of the course at any point shall not be less than 20 mm after compaction and to achieve this minimum figure the material immediately prior to rolling should be spread to a thickness of about 27.5 mm. Rolling shall start at not less than 70°C and the carpet shall be rolled to refusal by 2 smooth wheeled rollers of 6 to 10 tons in weight at least one of which shall be of the three-wheeled type."

The required use of hydrated lime and crushed limestone filler is in line with recommendations of the authors of this report. When hydrated lime is brought into intimate contact with wet aggregate prior to paving mixture production it acts as an antistrip device as well as filler. Furthermore, and in this vein, Plancher,et al. (26) reports the beneficial effects of hydrated lime in asphalt cement indicating that lime reacts with the carboxylic acids 2-quinoline types of asphalt to neutralize these acids and eliminate their interference with the aggregate-to-asphalt bond. Liddle, et al. (27) and Plancher, et al. (28) reported further on the use of hydrated lime for reducing the hardening rate of asphalt. The use of hydrated lime as an effective antistrip device is practiced by several contractors in Texas. The claimed additional benefit of reduced asphalt hardening has not been studied in Texas.

* British Standard

Gallaway and Epps (29) made reference to problems associated with design, construction and performance of open-graded bituminous surfaces. Among other things these writers warned that "Open-graded mixtures, however placed, must never be considered to form a waterproof cover on a pavement being modified by their use. To the contrary, they invite the intrusion of water." This statement is independent of the thickness of the open-graded layer. The design engineer should take this observation into account in maintenance planning.

Gallaway and Epps also reported on laboratory freeze-thaw tests on 21 different designs which utilized 11 different aggregates. Asphalt content as a variable was also included. The specimens used were cores taken from various in-service pavements, and the samples were fixed in jigs fitted into a rapid freeze-thaw cabinet meeting the general requirements of ASTM C-666-77. Special holders were designed to support the cores in the cabinet, and replicate tests were performed freezing first from the bottom and then from the top of the cores. The general conclusion from these tests is that no significant damage resulted from up to 100 rapid freeze-thaw cycles in any of the samples tested except for one set of specimens which utilized limestone as the major aggregate. High water absorption was probably a causative factor.

These authors also reported on water outflow or permeability measurements made on in-service porous surfaces. The data are shown in Figures 77 and 78 which show SN_{40} vs traffic for these surfaces. Most of these surfaces are still in service with some having accumulated more than 40 million vehicle repetitions. Current outflow values are at the four to five million vehicle level shown. An explanation for early closing of these surfaces is the limited thickness. It should be noted that most of these mixture designs contained little or no fines and therefore did not conform to recommended FHWA mixture design. In general these surfaces were 3/4 in (19 mm) in thickness or less initially and were ultimately reduced to about 1/2 in (13 mm) in thickness. True internal drainage is minimal today some four to six years after construction.

Smith (30) investigated, among other items, the rate of hardening of asphalt in asphalt concrete mixtures and concluded that within the normal range of voids for this type of mixture design that air void content permeability had a minimal effect on binder hardening rate. However, Smith's data appear to show that limestone filler reduced the rate of hardening (see Figure 79). These data are from a segment of the Blair County (Pennsylvania) experimental pavements utilizing slag, wyant conglomerate and limestone filler. This observation is mentioned here because open-graded friction courses require nominal amounts of filler. Further, the European practice favor hydrated lime and limestone dust, and, as mentioned previously, Texas' experience with hydrated lime is promising.

Smith also looked at inundation times for open-graded friction courses for various rainfall intensities. His reported theoretical drainage capacities are roughly an order of magnitude higher than those measured and observed by the Texas Transportation Institute.

White (31) looked at the performance of porous friction courses on airfields across the entire United States. The concluding remarks presented, as they may apply to highway pavements, are

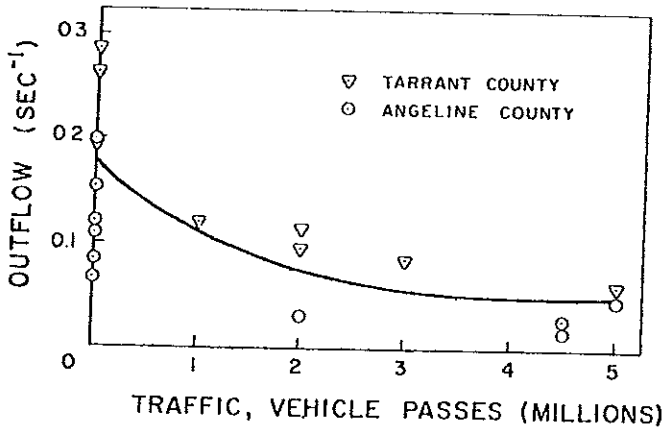

(After Gallaway & Epps (29))

Figure 77. Outflow meter shows traffic effects on open-graded friction course

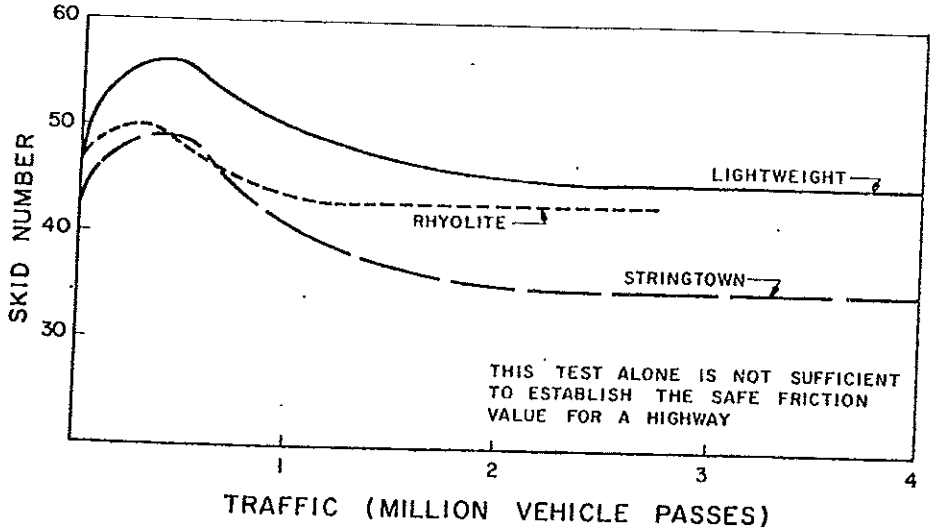

(After Gallaway & Epps (29))

Figure 78. Skid resistance of plant-mix surface course

a) Porous surfaces should be used only on structurally sound substrates.

b) The FHWA (32) mixture design procedure utilizing the relationship $2K_c + 4$ to estimate bitumen content can be used with confidence.

c) Consideration must be given to the temperature-viscosity relationship to optimize mixing and construction temperatures.

d) To verify bitumen drainage characteristics conduct a two-hour conditioning time at a temperature giving a viscosity of 275 centistokes (275 $\mu m^2/s$). Drain down should not be excessive.

Nystrup (33) of Denmark reported that open-graded surfaces placed in medium heavy service lost their permeability rather quickly; however, these surfaces continued to give good drainage on the top in connected surface channels giving reasonably high friction values even in heavier rainfall. After two years of service the Denmark surfaces produced less splash and spray and lower levels of night glitter than dense surfaces under the same wet-weather conditions.

Nystrup's data on permeability measured on field cores showed large standard deviations, and this was attributed to binder run down due to inadequate temperature control during construction. Similar observations have been made in the United States. The Federal Highway Administration has consistently recommended the use of some intermediate sized aggregate with fixed amounts of minus No. 200 mesh material, and the Federal Aviation Administration grading requirements include 3 to 5 percent passing the No. 200 sieve.

The controlled use of adequate filler broadens the range of construction temperature and thus reduces the problem of binder run-down.

Gerardu (34) reported on the comparative skid resistance of different types of road surfaces in the Netherlands, and these are summarized in Figure 80. . These are locked wheel values made with a smooth tire and at a water depth of 1 mm. Based on Dutch findings reported at the International Symposium on Porous Pavements, porous surfaces would be ranked above surface 5 (see Figure 80), open-textured asphalt concrete. Such surfaces would be less speed sensitive under wet conditions by a factor of about 4 as determined by the equation:

Relative decrease (RD) of the coefficient of friction

$$RD = \left(\frac{f\ 50 - f\ 70}{f\ 50}\right)(100\%)$$

where $f\ 50$ = friction at 50 km/h

$f\ 70$ = friction at 70 km/h

Hatherly and Lamb (35) pointed out the problems of silting of open-graded surfaces on curbed streets in urban areas particularly where the longitudinal grade was limited. These authors also reported on the use of additives to porous surfaces. Included were natural rubber, polyethylene powder and special asphalts with high penetration indices. As thin overlay surfaces none of these

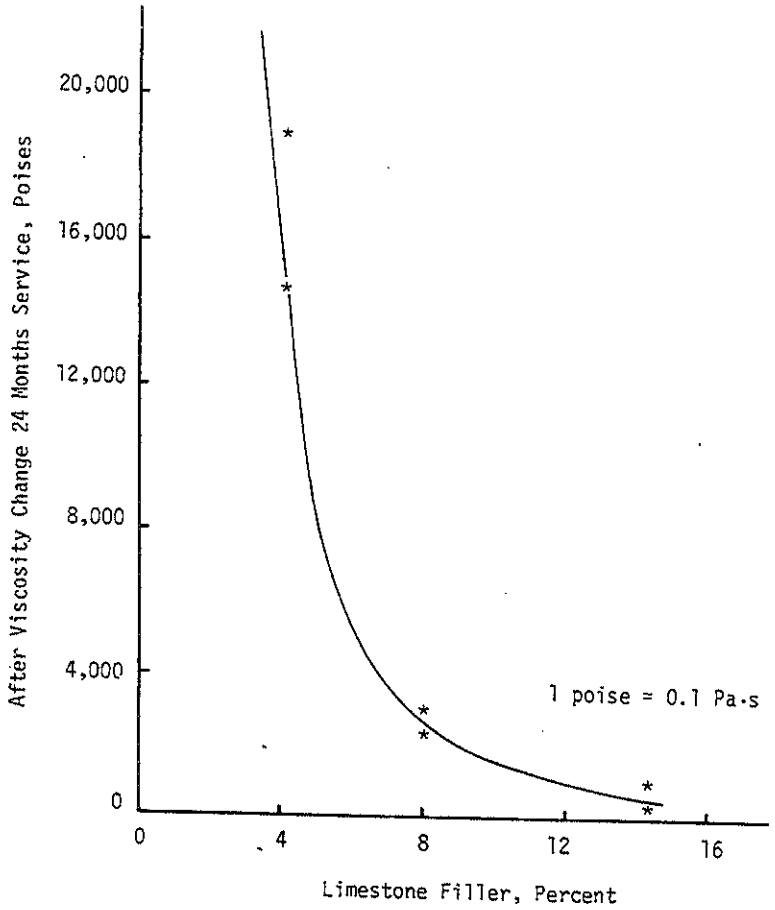

Figure 79. Effects of limestone filler on asphalt hardening rate

(After Smith (30))

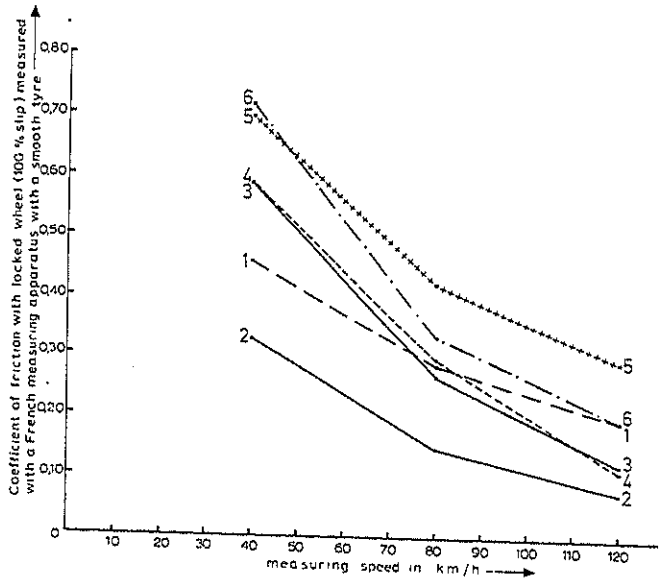

Section	Type of Pavement	Age (years)	Average texture depth (mm)
1	Cement concrete	9	0.5
2	Coarse dense asphaltic concrete	14	0.3
3	Coarse dense concrete	2–4	0.4
4	Fine dense asphaltic concrete	2	0.4
5	Open textured asphaltic concrete	2	1.0
6	Surface dressing	2	0.8

Figure 80. Coefficient of friction as function of the speed on various pavements

(After Gerardu (34))

changes in selected and modified binder types was effective; however, epoxy-bitumen binders of high bond strength were quite cost effective.

Beaton (36) reporting at The Second International Conference on Skid Resistance had the following statements to make, which statements have a direct bearing on the problem of wet-weather accident reduction.

> "The paving engineer has the responsibility to provide adequate tire-pavement friction for contemplated operating conditions and for a satisfactory period of service. At the present time he does not have the required tools to fulfill these requirements with the necessary degree of confidence, especially when one considers the economic aspects of pavement design and construction. The following areas are recommended for high priority attention by researchers and paving engineers. A most important objective for the future is the development of laboratory methods, properly correlated with field studies, that will provide test specimens which represent all forms of pavement surfaces, a wear and polish system that simulates the action of traffic and, finally, methods of friction measurement that will recognize micro and macrotexture effects through the operating range of vehicle speeds. The accomplishment of these tasks is far from complete. Their importance cannot be overstressed since an increasing amount of effort is being extended on determining minimum standards for skid resistance. Once such standards are adopted, the designer must have the tools to design a surface to meet the standards.
>
> "Another immediate need is for intensive study of construction practices for both asphalt and portland cement concrete. Design of equipment to produce an adequate surface texture for portland cement concrete pavement is needed. Such a surface to provide the desired initial requirements for micro and macro-texture and prevent such values from falling below a minimum value during the assumed service life.
>
> "Studies should also be initiated on construction control parameters that influence the uniformity of pavement friction values and surface undulations (this latter is of special importance to runways)."

Smith (37) in assessing the need for a basic approach to improved tire-pavement interaction stated that:

> "...A reasonable approach to development of pavement skid-resistance requirements may be the determination of requirements for groupings of roadway site types such as a) level and nearly level tangents, b) steep grades, c) long-radius curves, d) short-radius curves, e) intersections, and f) special situations.

It should also be recognized that skid resistance is not the only factor that influences the safety or the hazard potential of a site. Traffic volume and speed plus the prospect for wet-pavement conditions all should be considered when determining surface characteristics for safe operation."

Good engineering judgment and economic limitations will continue to rule favorably in the direction that Smith has outlined above. Smith stated further in his summary that:

"There is increasing recognition of the importance of the macrotexture and surface drainage of pavements to reduce the effects of hydroplaning during wet weather. Use of adequate cross slope, particularly on long-radius curves, open-graded asphaltic concrete surfaces, and grooved or tined portland cement concrete surfaces should result in reductions in wet-weather accidents on highways."

Gramling (38) in summarizing his view on the development and implementation of a program to reduce skid accidents states:

"...Attainment of the objective to provide safe skid resistant pavements adequate to meet the needs of the motoring public requires a systematic approach. The elements of the system should include the ability to reliably determine skid resistance values with dependable test equipment, methods of locating and surveying pavement surfaces, and a means of rating pavement performance. Finally, specifications should provide for economic, predictable, and adequate friction properties through the anticipated life of new surfaces or for surfaces placed as a corrective action."

Hatherly and Young (39) presented findings on the location and treatment of urban skidding hazard sites and in general concluded that:

"1. In Great Britain about 70 percent of all road accidents occur in urban areas.

"2. In London, about 70 percent of all accidents occur on road junctions on about 10 percent of the total road network. Nationally about half of all road accidents occur on urban junctions.

"3. The skid resistance of asphalt roads can be predicted from a knowledge of the stone used in the surfacing, the traffic intensity, and whether or not the traffic is maneuvering (braking, turning or accelerating).

"4. Although the existing tentative minimum standards of skid resistance for city junctions are suspect, route measurements of skid resistance and accident data may be used to indicate junctions where a skid resistance improvement can be expected to reduce accidents.

"5. Over 800 junctions and other hazard areas such as the approaches to pedestrian crossings in London have been treated with epoxy resin/calcined bauxite which has reduced accidents by 31 percent or about £2,500* per annum, at the treated sites.

"6. The economics of this form of treatment are shown to be exceptionally favourable and an expenditure of £3m over a 10 year period is estimated to produce a saving in accident costs of at least £24m at 1970 values.

"7. The localized treatment of city road junctions could well be a successful method of accident reduction in many major cities."

It is doubtful that similar data gathered in major urban areas of the United States would indicate appreciably different accident rates and/or potential savings by the application of effective remedial measures.

In a recent report by Halstead (40) a number of points dealing with fundamental consideration and research needs were raised including:

1. The role of OGFC in minimizing hydroplaning danger during heavy rains,
2. Optimum gradation of OGFC for skid prevention,
3. Optimum asphalt content and grade for maximum durability,
4. Effect of OGFC on winter maintenance techniques and
5. Noise levels for OGFC.

The first of these items has been discussed at length. No further comment will be made. The second item dealing with aggregate grading is critically important since size and size distribution, although of primary importance, are not sufficient in themselves to fix the effect of grading. Particle shape and surface texture as well as hardness and toughness are critical factors. Such properties as water susceptibility,adsorption and absorption may well be the difference between success and failure of a given surface. Certain types of siliceous aggregates may, for example, require pretreatment with hydrated lime or possibly portland cement to minimize stripping.

The grade of asphalt cement that may be successfully used depends heavily on mixing, and laying temperatures and the type and amount of filler and/or additive (such as rubber or carbon black) that may be included in the design. For those who are new users of this friction improvement system an AC-20 or equal is suggested as a starting point. With experience and select types and gradations of aggregates the use of a softer or harder asphalt cement might be advisable.

Maintenance of OGFC is difficult any time since the use of standard patching materials creates an undesirable difference in permeability of the overall surface. Current experiments in Texas indicate that delaminated

*British pound sterling

areas may be successfully repaired by a formed-in-place open-graded patch. The technique involves filling the area with selected uniform graded aggregate, bring this to line and grade and then spraying the area with a rapid setting emulsion. The voids are filled about three-fourths full of emulsion. After the emulsion breaks the surface may be released to traffic.

Field Experiments by TTI

In the total array of pavement construction and maintenance techniques there exists a limited number of economically practical measures that may be taken to assure long lasting high performance surfaces for medium-to-heavy traffic.

Efforts to develop new techniques to be used as partial or complete solutions to the problem have been reasonably successful. Among the several methods now in use, open-graded friction courses (OGFC) offer considerable promise.

Since the introduction of OGFC in the United States several years ago, a large number of states has developed mixture designs suited to their individual materials, traffic and environment. This has resulted in some cross pollenization, some of which has resulted in improved performance and some of which has caused unanticipated problems.

Theoretical mixture designs have been developed to allow control of air voids which in turn control to a reasonable degree the permeability of the in-place surface layer. However, the variables encountered have, in many instances, raised questions about the total drainage capability of OGFC, particularly under medium-to-heavy traffic.

Generally speaking, after about one to three million vehicle passages (applied at a rate of one million passages per year or greater) current applications of OGFC stabilize with respect to splash and spray, drainage and SN_{40}. This assumes that the thickness of the layer placed is in the approximate range of 20 to 30 mm and the aggregate is nonpolishing.

Field measurements made in Texas indicate that OGFC offer a positive means to control macrotexture at a generally higher level than current dense-graded asphalt concrete designs permit. This controlled greater macrotexture allows better drainage at the tire-pavement interface, irrespective of any internal drainage. Internal drainage in the dynamic sense is appreciably reduced after the surface layer stabilizes.

An extensive testing program was therefore initiated to assist in the classification of the performance of OGFC. The test plans for the various experiments carried out on different pavement sections are shown below.

Plan No. 1:

4 - Pavements (Section 1, >25 percent voids; Section 2, 25 percent voids; Section 3, 20 percent voids; and Section 4, 15 percent voids.)

2 - Rainfall Rates 1/2 and 2 in/h (13 and 51 mm/h)

4 - Tires - ASTM E501 (Full tread depth)
Steel Belted Radial (2/32 in) (1.6 mm)
Bias Ply (2/32 in) (1.6 mm)
Glass-Belted Wide Tire (2/32 in) (1.6 mm)

2 - Tire Pressures - 18 psi and 24 psi (124 and 165 kPa)
ASTM E501
Steel Belted Radial
Bias Ply
Recommended and 75 percent of recommended
Glass Belted Wide Tire

1 - Lane - Outside Wheel Path - Outside Lane

1 - Wheel load of 1085 lbs (4830N)

3 - Speeds of 30, 40 and 55 mph (48, 64 and 88 km/h)

5 - Runs per combination of conditions for repeatability

Total number of runs this plan = 4 x 2 x 4 x 2 x 3 x 5 = 960

Plan No. 2:

Same as Plan No. 1 as related to Rainfall Rates, Tire, Tire Pressures, Loads, Speeds and Number of Runs for Repeatability.

In this plan, on pavement Section No. 2 (25 percent voids), the program will be run in the outside wheel path of the inside lane.

Plan No. 3:

Same as Plan No. 1 as related to Rainfall Rates, Tires, Tire Pressures, Load, Speeds and Number of Runs for Repeatability.

In this plan, on pavement Section No. 2 (25 percent voids) the program will be run in the outside wheel path of the outside lane.

Also an impermeable shoulder will be created by sealing the outside edge of the surface to prevent the water from draining out.

The test sequence used in carrying our these plans was as follows:

	Master Plan
	Test Sequence
	Highway 21 Phase
SECTION NO. 1 -	Outside Lane - Outside Wheel Path
	Test Plan No. 1
SECTION NO. 2 -	Outside Lane - Outside Wheel Path
	Test Plan No. 3
	Outside Edge of Surface sealed to Simulate Impermeable Shoulder

SECTION NO. 2 - Outside Lane - Outside Wheel Path
Test Plan No. 2

SECTION NO. 3 - Outside Lane - Outside Wheel Path
Test Plan No. 1

A schematic of the layout of the four subsections of OGFC is shown in Figure 81. Each section is two lanes wide and about 500 ft (152 m) long and all sections are cross sloped at 1 percent toward the paved shoulder (see Figure 82). When constructed the voids in the four sections varied from more than 25 percent in Section 1 to about 15 percent in Section 4. Mat thickness was controlled at 1 in (25 mm) (see Figure 83).

Water on these sections was supplied by use of a rain simulator shown in Figure 84. Details of this apparatus have been reported previously (9) and will therefore not be repeated here.

In the operation of the rain simulator the correct rainfall intensity was controlled by pump discharge pressure and carefully monitored by actual "rainfall" measurements made under the simulator. Twin tankers are shown in Figure 85.

Since the depth of water on the test surface was a critical parameter, this was measured at designated points on the pavement with a point gage as reported (9) and shown in Figure 86. After the rain simulator was put into operation and the pump discharge pressure had stabilized, water depth measurements were taken in the lane to be tested at five minute intervals until the water depth became stable. When water depth stability was attained, testing began. The rainfall intensities investigated were 0.2 to 2 in/h (5.1 to 50.8 mm/h). Tests are underway in a 2 in/h (50.8 mm/h) rainfall in Figure 87.

Tire-Pavement Interaction on OGFC

Results of about 4000 tire-pavement interaction tests on the four pavement sections are presented in the following 31 graphs. For convenience of discussion these graphs have been grouped as follows:

Group A

Skid number vs speed ASTM E274 standard test method with ASTM E501 tire with 11/32 in (8.7 mm) tread depth -- all test sections.

Group B

Skid number vs water depth for ASTM E501 tire with 11/32 in (8.7 mm) tread depth -- all test sections.

Group C

Skid number vs water depth for steel belted radial (SBR) with 2/32 in (1.6 mm) tread depth -- all test sections.

Group D

Skid number vs water depth for glass belted, bias ply tire (F-78-14) with 2/32 in (1.6 mm) tread depth -- all test sections.

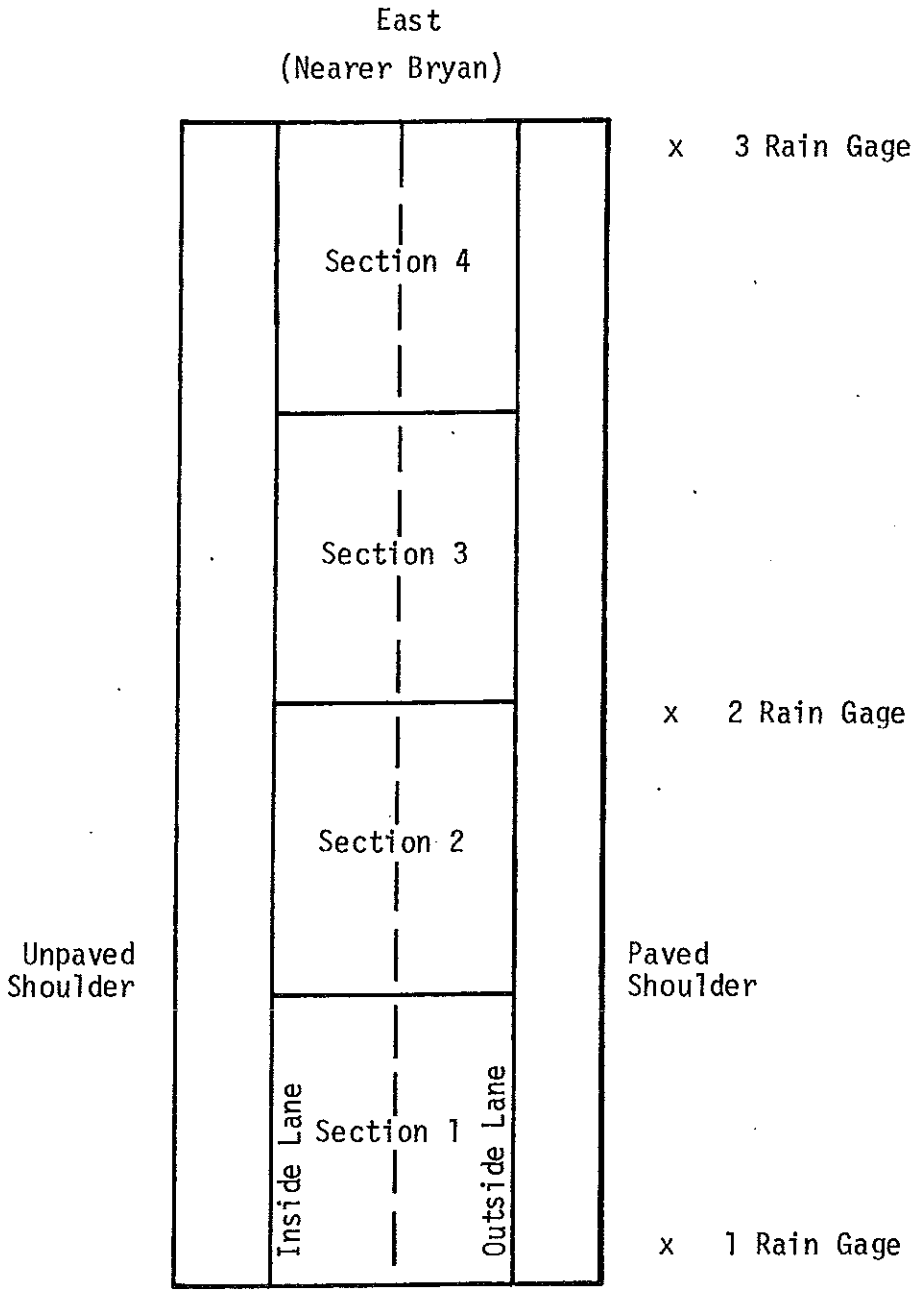

Figure 81 . Test layout and rain gage locations - SH-21.

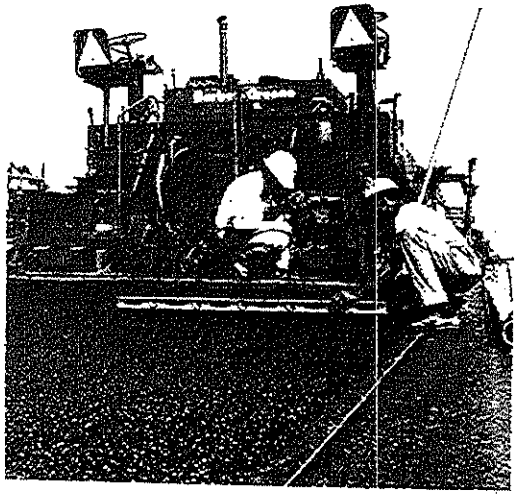

Figure 82. Cross slope of the finished OGFC on SH-21 was checked at regular intervals during construction

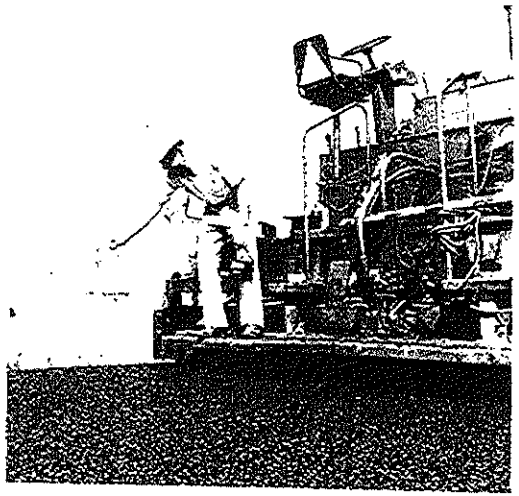

Figure 83. During construction mat thickness was monitored closely on SH-21 Brazos County

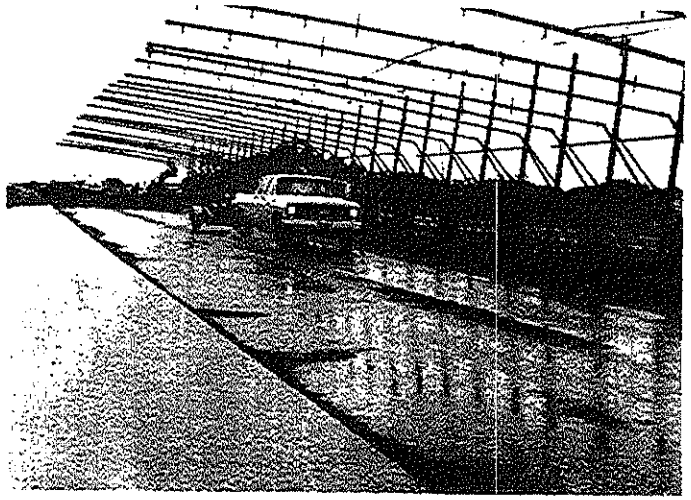

Figure 84. Testing OGFC at 30 mph (48 km/h) on SH-21 Brazos County (Rainfall intensity about 0.5 in/h (13 mm/h))

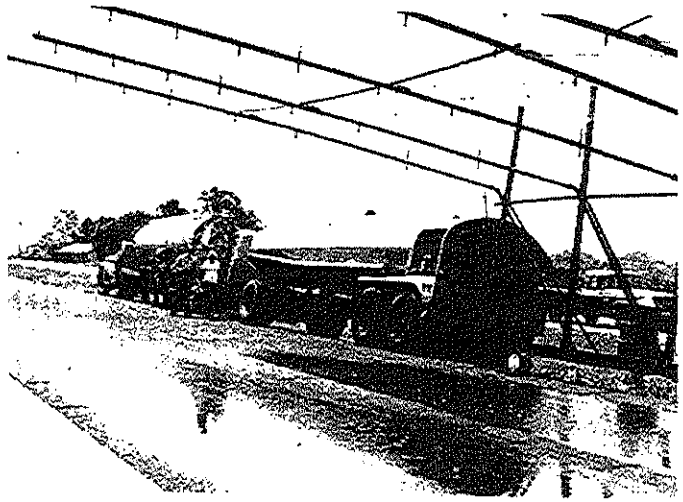

Figure 85. Water was supplied to the rain simulator on SH-21 by two 5000-gallon (19 m^3) tankers. Both tankers were equipped with separately powered centrifugal pumps mounted at the rear of the tankers

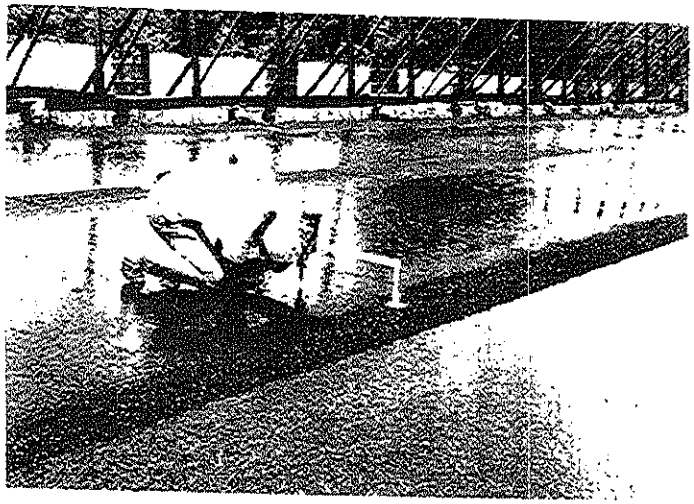

Figure 86. Prior to testing, water depths for each fixed rainfall intensity was carefully measured (Segments of rain simulator in the background)

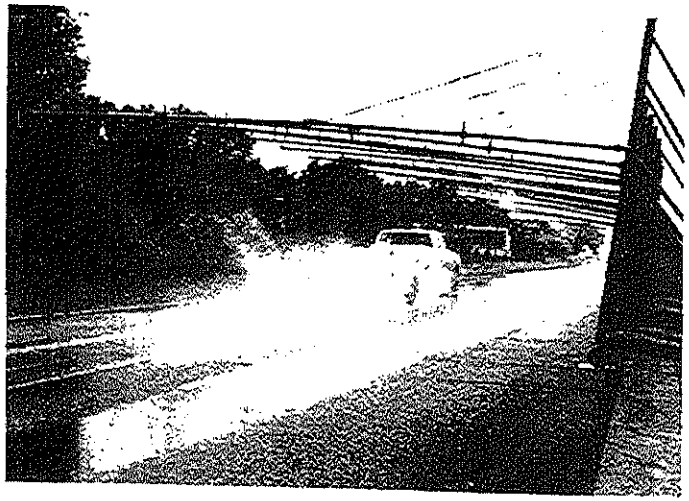

Figure 87. Testing OGFC at 55 mph (88 km/h) on SH-21 Brazos County (Rainfall intensity about 2 in/h (25 mm/h)

Group E

Skid number vs water depth for glass-belted bias-ply wide-oval tire (G-60-14) with 2/32 in (1.6 mm) tread depth -- all sections.

Group F

Skid number vs water depth for ASTM E501 with 11/32 in (8.7 mm) tread SBR* with 2/32 in (1.6 mm) tread, F-78-14 with 2/32 in (1.6 mm) tread and G-60-14 with 2/32 in (1.6 mm) tread. Section 2 with a simulated sealed shoulder.

Group G

Skid number vs water depth for glass-belted bias-ply F-78-14 and steel-belted radial FR-78-14 both at 24 psi (165 kPa) inflation pressure and 5/32 and 11/32 in (4.0 and 8.7 mm) tread depth -- Section 2 only.

Group H

Skid number vs water depth for glass-belted bias-ply (F-78-14) 2/32 in (1.6 mm) tread depth -- Section 2 only with sealed and unsealed shoulder and at various positions from the outside edge of the pavement.

Group I

Skid number vs speed for

1) ASTM E501 11/32 in (8.7 mm) tread depth 24 psi (165 kPa) and 0.5 in/h (12.7 mm/h) simulated rainfall -- all test sections.
2) ASTM E501 11/32 in (8.7 mm) tread depth 24 psi (165 kPa) and 2.0 in/h (51 mm/h) simulated rainfall -- all test sections.
3) Average of SBR* F-78-14, G-60-14 all at 24 psi (165 kPa) 2/32 in (1.6 mm) tread with 0.5 in/h (12.7 mm/h) simulated rainfall -- all sections.
4) Average of SBR F-78-14, G-60-14 all at 24 psi (165 kPa) and 2/32 in (1.6 mm) tread with 2.0 in/h (51 mm/h) simulated rainfall -- all sections.

Discussion of Performance of Open Mixes in Simulated Rain

Group A - The equipment and test procedures utilized to obtain those data presented in Figure 88 comply with ASTM Designation E274. These tests were conducted approximately midway in the overall test program, and check tests were made at the end of the simulated rain studies to determine whether or not significant changes as measured by ASTM E274 procedure had occurred. These check tests revealed no significant change in measurements obtained.

It is apparent from Figure 88 that all four surfaces have high skid numbers and are not very sensitive to speed.

*SBR - steel belted radial

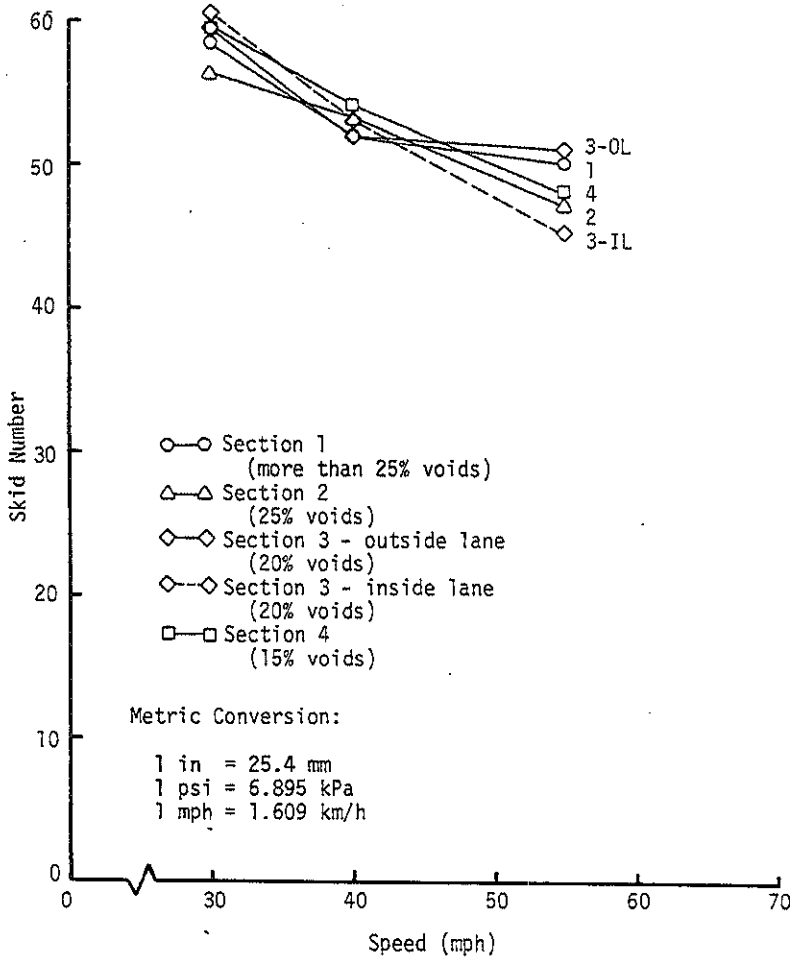

Figure 88. Skid number vs. speed from ASTM standard test method E274 (ASTM standard tire E501 with 11/32 in tread depth on all sections with internal water)

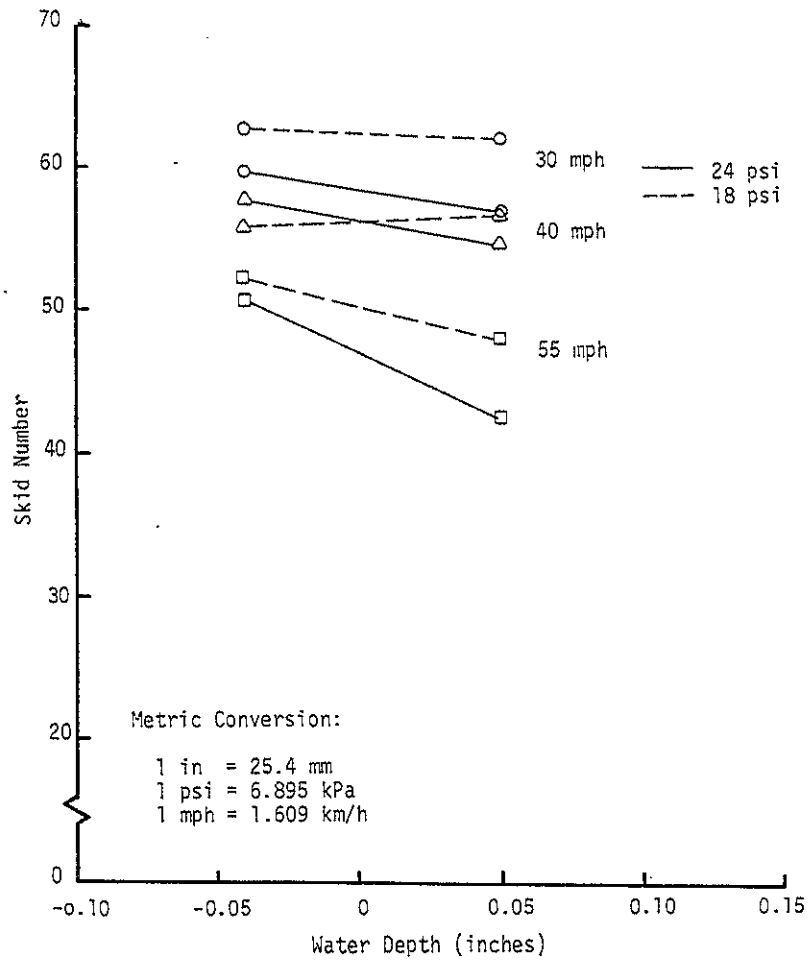

Figure 89. Skid number vs. water depth for ASTM standard tire E501 with 11/32 in tread depth on Section 1, outside wheel path of outside lane

In a study of the many graphs that follow, the reader will want to refer back to Figure 88 for comparison purposes.

Group B - Test Sections 1, 2, 3 and 4 were evaluated at 30, 40 and 55 mph (48, 64 and 88 km/h) using the ASTM E501 tire with 11/32 in (8.7 mm) tread in simulated rain. Rainfall rates were adjusted to produce water depths in the outside wheel path of the outside lane in the range of about 0.06 in (1.5 mm) above the asperity peaks to 0.05 in (1.3 mm) below the asperity peaks. Tests were made at tire pressures of 18 and 24 psi (124 and 165 kPa).

The results are presented in Figure 89, 90, 91, 92 and 93. A review of these figures will indicate that at speeds of 30 and 40 mph (48 and 64 km/h) all sections performed essentially alike. This, however, is not the case at 55 mph (88 km/h). The influence of voids becomes clearly evident in Section 3 in the outside wheel path of both lanes. In Figure 91 water was increased to about 0.12 in (3 mm). At 55 mph (88 km/h) and with a tire inflation pressure of 18 psi (124 kPa) the skid number is minimal. However, even at this speed, tire inflation pressure and water depth, the full tread of the tire and pavement macrotexture coupled with some internal pressure relief, dynamic hydroplaning did not occur.

The speed sensitivity of pavement Section 4 (high percentage of minus No. 8 material and low voids) was not unexpected. An extrapolation of the 55 mph (88 km/h) data to a water depth of approximately 0.12 in (3 mm) would indicate probable dynamic hydroplaning in spite of the drainage furnished by the full tread.

Group C - In this series of tests a steel-belted radial tire with the legal minimum of 2/32 in (1.6 mm) of tread was evaluated at speeds of 30, 40 and 55 mph (48, 64 and 88 km/h) under simulated rainfall. Again, tire inflation pressures were at two levels, namely 18 and 24 psi (124 and 165 kPa). Water depth values varied from 0.07 in (1.8 mm) below the asperity peaks to about 0.12 in (3 mm) above the asperity peaks. Rainfall intensities required to create this range of water depths was about 0.2 to 2.0 in/h (5 to 51 mm/h). Graphs are shown in Figure 94, 95, 96, 97 and 98.

A study of the composite trends shown in this series of graphs reveals that, as was generally true in the Group B curves, at speeds of 30 and 40 mph (48 and 64 km/h) skid numbers were in the 40 to 60 range; two exceptions being a value of SN_{40} equal to 35 for Section 3 outside wheel path of the inside lane with the tire pressure at 18 psi (124 kPa) and Section 4 with an SN_{40} of less than 40 for a tire pressure of 18 psi (124 kPa).

The picture for 55 mph (88 km/h) is quite different, particularly, for positive water depths. Skid numbers at 55 mph (88 km/h) are in the 15 range for Sections 3 and 4.

Figure 98 spans a rather restricted water depth range because of accident risk that was minimized by reduced water depths. Simulated rainfall intensity was approximately 0.2 in/h (5 mm/h).

Group D - The Group D series of tests was carried out in simulated rain with the intensity adjusted to produce an acceptable range of water depths

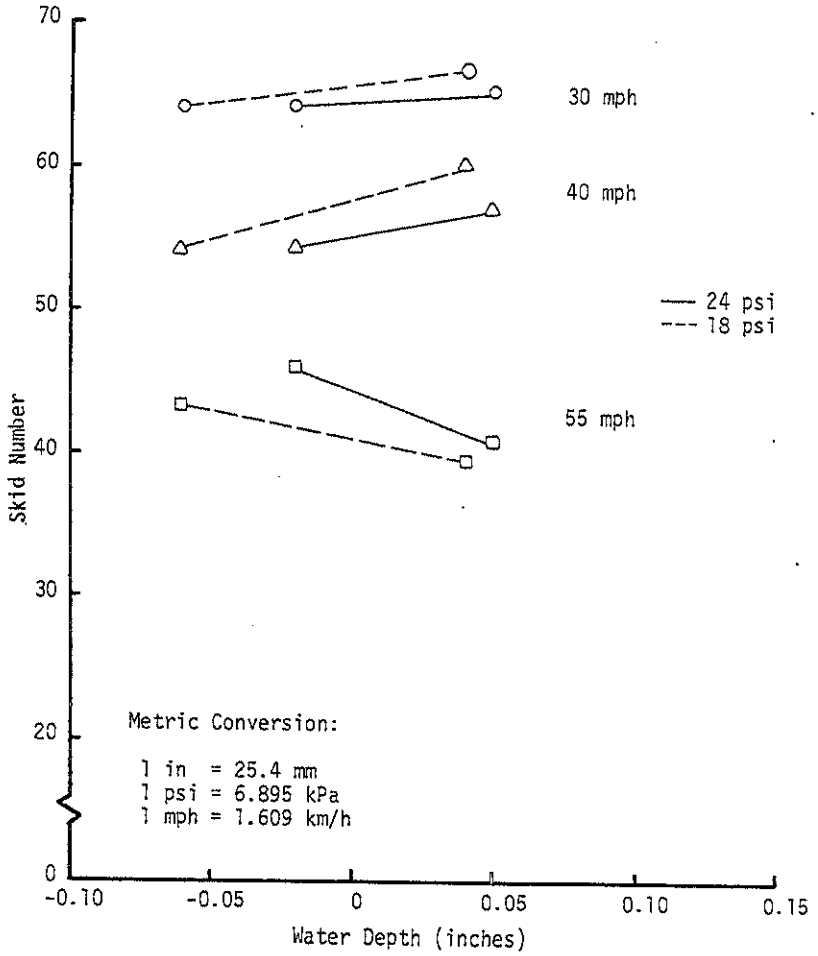

Figure 90. Skid number vs. water depth for ASTM standard tire E501 with 11/32 in tread depth on Section 2, outside wheel path of outside lane

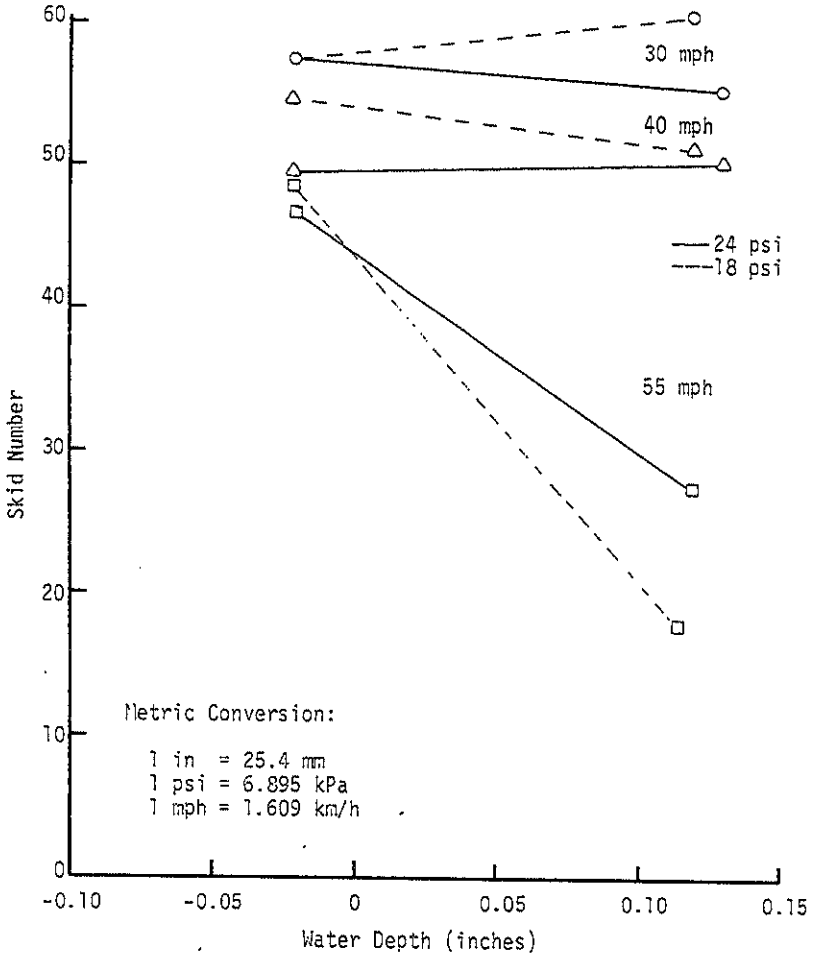

Figure 91. Skid number vs. water depth for ASTM standard tire E501 with 11/32 in tread depth on Section 3, outside wheel path of inside lane

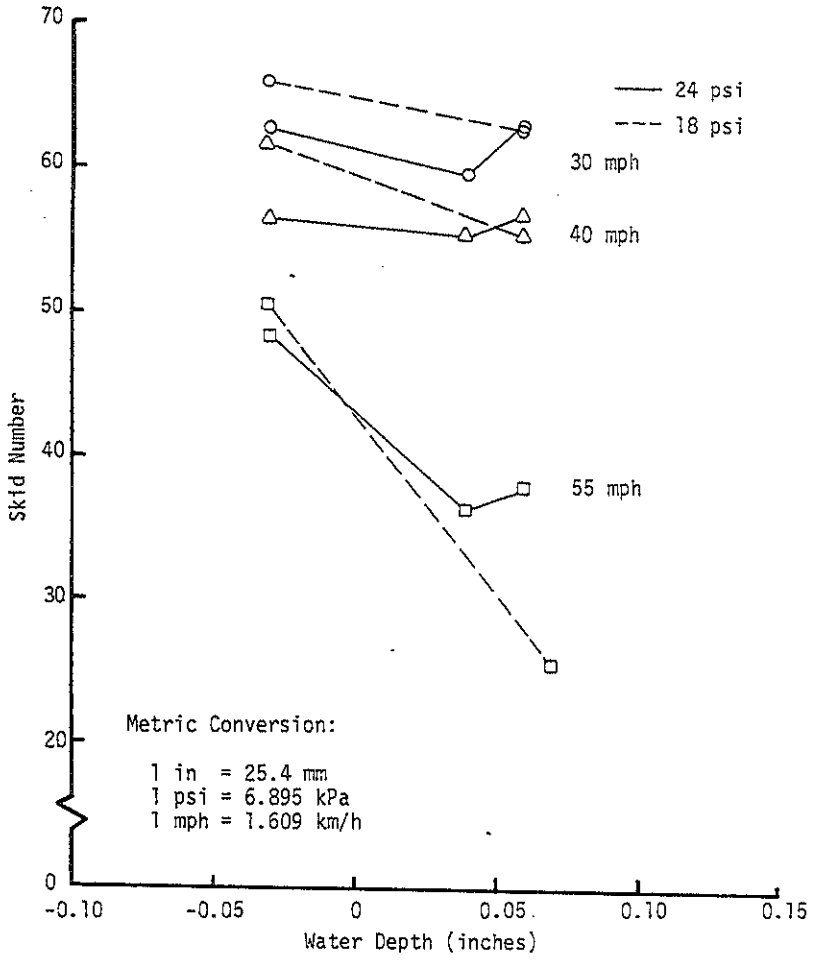

Figure 92. Skid number vs. water depth for ASTM standard tire E501 with 11/32 in tread depth on Section 3, outside wheel path of outside lane

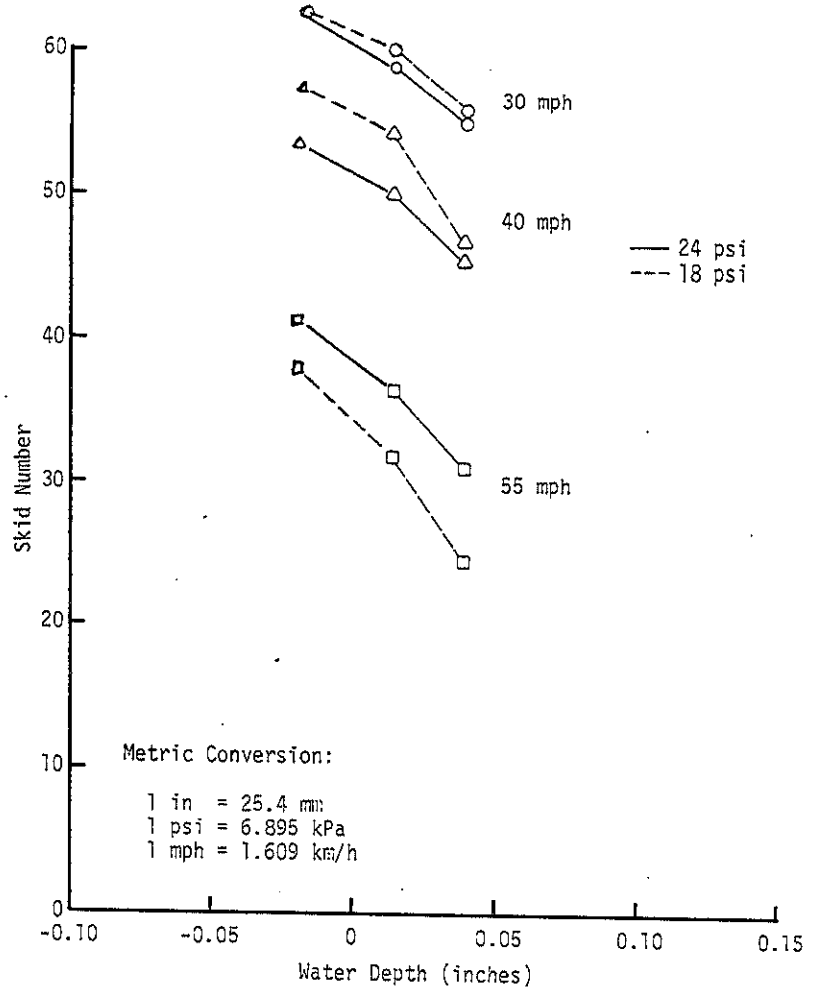

Figure 93. Skid number vs. water depth for ASTM standard tire E501 with 11/32 in tread depth on Section 4, outside wheel path of outside lane

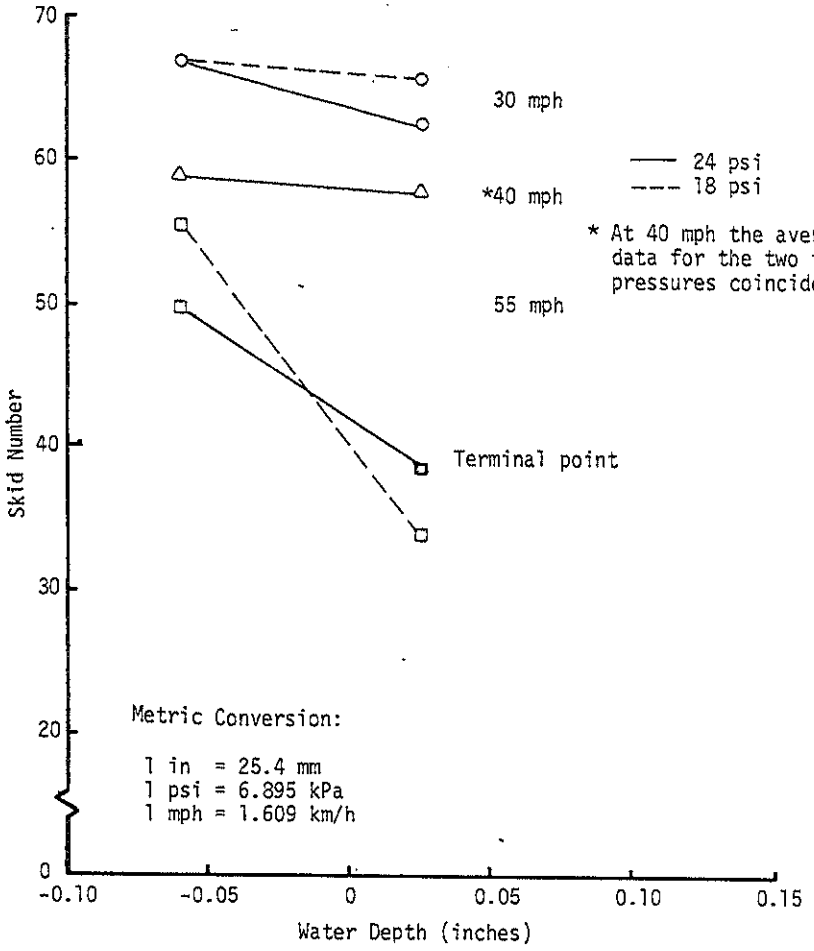

Figure 94. Skid number vs, water depth for steel-belted radial (SBR) with 2/32 in tread depth on Section 1, outside wheel path of outside lane

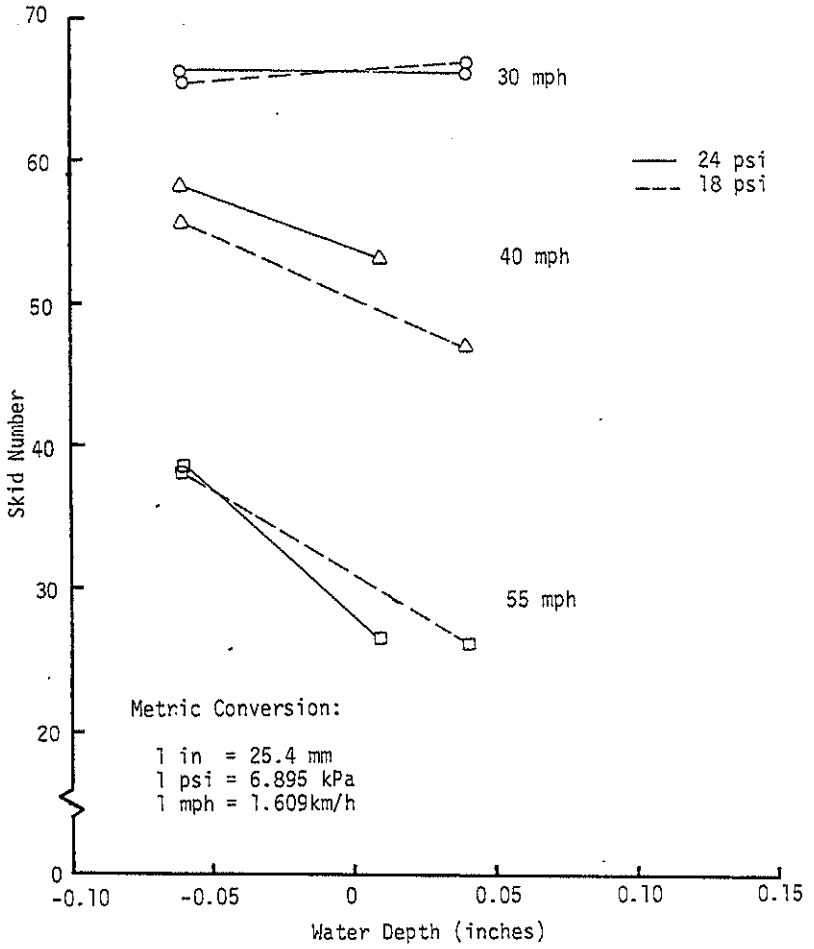

Figure 95. Skid number vs, water depth for steel-belted radial (SBR) with 2/32 in tread depth on Section 2, outside wheel path of outside lane

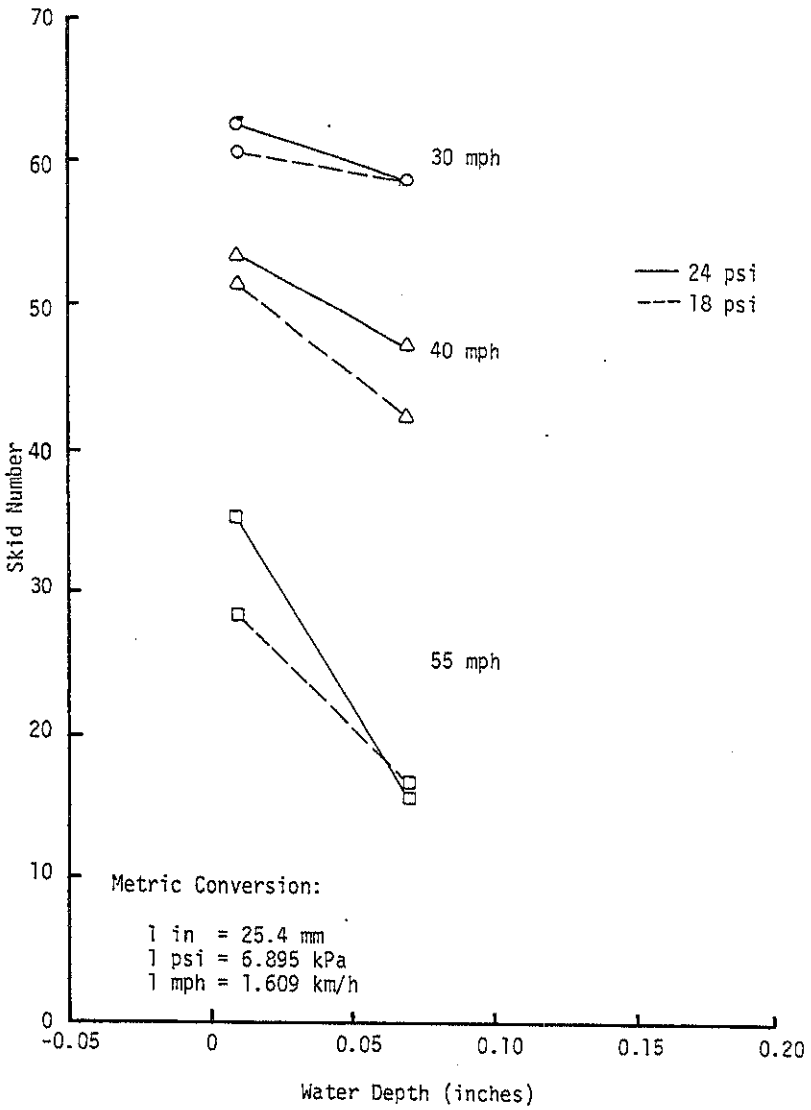

Figure 96. Skid number vs. water depth for steel-belted radial (SBR) with 2/32 in tread depth on Section 3, outside wheel path of outside lane

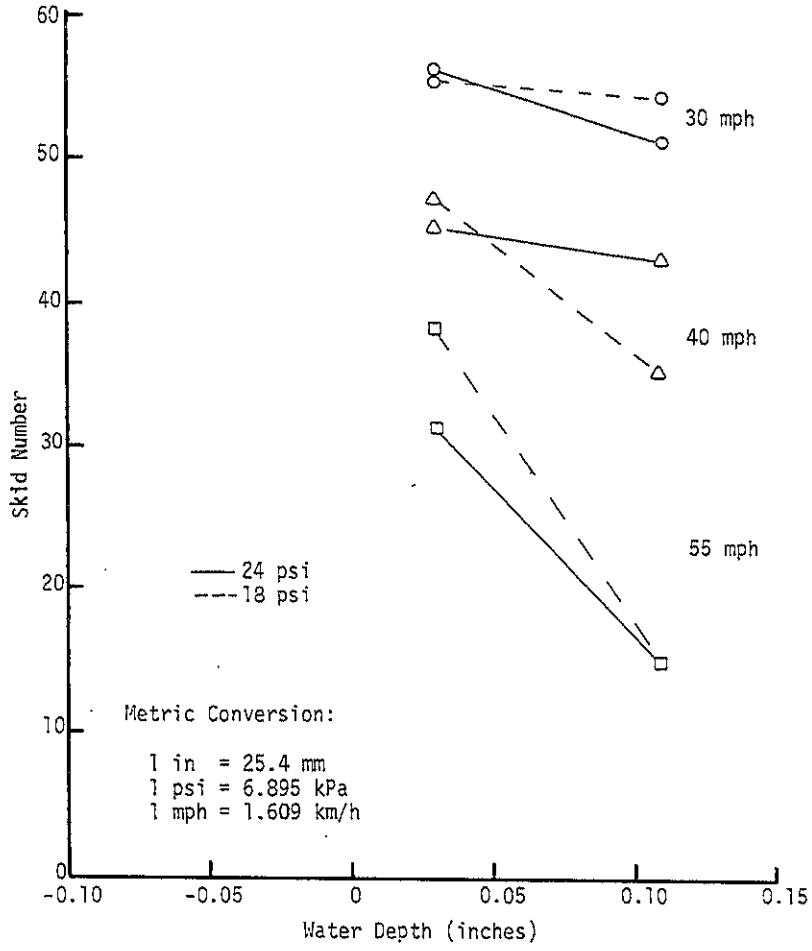

Figure 97. Skid number vs. water depth for steel-belted radial (SBR) with 2/32 in tread depth on Section 3, outside wheel path of inside lane

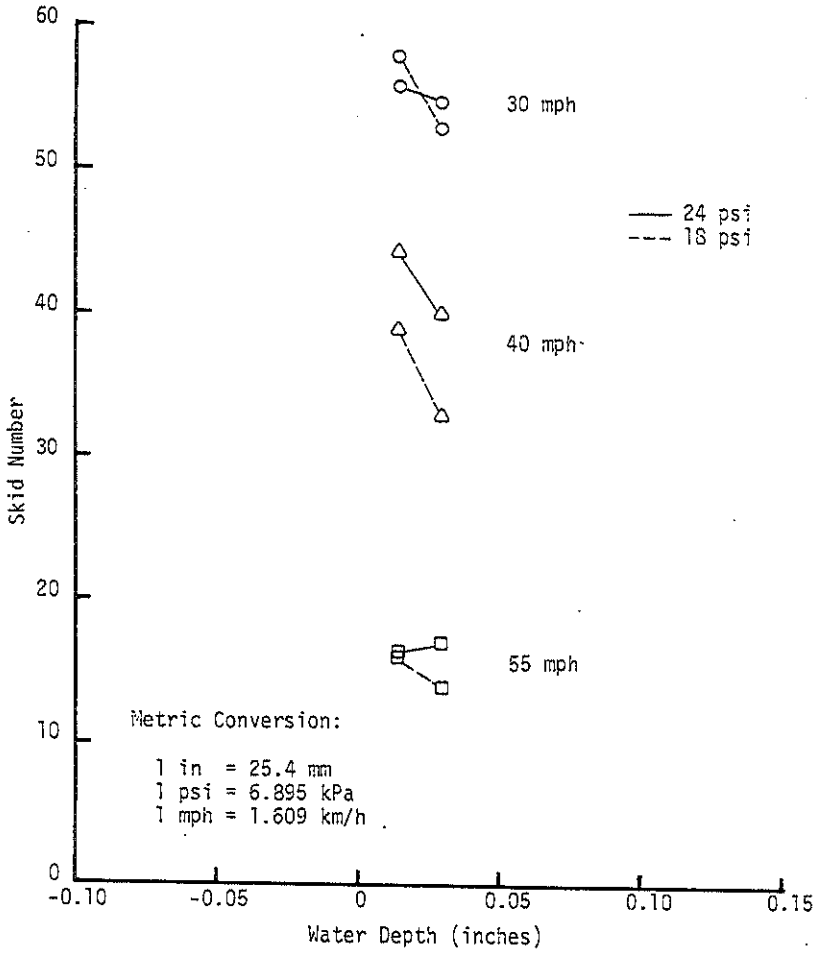

Figure 98. Skid number vs water depth for steel-belted radial (SBR) with 2/32 in tread depth on Section 4, outside wheel path of outside lane

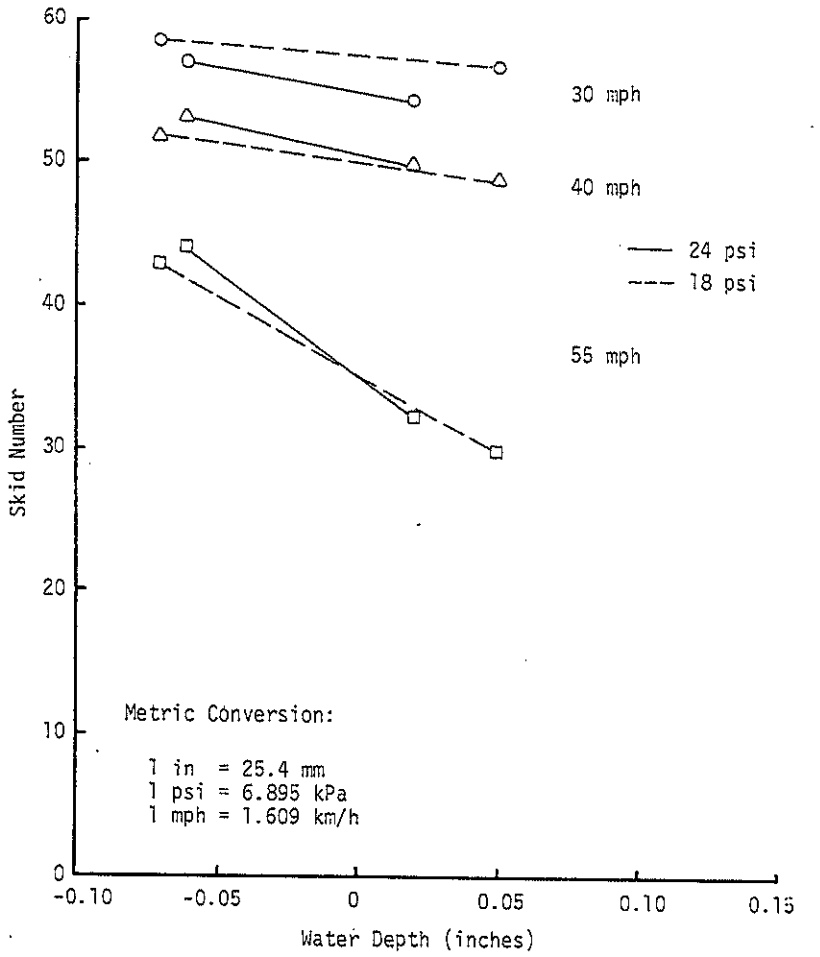

Figure 99. Skid number vs. water depth for glass-belted bias-ply tire (F-78-14) with 2/32 in tread on Section 1, outside wheel path of outside lane

on the pavement areas under test. The glass-belted bias-ply tire was an F-78-14 with a 2/32 in (1.6 mm) tread. Tire inflation pressures used were 18 and 24 psi (124 and 165 kPa). Skid numbers at 30, 40 and 55 mph (48, 64 and 88 km/h) were measured as shown in Figure 99, 100, 101, 102, and 103.

A comparative analysis of the performance characteristics of the surfaces as affected by tire type may be made by comparing the positions and the slopes of the curves in Groups C and D. The rainfall intensities and associated water depths were purposely repeated in these two series of tests. Considering the fact that the drainage capability of the surfaces decreases as the section number increases, the reader may note that the rainfall intensities utilized have caused a drift in the two sets of curves (Groups C and D), this drift being from negative toward positive water depths. It may also be noted that the Group D series of curves has shifted downward to generally lower skid numbers. At 55 mph (88 km/h) and water depths in the range of 0.1 in (2.5 mm) the skid numbers of approximately 10 on Sections 3 and 4 indicate probable loss of vehicle control due to dynamic hydroplaning -- this in spite of good surface drainage and some internal drainage.

Group E - The glass-belted bias-ply wide oval tire (G-60-14) was used in the Group E series of tests. The test variables were the same as those in Groups B, C and D. Again the reader may note friction deterioration at 55 mph (88 km/h) as the tests progressed from Section 1 to Section 4. It is apparent that at water depths of 0.05 to 0.10 in (1.3 to 2.5 mm) definite evidence of dynamic hydroplaning existed with skid numbers in the 7 to 10 range. With the rather large tire foot print presented by the G-60-14 the results are not surprising. One might be considered remiss in these analyses, if the superior performance of the G-60-14 at low speed were not mentioned. Indeed, throughout this series of tests the wide oval tire gave higher skid numbers at 30 and 40 mph (48 and 64 km/h) than did the F-78-14. Low-speed skid numbers for the SBR and the G-60-14 were essentially the same. Data are presented in Figures 104, 105, 106, 107 and 108.

Group F - Past experience with pavements overlaid with open-graded friction course on travelled lanes and the shoulder has indicated that the shoulder area is soon filled with debris thus reducing the permeable surface to a nonpermeable one. In some cases dense mixture designs have been placed on the shoulder directly against an OGFC on the travelled lane. To investigate the effect on skid performance of OGFC with abutting dense overlays, a series of tests was performed on Section 2 with a water seal placed at the outside edge of the outside lane.

Rainfall rates were adjusted to create both positive and negative water depths. Four tires were utilized in these tests

1) ASTM E501, full tread
2) SBR, minimal tread
3) F-78-14, minimal tread
4) G-60-14, minimal tread

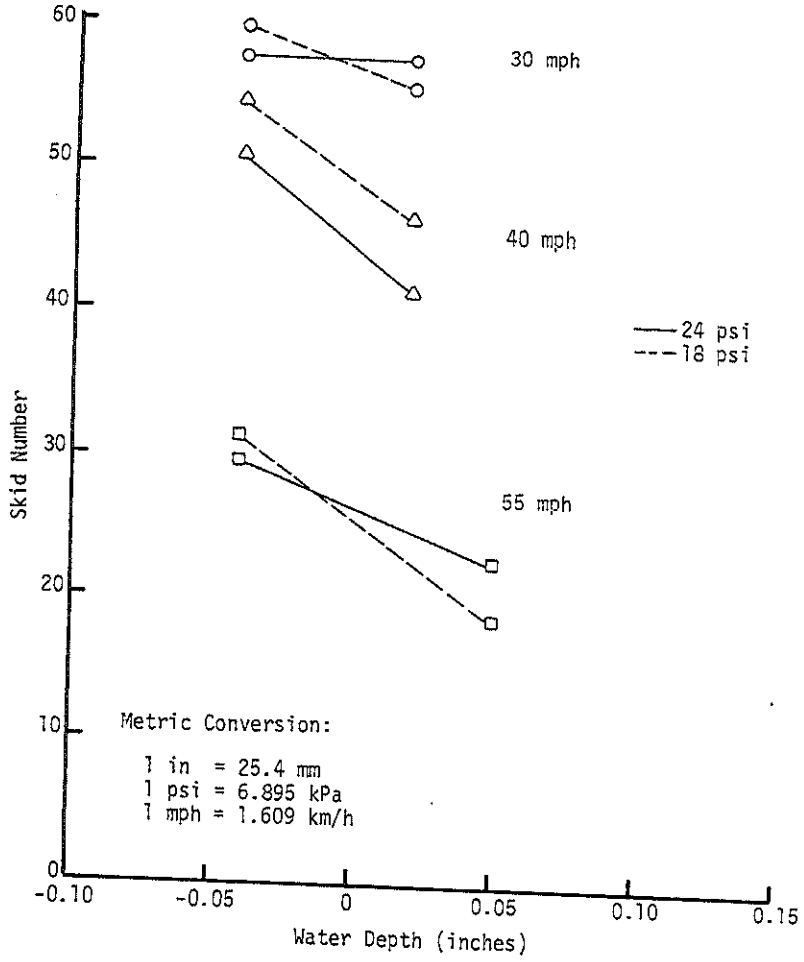

Figure 100. Skid number vs. water depth for glass-belted bias-ply tire (F-78-14) with 2/32 in tread depth on Section 2, outside wheel path of outside lane

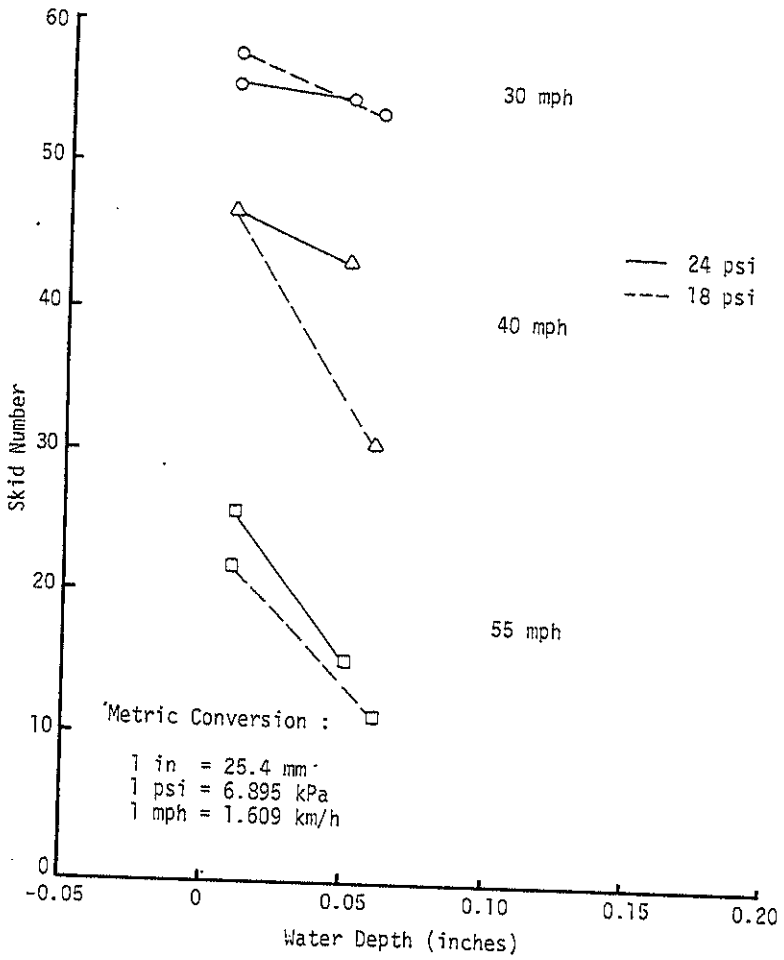

Figure 101. Skid number vs. water depth for glass-belted bias-ply tire (F-78-14) with 2/32 in tread depth on Section 3, outside wheel path of outside lane

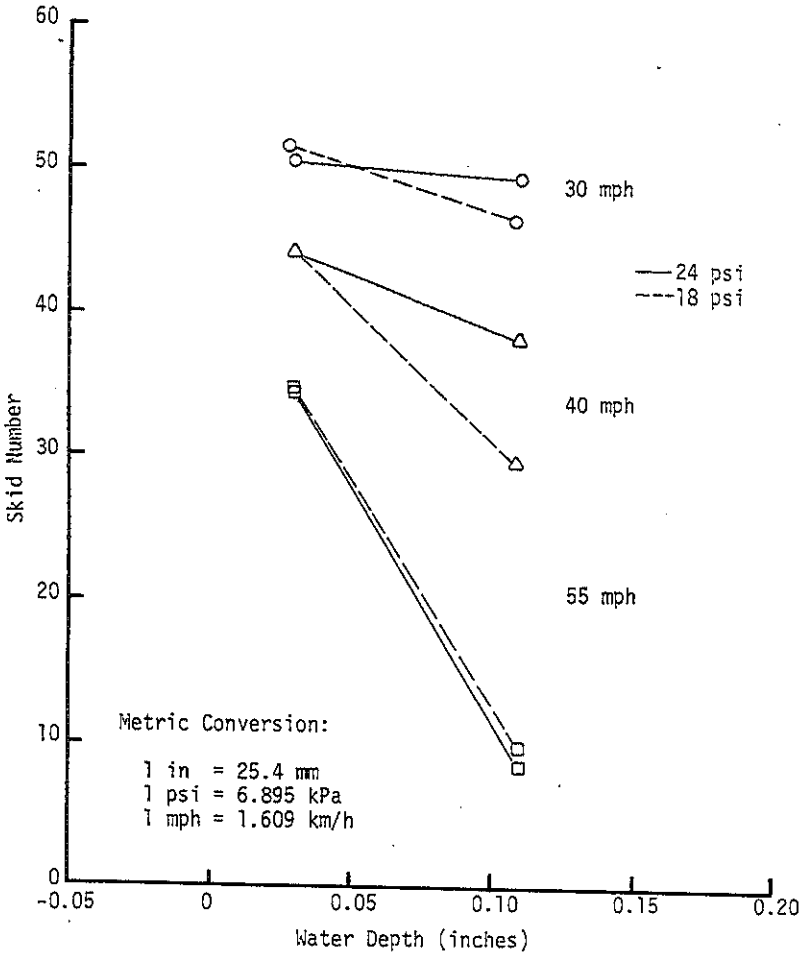

Figure 102. Skid number vs. water depth for glass-belted bias-ply tire (F-78-14) with 2/32 in tread depth on Section 3, outside wheel path of inside lane

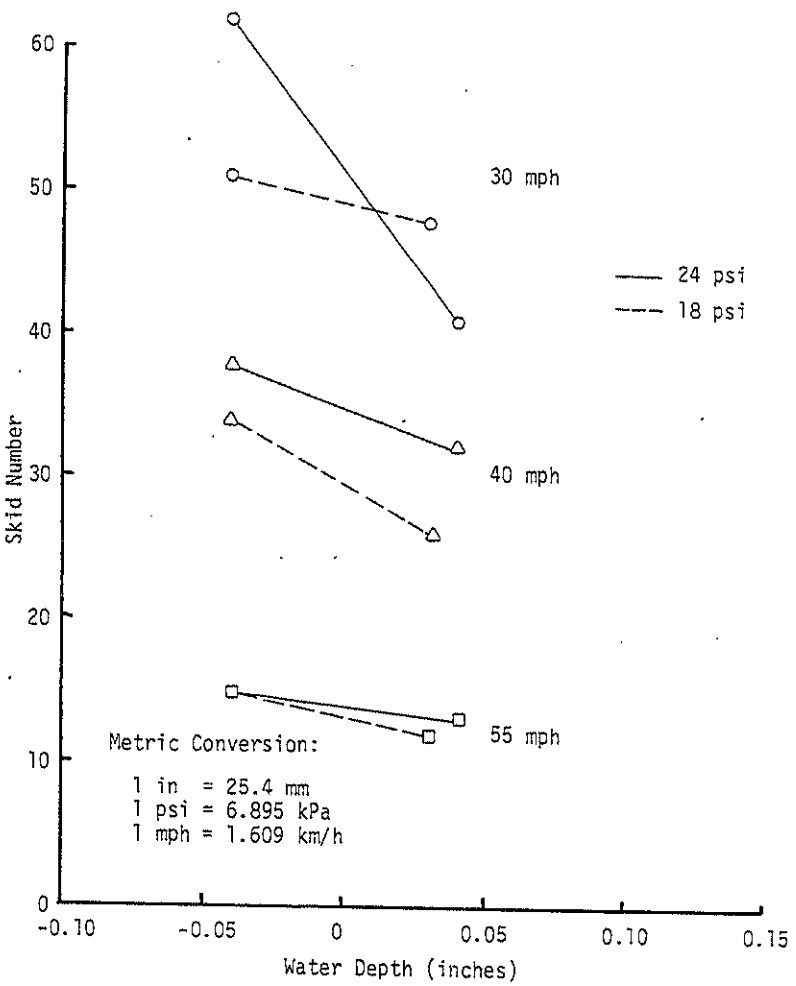

Figure 103. Skid number vs. water depth for glass-belted bias-ply tire (F-78-14) with 2/32 in tread depth on Section 4, outside wheel path of outside lane

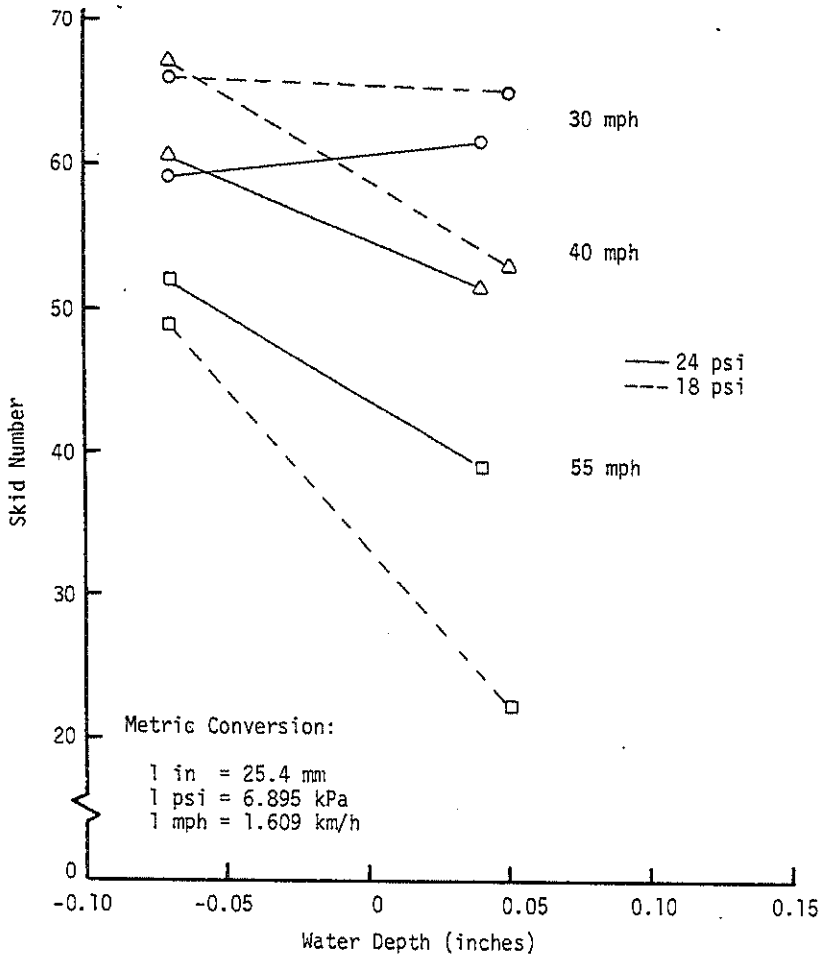

Figure 104. Skid number vs. water depth for glass-belted bias-ply wide tire (G-60-14) with 2/32 in tread depth on Section 1, outside wheel path of outside lane

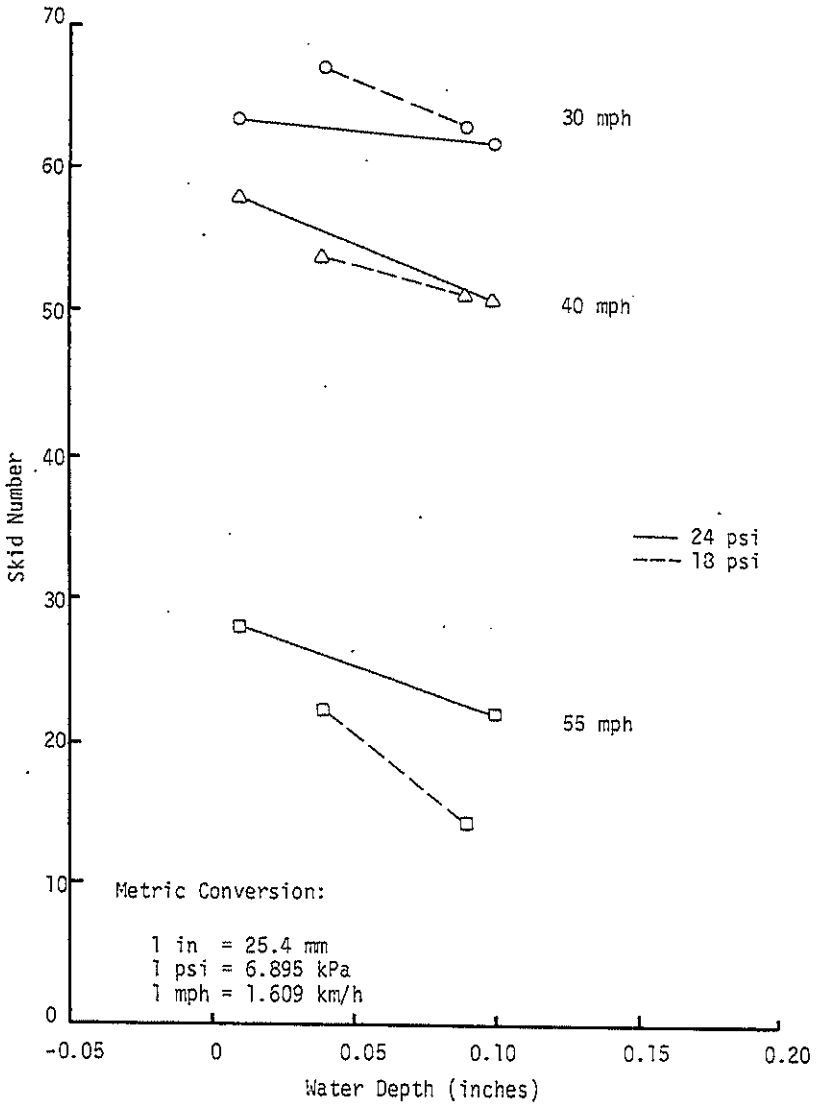

Figure 105. Skid number vs. water depth for glass-belted bias-ply wide tire (G-60-14) with 2/32 in tread depth on Section 2, outside wheel path of outside lane

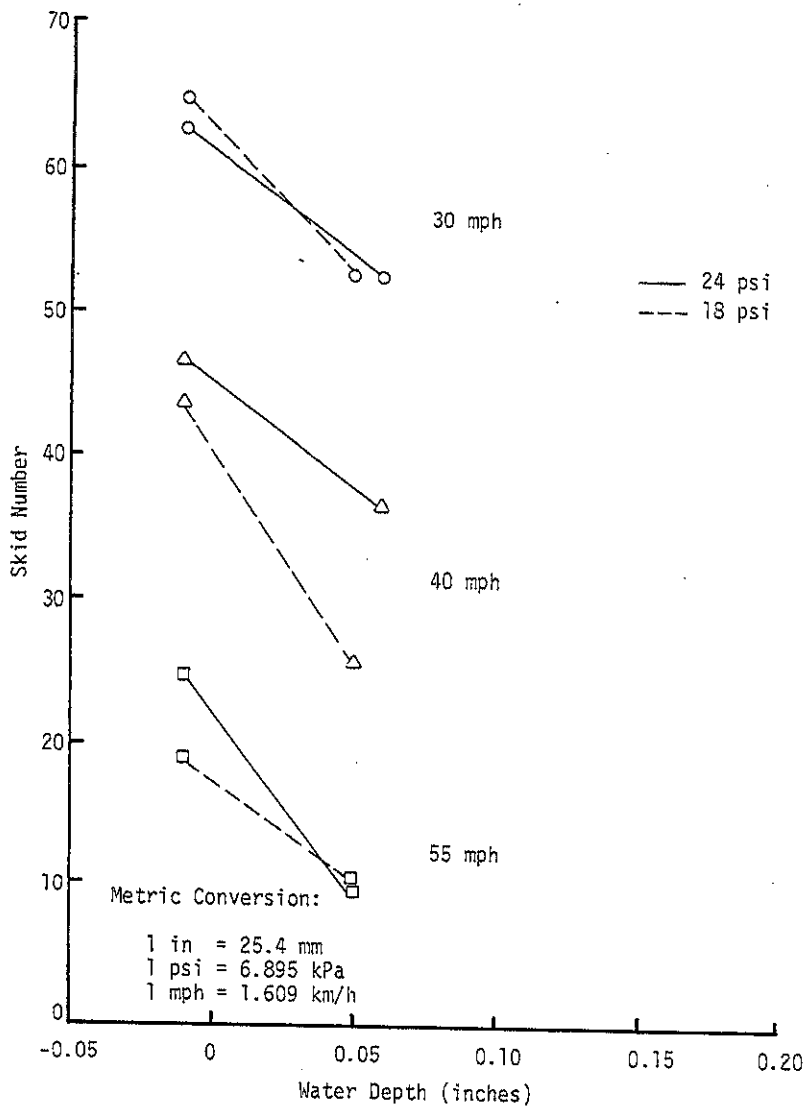

Figure 106. Skid number vs, water depth for glass-belted bias-ply wide tire (G-60-14) with 2/32 in tread depth on Section 3, outside wheel path of outside lane

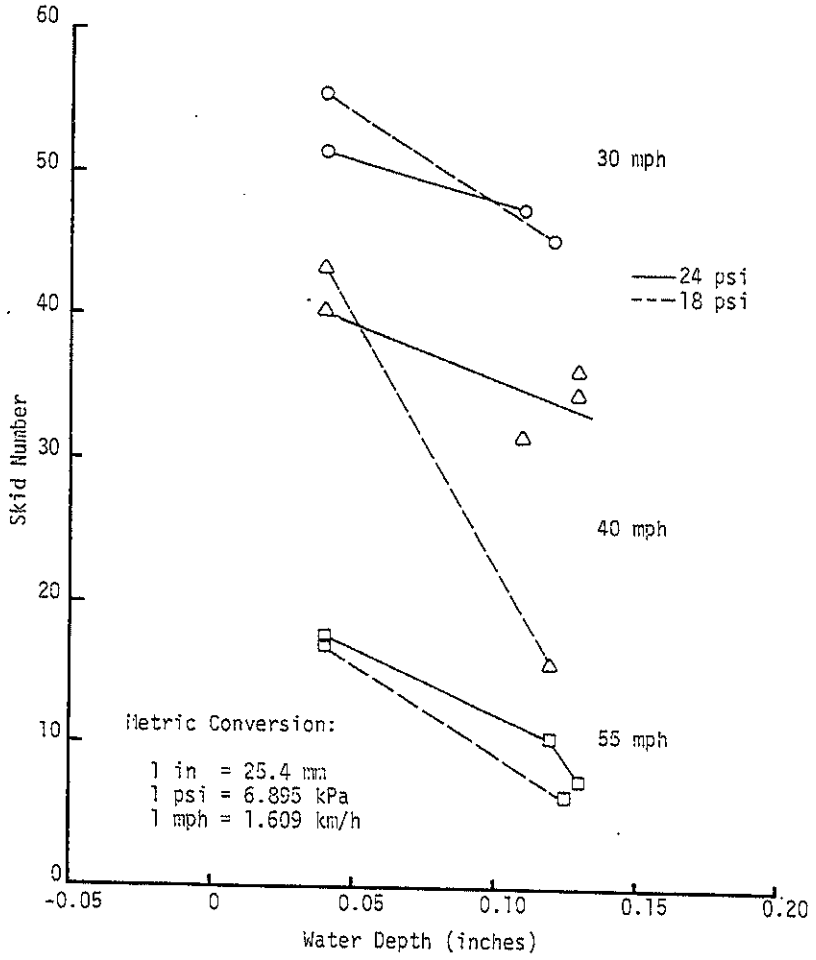

Figure 107. Skid number vs, water depth for glass-belted bias-ply wide tire (G-60-14) with 2/32 in tread depth on Section 3, outside wheel path of inside lane

All tires were loaded with the standard 1085 lbs (4826 N) load and tests were performed at 18 and 24 psi (124 and 165 kPa) tire inflation pressure. Graphical presentations are depicted in Figures 109, 110, 111 and 112.

A comparison of the performance of Section 2 with the shoulder sealed should be made, taking into account the rainfall intensity required to produce the water depths shown in Figure 112. The rainfall intensity was 0.46 in/h (12 mm/h) for the negative water depth of 0.03 in (0.8 mm) and 2.2 in/h (56 mm/h) for the positive value of 0.05 in (1.3 mm) for the shoulder sealed. Without the shoulder sealed the rainfall intensity was 0.59 in/h (15 mm/h) for a negative water depth of 0.04 in (1 mm) and 1.8 in/h (46 mm/h) for a positive depth of 0.05 in (1.3 mm). In an analysis of these data one should take into account the fact that data taken at, say, 40 mph (64 km/h) were gathered at different points in real time bringing wind direction and velocity into the picture. Consideration of the probable effect of wind direction and speed is offered as a plausible explanation for contradictions in the data. Stated another way, tests were made using a selected tire, tire inflation pressure and water depth at three different speeds and then, without changing anything but the tire inflation pressure, the tests were repeated at the three test speeds. This generated the group of points on, say, Figure 111, at -0.03 in (-0.8 mm) water depth and levels of SN from about 41 to 61. Later that day or even days later the other points positioned at + 0.05 in (1.3 mm) water depth were obtained; hence, the very likely possibility of differences in wind effects.

A general comparison of the data on Section 2 with and without the shoulder sealed indicates somewhat higher values of SN for the sealed shoulder condition. One logical explanation for this observation is that time and wear had their effect on the measured SN. The test sections were relatively immature when testing started and were therefore going through changes such as removal of the rather heavy film of asphalt on the aggregate and changes in the microtexture of the surface contacting the tire.

Group G - Since the normal tire population contains among the other variables a mixture of tire tread depths, a limited series of tests was performed using two tires, one a glass-belted bias-ply (F-78-14) and the other a steel-belted radial (FR-78-14) each at tread depths of 11/32 in (8.7 mm) and 5/32 in (4.0 mm). A tire inflation pressure of 24 psi (165 kPa) was used during the Group G tests. The relative performance of Section 2 of the OGFC measured by these two tires of different tread depths is shown in Figures 113 and 114. Attention is directed to two indicated findings, namely, the steel belted radial definitely delivers higher skid numbers for both tread depths, the difference being about 10 skid numbers for the 5/32 in (4.0 mm) tread depth and 55 mph (88 km/h) speed. This comparison of the effect of tread depth for the glass-belted bias-ply (F-78-14), is extended to include the 2/32 in (1.6 mm) tread depth in Figure 115. A marked sensitivity to reduction in tread depth is evident. The reduction at 55 mph (88 km/h) is in the range of 15 to 20 skid numbers when the tread depth is reduced from 5/32 to 2/32 in (4.0 to 1.6 mm). However, it may be noted that the OGFC delivers adequate friction at 55 mph (88 kn/h) and a water depth of 0.05 in (1.3 mm).

Group H - For a 12 ft (3.7 m) traffic lane the approximate center of the wheel path is 30 in (0.76 m) from the edge of the lane. This lateral

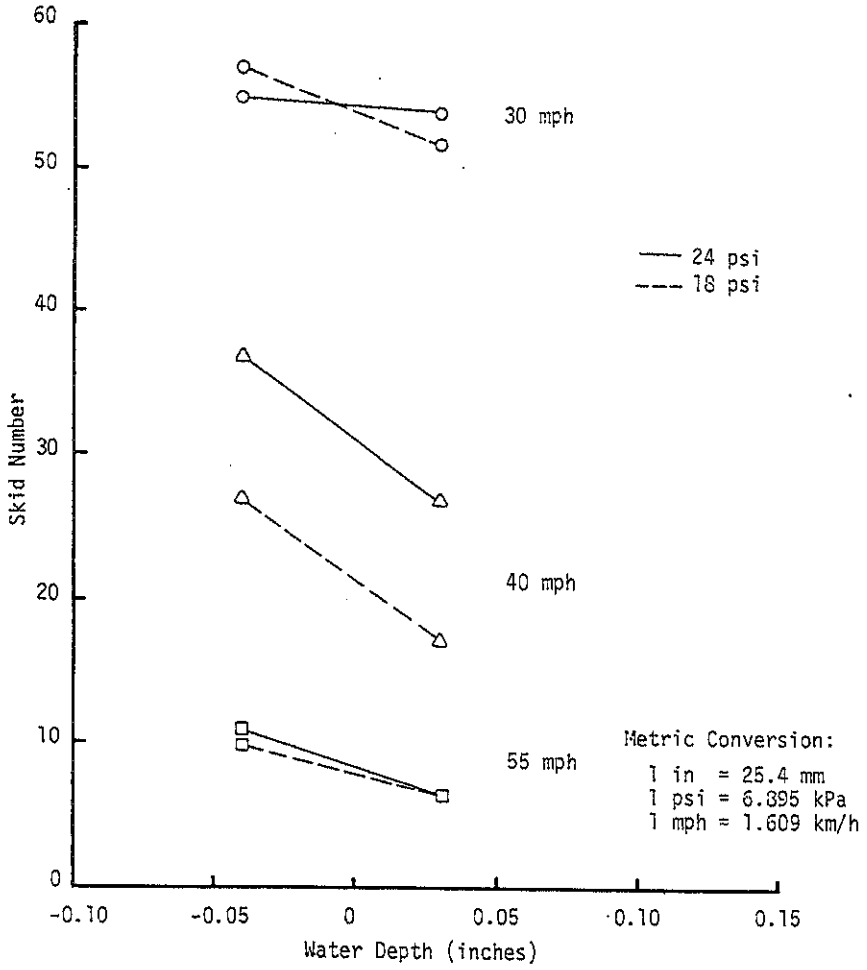

Figure 108. Skid number vs, water depth for glass-belted bias-ply wide tire (G-60-14) with 2/32 in tread depth on Section 4, outside wheel path of outside lane

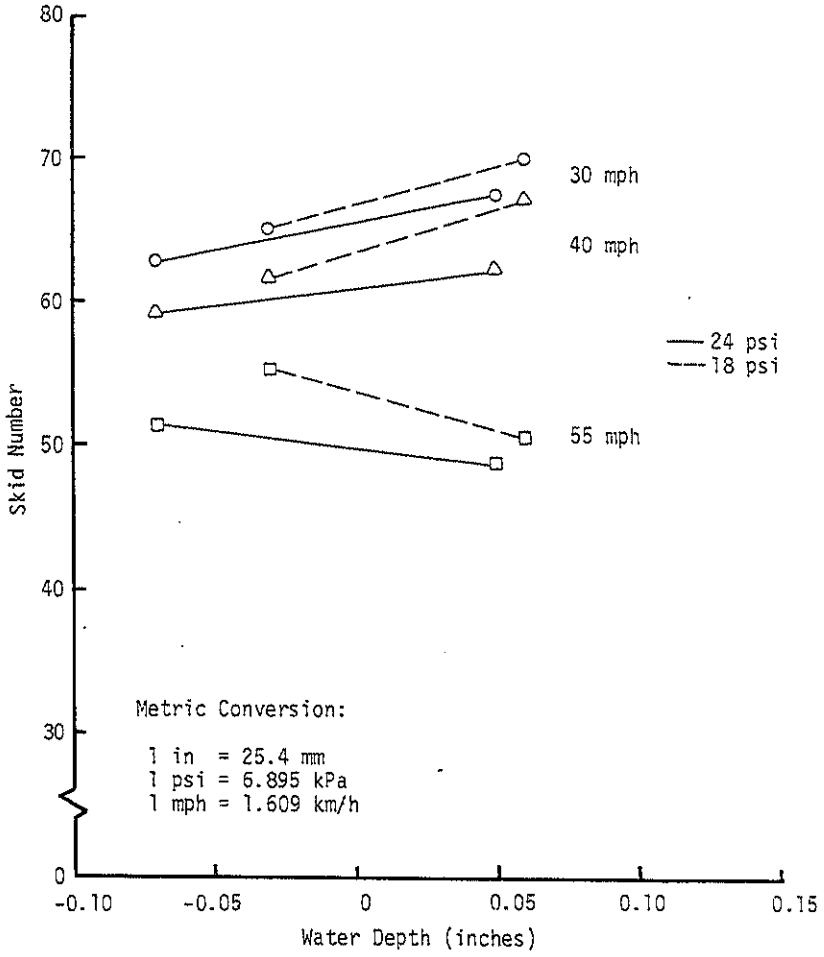

Figure 109. Skid number vs water depth for ASTM standard tire E501 with 2/32 in tread depth on Section 2 with simulated sealed shoulder, outside wheel path of outside lane

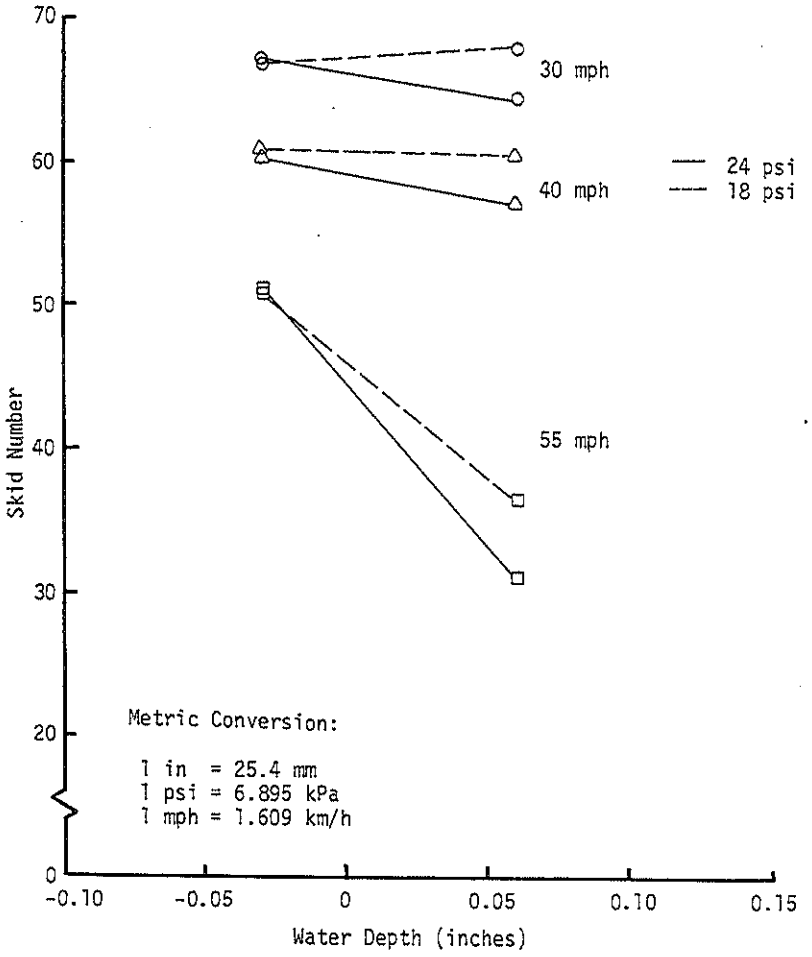

Figure 110. Skid number vs. water depth for steel-belted radial (SBR) with 2/32 in tread depth on section 2 with simulated sealed shoulder, outside wheel path of outside lane

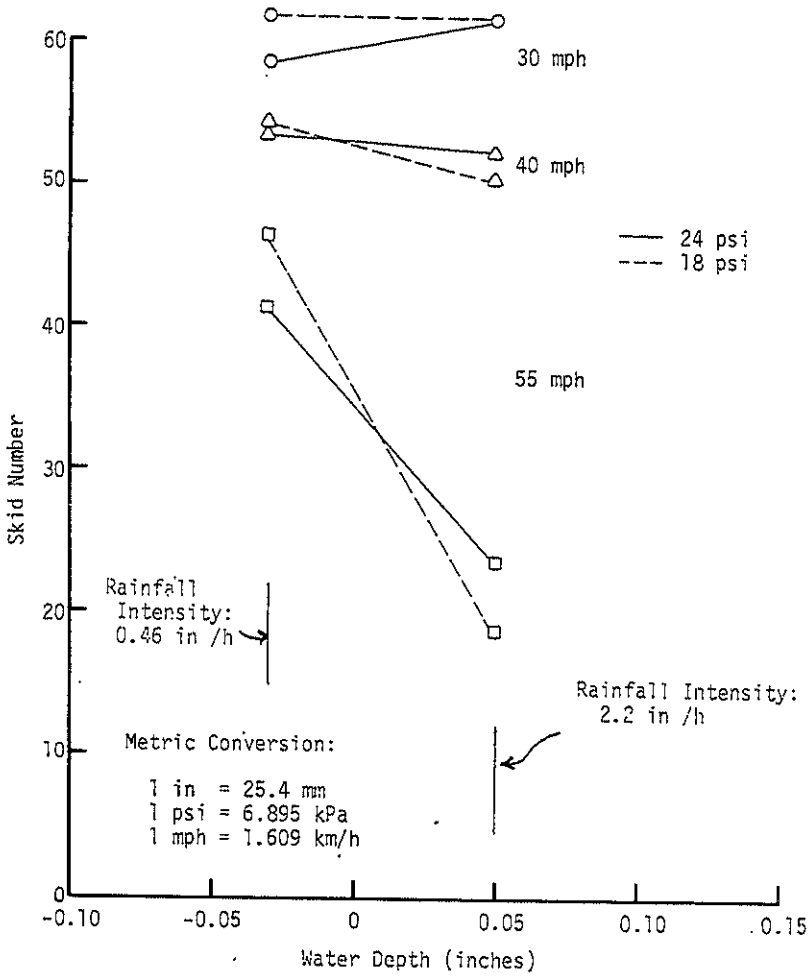

Figure 111. Skid number vs. water depth for glass-belted bias-ply tire with 2/32 in tread depth on Section 2 with simulated sealed shoulder, outside wheel path of outside lane

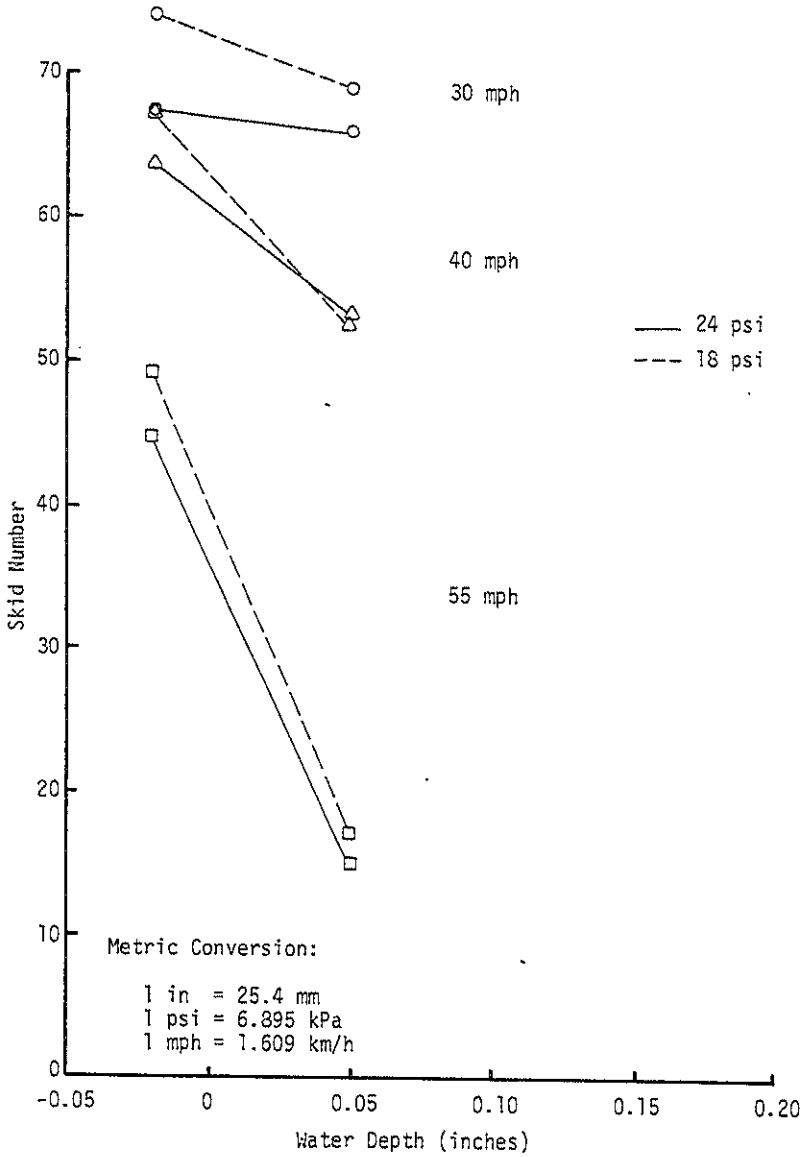

Figure 112. Skid number vs. water depth for glass-belted bias-ply wide tire (G-60-14) with 2/32 in tread depth on Section 2 with simulated sealed shoulder, outside wheel path of outside lane

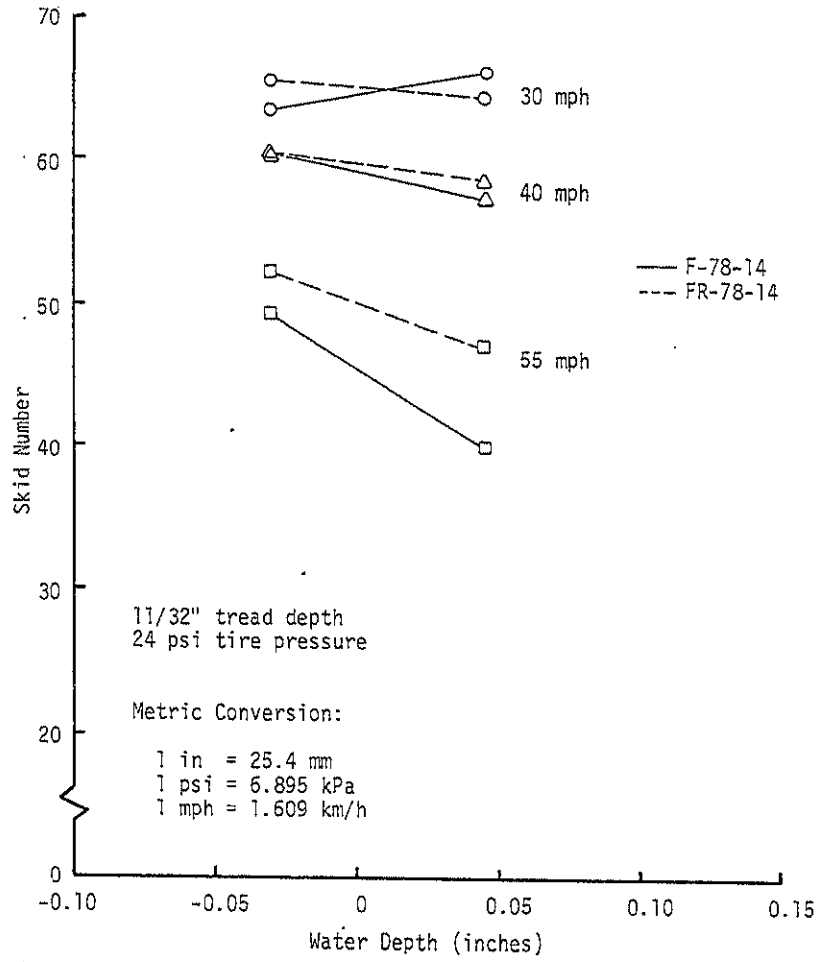

Figure 113. Skid number vs. water depth for glass-belted bias-ply tire (F-78-14) and steel belted radial (FR-78-14) having 11/32 in tread depth and inflated to 24 psi. Testing done on Section 2, outside wheel path of outside lane

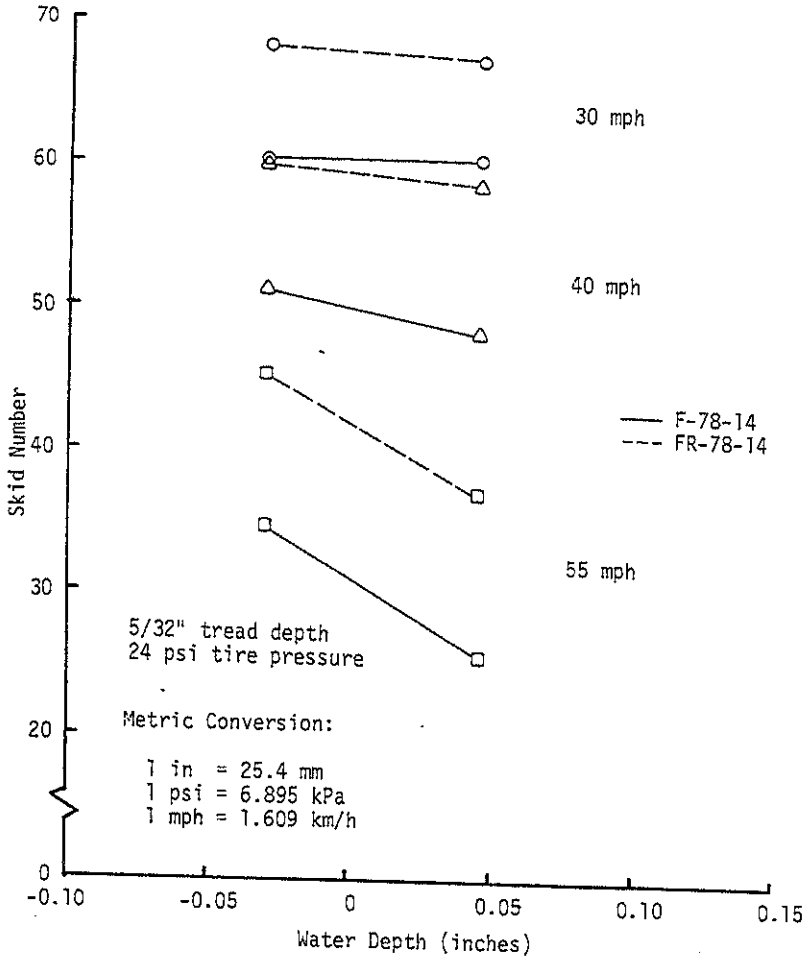

Figure 114. Skid number vs. water depth for glass-belted bias-ply tire (F-78-14) and steel belted radial (FR-78-14) having 5/32 in tread depth and inflated to 24 psi. Testing done on Section 2, outside wheel path of outside lane

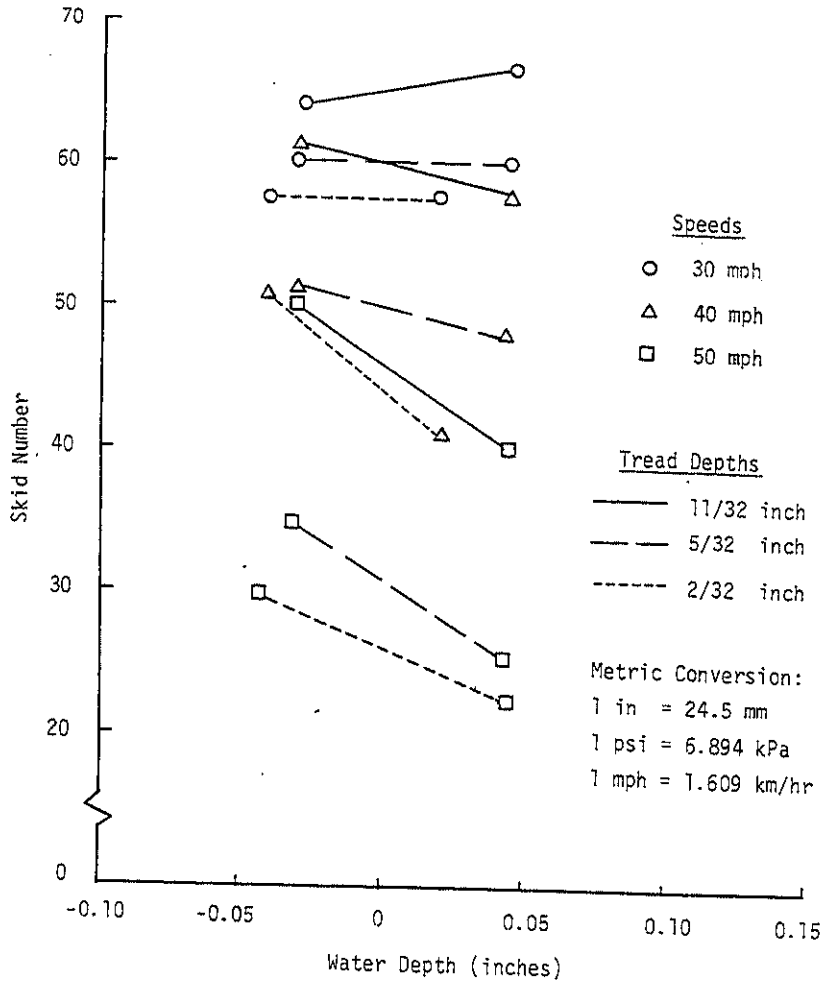

Figure 115. Skid number vs. water depth for glass-belted bias-ply tire (F-78-14) inflated to 24 psi. Testing done on Section 2, outside lane, outside wheel path

position was therefore chosen as the position for wheel lockup on the various sections and lanes through the described test program. When it was observed that the skid numbers for Section 2 with the shoulder sealed were somewhat higher than measurements made earlier, an effort was made to determine whether or not there was an appreciable variation in skid number across the pavement. The results presented in Figure 116 were taken at three different points in real time with a considerable delay between the time the measurements were taken on Section 2 with and without the shoulder sealed and a very short delay between the times data on the sealed shoulder and the position across the pavement were taken. Mention was made earlier in the discussion of the higher skid numbers on Section 2 at the time the shoulder was sealed. The skid numbers measured at points of 36 in (0.9 m), 42 in (1.1 m) and 68 in (1.7 m) from the outside edge of the outside lane appear to verify the change in the surface properties of Section 2 with time and exposure to test associated with traffic as deduced earlier in this segment of the report.

Group I - Although the data presented in this series of tests were gathered early in the test program the analyses have been relegated to a latter position in the discussion. The reader should note that Figures 117, 118, 119 and 120 are plots of skid number vs speed, not skid number vs water depth as has been the case in most of the past discussions. The three primary variables are rainfall intensity, vehicle speed and test section or pavement voids. This complete series of tests was performed in the outside wheel path of the outside lane in each of the sections. Similarly, this series of tests might be considered to correspond to the procedures and equipment in ASTM E274 with water depth and speed as variables. This, of course, means that for a fixed rainfall intensity of, say, 0.5 in/h (13 mm/h) the water depth increased with the section number. It should be noted, however, that the effect on water depth of a given rainfall intensity is also a function of the mat thickness as well as the average void content of the OGFC. In spite of differences in mat thickness the general trend of the data is an increase in the slope of the SN vs speed curves and a lowering of skid numbers.

In Figures 119 and 120, skid number vs speed data for all tires except the ASTM E501 are presented. Tire tread depth and tire inflation pressure were fixed at 2/32 in (1.6 mm) and 24 psi (165 kPa), respectively. Again, all four sections of pavement were examined for their performance characteristics during simulated rainfall rates of 0.5 and 2 in/h (13 and 52 mm/h).

This overall analysis clearly indicates that the OGFC provided adequate friction in all cases except at 55 mph (88 km/h) on Section 4 where the as-constructed voids were in the range of 15 percent. The slope of SN vs speed curve for Section 4 is quite steep indicating a rapid approach to dynamic hydroplaning in the 55 to 60 mph (88 to 97 km/h) speed range with the associated potential danger of this phenomenon. In a general comparison of the effect of the two rainfall intensities it is evident that the greater water depths, associated with the higher rainfall, caused a general downward, lower SN's, shift of the curves.

Macrotexture of SH-21 OGFC

Shortly after the above described testing was completed, macrotexture measurements of the four test sections were made using the Silicone

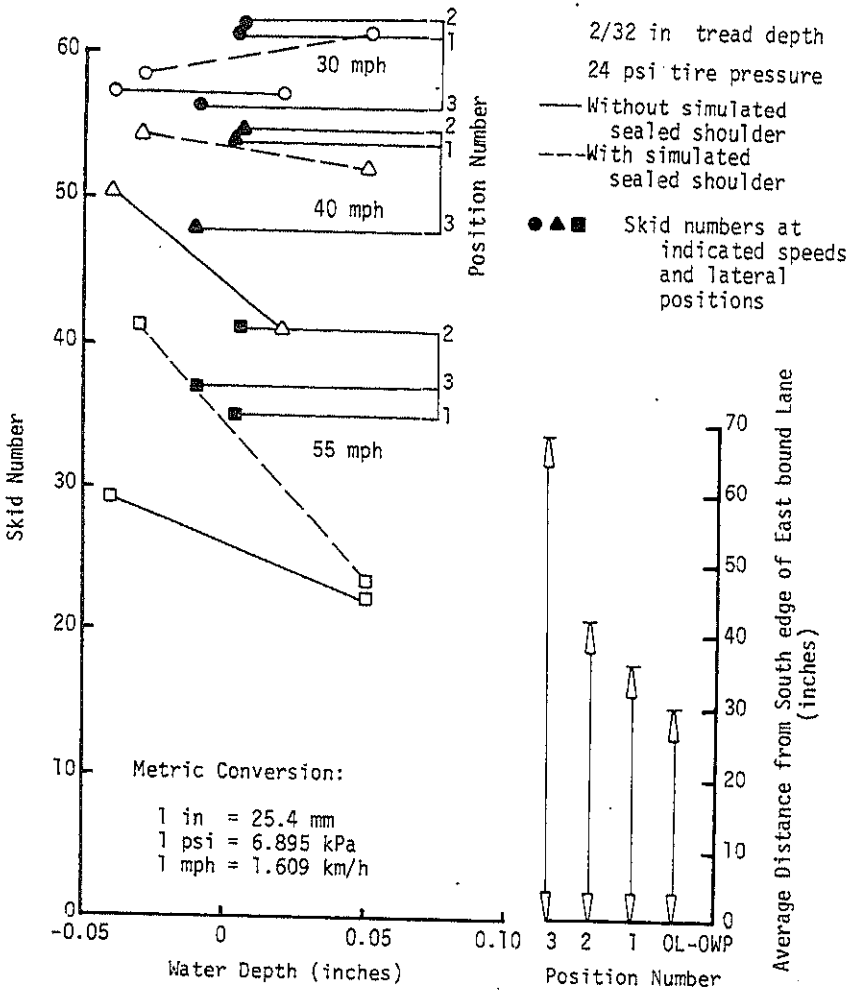

Figure 116. Skid number vs. water depth for belted-bias ply tire (F-78-14) on Section 2 at various positions across the lane

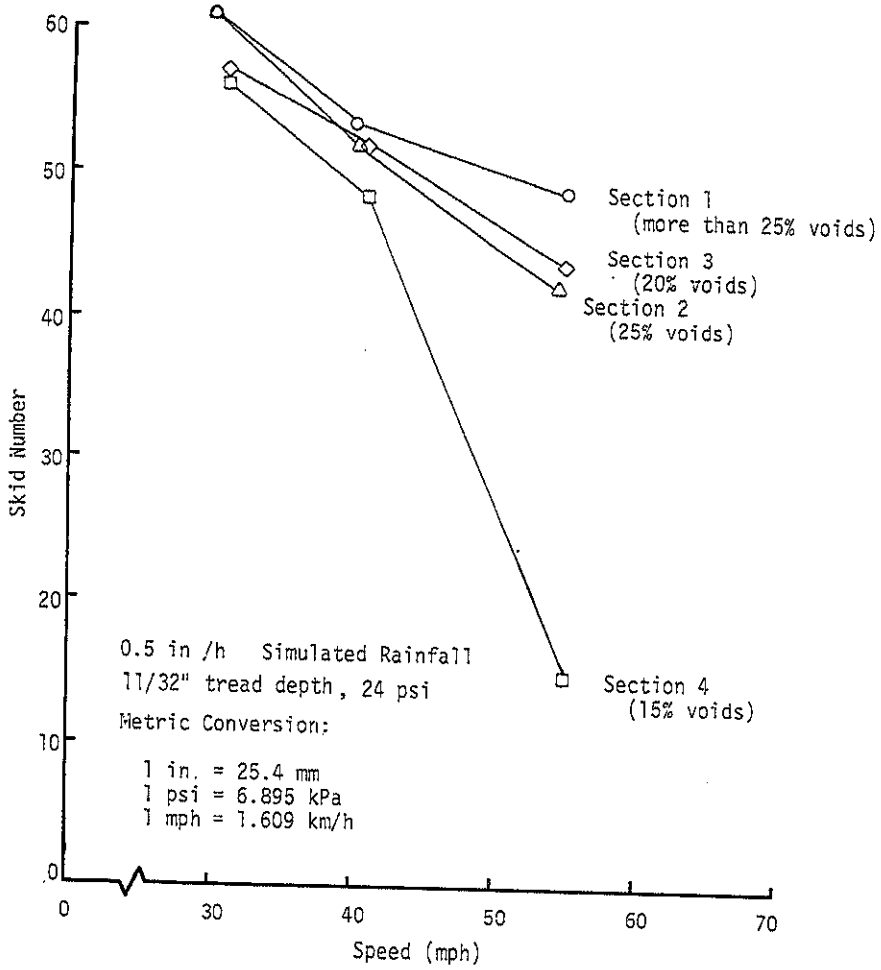

Figure 117. Skid number vs. speed for all sections, average of ASTM E501 tire only

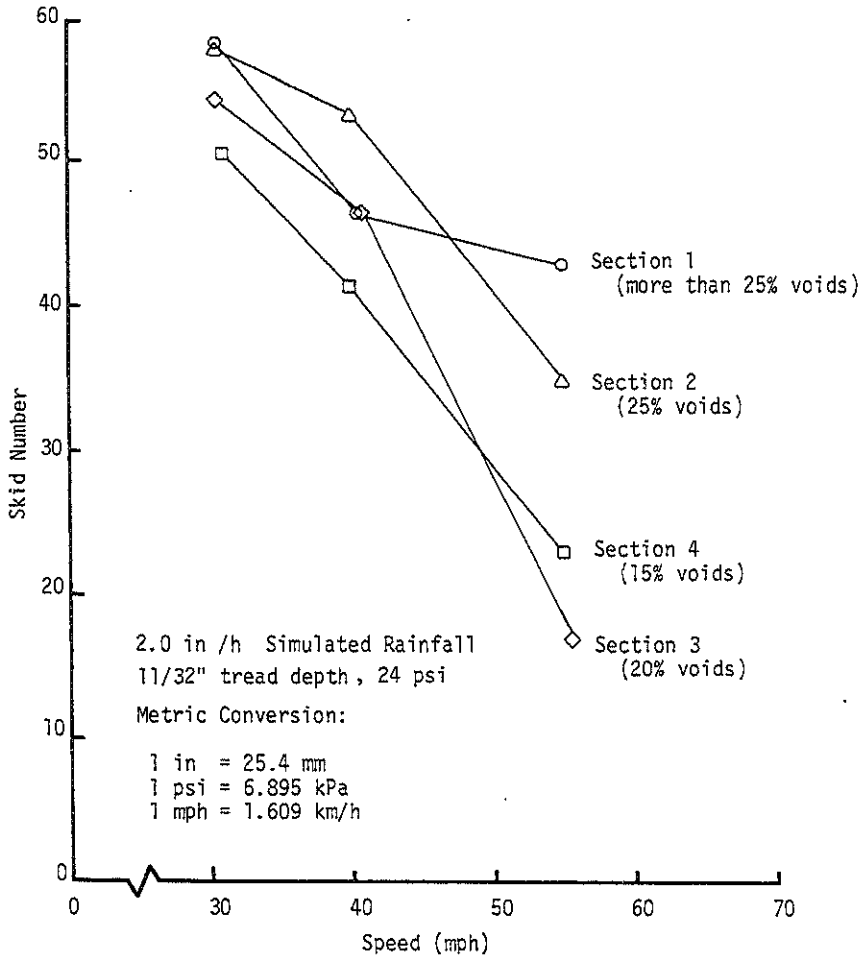

Figure 118. Skid number vs. speed for all sections, average of ASTM E501 tire only

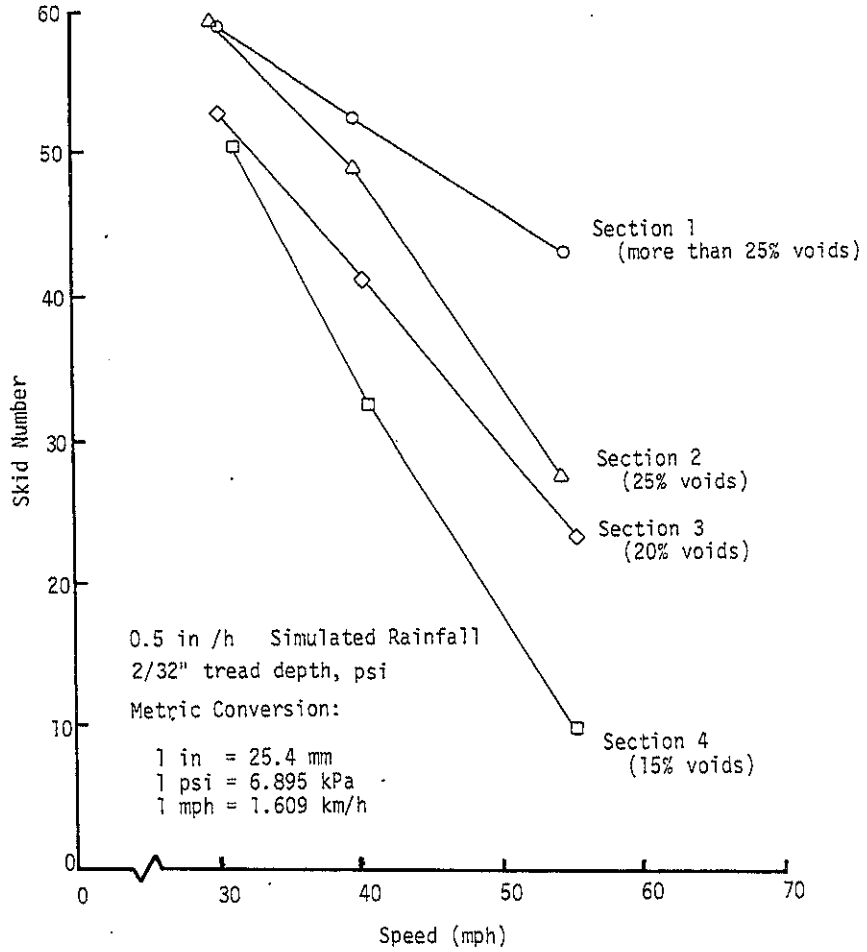

Figure 119. Skid number vs. speed for all sections, average of all tires except ASTM E501

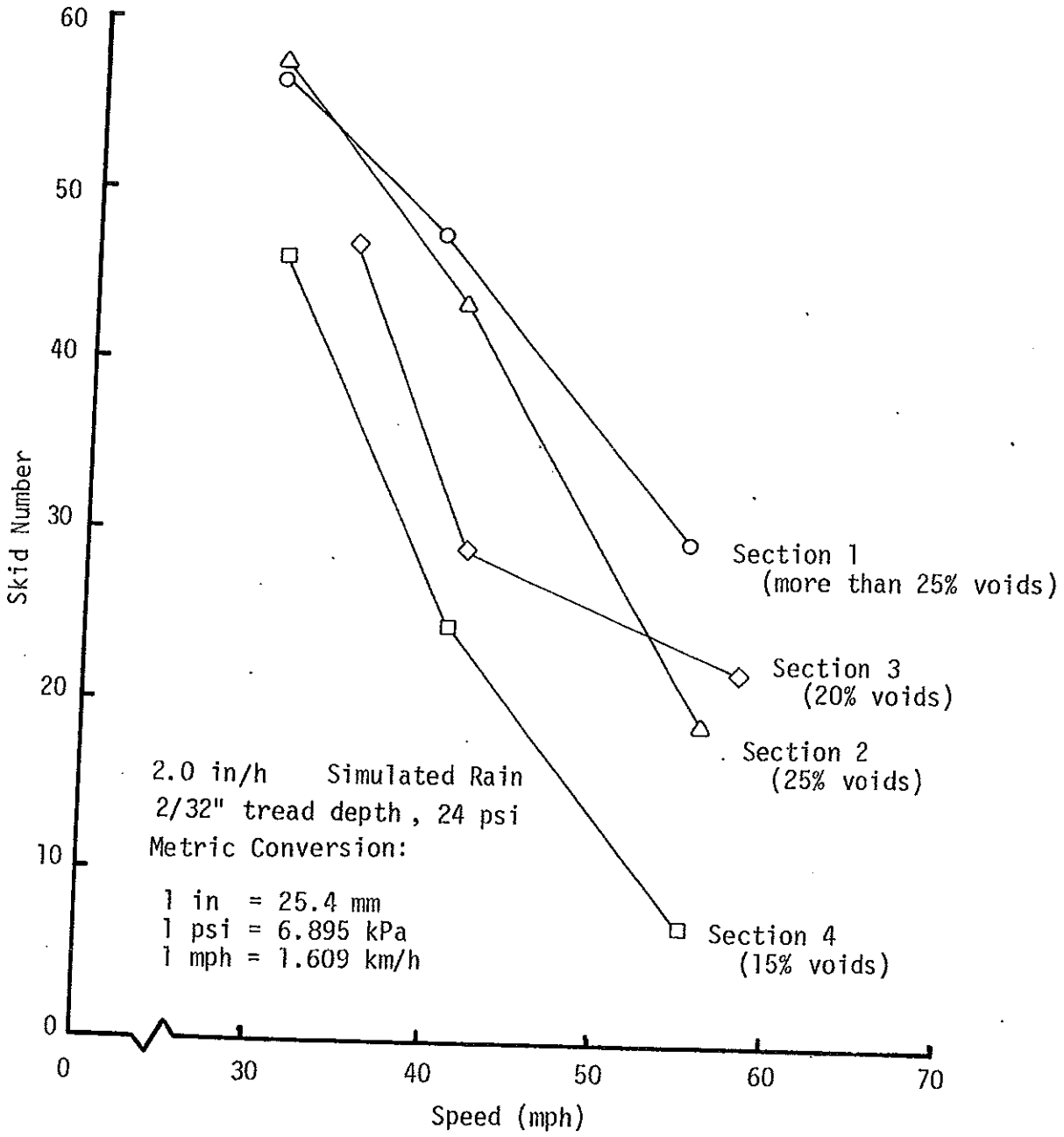

Figure 120 Skid number vs speed for all sections, average of all tires expect ASTM E501

Putty Method. The results of these measurements are presented in Table 15 .

Additional macrotexture measurements were made in the wheel path (IWP) and between the wheel path (BWP) of Section 3 with values of 0.110 in (2.79 mm) and 0.122 in (3.10 mm), respectively. The average of the three sets of measurements was 0.107 in (2.72 mm). To determine the probable effect of macrotexture on the skid number at those lateral positions, macrotexture measurements were made in this section at the same lateral positions and locations, and data are presented in Table 16.

The overall average macrotexture including all texture measurements made after all simulated rain testing was done was 0.107 in (2.72 mm). The range of values was from 0.084 to 0.134 in (2.13 to 3.40 mm).

A falling head water outflow apparatus was used to evaluate the permeability of these surfaces after all testing had been completed. These measurements indicate a definite reduction in permeable voids from Section 1 to Section 4 with outflow time measurements of 5.9, 8.2, 9.7 and 17.6 seconds for Sections 1, 2, 3 and 4, respectively. Again, precise thicknesses of the mat at the points of measurement were not measured; however, mat thicknesses measured about 1 in (25.4 mm) based on material quantities and thickness measurements made on cores taken from the several sections.

Performance of OGFC Under Natural Rain

The question of the comparative performance of OGFC under simulated and natural rainfall has been raised. To shed some light on this question five field sites were established in Texas to gather data on existing open-graded surfaces that have been in service for time intervals of two to five years. Traffic on these sections varies from light to very heavy. General properties of the various sites and surfaces are given in Table 16.

The real impact of the nature of the variation of rain was not truly appreciated until the researchers became acquainted with the difficulty of securing natural rainfall and associated tire pavement interactions on a specific segment of highway. Time and timing became most critical problems at all sites. Equipment availability was another critical factor at all sites except the SH-21 Bryan, Brazos County site. Even at this site it was not economically feasible to have a trained crew on a 24-hour, 7-day a week stand-by basis.

The five selected sites included Austin, Fort Worth, Lufkin, Beaumont and Bryan, Texas. There was one skid trailer available at Bryan (the property of Texas Transportation Institute), one trailer at Austin and one for Fort Worth, Lufkin and Beaumont (a single unit normally stationed at Lufkin). All three units were equipped with three or more rain gages, a stop watch and two mounted tires. The tires were ASTM E501's, one with full tread and the other shaved to minimal tread depth.

Operators at each site were instructed to place primary emphasis on collecting data at 40 mph (64 km/h) with the full tread E501 tire in natural rain in the general intensity range of 0.01 to 0.5 in/h (0.3 to 13 mm/h) on their typical open-graded surfaces. Following this they were instructed to collect data at 55 mph (88 km/h) then change to the minimal tread tire and repeat the data collection at the two stated speeds.

Table 15. Macrotexture of OGFC surfaces SH-21

Section	OWP Passing Lane	OWP Passing Lane	BWP Travel Lane
No. 1	0.093 in (2.36 mm)	0.096 in (2.44 mm)	0.101 in (2.57 mm)
No. 2	0.099 in (2.51 mm)	0.123 in (3.12 mm)	0.109 in (2.77 mm)
No. 3	0.166 in (4.22 mm)	0.099 in (2.51 mm)	0.108 in (2.74 mm)
No. 4	0.125 in (3.18 mm)	0.105 in (2.67 mm)	0.105 in (2.67 mm)

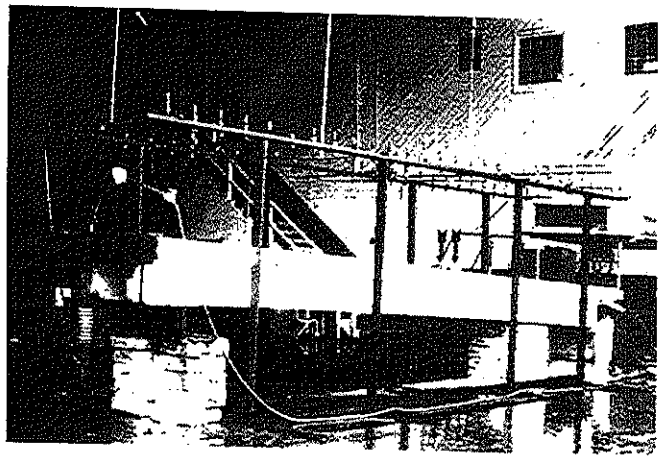

Figure 121. Model surface used to examine runoff from multilane pavements (Note water input at left (upper) end of pavement segment and simulated rain capability on two outer lanes.)

Table 16. Comparative performance of open mixes under various conditions

Site Location	Highway	Age (Yrs.)	Thickness (inches)	Texture (inches)	Traffic (Millions of Vehicle Passes)	Internal Water E-501 Full Tread SN_{40}	Internal Water E-501 Full Tread SN_{55}	In Rain 2/32" Tread SN_{40}	In Rain 2/32" Tread SN_{55}	In Rain E-501 Full Tread SN_{40}	In Rain E-501 Full Tread SN_{55}	Rainfall Intensity in/hour
Bryan												
Sec.1	SH 21	2	1± *	0.091		52	50	50	32	54	43	2.0**
Sec.2	Sh 21	2	1±	0.111		53	48	41	23	56	42	2.0**
Sec.3	Sh 21	2	1±	0.111		52	51	43	16	56	37	2.0**
Sec.4	SH 21	2	1±	0.107		54	49	39	9	45	30	2.0**
Austin												
	US 290	1.2	3/4-	0.105	2.5	46	40	45	25	46	39	0.05
	US 290	1.2	1±	0.030	2.5	37	28	44	18	35	27	-
Ft. Worth												
	IH 30	5	3/4-	0.033	35.1	46	37	-	-	42	29	0.02
	IH 820	5	3/4-	0.048	38.3	43	31	-	-	40	28	-
Lufkin												
	US 59	5	1/2±	0.026	6.2	49	-	-	-	-	-	-
	US 59	6.5	1/2-	0.019	7.8	34	-	-	-	-	-	-
	US 59	6.5	1/2-	0.018	8.0	54	-	-	-	-	-	-
	US 59	6.5	1/2-	0.044	7.9	61	-	-	-	-	-	-
	US 59	5	1/2±	0.028	5.0	50	-	-	-	-	-	-
	US 59	5	1/2±	0.040	8.0	44	-	-	-	-	-	-
Beaumont												
Sec.1	IH 10	2.5	3/4-	0.093	4.0	47	33	-	-	47	-	0.30
Sec.2	IH 10	2.5	3/4-	0.061	5.4	45	30	-	-	46	-	0.25
Sec.3	SH 87	4.2	3/4-	0.032	1.6	33	20	-	-	28	-	0.05
Sec.4	SH 87	2.7	3/4-	0.105	1.5	44	28	-	-	43	-	0.05

* Metric Conversion: 1 in = 25.4 mm
** Simulated Rain

Rain gages used were Model Tru-202 Tru-Check Gage manufactured by Edwards Manufacturing Company, Albert Lea, Minnesota. These gages are easily read to 0.01 in (0.3 mm) for the first 0.5 in (13 mm) and had a 2 in (51 mm) capacity.

Normally the crews were available during the regular work week, and it was difficult to estimate when a given rain shower would be at a given site. Further, a rain of uniform intensity covering an area of sufficient size to include a reasonably sized test area occurred with great rarity.

Measurements made on SH-21 in Brazos County, Texas, showed a wide variation in intensity and duration within the 2200 ft (671 m) test site. Variations in intensity of 100 percent or more were not uncommon, with such variations taking place in a distance of 1000 ft (305 m) or less. These observations were most particularly true for rainfall intensities in the 0.1 to 0.5 in/h (2.5 to 13 mm/h) range. It was noted that light rains in the 0.01 to 0.1 in/h (0.3 to 2.5 mm/h) range were much more nearly uniform in intensity and usually extended over longer periods of time. The impact of this observation on the probability of wet-weather accidents is important. The time factor is all-important and in this connection the reader is referred to Figure 18 of Chapter II, where the probability of a rainfall of a given intensity is graphed.

Given the observed facts regarding the measured variations in rainfall intensity and duration, it is considered advisable to look at recession curves for various flow lengths, particularly for open-graded friction courses before we complete the trials and tribulations of gathering skid data in natural rain.

The time required for a given surface to drain after rainfall has ceased is a definite factor contributing to wet-pavement exposure time.

To this end and in keeping with the work plan a pavement surface drainage study was made utilizing a 4 by 28 ft (1.2 by 8.5 m) segment of open mixture placed 1 in (25.4 mm) thick on a double tee beam as shown in Figure 121. By using simulated rain and different cross slopes recession curves were developed for different flow lengths.

Recession curves for flow lengths of 9, 14, 18 and 28 ft (2.7, 4.3, 5.5 and 8.5 m) are plotted on Figures 122 through 129. The recession curves, which show runoff rates in inches per hour versus time after stoppage of the rainfall supply, are characteristic of recession curves of flow from drainage areas.

At time zero the runoff rate is equal to the supply rate, so that each curve plotted may be identified as to its initial supply rate or time zero supply rate. Stoppage of rainfall in these experiments was done in a short period of time, resulting in a decrease in runoff after time zero. If rainfall could have been stopped instantly, there would have been a sudden increase of about 5 percent in the discharge rate due to the release of the frictional effect (rain drop impact) of the rainfall on the runoff. The flow would then have decreased in approximately the same manner as shown in Figures 130 through 131. The recession curves shown on Figures 122 through 129 should be representative of actual runoff curves on highway pavements subjected to natural rainfall patterns.

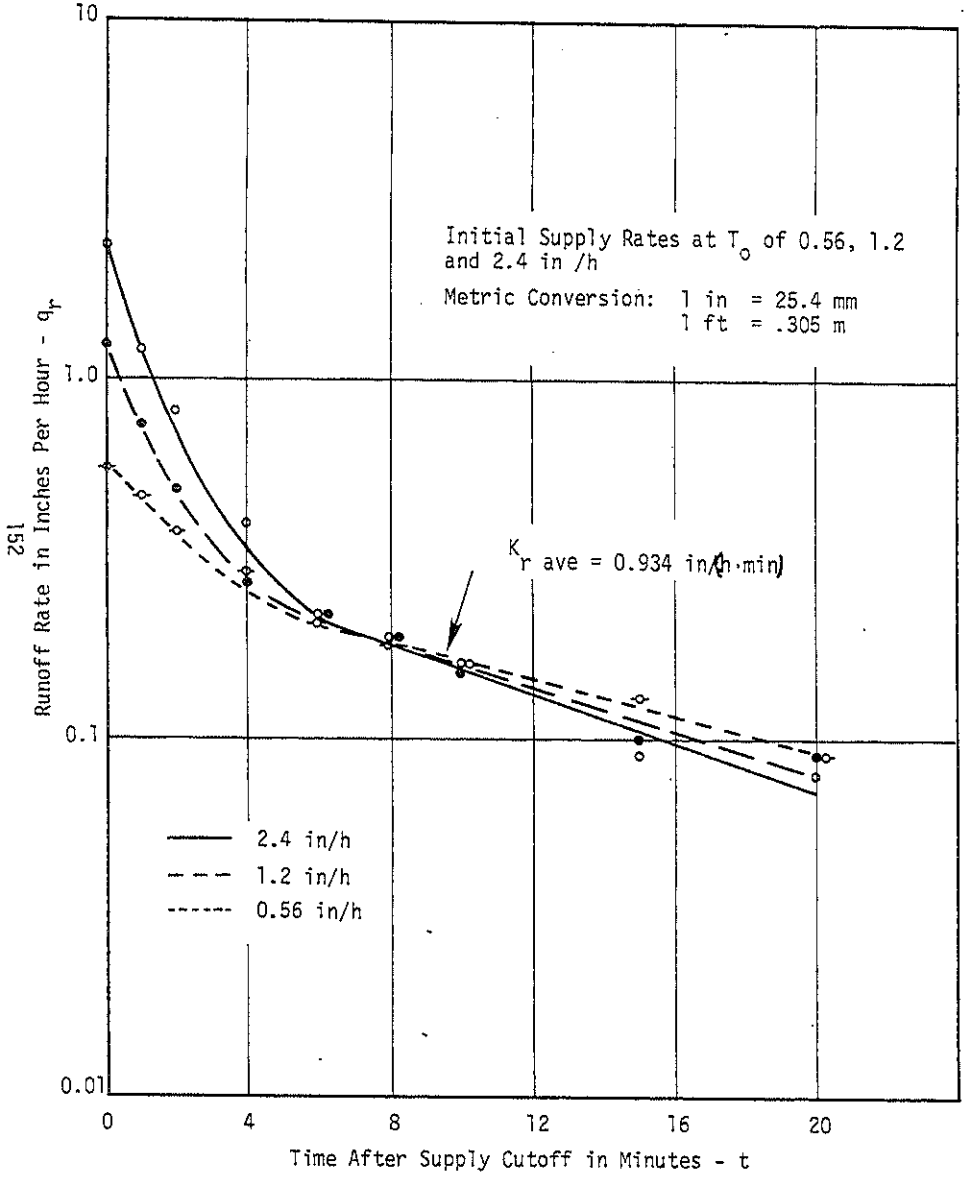

Figure 122. Recession curves 9 ft - flow length slope = 4%

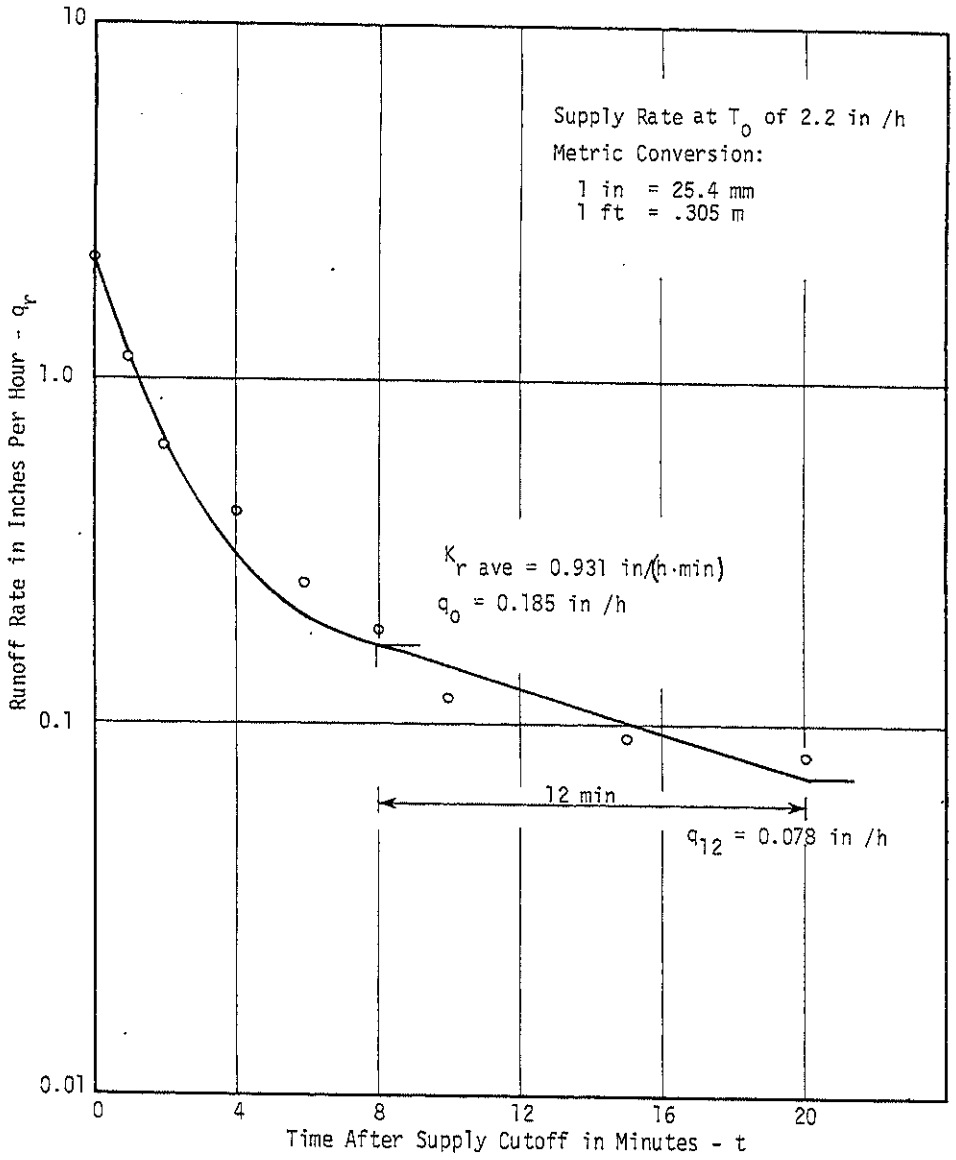

Figure 123. Recession curve 9 ft - flow length slope = 8%

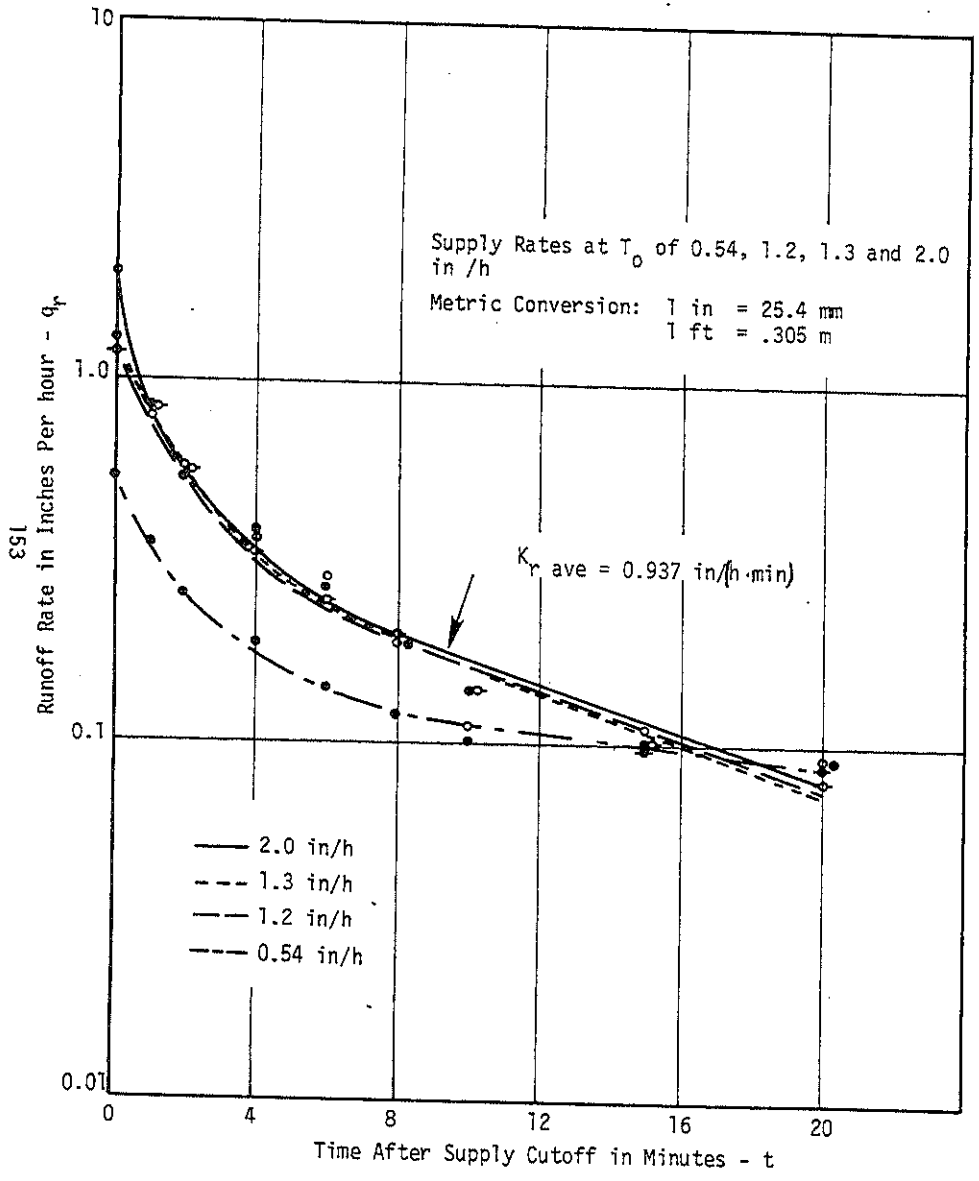

Figure 124. Recession curves 14 ft - flow length slope = 4%

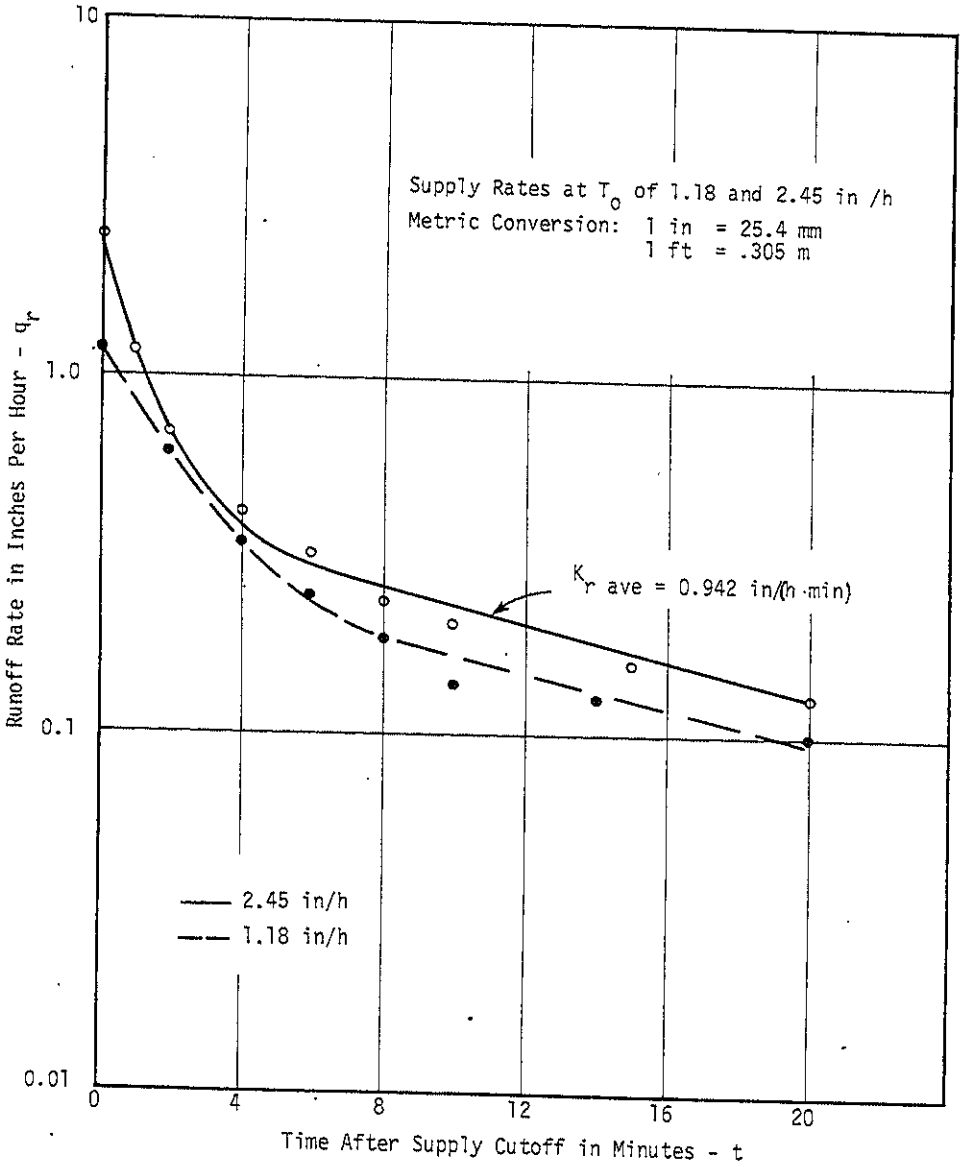

Figure 125. Recession curves 18 ft - flow length slope = 4%

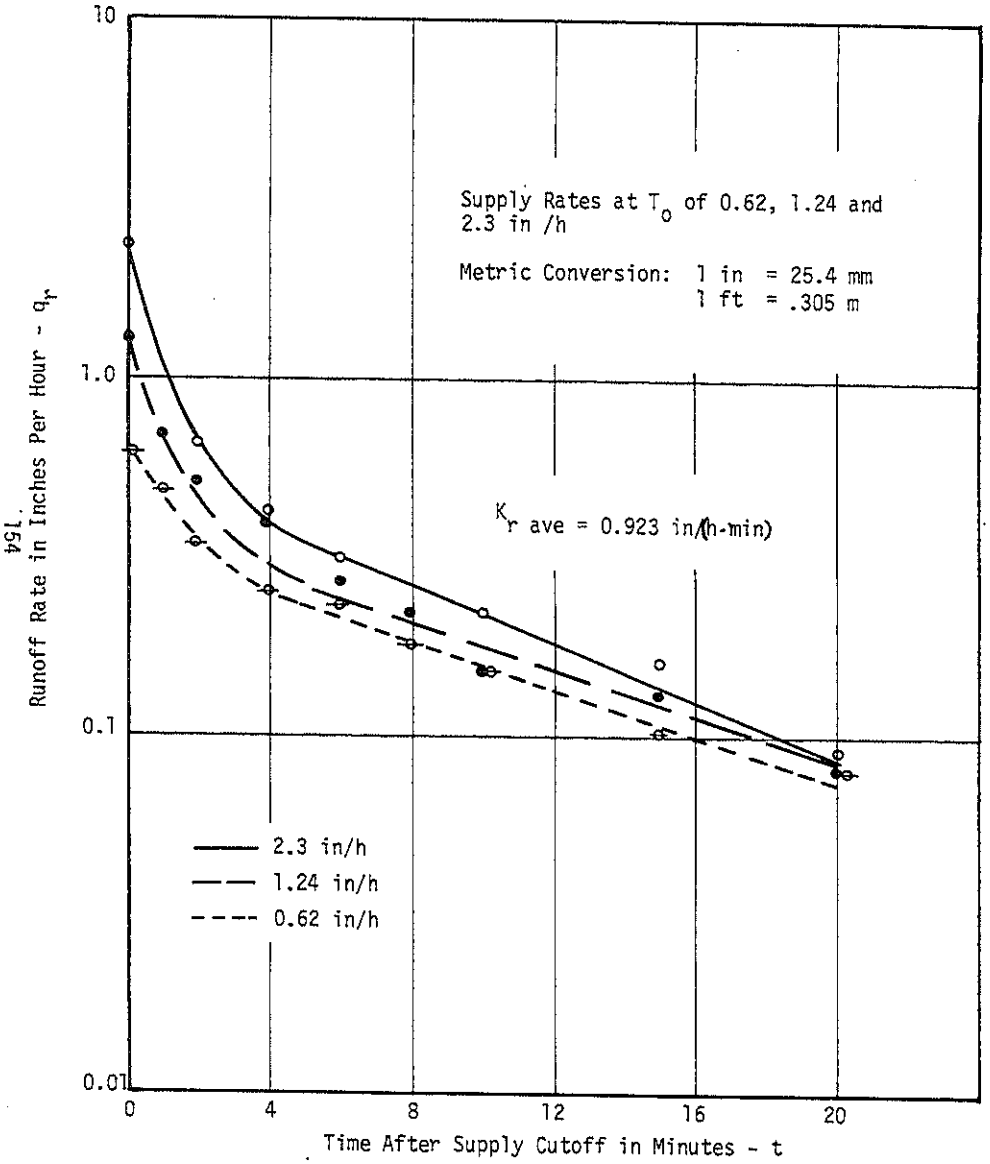

Figure 126. Recession curves 18 ft - flow length slope = 8%

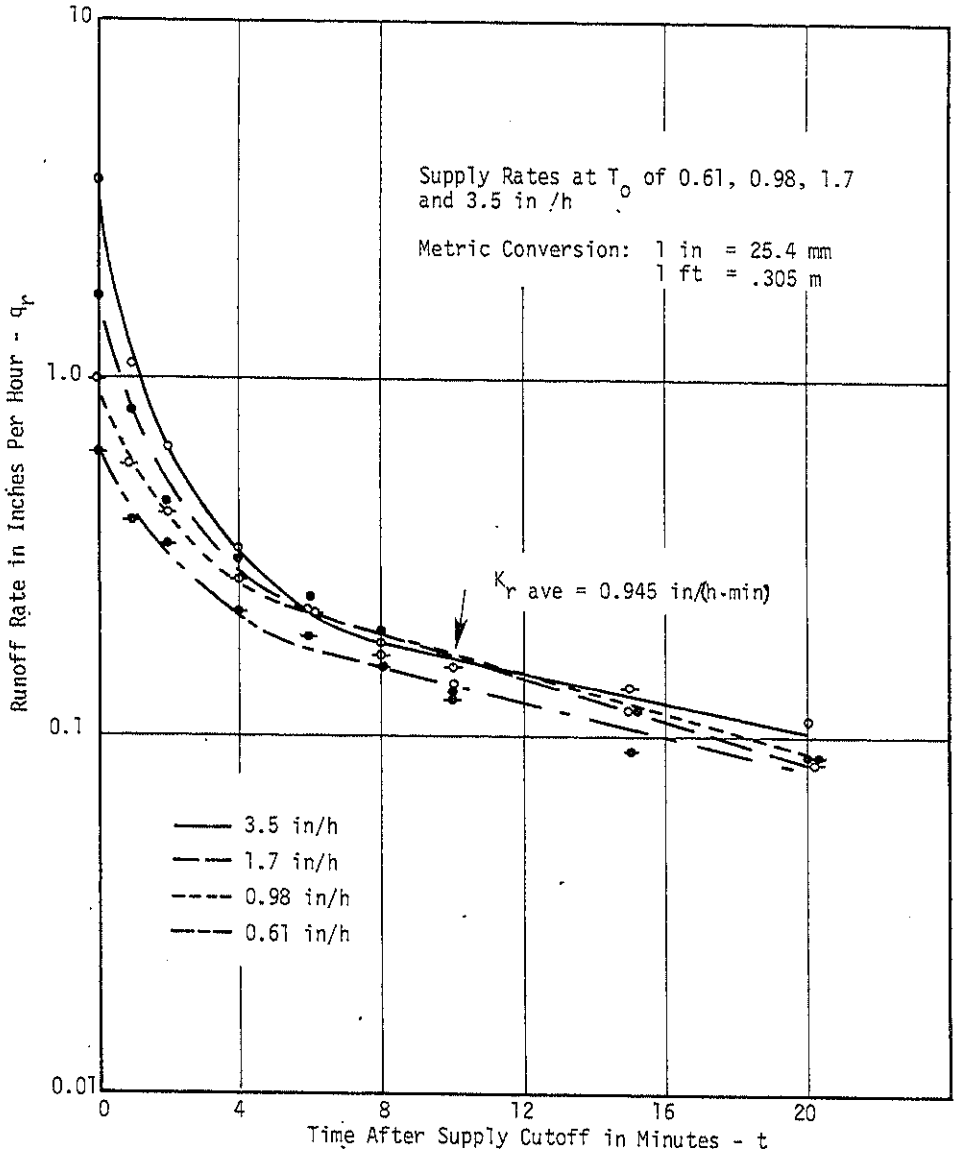

Figure 127. Recession curves 28 ft - flow length slope = 0.5%

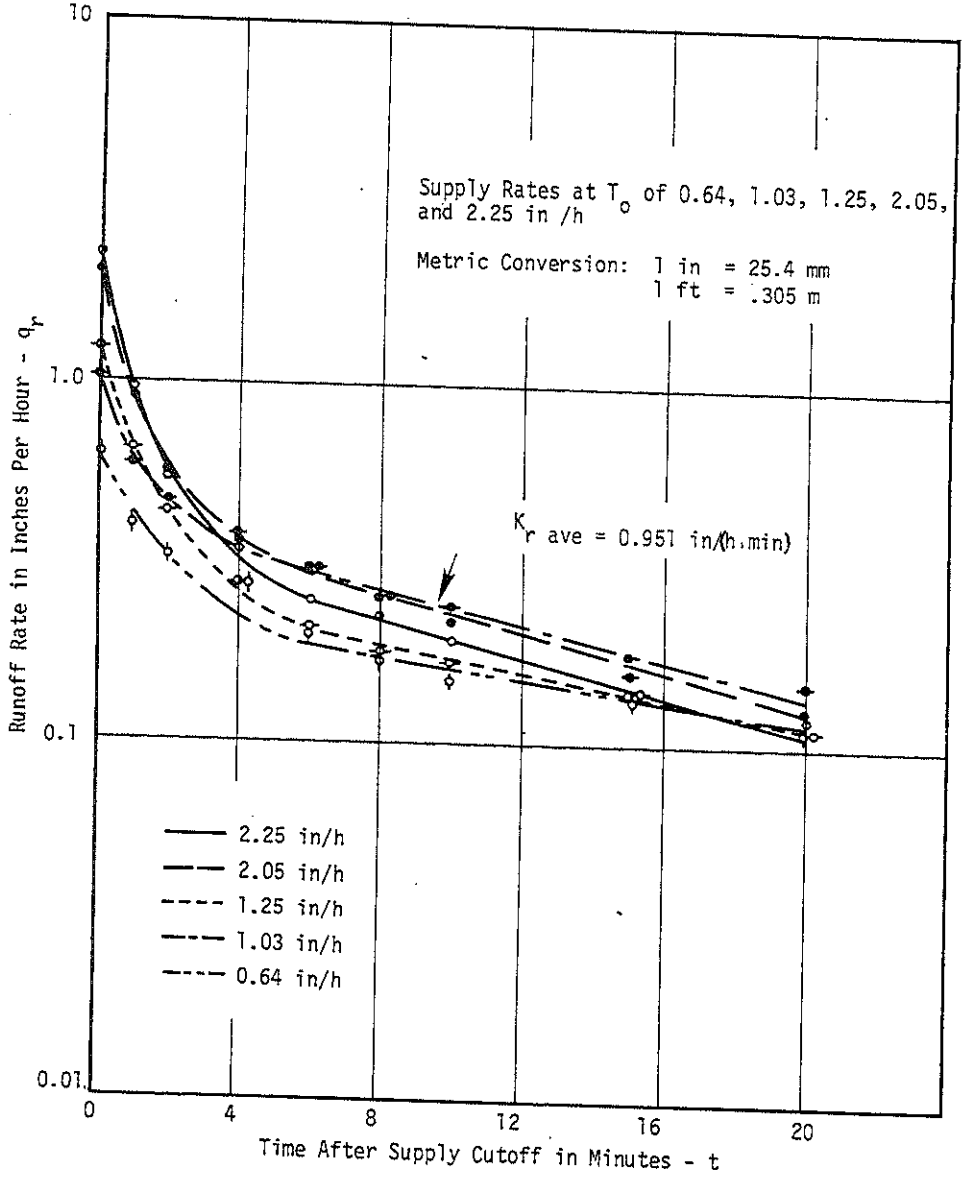

Figure 128. Recession curves 28 ft - flow length slope = 4%

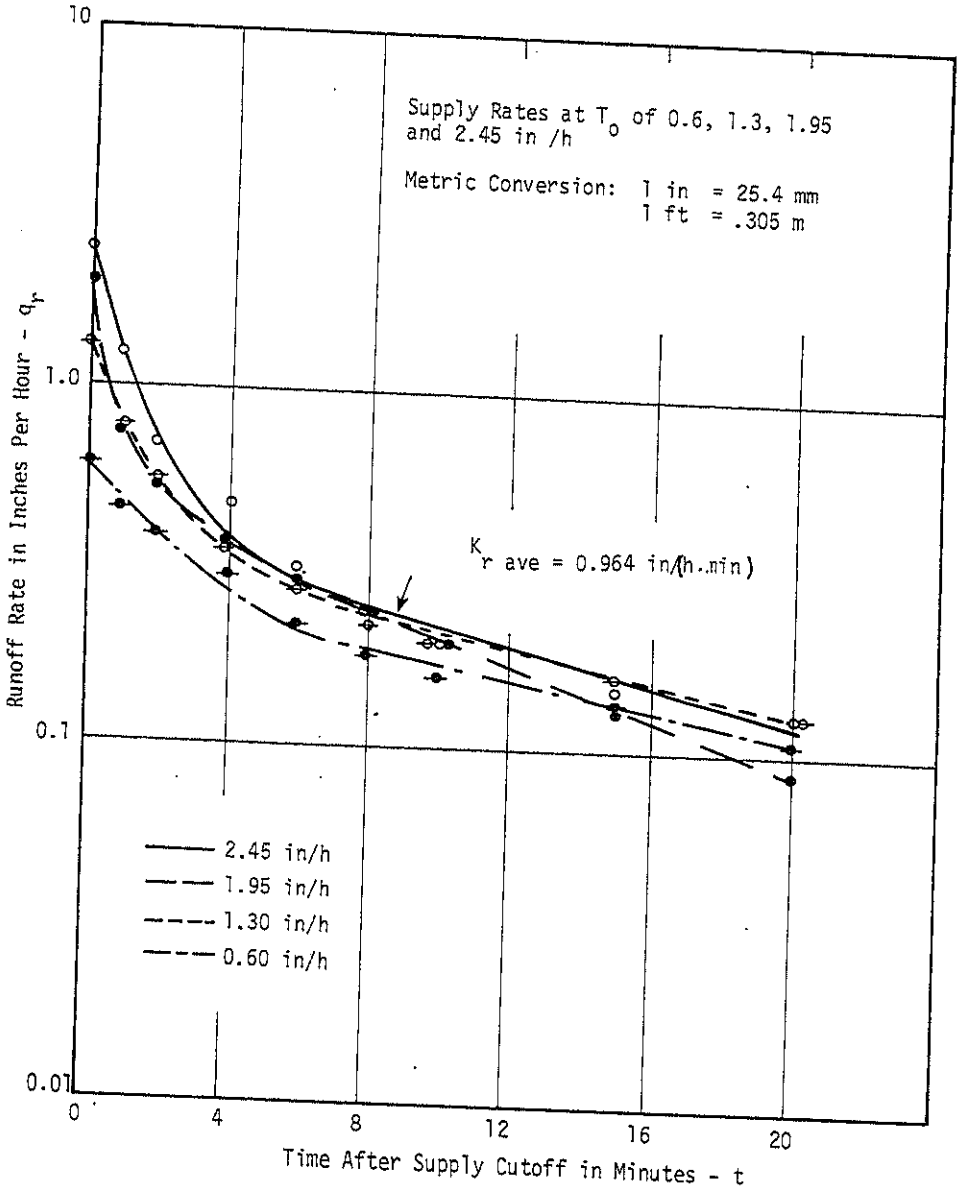

Figure 129. Recession curves 28 ft - flow length slope = 8%

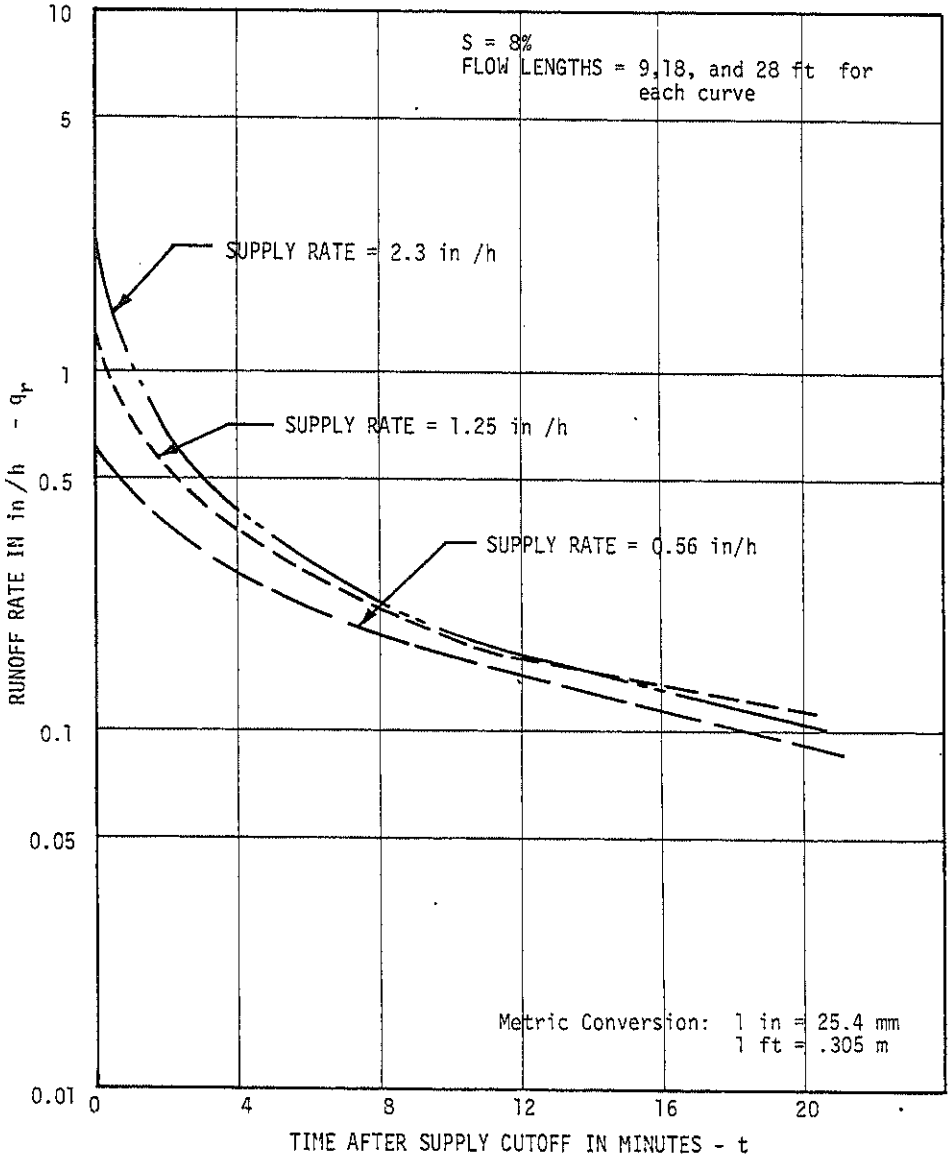

Figure 130. Average recession curves for slope = 8%
9 ft, 18 ft and 28 ft flow lengths

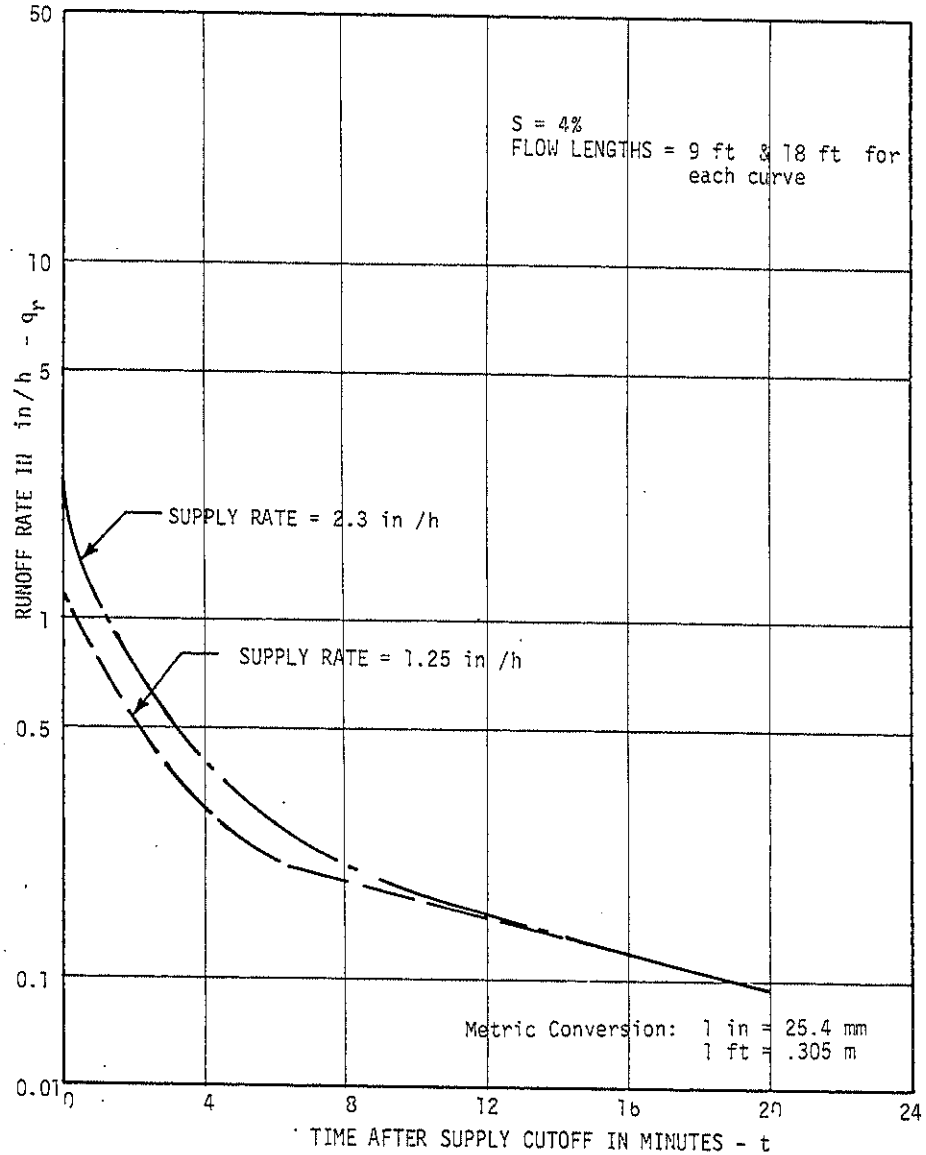

Figure 131. Average recession curves for slope = 4%
9 ft and 18 ft flow lengths

After time zero (or stoppage of rainfall), the runoff rate decreases rapidly until about 6 minutes after stoppage of rainfall and a straight line recession begins. The per minute recession coefficient, K_r may be computed from two points on the exponential (straight line) regression line by the following equation:

$$K_r = \sqrt[t]{\frac{q_t}{q_o}} \qquad \text{Eq (33)}$$

where: q_o = discharge at first point, in/h units

q_t = discharge at second point, in/h units, and

t = time intervals, in minutes between points 1 and 2.

From Figure 123, point 1 is 0.185 in/h (4.7 mm/h) at time = 8 minutes, and point 2 is 0.078 in/h (2.0 mm/h) at time = 20 minutes. The recession coefficient is then

$$K_r = \sqrt[12]{\frac{0.078}{0.185}} = 0.931 \text{ in/h/min.}$$

The discharge rate at any time after point 1 (or any other selected point on the exponential recession line) may be found from the expression

$$q_t = (q_o)(K_r)^t. \qquad \text{Eq (34)}$$

Using the example above:

$$q_{12} = (0.185)(0.931)^{12} = 0.078 \text{ in/h.}$$

The volume in storage at a particular point on the exponential regression line may be found from:

$$\text{Volume in Storage} = \frac{-q_o}{\ln(K_r)}. \qquad \text{Eq (35)}$$

Again using the example on Figure 123, the volume in storage at the time when q_o = 0.185 in/h is

$$\text{Volume} = \frac{-0.185}{\ln(0.931)} = 2.588 \frac{\text{in}}{\text{h}} \text{ minutes.}$$

The volume may be reduced to water depth over the drainage area by dividing by 60 minutes, giving in this case a depth of 0.043 in (1.1 mm). This division by 60 may be carried out for any size of drainage area when q is in in/h and K_r has unites of in/h/min.

Examination of the regression curves for the various lengths indicates a slight trend for the regression coefficient, K_r, to increase with length. The data are, however, scattered too much to give a reliable expression for this trend. The recession coefficient K_r should also decrease with increase

in slope. The data for the 18 ft (5.5 m) flow length show this trend; whereas, the data for the 28 ft (8.5 m) flow length show an opposite trend.

From the plots on Figures 122 through 129, it appears that a considerable amount of drainage occurs in the first 6 minutes after cessation of rainfall. For example, on Figure 128, the curve for a time zero supply rate of 2.0 in/h (51 mm/h) reduces to 0.30 in/h (7.6 mm/h) 6 minutes after stoppage of rainfall. A summation of the area under the 2.0 in/h (51 mm/h) supply curve from zero to 6 minutes gives the volume discharged in this time as 3.51 in/h/minutes. The volume remaining in storage at time = 6 minutes is

$$\text{Volume} = -0.30/\ln(0.951) = 5.97 \text{ in/h/min.}$$

The total volume discharged after time zero would be the sum of these two values or 9.48 in/h/min, equivalent to a water depth of 0.158 in (4.7 mm) over the drainage area.

This discharge rate at 6 minutes after stoppage of rainfall shows a rough trend of increasing values with increase in cutoff supply rate. A plot of the values for a flow length of 28 ft (8.5 m) and a slope of 4 percent is shown on Figure 132.

The scatter of the data for the recession curves may be attributed in part to the accuracy of the measurement of the discharge rates. The experimental apparatus gave sufficient accurate results for determination of rainfall supply rates above 0.6 in/h (15 mm/h). However, when the discharge rates dropped below about 0.2 in/h (5 mm/h) (on a 28-ft (8.5m) flow length), the results became erratic. When shorter flow lengths were used, the results were even more scattered. The following summary statements appear in order.

1. Recession curves of runoff from open-graded asphaltic concrete mixtures have the same characteristics as recession curves from any natural drainage area.

2. The recession coefficient for flow lengths of 24 ft (7.3 m) will be about 0.95 in/h/min for most conditions of slope and rainfall intensity.

3. The exponential recession curve will start at about 6 minutes for flow lengths of 9 to 28 ft (2.7 to 8.5 m) and slopes of 0.5 percent to 8 percent. A rough approximation of the 6-minute discharge rate for a 24-ft (7.3 m) flow length is

$$q_6 = 0.22\,\sigma^{44} \qquad \text{Eq (36)}$$

where q_6 is in in/h and

σ = cutoff supply rate in in/h.

The reader's attention is now redirected to the experimental work conducted in the field under natural rainfall.

Table 17 is a summary of the data collected, for the most part, during natural rain over a period of eight months on SH-21 in Brazos County.

The data collection system consisted of the standard TTI locked-wheel trailer which utilized the ASTM E501 full tread tire inflated to 24 psi (165 kPa). The first column of data includes SN's obtained using the

Table 17. Performance of open-graded friction courses on SH-21 Brazos County in natural rain

Metric Conversion: 1 mph = 1.609 km/h
1 in = 25.4 mm

Section No. 1	DATE INTERNAL WATER Avg. SN	DATE RAINFALL RATE in /h Avg. SN	DATE RAINFALL RATE in /h Avg. SN	DATE RAINFALL RATE in /h Avg. SN	DATE RAINFALL RATE in /h Avg. SN	DATE RAINFALL RATE in /h Avg. SN	DATE RAINFALL RATE in /h Avg. SN	DATE RAINFALL RATE in /h Avg. SN	DATE RAINFALL RATE in /h Avg. SN	DATE RAINFALL RATE in /h Avg. SN
40 mph O.O.*	5/21 Int. 52	6/15 0.57 52	9/9 0.07 50	11/1 0.01 52	11/8 0.42 53	1/11 0.14 47	1/16 0.47 49	1/11 1.3 43	1/16 0.62 44	1/18 0.08 45
40 mph I.O.**	5/21 Int. 55	6/15 0.34 60	9/9 0.07 64	11/1 0.06 61	11/8 0.26 54	1/11 0.11 57	1/16 0.11 58	1/11 1.2 53		
55 mph O.O.	5/21 Int. 46	6/15 0.10 51		11/1 0.06 52	11/8 0.33 50	1/11 0.09 48	1/16 0.10 46	Goodyear Custom Belted-Polyglass		
55 mph I.O.	5/21 Int. 47	6/15 0 57		11/1 0.01 50	11/8 0.28 52	1/11 0.13 48	1/16 0.09 47	G 78 x 15 2/32-inch Tread		
Section No. 2										
40 mph O.O.	5/21 Int. 52	6/15 0.57 60	9/9 0.07 45	11/1 0.01 56	11/8 0.42 60	1/11 0.14 53	1/16 0.47 53	1/11 1.3 55	1/16 0.62 54	1/18 0.08 53
40 mph I.O.	5/21 Int. 51	6/15 0.34 58	9/9 0.07 49	11/1 0.06 53	11/8 0.26 54	1/11 0.11 48	1/16 0.11 46	1/11 1.2 43		
55 mph O.O.	5/21 Int. 46	6/15 0.10 54		11/1 0.06 53	11/8 0.33 52	1/11 0.09 47	1/16 0.10 48	Goodyear Custom Belted-Polyglass		
55 mph I.O.	5/21 Int. 48	6/15 0 51		11/1 0.01 52	11/8 0.28 52	1/11 0.13 50	1/16 0.09 48	G 78 x 15 2/32-inch Tread		
Section No. 3										
40 mph O.O.	5/21 Int. 53	6/15 0.57 61	9/9 0.07 50	11/1 0.01 57	11/8 0.42 58	1/11 0.14 56	1/16 0.47 54	1/11 1.3 50	1/16 0.62 5	1/18 0.08 52
40 mph I.O.	5/21 Int. 53	6/15 0.34 62	9/9 0.07 51	11/1 0.06 57	11/8 0.26 59	1/11 0.11 57	1/16 0.11 52	1/11 1.2 49		
55 mph O.O.	5/21 Int. 44	6/15 0.10 55		11/1 0.06 51	11/8 0.33 47	1/11 0.09 48	1/16 0.10 47	Goodyear Custom Belted-Polyglass		
55 mph I.O.	5/21 Int. 46	6/15 0 52		11/1 0.01 50	11/8 0.28 54	1/11 0.13 51	1/16 0.09 49	G 78 x 15 2/32-inch Tread		
Section No. 4										
40 mph O.O.	5/21 Int. 50	6/15 0.57 59	9/9 0.07 56	11/1 0.01 60	11/8 0.42 53	1/11 0.14 53	1/16 0.47 51	1/11 1.3 51	1/16 0.62 49	1/18 0.08 53
40 mph I.O.	5/21 Int. 52	6/15 0.34 61	9/9 0.07 55	11/1 0.06 58	11/8 0.26 56	1/11 0.11 53	1/16 0.11 53	1/11 1.2 52		
55 mph O.O.	5/21 Int. 47	6/15 0.01 55		11/1 0.06 52	11/8 0.33 47	1/11 0.09 49	1/16 0.10 44	Goodyear Custom Belted-Polyglass		
55 mph I.O.	5/21 Int. 46	6/15 0 55		11/1 0.01 49	11/8 0.28 44	1/11 0.13 43	1/16 0.09 47	G 78 x 15 2/32-inch Tread		

*O.O. = outside lane, outside wheel path
**I.O. = inside lane, outside wheel path

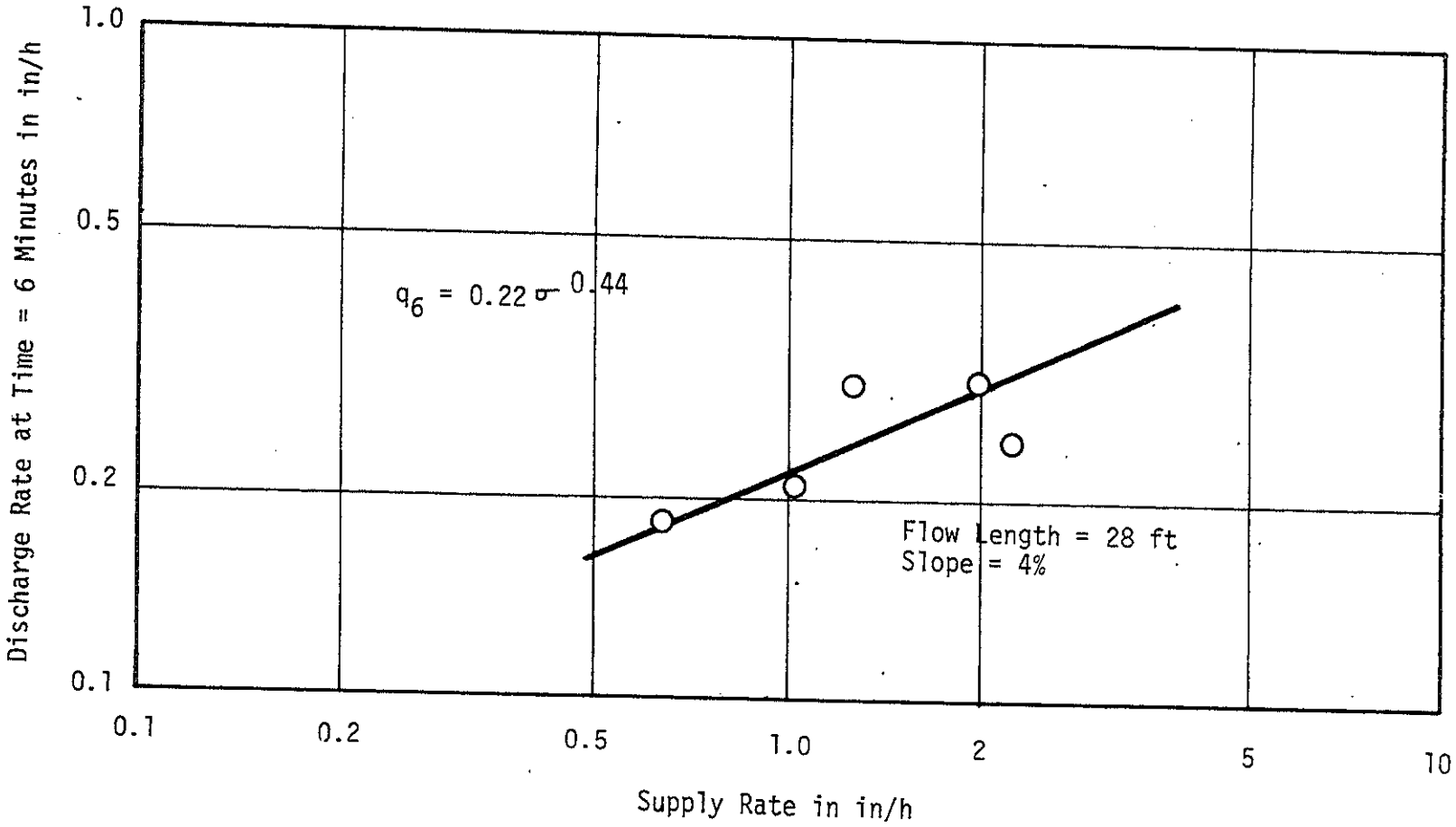

Figure 132. Value of discharge after 6 minutes with respect to cutoff supply rate, σ

Metric Conversion: 1 in = 25.4 mm
1 ft = 0.305 m

internal watering systems as per ASTM E274. These data indicate no significant difference among the four test sections.

The next six columns of data represent information collected during natural rain, the intensity of which varied from zero to 0.57 in/h (14.5 mm/h). An examination of these data indicates that all four sections of the OGFC performed in a highly acceptable manner. To picture this conclusion more clearly the more than 260 data points at SN_{40} and SN_{55} were averaged for each lane of each section at the two test speeds, and these were plotted and are shown in Figure 133. A spread in the SN_{40} of eight skid numbers (from 51 to 59) is apparent; whereas, the SN_{55} ranged from 49 to 51, a remarkably small variation. If all these data are averaged for both lanes and all sections, the SN_{40} is found to be 55 and the SN_{55} is found to be 50, a drop of only five skid numbers for a speed increase of 15 mph (24 km/h).

In columns 8, 9 and 10 limited data are presented depicting skid numbers in natural rain on these same test sections wherein a G 78-15 custom belted polyglass tire with 2/32 in (1.6 mm) tread was substituted for the full tread ASTM E501.

Observations were made during rains of three different intensities varying from 0.08 in/h (2 mm/h) to 1.3 in/h (33 mm/h). Data at 40 mph (64 km/h) ranged from 43 to 55 with no particular pattern.

The data presented in Table 18 and Figure 134 were obtained from the four test sections of OGFC on SH-21 in Brazos County. Six-inch (152 mm) diameter cores were taken from each of these sections and tested for water permeability in the laboratory. Both constant head and falling head measurements were taken. Except as noted the cores came from the outside lane of each section.

It will be recalled that Section 1 contained no crusher fines and that increasing amounts of fines were used in Sections 2, 3 and 4. From the data points it appears that 10 to 15 percent crusher fines produce the most permeable surface for the materials and mixture design utilized on this project.

Apparently the zero fines mixture suffered particle degradation due to the limited number of aggregate contact points and the associated stress at these points of contact. It should be recalled that the coarse aggregate used on this project is a manufactured lightweight aggregate sized predominantly from 1/2 in (13 mm) to No. 4 (4.8 mm) sieve sizes.

Field measurements made with the skid trailer at most of the sites were limited for reasons stated; however, extensive photographs were taken, coordinated with rainfall intensity readings. Selected photographs from several of the sites follow with captions and added explanations in the text as seems appropriate.

With the exception of the data gathered on the SH-21 sections in Brazos County personnel of the State Department of Highways and Public Transportation were generally responsible for data gathering at the other four field sites. The coordinated assistance of State and Federal agencies is a necessary part of research of this type.

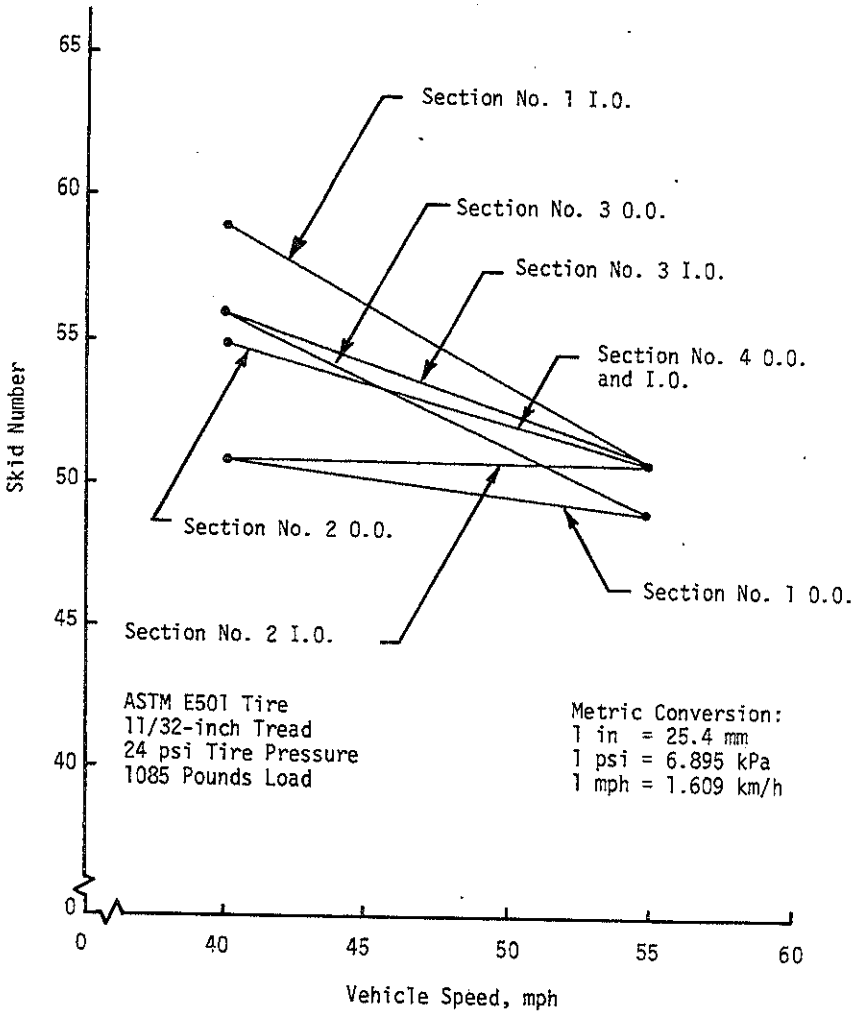

Figure 133. Average skid numbers in natural rain of various intensities on SH-21 OGFC for outside lane, outside wheel path (O.O.) and inside lane, outside wheel path (I.O.)

Table 18. Properties of field cores from SH-21 open-graded surfaces

Sec. No.	Lane	Percent Fines	Core Location	Thickness mm	K cm/sec	
					Const. Head	Falling Head
1	outside	0	BWP	22	0.058	0.053
1	outside	0	OWP	10	0.035	0.034
2	outside	8	OWP	25	0.080	0.079
2	inside	8	OWP	26	0.048	0.048
3	outside	15	OWP	24	0.118	0.121
4	outside	22	OWP	23	0.027	0.025

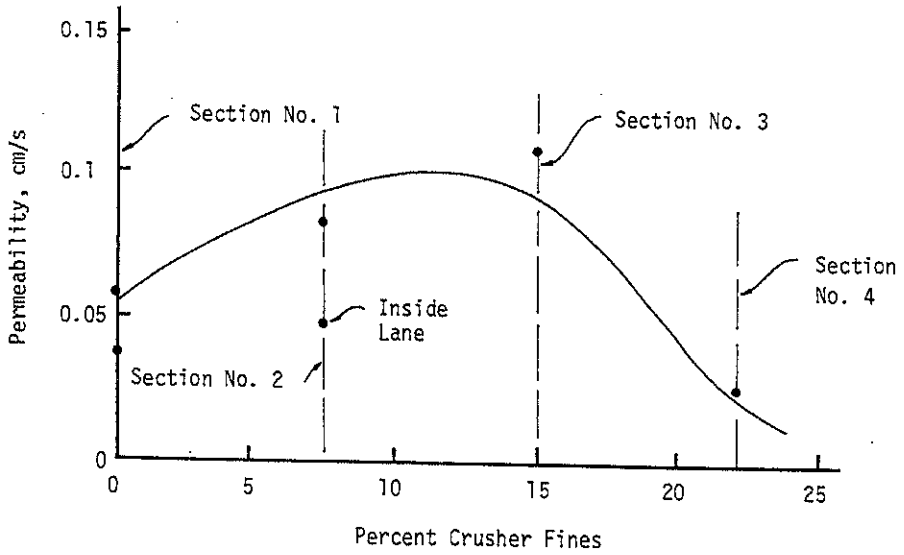

Figure 134. Modified U. S. Corps of Engineers Waterways Experiment Station permeameter values for field cores from SH-21 open-graded surfaces

Natural Rainfall on Open-Graded and Dense Surfaces in Austin, Texas

Limited data were gathered during and after rain in the Austin, Texas, area on both dense and open-graded surfaces. Photographic evidence is presented depicting the several events in Figures 135 through 143.

Figure 135 presents a thru lane facility on a crest vertical curve with a drainage path length of about 50 ft (15 m). Cross slope in this area of the pavement is about 2 percent. Water flow lines are in evidence but complete flooding of the surface asperities occurs in only a small part of the off-ramp area (see left center of photograph). The condition being observed was photographed about three minutes after rain had ceased.

Figure 136 is the same general area but somewhat upstream. This picture was taken three minutes after rain had ceased. In both cases the two higher lanes of the road appear "dry". Open mix extends completely across the road.

In Figure 137 only the two travelled lanes are surfaced with OGFC. This picture was taken ten minutes after rainfall had ceased. Water continues to sheet across the dense shoulder, a potential hazard area.

Rainfall intensity in Figure 138 is 0.06 in/h (1.5 mm/h). The skid trailer wheel is locked. The line left behind the locked wheel indicates that the tire has purged the voids in the surface layer. High SN_{40} recorded during the lockup indicate adequate rubber-to-aggregate contact. It is evident from Figure 139 that the light rain has caused some spray in the outside lane of this four-lane divided highway.

For a passenger vehicle there is a minimal amount of spray in Figure 140.

In Figure 141 a "bow wave" is visible in front of the locked wheel of the skid trailer operating on a dense pavement surface in 0.06 in/h (1.5 mm/h) intensity. Glare is more pronounced on this surface than that on an open surface subject to the same conditions (see Figure 170).

In Figure 142 rain had ceased five minutes before this picture was taken. Surface drainage continues in the outside lane and is creating spray. Even ten minutes after rain ceased spray continued to trail passenger vehicles for 50 ft (15 m) or more (see Figure 143).

Fort Worth Pavements in Natural Rain

Pictorial evidence of splash and spray on pavements subjected to heavy traffic is presented in the photographs that follow. These pictures are grouped and include variables of pavement type (open-graded or dense), rainfall intensity, lane position of vehicle being observed, type of vehicle and geometrics.

The photographs presented in Figures 144, 145, 146 and 147 were taken during a rainfall intensity of 0.04 in/h (1 mm/h). All observations were on I-30 where a lightweight aggregate was used to form a thin open-graded surface of limited internal permeability.

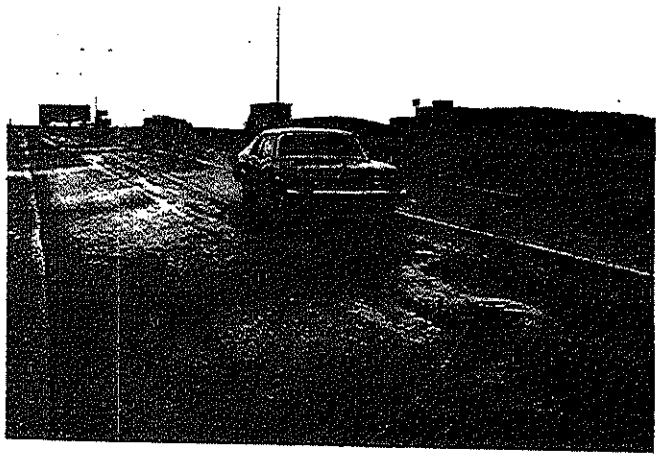

Figure 135. Austin, Texas, U. S. 290 open-graded friction course on crest vertical curve (Note direction of water flow and spray. Rain had ceased about 3 minutes before photo was taken.)

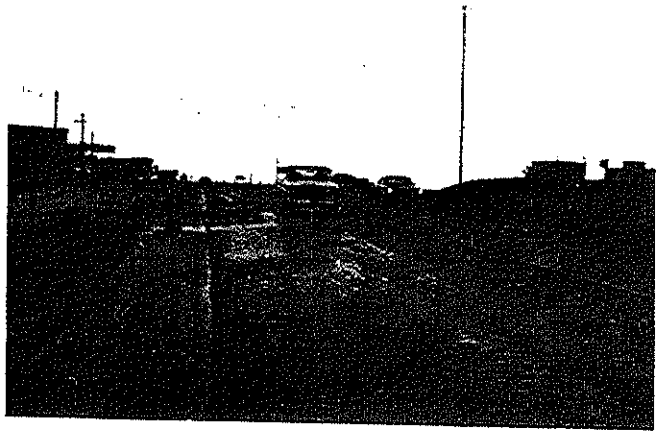

Figure 136. Austin, Texas, U. S. 290 OGFC 3 minutes after rain ceased. (Note flow line of water and absence of visible water on inside (high) lane.)

Figure 137. Austin, Texas, U. S. 290, 10 minutes after rainfall ceased on open mix (Note water ponding at transition to curve.)

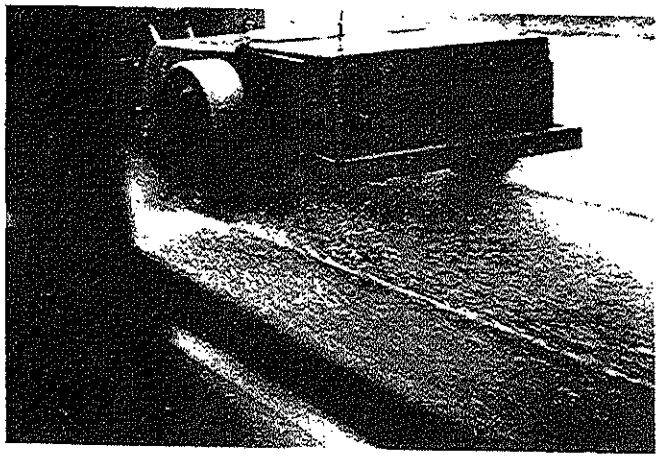

Figure 138. Austin, Texas, U. S. 290 open-graded surface 3/4 inch (19 mm) thick after skid trailer lockup. (Note light line behind left wheel caused possibly by purging of water and air into and out of pavement voids. Rainfall 0.06 in/h (1.5 mm/h))

Figure 139. Austin, Texas, U. S. 290 open-graded friction course in 0.06 in/h (1.5 mm/h) rainfall before wheel lockup

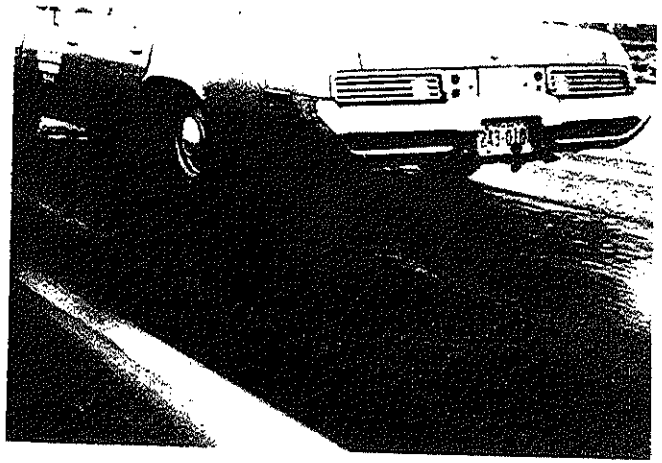

Figure 140. Austin, Texas, U. S. 290 "light" rain. (Vehicle traveling 55 ± mph (88 km/h). Spray from open mix not serious.)

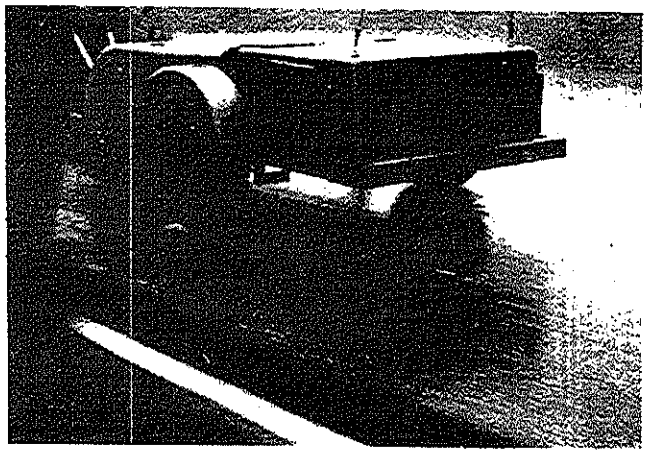

Figure 141. Austin, Texas, U. S. 290 dense pavement in 0.06 in/h (1.5 mm/h) rainfall - locked wheel skid tests (Note bow wave at left wheel and glare from reflected light.)

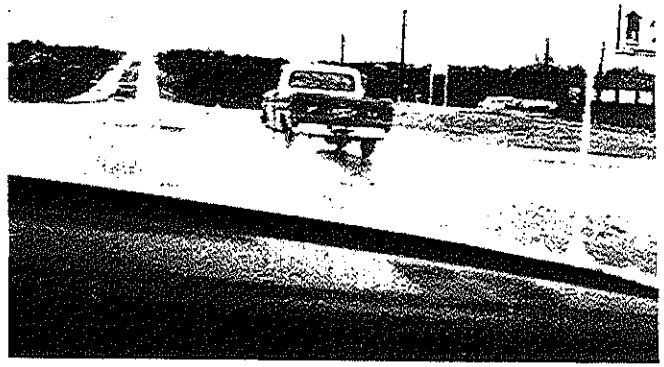

Figure 142. Austin, Texas, U. S. 290 5 minutes after rainfall ceased on dense pavement (Note heavy spray in outside (lower) lane.)

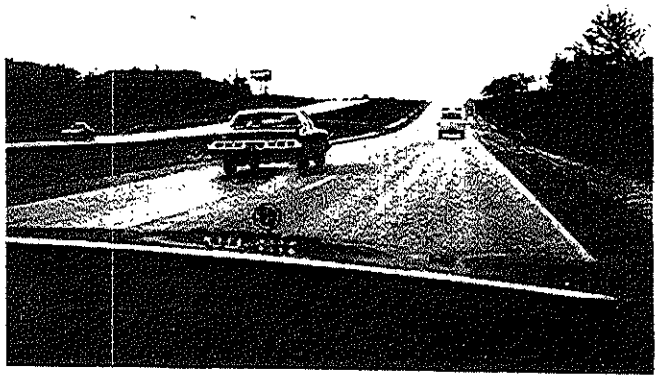

Figure 143. Austin, Texas, U. S. 290, 10 minutes after rainfall ceased on dense pavement (Note spray on inside (high) lane.)

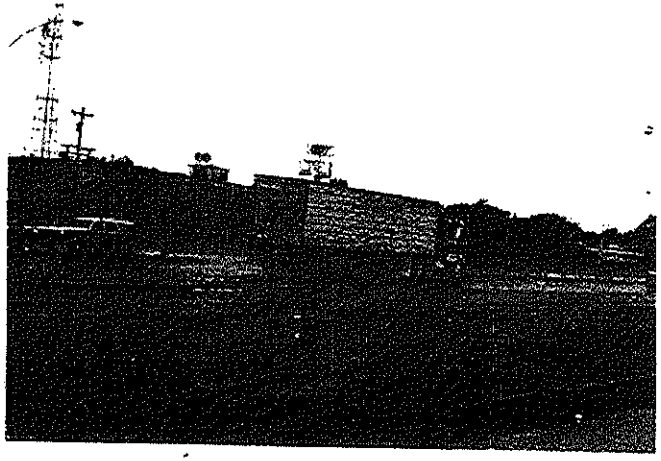

Figure 144. Fort Worth, Texas, I-30, open-graded surface 3/4 inch (19 mm) thick in 0.04 in/h (1 mm/h) rainfall (Spray from truck would be objectionable particularly at night.)

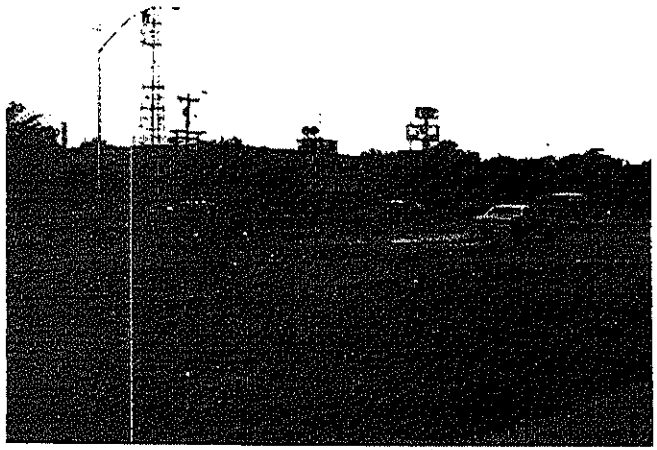

Figure 145. Fort Worth, Texas, I-30, 0.04 in/h (1 mm/h) rainfall (Spray from automobiles is evident but not severe.)

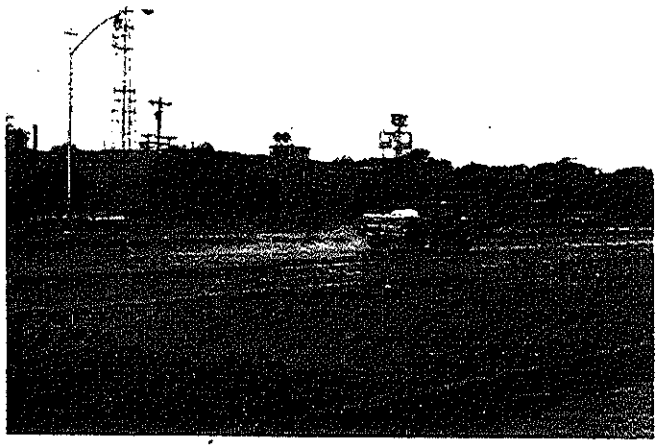

Figure 146. Fort Worth, Texas, open-graded lightweight aggregate surface about 3/4 inch (19 mm) thick in 0.04 in/h (1 mm/h) rainfall

Figure 147. Fort Worth, Texas, I-30, open-graded surface on compound curve in 0.04 in/h (1 mm/h) rainfall.

Figure 148. Fort Worth, Texas, I-30, concrete pavement (Note spray from outer lane of superelevated curve in 0.04 in/h (1 mm/h) rainfall.)

A large truck, passenger vehicle and a pickup truck may be observed with each one producing spray. It is apparent and expected that the tractor-trailer causes much more spray.

In Figure 145 there is a marked difference in the spray when the vehicles in the inner and outer lanes are compared.

The pickup in Figure 146 creates more spray than a passenger vehicle on the same lane and in the same weather condition. The vehicle on the inside lane of a compound curve in Figure 147 presents more spray than might be expected. The crest vertical curve is a factor in this case.

Figures 148, 149, 150 and 151 involve another segment of I-20 in Fort Worth where the old existing portland cement concrete pavement is exposed directly to traffic. Rainfall intensity is 0.03 to 0.04 in/h. Spray generally extends further behind all types of vehicles and is noticeably denser. Although not critical during daylight hours the level of light reflectance is much greater on these dense pavements of low macrotexture. Headlamp glare at night would add to the driving task. The driving task would be further complicated on undivided highways.

Photographs presented in Figures 152, 153 and 154 were taken during a rain of 0.03 in/h (0.8 mm/h) intensity and all three show large trucks. The VW bug along the side of the tractor-trailer of Figure 152 represents only limited hazards but these hazards would be more severe at night.

The side view of the tractor-trailer of Figure 154 gives reasonably clear evidence that the OGFC gives adequate spray control. Spray extends behind the vehicle about 50 ft (15 m) and is rather light. The pickup drawn house trailer of Figure 155 is travelling at about 55 mph (88 km/h) in the outside lane of this heavily travelled freeway. Low level spray extends about two car lengths behind the trailer. Macrotexture of this pavement is in the range of 0.04 to 0.05 in (1 to 1.3 mm).

In Figures 156, 157, 158 and 159 the observed rainfall intensity is 0.02 in/h (0.5 mm/h). These pavements are all of the open-graded type but the overlay thickness is, as has been the case throughout the entire Fort Worth area, quite minimal with little or no true internal drainage. One might refer to these overlays as special surface treatments designed for heavy traffic.

The surfaces do have a good macrotexture and the aggregate selection procedure is generally structured to avoid the inclusion of polishing types of stone. The light spray behind the tractor-trailer of Figure 158 is typical for these surfaces in this intensity of rain. The low level of light reflectance is evident in Figure 159.

Natural Rainfall on OGFC in Beaumont

A group of selected photographs is presented to show splash and spray of passenger vehicles and trucks in natural rain on open-graded surface courses in the Beaumont, Texas area. Two rainfall intensities, namely 0.25 in/h and 0.05 in/h (6.4 mm/h and 1.3 mm/h) were observed on state and interstate highways surfaced with thin overlays of open-graded hot-laid asphalt surfacing.

Figure 149. Fort Worth, Texas, Hulen Street, portland cement concrete 0.04 in/h (1 mm/h) rainfall (Note high level of light reflection.)

Figure 150. Fort Worth, Texas, I-30, concrete pavement in 0.03 in/h (0.8 mm/h) rainfall (Note light reflectance, a night hazard.)

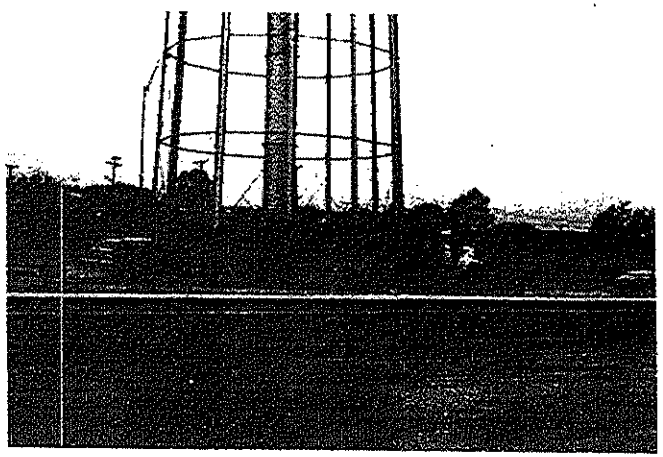

Figure 151. Fort Worth, Texas, I -30, concrete pavement in 0.03 in/h (0.8 mm/h) (Note spray in area of windshield of trailing passenger vehicle.)

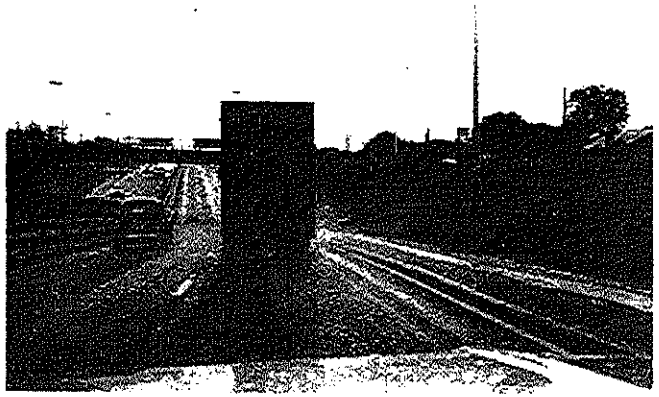

Figure 152. Fort Worth, Texas, I-30, open-graded friction course in 0.03 in/h (0.8 mm/h) rainfall on downgrade to sag-vertical curve (Spray is evident but not excessive.)

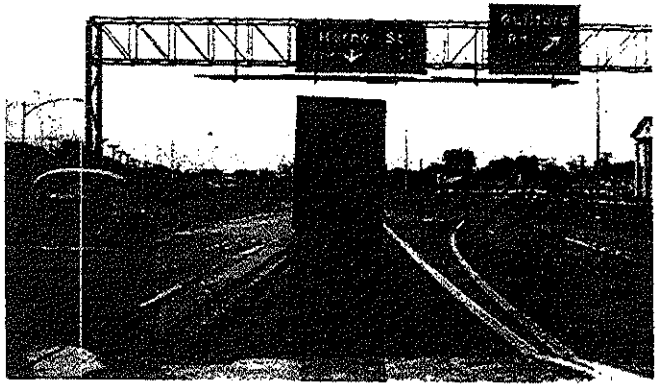

Figure 153. Fort Worth, Texas, I-30, lightweight aggregate open mix in 0.03 in/h (0.8 mm/h) rainfall (Note "dry" tire marks behind truck.)

Figure 154. Fort Worth, Texas, I-20, during 0.03 in/h (0.8 mm/h) rainfall (Truck speed about 55 mph (88 km/h))

Figure 155. Fort Worth, Texas, I-20, during 0.03 in/h (0.8 mm/h) rainfall (Heavy traffic, medium macrotexture, surface course generally less than 3/4-inch (19 mm) thick.)

Figure 156. Fort Worth, Texas, I-20, rhyolite aggregate open mix in 0.02 in/h (0.5 mm/h) (Note visible water in outside wheel path of inside lane.)

Figure 157. Fort Worth, Texas, I-20, OGFC utilizing rhyolite (Rainfall 0.02 in/h (0.5 mm/h), truck traveling 55± mph (88 km/h). Spray would be less in inside lane.)

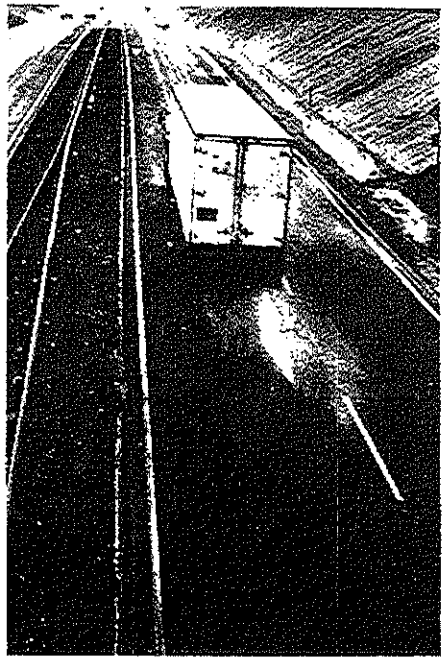

Figure 158. Fort Worth, Texas, I-20, during 0.02 in/h (0.5 mm/h) rainfall (Spray trails the truck 100 to 150 feet (30 to 46 m) on rhyolite open-graded surface.)

Figure 159. Fort Worth, Texas, I-20, open mix using rhyolite aggregate rainfall 0.02 in/h (0.5 mm/h) (Cut section with some spray from dual wheel vehicles and very little from passenger car and pickup.)

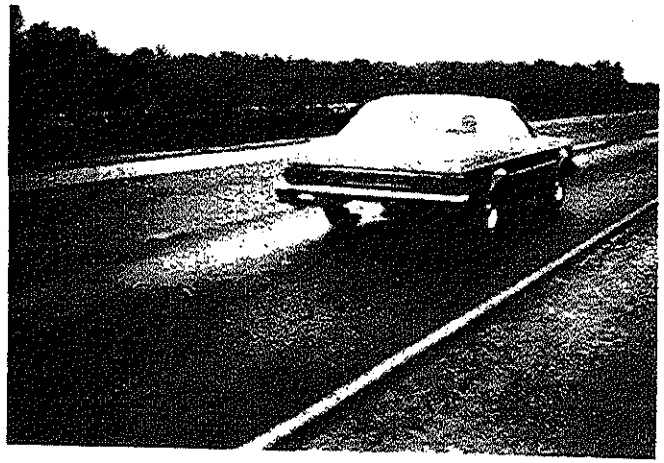

Figure 160. Beaumont, Texas, I-10, open mix in 0.25 in/h (6.4 mm/h) rainfall (Highly acceptable performance. Total traffic about 4.5 million passages.)

The coarse aggregates used in all but one of the surfaces consisted of selected manufactured lightweight aggregate with good and lasting microtexture. This material was sized from 1/2 in (13 mm) to No. 4 (4.75 mm) mesh. Fine aggregate formed about 10 percent by weight of the total aggregate. The combination resulted in a blend containing about 3 percent filler.

One section of pavement utilized a crushed traprock sized similarly to the lightweight material. A major difference in particle-shape existed between the two materials. The lightweight was blocky in form while the traprock particles were quite flat. Constrast Figures 164 and 167.

Reference is made to Figures 160, 161 and 162 taken during rain on I-10. It is apparent in Figure 160 where a passenger vehicle is travelling about 55 mph (88 km/h) in the outside lane in rainfall of intensity 0.25 in/h (6.4 mm/h) that the open-graded surface is performing quite well. On the other hand the tractor-trailer in Figure 161 is creating a noticeable amount of spray but no splash. The truck is travelling about 55 mph (88 km/h) and on a slight upgrade of about 2 percent.

Figure 162 presents a truck on another segment of I-10. Truck speed was estimated at 45 mph (72 km/h). There is no splash and the spray is much less than that to be observed in Figure 161.

Rainfall intensity in Figures 163, 164 and 165 is about 0.05 in/h (1.3 mm/h). These photographs clearly show that none of the three vehicles causes any splash or spray on this segment of SH-87. Again the surface is open-graded with fines used in the mixture design. Cross slope of the travelled lanes is 2 percent. The shoulder is also surfaced with an open-graded surface and is cross sloped at 3 percent. Performance is judged excellent.

The effects of accumulated water in and on open-graded pavement surfaces are functions of several factors. Figure 166 depicts a situation where surface performances were observed about three minutes after cessation of heavy rain. The eighteen-wheel truck produced some spray but no splash. Now contrast this with a similar truck on SH-87 in a 0.06 in/h (1.5 mm/h) rainfall. Note that the macrotexture on the I-10 pavement is 0.08 in (2 mm) and that on SH-87 is 0.03 in (0.8 mm). Additionally, there is less cross slope on SH-87 (see Figure 167).

Natural Rainfall on OGFC in Bryan on SH-21

The probability of securing tire-pavement interaction data during natural rainfall was greatest for Brazos County SH-21 site. Proximity to the test site and availability of a trained crew and the necessary equipment made it possible to obtain skid data during several rains. The range of the rainfall intensity was fairly broad and covered those intensities for which data were considered most desirable.

Instructions to the data gathering crew were essentially the same as those issued to the other four sites in Texas. Emphasis was placed on gathering data at 40 mph (64 km/h) with a full tread ASTM E501 tire followed by a reading at 55 mph (88 km/h). Wheel load and tire inflation pressure corresponded to that called for in ASTM E274.

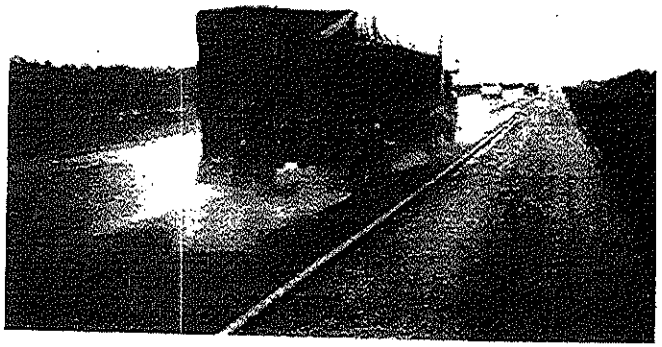

Figure 161. Beaumont, Texas, I-10, open-graded surface in 0.25 in/h (6.4 mm/h) rainfall (Traffic about 4.5 million passages. Cross Slope is about 2 percent.)

Figure 162. Beaumont, Texas, I-10, open-graded surface in 0.25 in/h (6.4 mm/h) rainfall (Surface performance considered quite successful.)

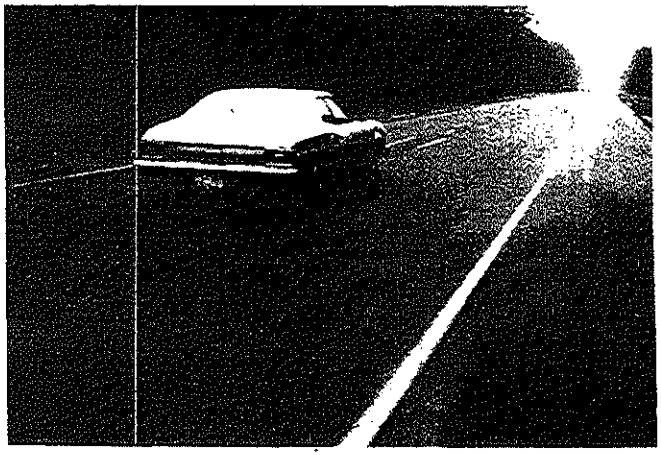

Figure 163. Beaumont, Texas, SH-87, open mix in 0.05 in/h (1.3 mm/h) rainfall (Complete internal drainage after 1.5 million vehicle passages. Cross slope 2 percent.)

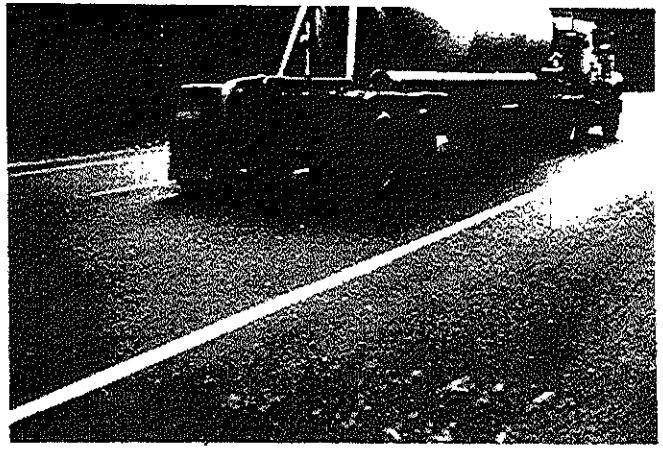

Figure 164. Beaumont, Texas, SH-87, open-graded friction course in 0.05 in/h (1.3 mm/h) rainfall (Contrast performance with that shown in Figure 167).

Figure 165. Beaumont, Texas, SH-87, open mix including the shoulder effective in 0.05 in/h (1.3 mm/h) rainfall (Cross slope of 2 percent, macrotexture 0.04 to 0.5 inches (1 to 1.3 mm))

Figure 166. Beaumont, Texas, I-10. open mix shortly after heavy shower (about 3 minutes) (Some spray but no splash, cross slope 2 percent, macrotexture about 0.08 inches (2 mm))

Pavement surface conditions were observed with respect to drainage and free surface water on each of the four subsections of the SH-21 test site. As the reader may recall from an earlier segment of this chapter of the report, the 2200 ft (670 m) test site consists of four subsections each designed with a different percent of voids as constructed. The range of these voids was from more than 25 to about 15 percent. The actual permeable voids in the field were about 20 percent less than the as-constructed void contents.

During the several months of data gathering it was possible to obtain data in rainfalls ranging from 0.02 in/h (0.5 mm/h) to 0.8 in/h (20 mm/h). The duration and the intensity were variables for each rain; therefore, it was quite important that tire-pavement interaction data be carefully referenced to rainfall intensity.

Recording of pictorial information and referencing these data to rainfall intensity were less difficult. Rainfall intensity was usually measured at 10-minute intervals; hence, pictures made in these intervals were assumed to represent the conditions associated with the intensity recorded. The usual practice was to allow the system to stabilize for at least 15 minutes before any data were taken.

In Figures 168 and 169 the effect of a rainfall of 0.02 in/h (0.5 mm/h) may be observed. In Figure 168 one may observe the highly reflective dense surface in the foreground with the passenger vehicle on Section 4 of the OGFC. Section 4 has the lowest void content, about 12 percent of permeable voids at the time the picture was taken. Essentially no water existed above the surface asperities in the outside wheel path of the outside traffic lane. Splash and spray would be a problem on the dense pavement in the foreground. Evidence of this splash and spray is presented in Figure 169 where the passenger vehicle in the background has spray trails 150 ft (46 m) behind the car.

In Figure 170 tests are being conducted in the outside wheel path of the outside lane in Section 3. The light streaks in the wheel path indicate that water is near the top of the surface asperities but does not completely cover these peaks. Frictional drag is essentially the same as that for internal water only. During this same rainfall of 0.08 in/h (2 mm/h) a photograph was made on the westbound dense pavement paralleling the test site. Splash and spray for this figure are shown in Figure 171.

Further evidence of the high frictional drag on the OGFC is presented in Figure 172. Here the locked tire of the trailer is creating a black mark on the pavement.

Again in Figure 173 the comparative performance from the splash and spray viewpoints for a dense surface (left portion of picture) and the OGFC on the right foreground are evident. The vehicle in the background has just left Section 4.

Very little spray is being produced in Figure 174 on Section 3 in a rain of 0.08 in/h (2 mm/h). No splash was observed.

The most open surface of the SH-21 test site is being subjected to a rain of 0.2 in/h (5 mm/h) in Figure 175. Reflectance of the headlamps is

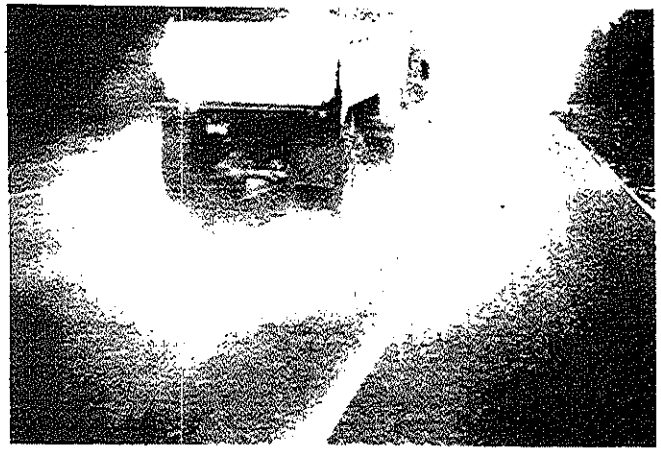

Figure 167. Beaumont, Texas, SH-87, open mix made from crushed trap rock (Rainfall 0.06 in/h (1.5 mm/h)) (Traffic and minimal cross slope coupled with an aggregate particle shape factor has caused the mat to close allowing little or no internal drainage. Cross slope 2 percent, macrotexture about 0.03 (0.8 mm))

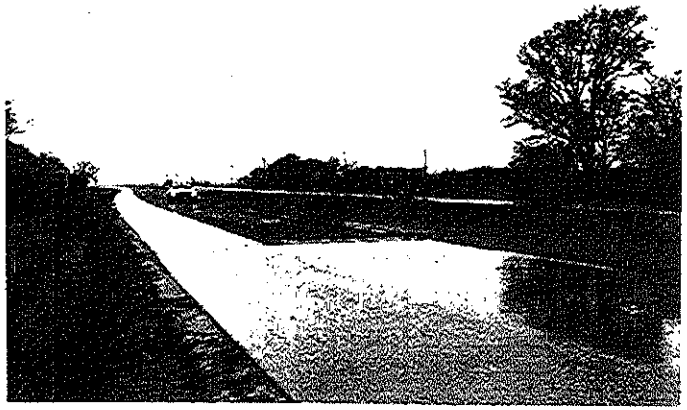

Figure 168. Natural rain 0.02 in/h (0.5 mm/h) on OGFC SH-21 Brazos County at intersection of Section No. 4 (Note reflected light in foreground and absence of same on OGFC.)

Figure 169. Natural rain 0.02 in/h (0.5 mm/h), SH-21 Brazos County. Section No. 2 (Note spray from vehicles on westbound dense surface in background. Note sheeting of water on dense shoulder of OGFC right foreground.)

Figure 170. Natural rain 0.08 in/h (2 mm/h) OGFC SH-21 Brazos County Section No. 3 (Note offset of test trailer. All testing utilized this trailer position.)

Figure 171. Natural rain 0.08 in/h (2 mm/h) on westbound dense pavement (SH-21); cross slope about 1 percent (Note lateral splash at front wheel.)

Figure 172. Natural rain 0.08 in/h (2 mm/h) Section No. 3, SH-21 Brazos County (Note black tire mark on pavement behind locked left trailer wheel.)

a key item to observe here. Compare the reflectance on the dense surface which is covered with a sheet of water with that of the OGFC. The possible hazards of driving on wet pavements at night is minimized where OGFC are used.

The comparative drainage efficiency of Sections 1 and 3 may be observed in Figure 175 and 176. In some areas of Section 3 water is above the asperity peaks. The corresponding west bound dense surface lanes may be observed in Figure 177. Spray follows both vehicles several hundred feet.

Lack of uniformity of the test section is apparent in Figure 176. Slight differences in density, lack of a perfect section and differences in mat thickness contribute to the evident non-uniform drainage.

Tests at 55 mph (88 km/h) in a rain of 0.3 in/h (7.6 mm/h) are being conducted in Figure 178. The outside lane produces some spray but no splash.

Pickup trucks are presented in Figure 179 during a rain of 0.25 in/h (6.4 mm/h). The truck in the left foreground is on Section 2 and the truck immediately behind is leaving Section 1 and is in the outside wheel path of the outside lane. There is essentially no spray from the inside lane.

In Figure 180 the inside or passing lane is free of surface water; whereas, the outside lane produced short spray trails on Section 3 (foreground) and longer trains on Section 4 in the far background.

At a natural rainfall intensity of 0.4 in/h (10 mm/h) the skid trailer created considerable spray but still no splash (see Figure 181). The SN_{40} with a full tread ASTM E501 is in the range of 45 to 55 on these surfaces and under the prevailing 0.4 in/h (10 mm/h) rainfall.

The tractor-trailer shown in Figure 182 is travelling about 55 mph (88 km/h) on Section 3 of the SH-21 test site in a rain of 0.6 in/h (15 mm/h). Both splash and spray are being produced in the outside lane. This situation would be hazardous at night, particularly if passing were involved.

In Figure 183, Section 4, the section with the least voids, flooding of the outside lane is critical. Approximately 8 ft (2.4 m) of this lane are flooded for the entire length of this section. In Figure 184 (taken from behind the steering wheel of a trailing vehicle) the skid trailer is almost obscured by the spray. The trailing vehicle is about 100 ft (30 m) behind the trailer. Under these conditions of water the SN_{40} for the full tread ASTM E501 was 54 and the SN_{55} was 49.

It is evident that when an OGFC of the type described here is flooded by heavy rainfall, ample friction is available provided the tire being used has good tread.

General Conclusions and Summary Statements

Several conclusions regarding the performance characteristics of OGFC may be listed, and based on field observations as well as background information, brief summary statements regarding the interacting technical and economic factors will be presented.

Figure 173. Natural rain of 0.08 in/h (2 mm/h) OGFC SH-21 Brazos County (Section No. 3 in foreground and truck leaving Section No. 4 in background. Note intense and long trailing spray to the left on westbound dense surface.)

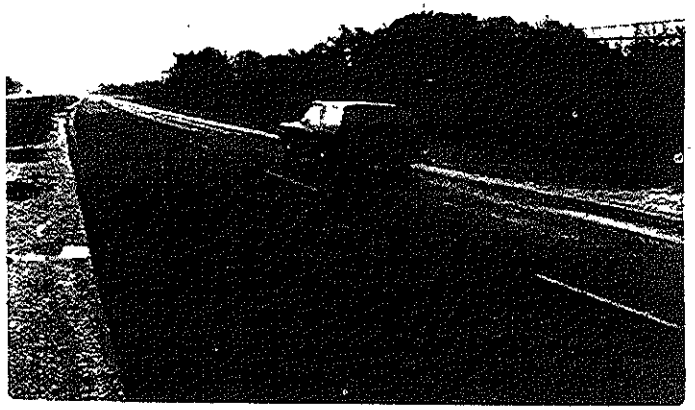

Figure 174. Natural rain of 0.08 in/h (2 mm/h) on SH-21 Section No. 3 (Vehicle traveling about 55 mph (88 km/h). Note areas of reflected light indicating surface water among the asperity peaks of the surface.)

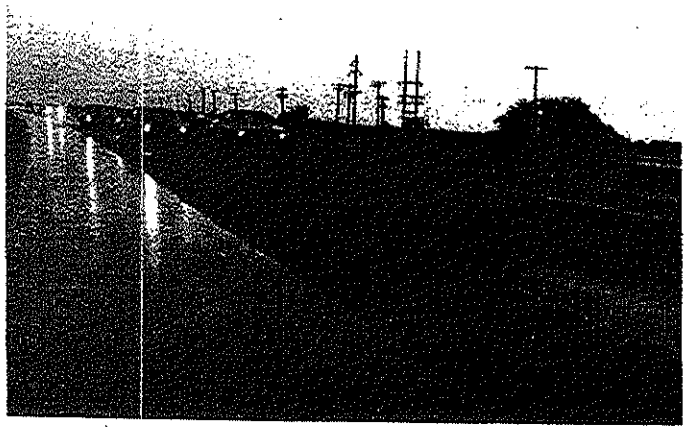

Figure 175. Natural rain 0.2 in/h (5 mm/h) SH-21 Brazos County Section No. 1 (Note contrast of reflected light on OGFC and dense shoulders.)

Figure 176. Natural rain 0.2 in/h (5 mm/h) SH-21 Brazos County Section No. 3 in foreground; Section No. 4 in background

Figure 177. Dense surface on SH-21 with 1 percent cross slope in 0.2 in/h (5.1 mm/h) rainfall (Note that spray persists for more than 200 feet (61 m) behind a passenger vehicle.)

Figure 178. Natural rain of 0.3 in/h (7.6 mm/h) on SH-21 Section 3 outside lane (Vehicle speed 55 mph (88 km/h). Some spray but little or no splash.)

Figure 179. Natural rain 0.25 in/h (6.4 mm/h) SH-21 Brazos County Section No. 1 (Note difference in spray of the two pickup trucks - inner and outer lanes.)

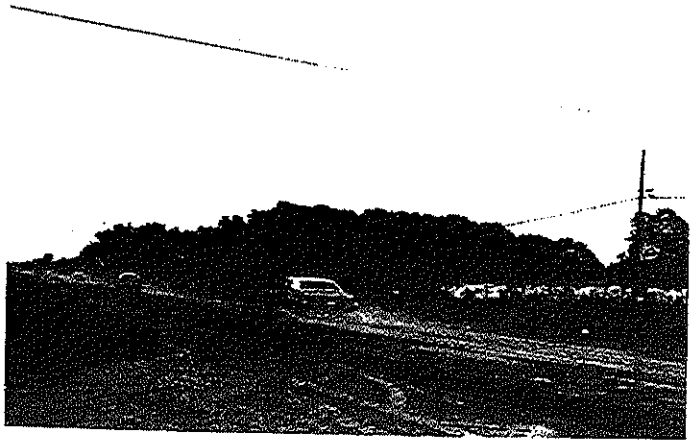

Figure 180. Natural rain 0.25 in/h (6.4 mm/h) on OGFC SH-21 Brazos County Section No. 3 in foreground and Section No. 4 in background (Note passing lane is essentially free of surface water.)

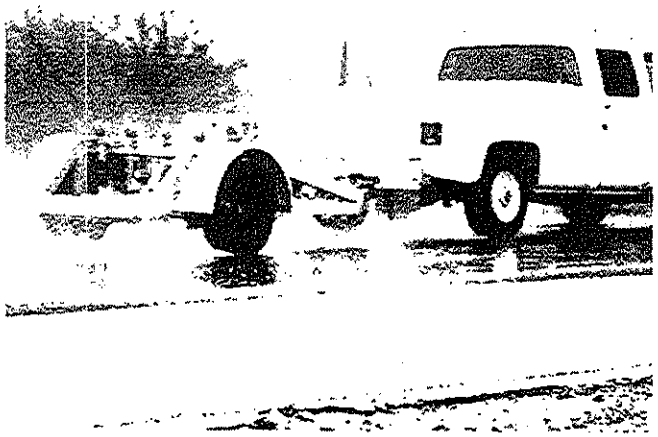

Figure 181. SH-21 open-graded friction course Section 3 in 0.4 in/h (10 mm/h) rainfall (Splash and spray objectionable but not critical during daylight.)

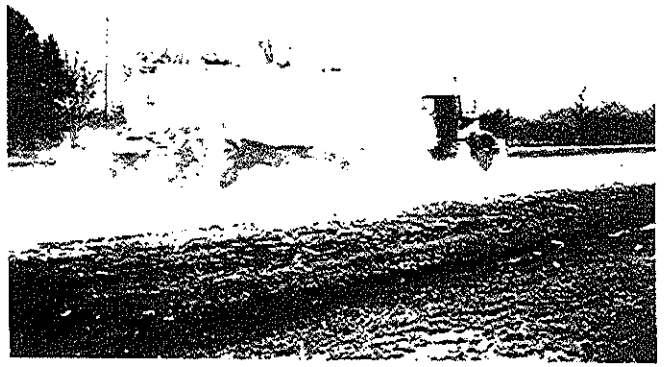

Figure 182. Splash and spray on SH-21 Section 3 in 0.6 in/h (15 mm/h) rainfall (Truck traveling about 50 mph (80 km/h) on outside lane of two-lane facility.)

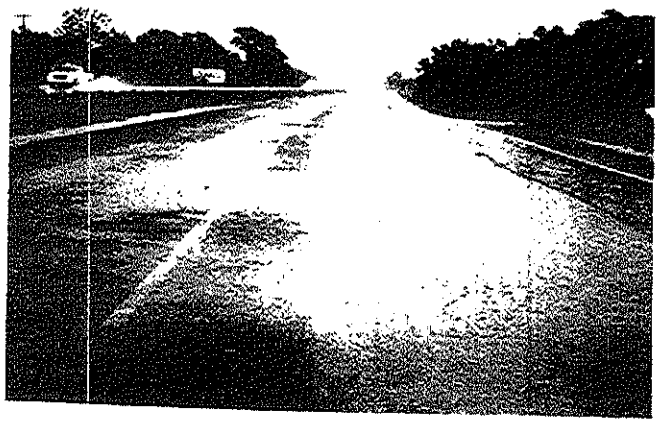

Figure 183. Natural rainfall 0.8 in/h (20 mm/h) intensity on SH-21 Section 4 (About 8 feet (2.4 m) of outside lane is completely flooded.)

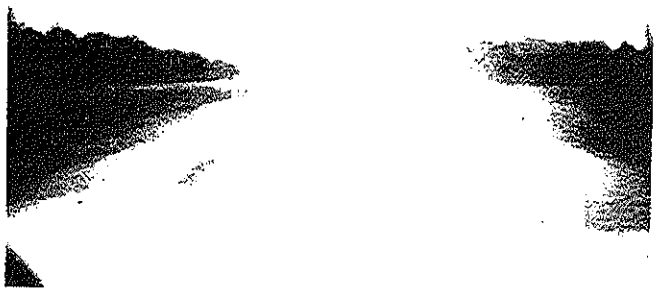

Figure 184. Trailing test trailer at 55 mph (88 km/h) in 0.8 in/h (20 mm/h) rainfall (View from the driver's position in a trailing vehicle.)

Current OGFC mixture design procedures recommended by the Federal Highway Administration are entirely satisfactory. The inclusion of fine material in sufficient amounts that result in about three percent filler in the final mixture is a highly beneficial construction aid that permits a wider range in placement temperature.

For prolonged internal drainage, minimum compacted mat thickness should be about 1 inch (25.4 mm). This assumes high quality aggregates properly graded and correctly placed.

Open-graded mixtures offer one of the best known methods of controlling macrotexture. Large top size aggregate may be used without creating unacceptable noise levels, since the asperity peaks lie in essentially one plane and there are few percussion cups in the face of the surface mat.

As indicated by the hard data presented, OGFC will deliver relatively high levels of friction at legal, rural speed limits and at water depths up to 0.1 inches (2.5 mm) provided tread depth is at or above approximately 0.2 inches (5 mm) and tire inflation pressure is at or above approximately 20 psi (138 kPa).

Splash and spray are materially reduced in rainfalls ranging from about 0.2 to 0.5 in/h (5 to 13 mm/h), and at lesser rainfall rates correctly designed and constructed OGFC may be expected to present essentially completely drained surfaces with the associated performance characteristics. Sustained rainfall in excess of about 0.3 in/h (7.6 mm/h) was found to cause flooding of acceptable OGFC where the flow path exceeded about 12 feet (3.7 m); however, no serious problems were encountered in flow lengths up to 24 feet (7.3 m).

Sealing the outside edge of a 24-foot (7.3 m) pavement caused no significant problem with the skid performance of the surface investigated; however, long-time storage of water in the mat could cause substrate instability problems.

Tires with minimum tread pattern depth or less, especially the wide oval type, performed poorly at 55 mph (88 km/h) on those surfaces with water depths in excess of about 0.08 inches (2 mm) irrespective of the macrotexture and internal drainage.

Although initial costs, maintenance costs and vehicle operating costs were not investigated in this study, these are factors which warrant consideration in a systematic friction improvement program.

Economic Factors

When we consider all aspects of the economic problem related to increases in levels of highway surface texture and skid resistance, it appears the justification must lie primarily on humanitarian grounds. The gross relationship between surface friction and wet-accident rate has been shown in a number of studies through the years. Increasing tire-pavement friction, however, results in a variety of economic influences. The most obvious positive influence is accident reduction, but other influences are not positive. Figure 185 summarizes these influences.

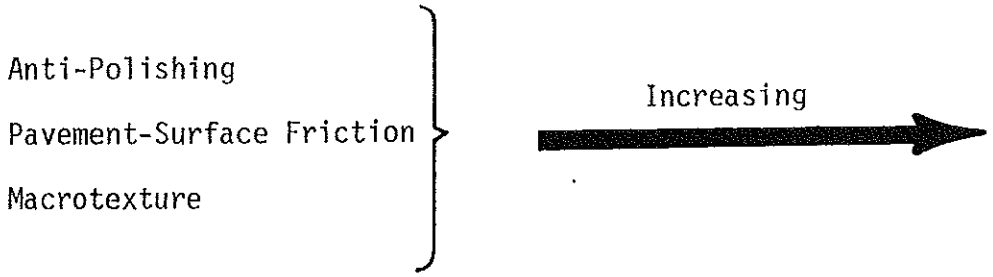

Positive Economic Influences

- Reduction in Wet-Weather Accidents
- Resurfacing Required Less Frequently

Negative Economic Influences

- Increased Fuel Consumption
- Increased Tire Wear
- Increased Surfacing Costs

Other

- Increased Noise and Vibration Levels Imposed on Vehicle Occupants

Figure 185. Influences of increasing anti-polishing characteristics on pavement friction

It is apparent that arbitrarily increasing pavement macrotexture to produce increases in friction and reduce hydroplaning tendencies must be subject to some compromise to prevent the negative influences from growing intolerable. The recommendations for combinations of surface slope, drainage path length and texture made in Chapter VII, have been made with the positive as well as negative economic influences in mind.

CHAPTER VI

PAVEMENT DRAINAGE

Field Investigations of Puddle and Texture Depth

Measurements were made at 314 sites in Texas to determine (1) ocurrence of significant puddling on traffic lanes and (2) amount of texture depth at the puddling areas. The locations of these sites and highway category are shown in Table 19.

Test Procedures

Three types of measurements were taken to investigate puddle depths and texture depths on typical highways, interstate, U.S. and state routes.

1. A rod and level were used to measure cross-section elevations on the pavement.
2. A 6 ft (1.83 m) steel bar and calibrated step gauge were used to measure rut depths at these cross sections.
3. The Silicone Putty Method was employed to measure texture depths in wheel paths.

The first two measurements provided information to calculate puddle depths. The elevations were used to determine the cross slope of the pavement. Readings were taken at the centerline, edge of pavement and at an intermediate point on the traveled way. A 6 ft (1.83 m) steel bar was placed on the traveled way, and rut depths were measured by using a calibrated step gauge. The step gauge was fabricated from 17-4 PH stainless steel heat treated to H-900 condition. Details of the instrument are shown in Figure 186. Previous research indicated 2.5 ft (0.76 m) for the wheel path width. This width was checked at more than 200 sites. The average width was approximately 2.5 ft (0.76 m).

Cross sections were plotted, cross slopes were determined and puddle depths were computed.

Computation methods:

$$PD = \Delta - \frac{W_p}{2} \tan \theta$$

(see Figure 187)

where $\tan = \frac{C}{WL}$ (see Figure 188)

Positive or negative puddle depths may exist. Positive puddle depths, as shown in Figure 187 represent measureable depths in the wheel path where puddling may occur. As shown in Figure 188, negative puddle depths indicate the slope of the road was adequate to permit water to flow to the edge of the pavement.

Table 19. Locations of test sites in Texas

District No.	Highway Category				Total
	IH	US	SH*	FM	
2		8	34	14	56
10			46		46
11		11	17		28
12			3		3
14		22			22
15	18	4	8	6	36
16		11			11
18		14	50	10	74
19		13			13
20		16	9		25
Total	18	99	167	30	314

* SH includes loops

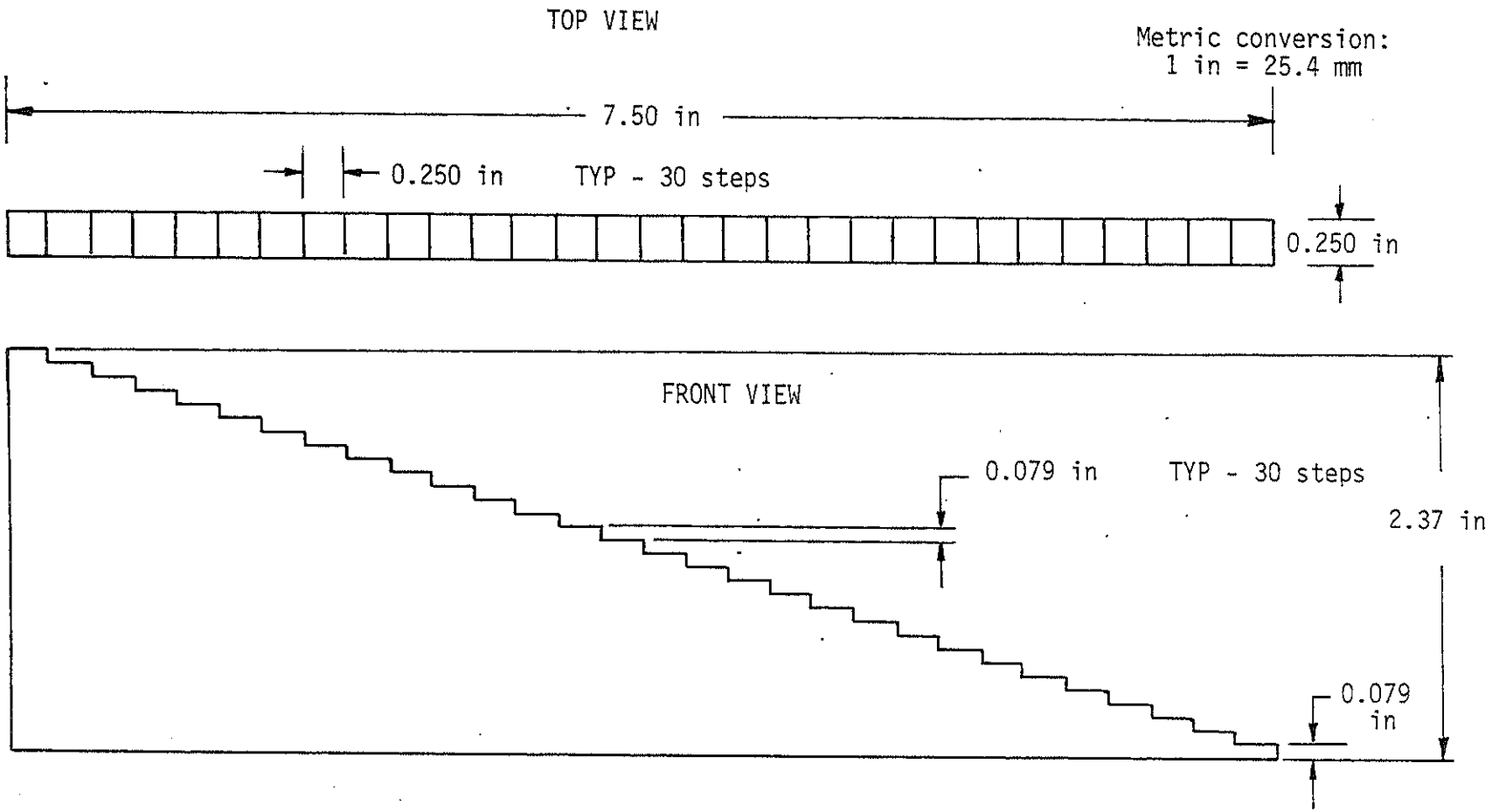

Figure 186. Step gauge details

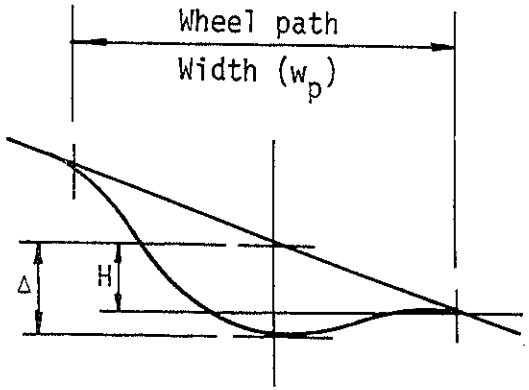

Figure 187. Positive puddle depth ($\Delta > H$)

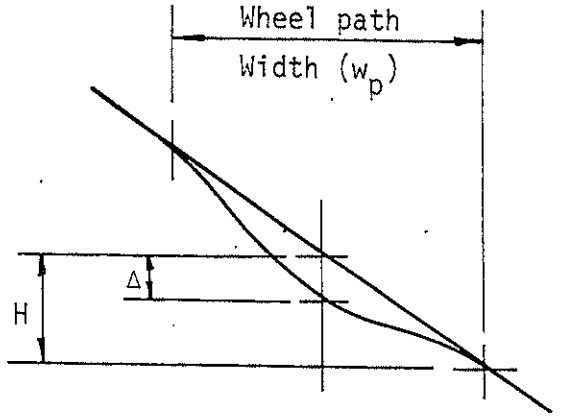

Figure 188. Negative puddle depth ($\Delta < H$)

$$\text{Puddle depth} = \Delta - H$$

$$= \Delta - \frac{w_p}{2} \tan \theta \quad \text{(for } \theta\text{, see Figure 189)}$$

$$= \Delta - \frac{w_p}{2} \left(\frac{C}{WL}\right) \quad \text{(for C and WL, see Figure 189)}$$

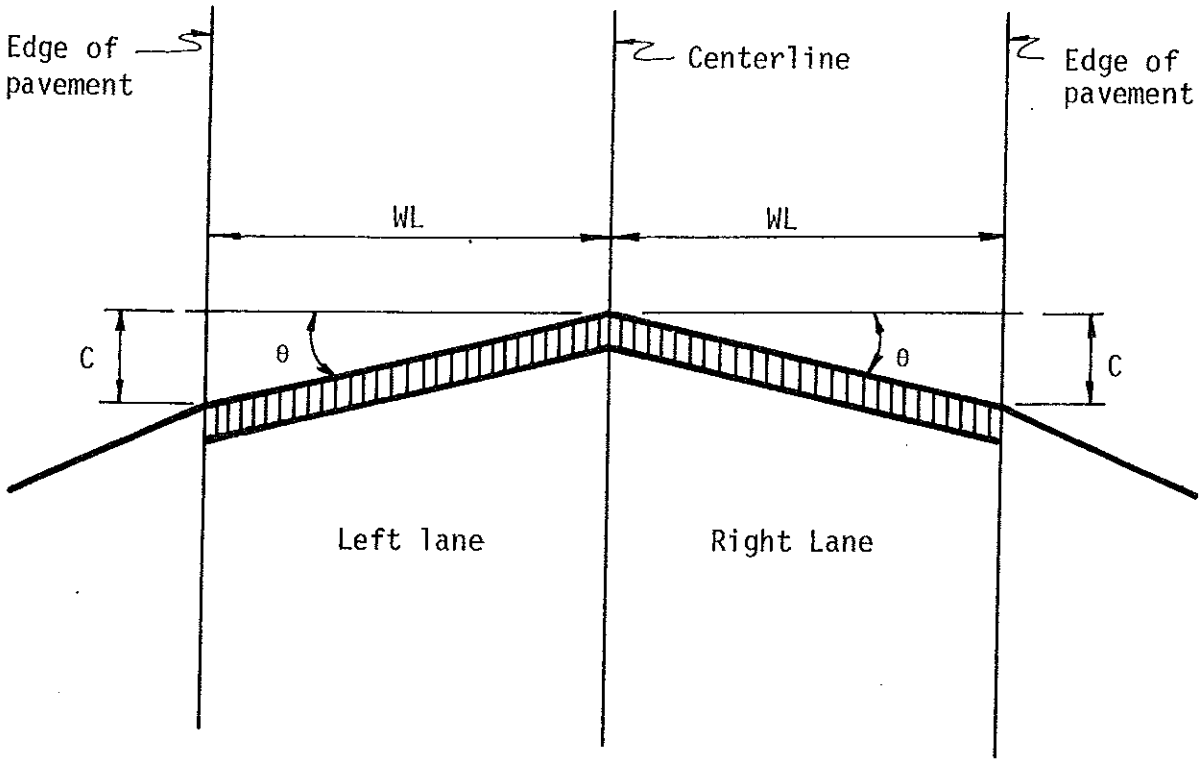

WL = Width of traffic lane

C = Change in height throughout WL

PD = Puddle depth

w_p = Wheel paths = 2.5 ft (0.76 m)

Δ = Largest rut depth that existed within WL

Figure 189. Cross section of traveled way.

Average texture depths were determined at each cross section by employing the equation:

$$TXD = \frac{1}{D_d^2} - 0.0625$$

where D_d = Average of four diameter measurements taken on the putty impression, in inches.

TXD = Average texture depth.

Note: To measure D_d in the metric system, the device would need to be calibrated with an appropriate metric weight.

Findings

Cross Slope - Readings were made at 547 locations. The measurements were analyzed and a histogram was plotted, see Figure 190. The mean slope was found to be 1.9 percent. The cumulative percent distribution of cross slopes is shown in Figure 191.

Puddle Depth - The puddle depths were analyzed and a histogram plotted. The data were erratically distributed as shown in Figure 192. The cumulative percent distribution of puddle depths in shown in Figure 193.

Texture Depth - A frequency histogram was prepared, and as shown in Figure 194, the mean depth was 0.043 in (1.09 mm). The cumulative percent distribution of texture depths at 131 locations is shown in Figure 195. These texture depths were measured on asphaltic concrete pavements.

In the summer of 1977 personnel from the Texas State Department of Highways and Public Transportation and the Texas Transportation Institute recorded texture depths at 213 locations in the eastern half of the state. At each of these 213 locations, four readings were taken

1. Sand 1 = Sand patch reading in the wheel path,
2. Putty 1 - Putty reading in the wheel path,
3. Sand 2 = Sand patch reading between wheel paths and
4. Putty 2 = Putty reading between wheel paths.

Sand patch measurements were taken in accordance with specifications set forth (41). Putty measurements were taken according to procedures outlined in Appendix B.

The pavement surfaces at these 213 locations consisted of asphaltic concrete, seal coats, portland cement concrete, and other materials (e.g., brick surfaces). In all, 125 sets of measurements were taken on asphaltic concrete, 50 on seal coats, 23 on portland cement concrete and 15 on other surfaces. The data in Table 20 indicate that the putty method consistently yields higher reading than the sand patch method. For example, the average "in path" texture reading on asphaltic concrete for the putty method is 0.041 in (1.04 mm); for the sand patch method, 0.025 in (0.635 mm).

Table 20. Surface texture depth (inches).

Metric conversion:
1 in = 25.4 mm

In Wheel Path	Asphaltic Concrete		Seal Coat		Portland Cement Concrete		Other	
	Sand 1	Putty 1	Sand 1	Putty 1	Sand 1	Putty 1	Sand 1	Putty 1
Mean	0.025	0.041	0.054	0.063	0.021	0.039	0.027	0.045
SD*	0.013	0.017	0.031	0.025	0.005	0.012	0.020	0.022
N	125	125	50	50	23	23	15	15

Between Wheel Paths	Asphaltic Concrete		Seal Coat		Portland Cement Concrete		Other	
	Sand 2	Putty 2	Sand 2	Putty 2	Sand 2	Putty 2	Sand 2	Putty 2
Mean	0.027	0.045	0.073	0.079	0.021	0.042	0.038	0.053
SD	0.015	0.018	0.028	0.023	0.004	0.014	0.022	0.032
N	125	125	50	50	23	23	15	15

*Standard Deviation

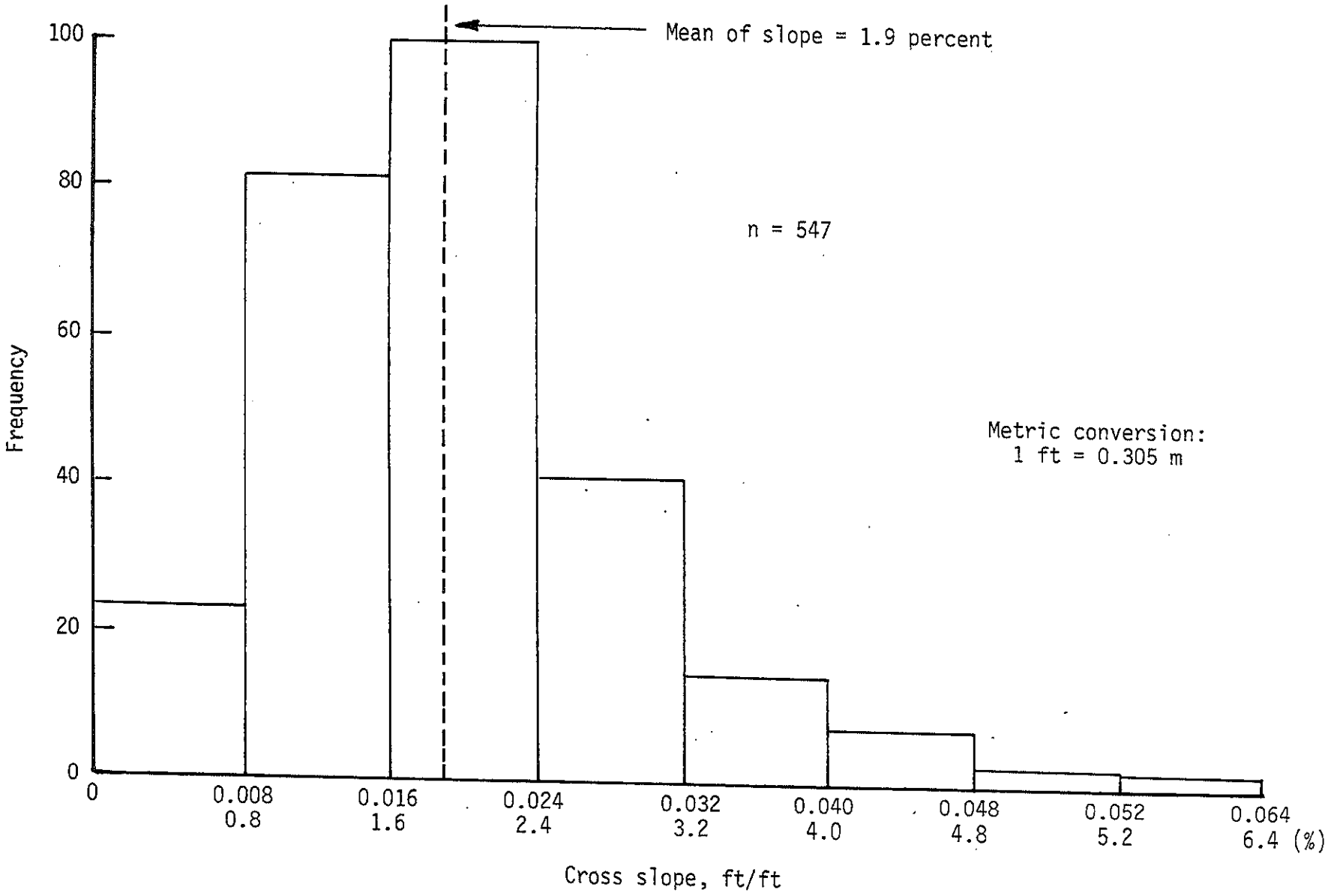

Figure 190. Relative frequency of cross slopes.

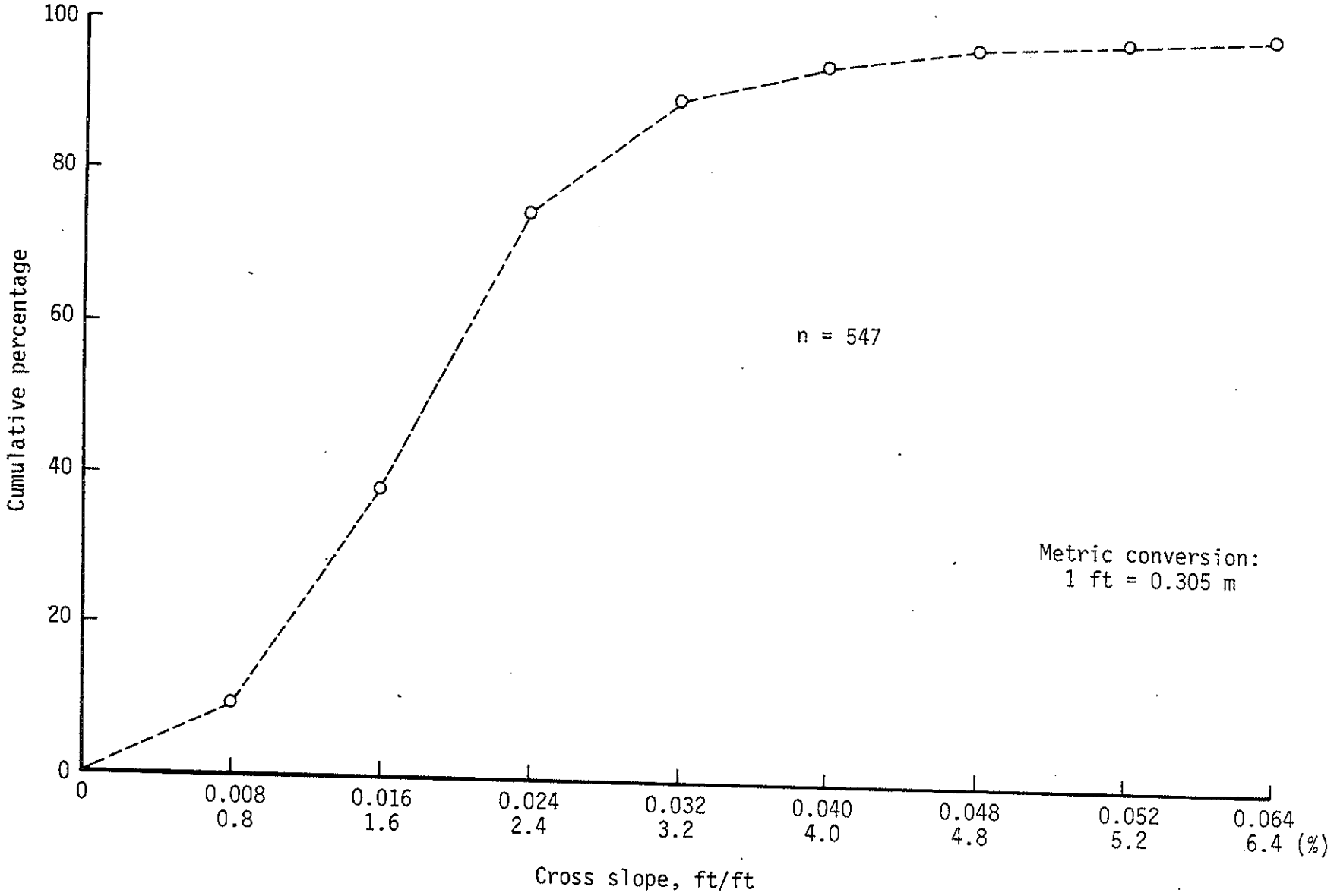

Figure 191. Cumulative percentage of cross slopes.

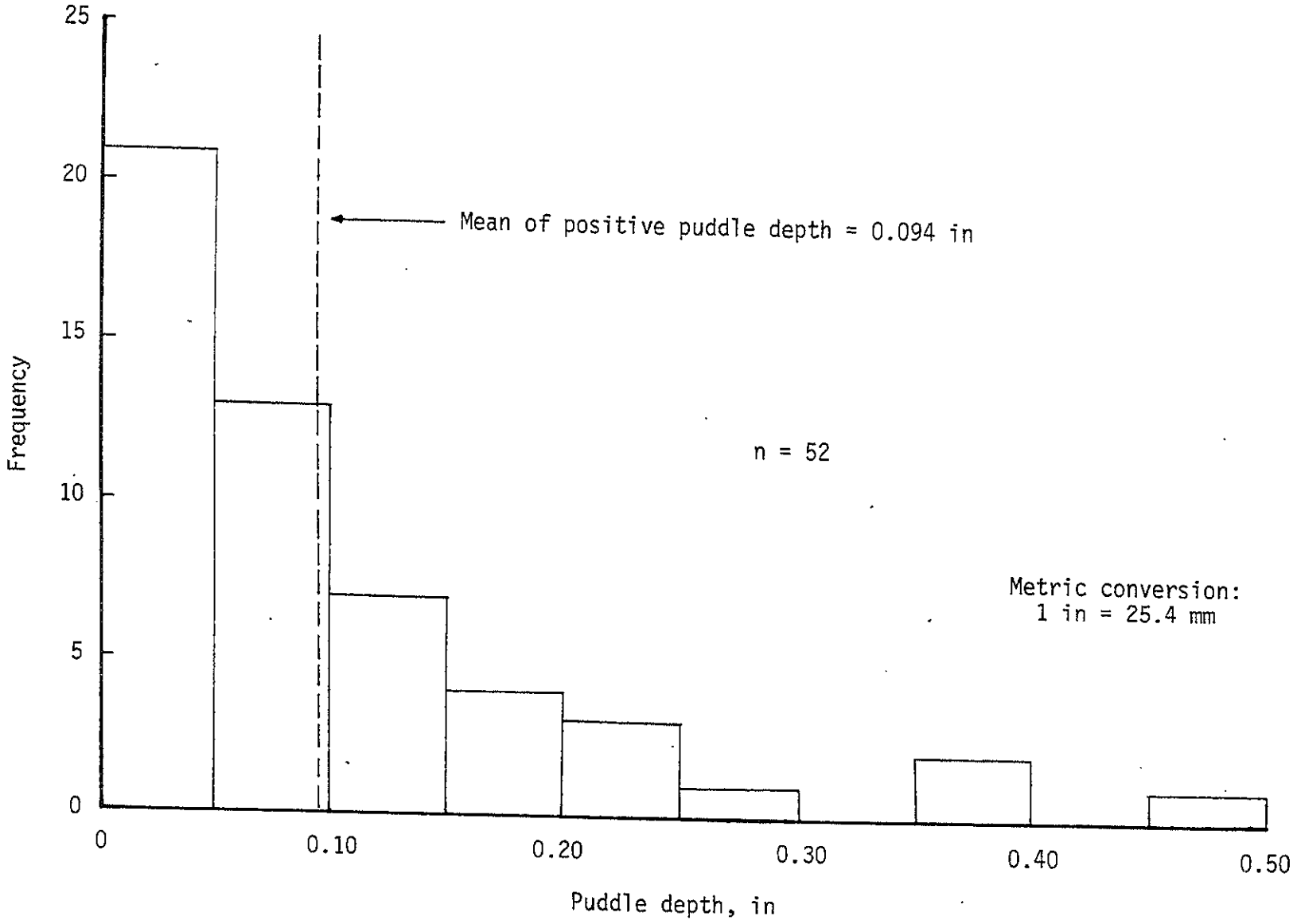

Figure 192. Relative frequency of puddle depth.

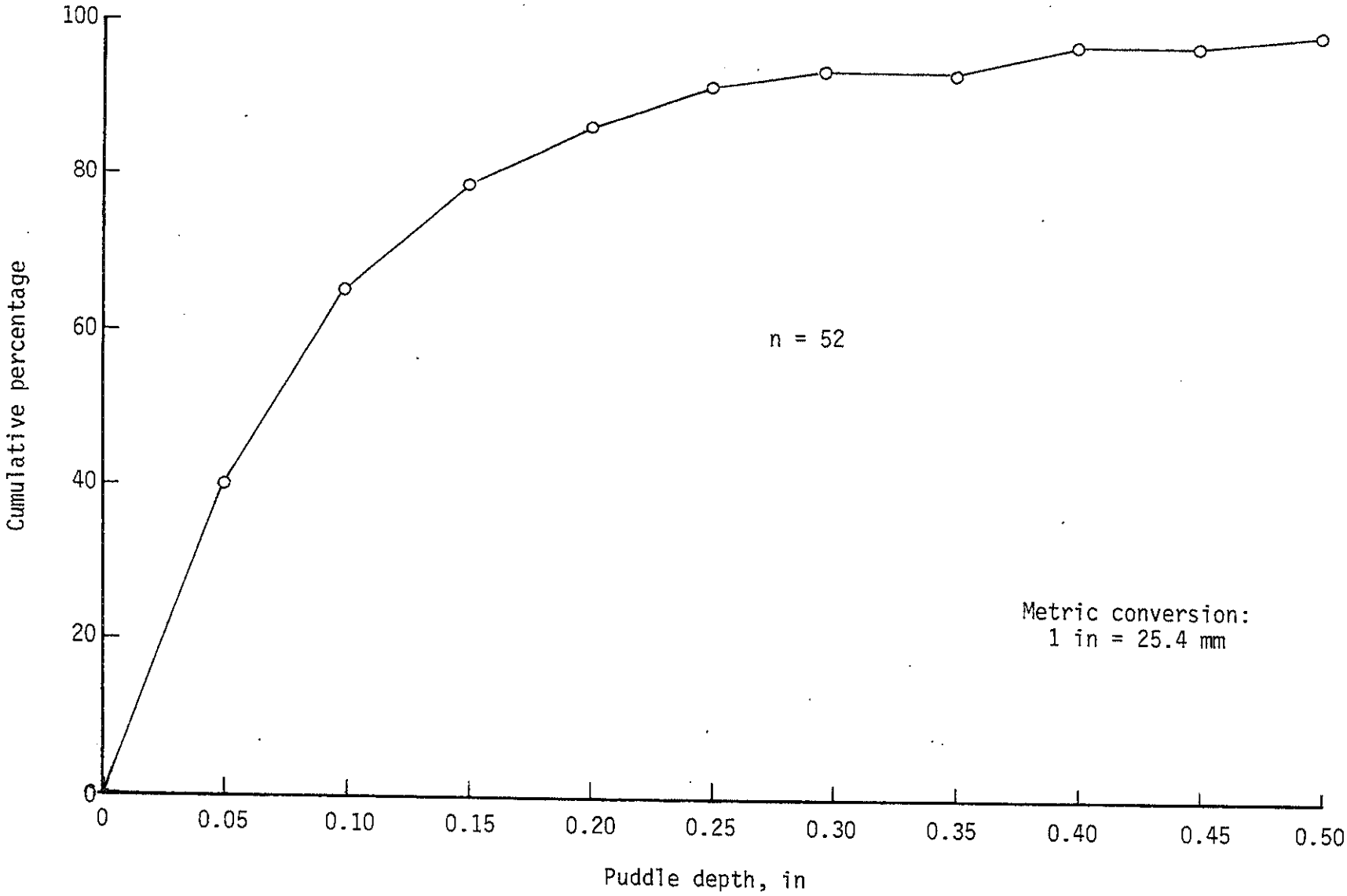

Figure 193. Cumulative percentage of puddle depth

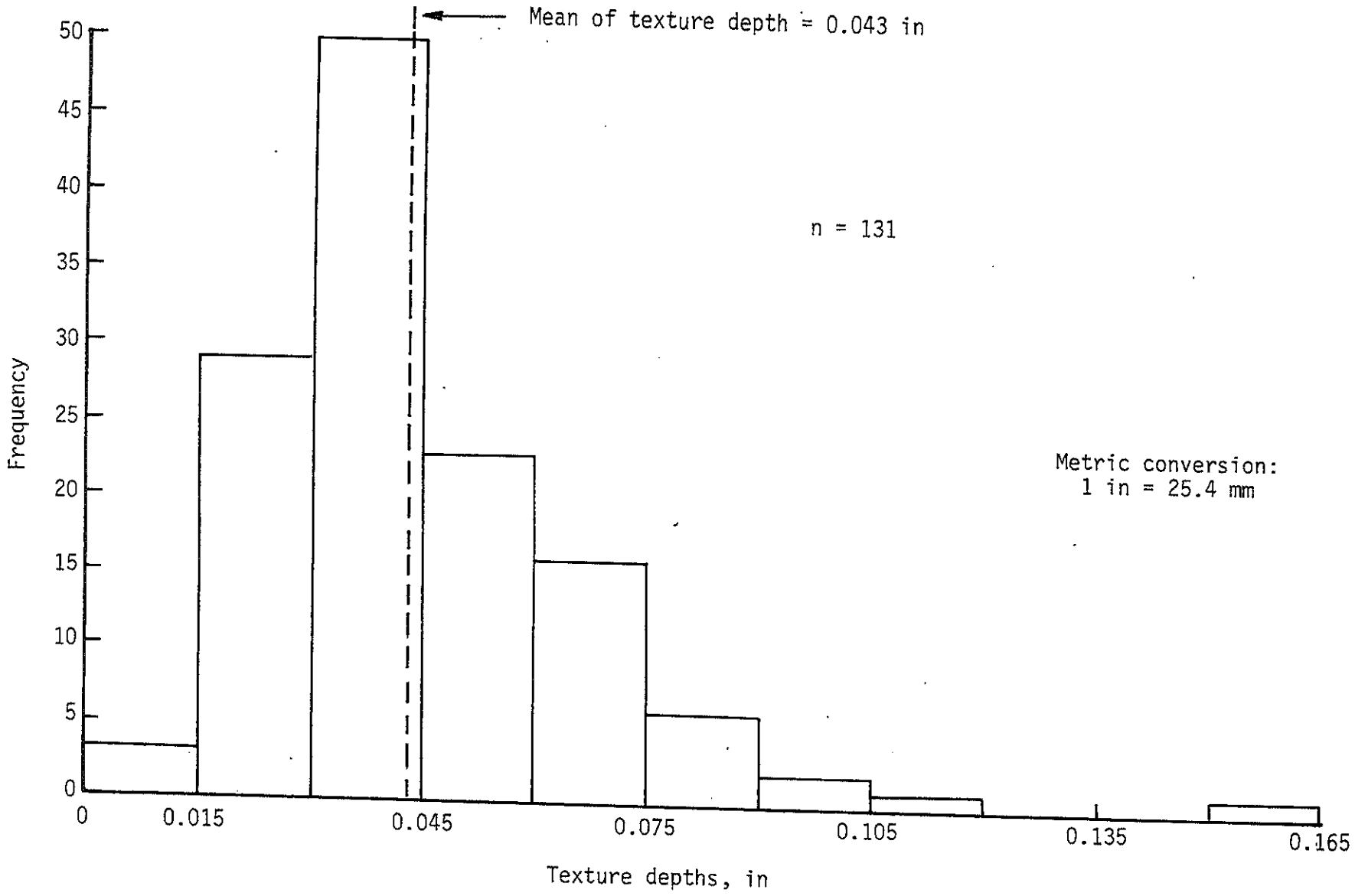

Figure 194. Relative frequency of texture depth

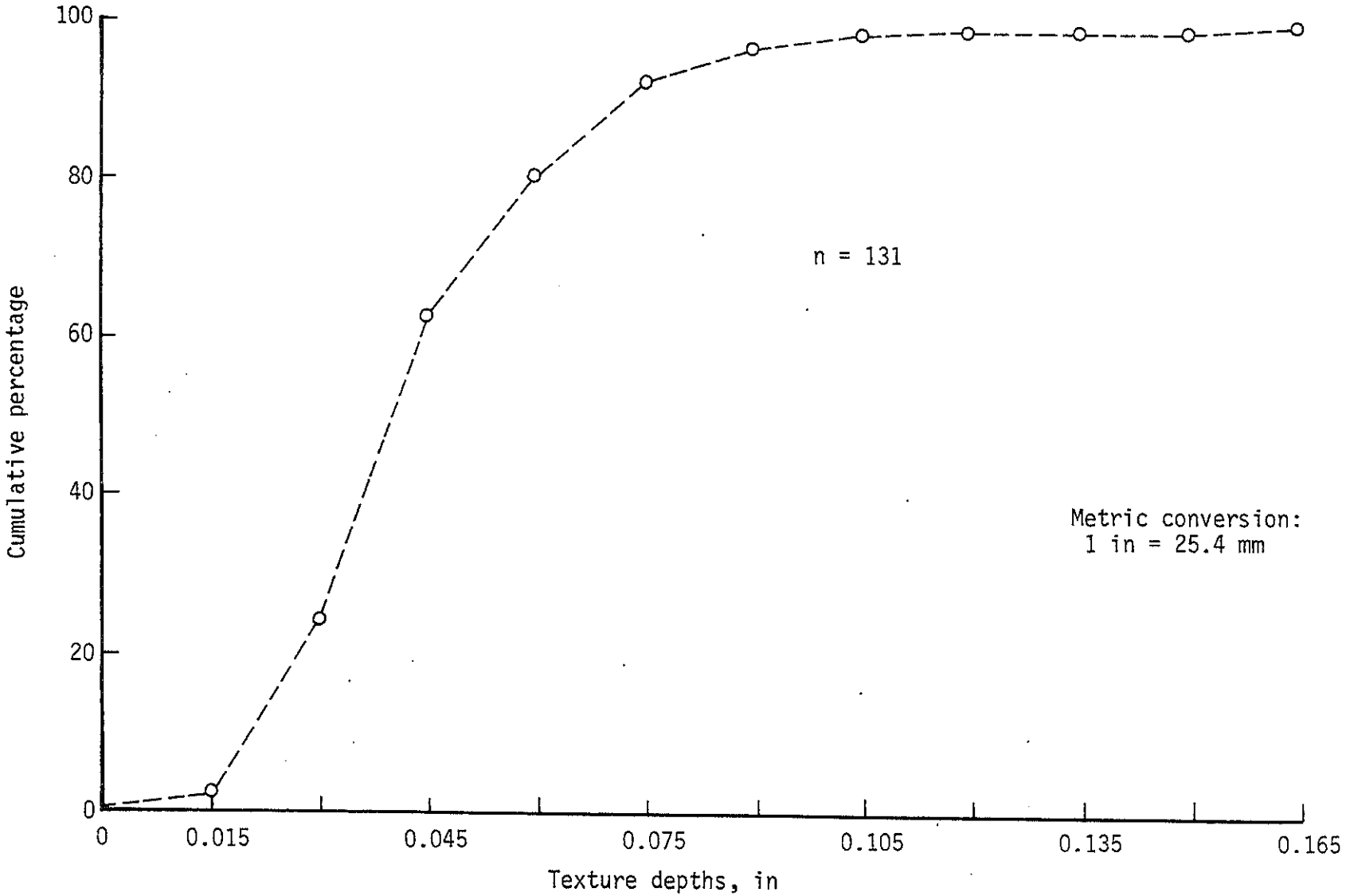

Figure 195. Cumulative percentage of texture depth

Figure 196 is a graphical representation of the averages (mean) shown in Table 20. It should be noted that the "in path" putty reading for asphaltic concrete in Table 20, 0.041 in (1.05 mm), is consistent with the value reported independently in Figure 194, 0.043 in (1.09 mm).

The consistently higher readings from the putty method bear further explanation. The putty method of measuring surface texture involved the use of a known amount of silicone putty pressed into the surface for a known length of time by a known dead weight. A change in any of the factors -- amount of putty, weight or length of weighted time -- could influence the resulting diameter of the putty impression patty. The factor most likely to vary is the weighted time which would be influenced by the operator's timing and technique. On busy highways the tendency would be to rush the test, resulting in less spread of the putty patty. Due to the inverse relation of texture depth to putty diameter the resulting texture depth measurement would be higher than in actuality. This seems to be the most likely explanation of the discrepancy. Texture depths measured on similar pavements using the Silicone Putty Method for a previous study (42) compared favorably with the sand patch data produced for this study. These similar data are presented in Figure 197, and the comparison can be seen in Figure 196.

Water Depths on Multilane Highways with Different Cross Slopes

Based on experimental studies of water film depths on pavements at Texas A&M University, the following empirical expression for water film depths was determined by regression analysis

$$WD = \left[(3.38 \times 10^{-3})(TXD^{0.11})(L^{0.43})(I^{0.59})(\frac{1}{S})^{0.42}\right] - TXD \qquad \text{Eq (16)}$$

where WD = Water depth above asperities in inches (mm/25.4)
TXD = Pavement texture depth in inches (mm/25.4) (putty test)
L = Length of flow in feet (m/0.305)
I = Rainfall intensity in inches per hour ($\frac{mm}{25.4}$/h)
S = Slope of drainage path in feet per foot (m/m).

The equation is applicable to laminar flow conditions generally. For laminar flow, an expression for water depth may be derived considering the forces acting on a liquid column of unit area above the plane A-A' in Figure 198. The shear stress above the plane A-A' due to the weight component of the liquid in the direction of flow is

$$\tau_o = \gamma(d-y)S \qquad \text{Eq (37)}$$

where τ_o = Bottom shear stress (F/L^2)
γ = Unit weight of liquid (F/L^3).

Newton's law of viscosity may be written as:

$$\tau_o = \mu \frac{dv}{dy} \qquad \text{Eq (38)}$$

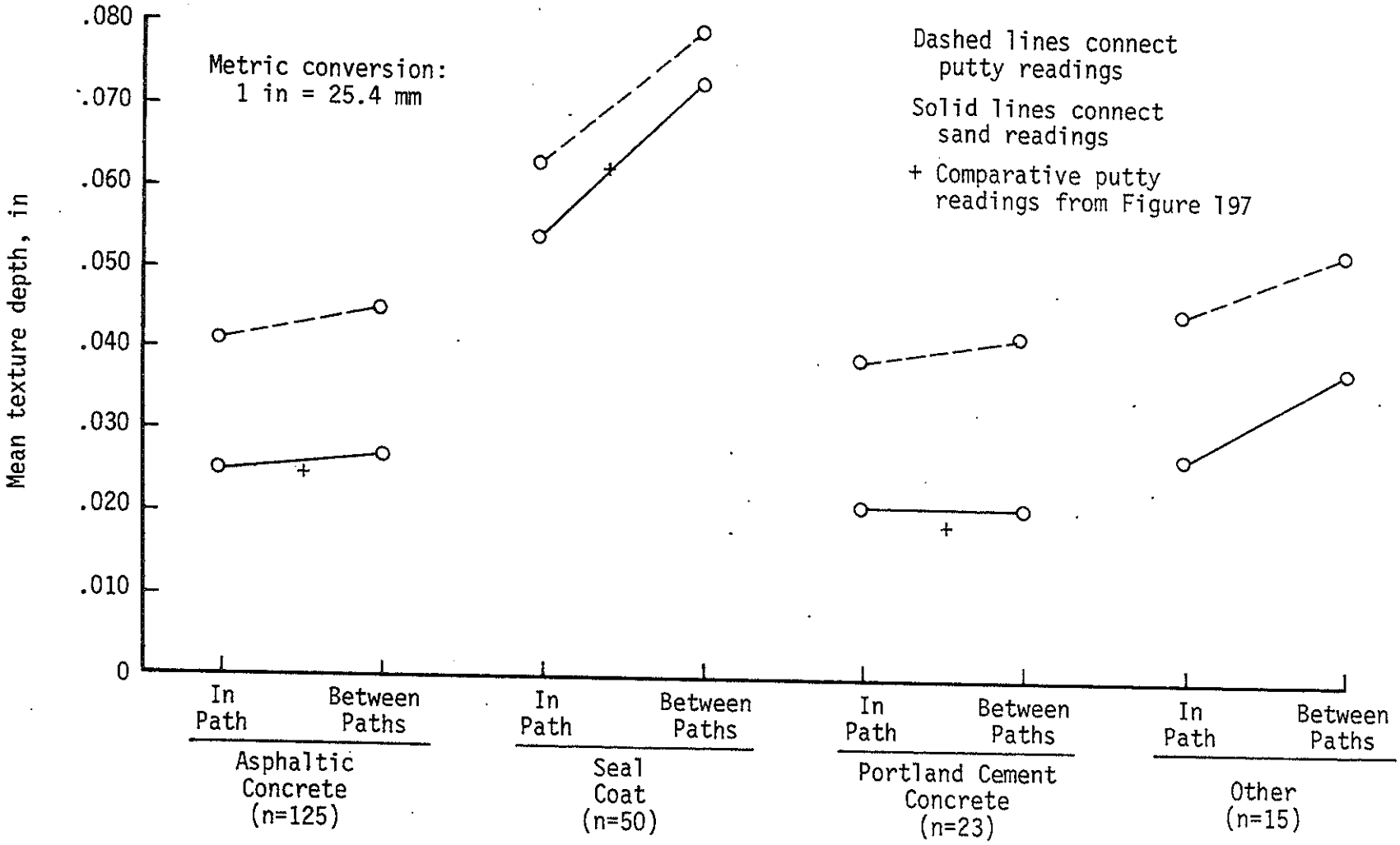

Figure 196. Texture depth as a function of surface material, measurement technique, and measurement location

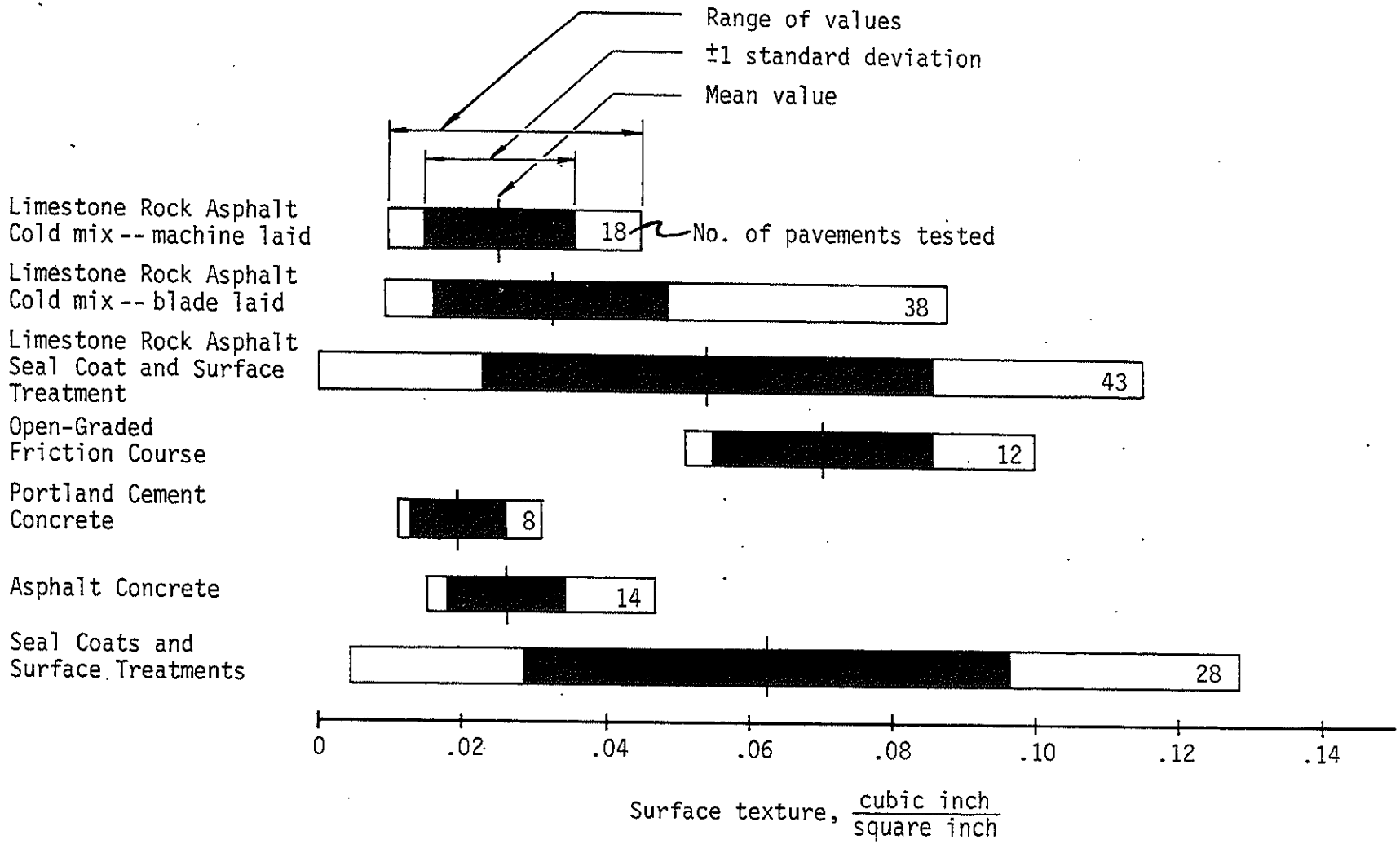

Figure 197. Typical values of surface texture as measured by putty test (After Epps and Button, 42)

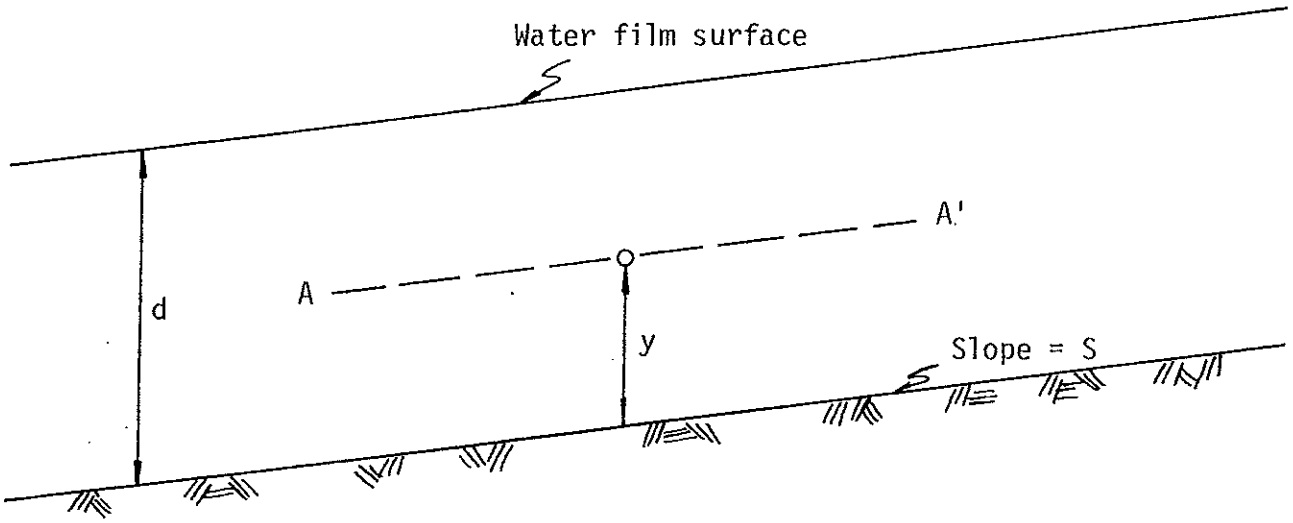

Figure 198. Laminar flow conditions

where μ = Absolute viscosity of the liquid (FT/L^2)

$\frac{dv}{dy}$ = Rate of change of velocity in the y direction (L/T^2)

$\tau = \mu \frac{dv}{dy}$ = (Newtonian Shear Stress equation) = bottom shear stress

$\tau = \gamma (d-y)S$ = bottom shear stress due to weight of liquid.

Equating the two expressions gives

$$\gamma(d-y)S = \mu \frac{dv}{dy}$$

$$dv = \frac{\gamma S}{\mu} (d-y)dy, \qquad \text{Eq (39)}$$

Integrating and evaluating the constant of integration for the condition that v = 0 when y = 0

$$v = \frac{\gamma S}{\mu} (yd - y^2/2)$$

which indicates a parabolic velocity distribution in the vertical direction. The mean velocity, Vm, is 2/3 v_{max} which occurs at y = d. Substituting d = y and multiplying by 2/3 gives

$$Vm = \frac{\gamma S d^2}{3\mu},$$

For a unit width, the area of flow is equal to d and the discharge per unit width is

$$q = \frac{\gamma S d^3}{3\mu}, \qquad \text{Eq (40)}$$

The profile of the sheet flow due to rainfall may be found by equating Equation 40 and the expression for discharge per unit width from rainfall which is

$$q = IL$$

where I = Rainfall supply rate (L/T) Eq (40a)

L = Length of supply (L),

Combining Equation 40 and Equation 40a gives

$$d = \left[\frac{3\mu IL}{\gamma S}\right]^{1/3}, \qquad \text{Eq (41)}$$

The theoretical expression (Equation 41) may be compared with the empirical expression (Equation 16), and it may be seen that d is a function if I, L, and 1/S to the 1/3 power for the theoretical expression whereas d is a function of $I^{0.59}$, $L^{0.43}$, and $(1/S)^{0.42}$ in the enpirical expression.

Example Calculation for Theoretical Water Depth

Calculate water depths at points A, B, C and D for Cases 1 and 2 in Figure 199 using the theoretical expression (Equation 41) and the empirical equation (Equation 16).

Case 1

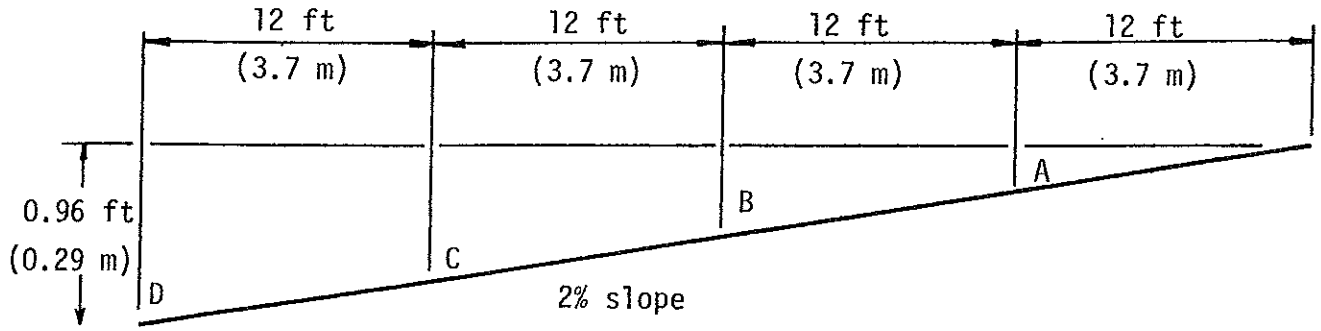

Case 2

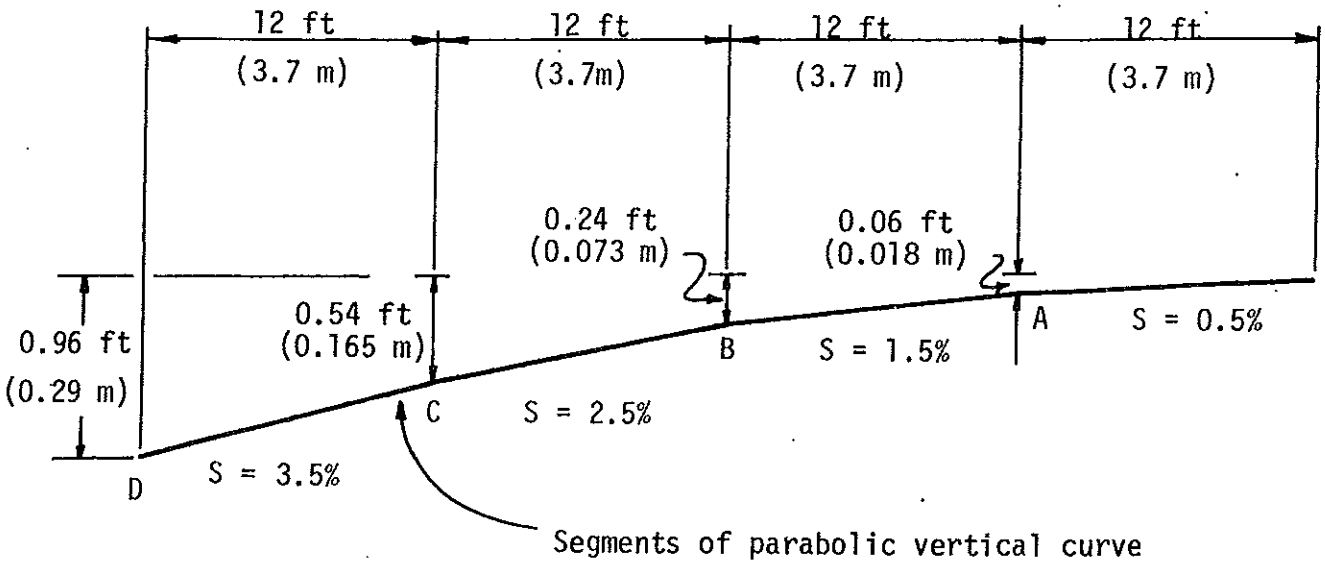

Given:

Rainfall intensity = 1 in/h (25.4 mm/h)
Texture = 0.035 in (0.9 mm)
Water temperature = 70°F (21°C)

Figure 199. Example of comparative water depths on multilane highways with different cross slopes

Example Case 2

$$d_t = \left[\frac{3\mu IL}{\gamma S}\right]^{1/3} = \left[\frac{(3)(2.05 \times 10^{-5})(0.0833)(12)}{(3600)(62.4)(0.005)}\right]^{1/3} = 3.80 \times 10^{-3} \text{ ft}$$

d_t at 12 ft (3.7 m) for a slope of 0.5 percent = 0.046 in (1.168 mm).

Note: Rainfall intensity I = 1 in/h (25.4 mm/h) = 0.0833 ft/3600 sec.

Example Case 2

At a distance of 24 ft (7.3 m) (slope of 0.5 percent for 12 ft (3.7 m) and 1.5 percent for 12 ft (3.7 m) the water depth is

$$d_t = \left[\frac{(3)(2.05 \times 10^{-5})(0.0833)(24)}{(3600)(62.4)(0.015)}\right]^{1/3*} = 3.32 \times 10^{-3} \text{ ft}$$

$$= 0.040 \text{ in } (1.02 \text{ mm}).$$

Example Case 2

Calculation for empirical water depth

$$d_T = \left[(3.38 \times 10^{-3})(TXD^{0.11})(L^{0.43})(I^{0.59})\left(\frac{I}{S}\right)^{0.42}\right] - TXD$$

$$= \left[(3.38 \times 10^{-3})(0.035^{0.11})(12^{0.43})(1^{0.59})\left(\frac{1}{0.005}\right)^{0.042}\right] - 0.035$$

$$= 0.028 \text{ in } (0.711 \text{ mm})$$

A comparison of Case 1 and Case 2 from Table 21 indicates that maximum water depths are approximately the same for the two cases but these maximum depths occur at different points of the flow. The depth d_B (empirical depth with respect to the bottom of the texture) when compared with the theoretical depth d_t (measured above a plane surface) is larger than the depth d_T, which is to be expected.

*Note: The question may arise as to what cross slope to use in the calculation of d_t. This may be related to a back water curve computation such as the Standard Step Procedure as outlined in Open Channel Hydraulics by V. T. Chow, McGraw-Hill, 1959, p. 269; however, this approach does not apply if the depth approaches normal depth or starts at normal depth. In Case 2 the upstream slope was used at the break in grade. This gives a conservative water film depth which exceeds the probable actual depth at the break in grade where the grade changes from 0.5 percent to 1.5 percent. Where the grade change is 1.5 percent to 2.5 percent the depth computed using the 1.5 percent will be very close to the actual depth and the distance used to compute this depth must be 24 feet (7.9 m) to get the proper supply rate q.

Table 21. Comparison of theoretical water depths with water depths from the empirical equation at several points along the slope.

Point	Case 1			Case 2		
	d_t	d_B	d_T	d_t	d_B	d_T
A	0.029	0.035	0.000	0.046	0.063	0.028*
B	0.036	0.047	0.012	0.040	0.053	0.018
C	0.041	0.056	0.021	0.038	0.051	0.016
D	0.046	0.064	0.029*	0.038	0.050	0.015

*Maximum water depth

Note: All depths are listed in inches for d_t = theoretical depth, d_T = empirical depth with respect to top of asperities, and d_B = empirical depth with respect to bottom of texture. The water depths listed are for I = 1 in/h (25.4 mm/h), water temperature = 70°F (21°C), and T = 0.035 in (0.9 mm).

CHAPTER VII

DESIGN OF SAG-VERTICAL CURVES TO REDUCE HYDROPLANING

Design Criteria for Drainage of Sag-Vertical Curves

In order to examine the present practices with regard to sag-vertical curve design to minimize hydroplaning, a questionnaire was sent to nine state design engineers. A summary of the significant findings of this survey are listed below.

1. No wet-weather speed limits are currently in use.
2. Surface drainage is a significant design consideration in most states.
3. No special drainage considerations are given to sag-vertical curves.
4. A storm recurrence interval of 8-15 years is commonly used.
5. A maximum water-film depth criterion is not currently being applied in the design process.
6. Maximum flow-path length is used as a design criterion by about 20 percent of the states.
7. A thirty-six foot (11 m) maximum width of drainage in one direction is common.
8. Cross-slope criteria for sag-vertical curves were also typical of standard criteria for tangent sections.
9. Few attempts have been made to incorporate experimental drainage features at critical drainage locations (i.e., sag-vertical curves). Those states whose policy prescribes the use of a storm recurrence design interval also encourages increasing the design interval for underpasses and intersection design for sag-vertical curves.

Based on a review of the AASHTO standards, the input from state design engineers and engineering judgment, a tentative design criterion for sag-vertical curves has been prepared. These criteria are presented in Table 22.

Some of the criteria in Table 22 are based on judgment. These must be applied and evaluated to confirm their utility in the design process.

Innovative Drainage Concepts for Sag-Vertical Curves

Hydroplaning has been identified as a contributing factor and possibly the principal causative factor in many high-speed, loss-of-control accidents. Dynamic hydroplaning occurs when water separates the tire from the pavement due to the forceful interaction of the tire, water and pavement (43). When the thickness of the water film exceeds the height of the asperities of the surface aggregate, steering control may be lost at high speeds. It is apparent that the removal of the water so as to reduce the water-film thickness is the key to reducing hydroplaning accidents.

Sag-vertical curves on modern highways are particularly susceptible to water accumulation. The two grades direct the runoff toward the bottom of the curve. The lack of longitudinal grade at the low point of the curve requires that the accumulated water must drain across the pavement. The efficiency of the drainage system could be a critical part of reducing the hydroplaning potential of sag-vertical curves. This section presents the findings from the research effort involved.

Table 22. Tentative sag-vertical curve drainage design criteria based on a survey of existing practice

Design Element	Desirable Design	Minimum Design
Maximum pavement width for one way drainage	36 ft (11 m)	36 to 48 ft (11 to 14.6 m)
Maximum inlet spacing	50-200 ft (15 to 61 m)	300 to 500 ft (91 to 152 m)
Storm recurrence design interval with crossroad intersection with underpass structure	25 year 25-50 year 25-50 year	10 year 10-25 year 25 year
Channelized curb flow encroachment	Containing ponding on the shoulder.	Containing ponding on the shoulder and 1/2 of the extreme right lane
Increase in roughness coefficient (Manning's N) for various materials due to small gutter slopes	0.005	0.002
Pavement cross slope for sag-vertical curve section	Slight increase in cross slope	No increase in cross slope

Objectives

The objectives of this phase of the research program were to:

1. Develop innovative drainage concepts and improvements to existing drainage design for sag-vertical curves,
2. Develop concepts for surface drainage that intercept the water at intermediate locations between the outer edges of wide, multiple lane pavements and
3. Identify feasible remedial measures for existing curbs and other structures and for pavement distortions because of rutting and/or subgrade heaving and swelling where they impede the rapid removal of water from the pavement surface.

Generalized Work Plan

To achieve the objectives, a work plan was conceived that includes seven basic steps. These are

1. Identify innovative surface drainage techniques,
2. Evaluate innovative surface drainage techniques for practicality,
3. Evaluate the interaction between grade, pavement cross slope and pavement deformations,
4. Rank innovative surface drainage techniques in accordance with their

ability to reduce the water accumulation on the surface and to minimize the associated maintenance,
5. Recommend a surface drainage technique for the design of sag-vertical curves,
6. Review the alternatives for curbs and
7. Recommend remedial treatments for sag-vertical curves with curbs.

The remainder of this document will be organized around these seven points.

Step 1 - Identify Innovative Surface Drainage Techniques

The removal of water from the pavement surface can, in concept at least, be accomplished in two ways: 1) over-the-surface drainage and/or 2) through-the-pavement drainage. Through-the-pavement drainage can be accomplished in two basic ways: First, drainage through an open-graded asphalt friction course and secondly by intercepting the water runoff through drop inlets on the surface of the pavement. The basic concepts are incorporated in seven innovative drainage concepts which can be adapted to two-lane pavements or multi-lane facilities (See Figures 200 through 206).

While not an innovative technique, the raising of the grade throughout the sag vertical can provide a larger drainage capacity of adjacent drainage facilities and reduce the probability of surface flooding. Increasing the grade does not reduce the need for adequate cross slope on the pavement surface or adequate downstream drainage capacity.

Step 2 - Evaluate Innovative Surface Drainage Techniques For Practicality

Many of these innovative concepts depend on open-graded pavements in part or totally for surface drainage. The first step then becomes one of identifying the amount of runoff or discharge (directly related to rainfall intensity) that can be accommodated through open-graded pavements. This requires an estimate of the drainage capacity of the open-graded mixture. Based on experimentally determined values, for a pavement with a 2 percent cross slope and a zero grade, research shows flooding occurs on an open-graded paving mixture 1 inch (2.5 cm) thick, 12 feet (3.7 m) wide composed of 0.3 inch (7.6 mm) aggregate if the rainfall intensity is in the approximate range of 0.3 to 0.5 in/h, (8 to 13 mm/h)(9).

The drainage capacity of the permeable pavements and the water flow velocity through them can be estimated from the above information and the following assumptions:

Assumptions

1. Fifteen percent of the cross-sectional area is available to remove surface water,
2. There is adequate drainage capacity at the shoulder or edge of the open-graded pavement section,
3. The critical rainfall intensity is 0.35 in/h (9 mm/h) (capacity of open-graded mixture),
4. There is no longitudinal grade and
5. The rainfall is uniformly distributed on the pavement.

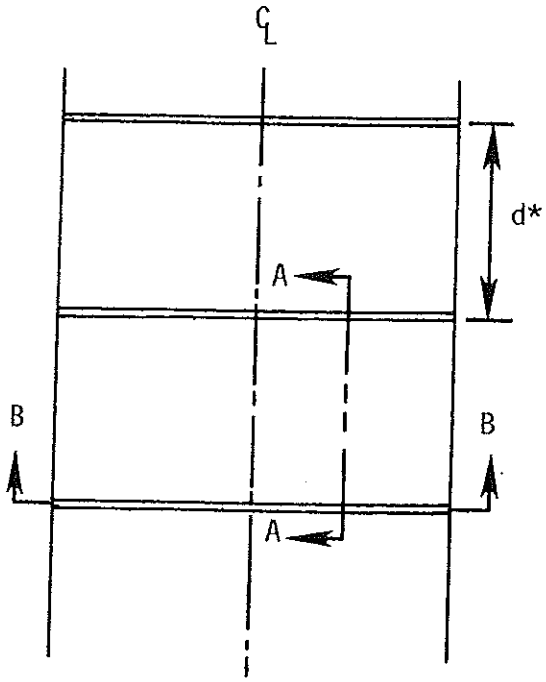

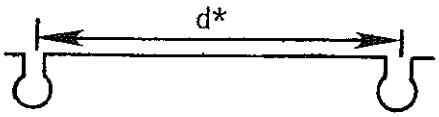

Section A-A

Open topped drainage pipes inlaid in the pavement.

Slope, S, is dependent upon grade.

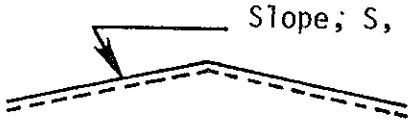

Section B-B

Figure 200. Surface transverse slotted pipe, System A

* d is dependent on the design rain discharge and grade.

ADVANTAGES

- Continuous draining.
- Can be extended on overlays.
- Pipes dump directly into ditches.
- Large drainage capacity.

DISADVANTAGES

- Rough surface (joints).
- Difficult construction.
- Possible clogging.
- If longitudinal pipes are used, they can be hazardous to motorcycles and bicycles.
- Reduced friction on pipe.
- Lack of adaptability to asphaltic concrete (AC) compaction could create frequent ponding in the wheel path.
- Requires special treatment on overlays.

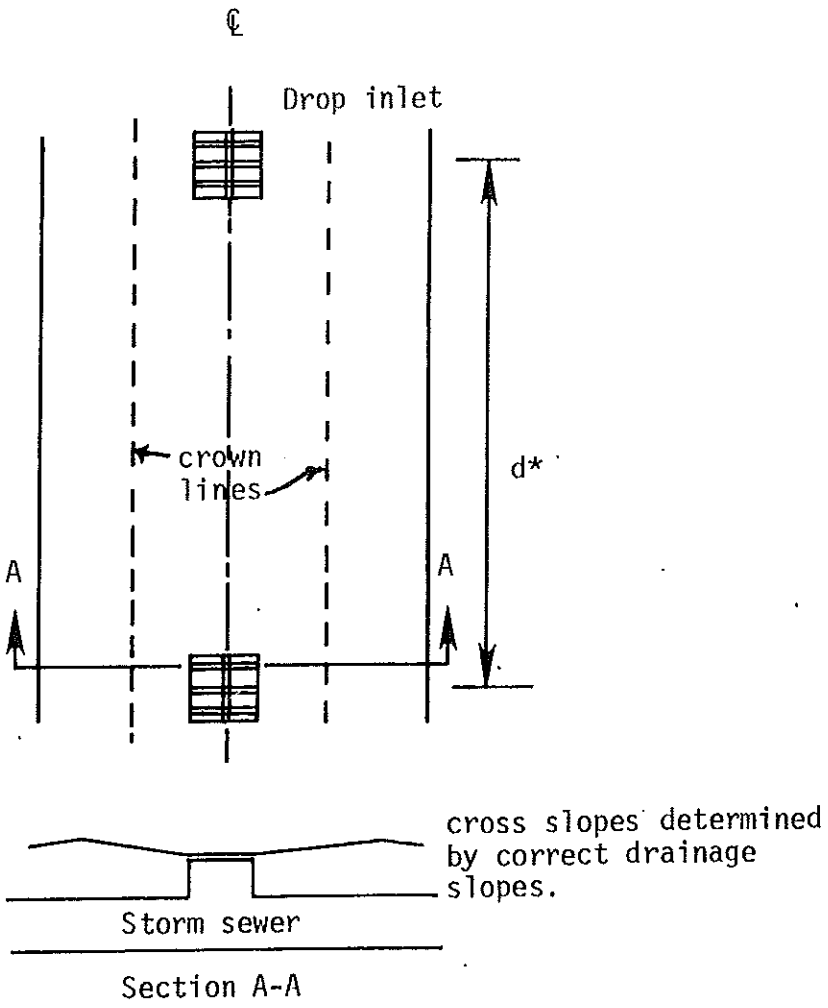

Figure 201. Surface drop inlets, System B

* d is dependent on the design rain discharge, and longitudinal grade

ADVANTAGES

- Can be extended on overlays.

DISADVANTAGES

- Rough surface.
- Ponding around drain occurs in the middle of the roadway which is critical.
- Must have storm sewer system under the inlet.
- Reduce friction on grates.
- Could be hazardous to motorcycles and bicycles.
- Additional noise.

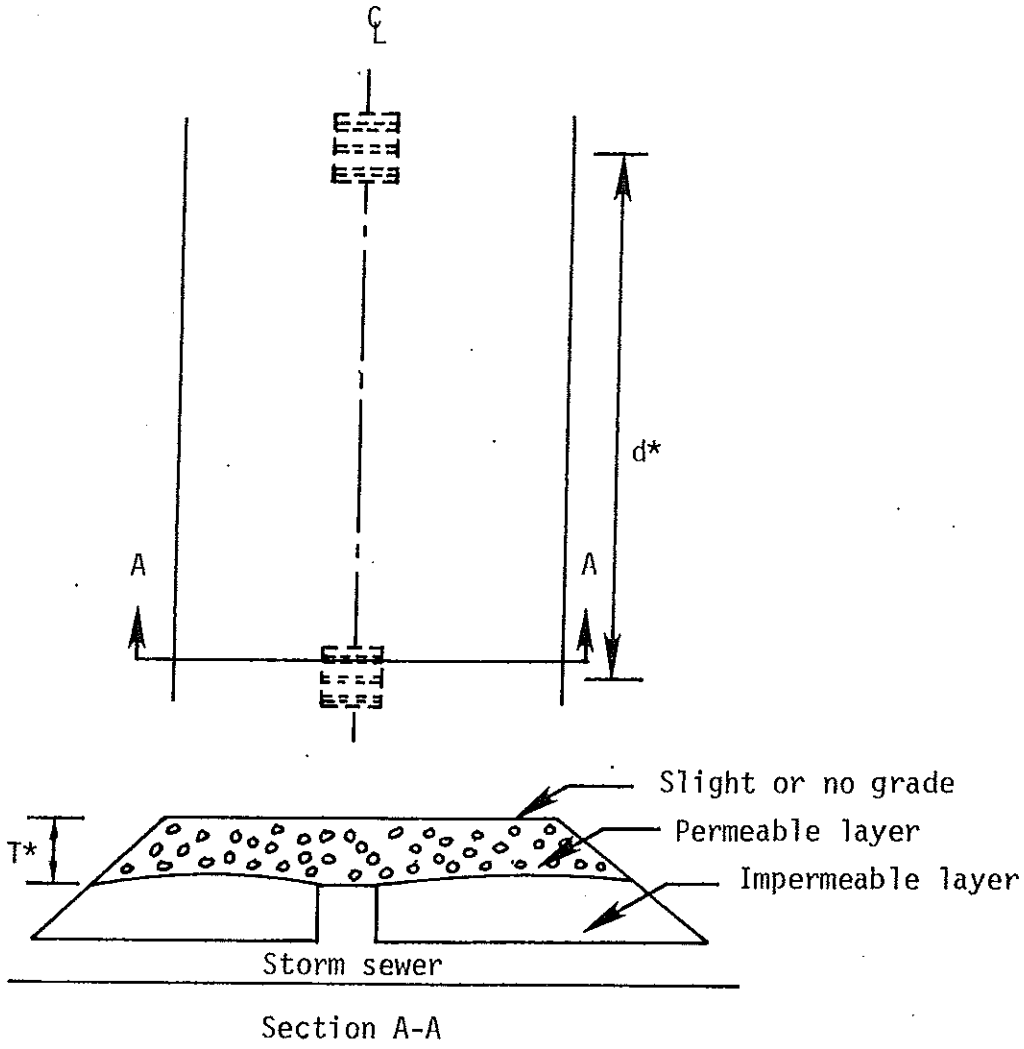

Figure 202. Subsurface drop inlet, System C

* T and d are dependent on design rain and discharge. Note: slotted pipe could be substituted for the drop inlet and run longitudinally for continuous drainage.

ADVANTAGES

- Permeable layer provides natural filter. Clogging by large material less likely.
- Continuous drainage if slotted pipe used.
- Fast and effective drainage.
- Edge drainage as well as subsurface drainage.

DISADVANTAGES

- If clogged difficult to correct.
- For drop inlet a storm sewer system must be used.
- Relatively low hydraulic capacity (i.e., 15% of area available to move water). Therefore, only suitable for low intensity rainfalls.

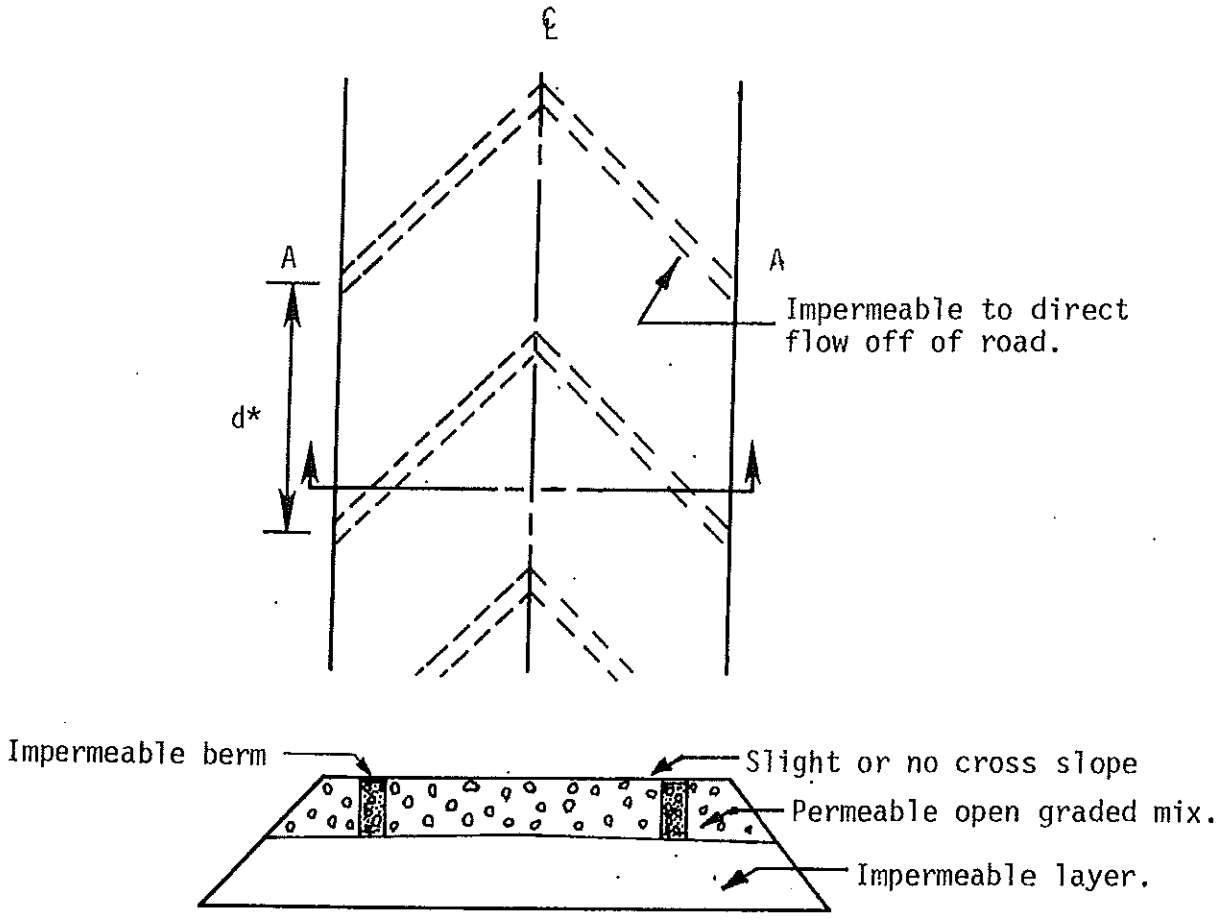

Figure 203. Subsurface directional berm, System D

* d is dependent on the design rain and discharge.

ADVANTAGES

- No subdrain system needed.
- Continuous drainage.
- Overlays easy.

DISADVANTAGES

- Difficult construction.

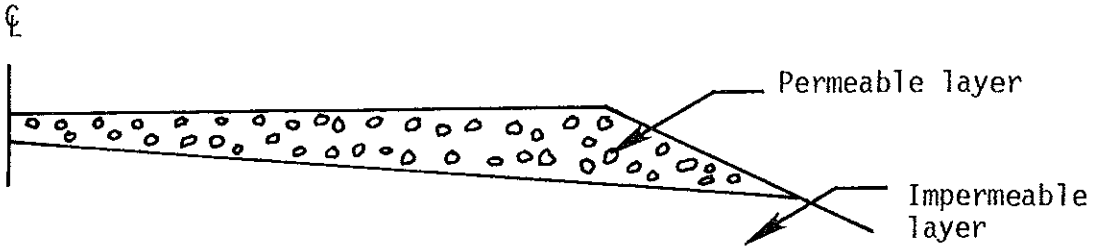

Figure 204. Subsurface cross-slope drainage, System E

ADVANTAGES

- Clogging limited.
- No surface water present up to drainage capacity of permeable layer.

DISADVANTAGES

- Difficult to overlay.
- Amount of drainage through permeable layer limited.

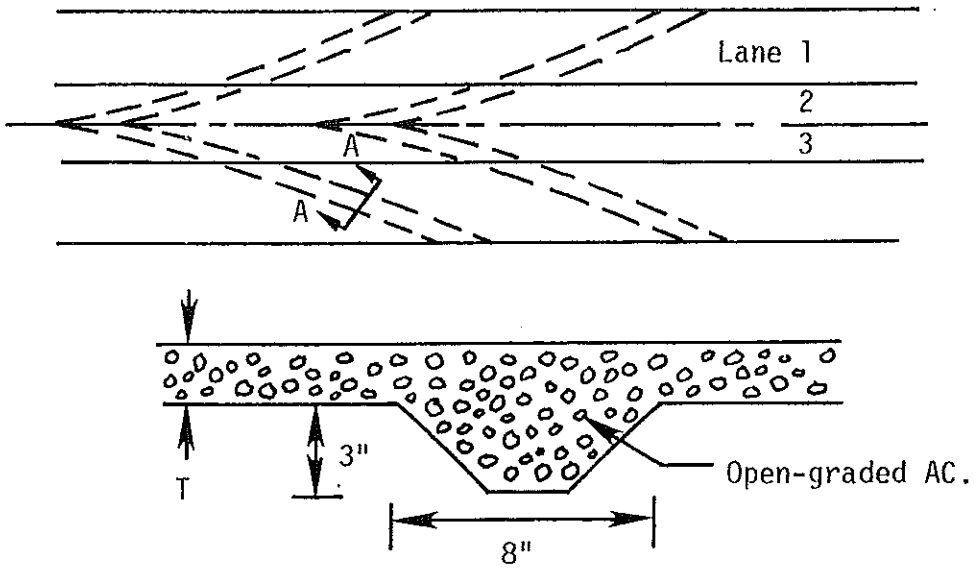

Section A-A

Figure 205. Subsurface channel drainage, System F

* T dependent upon design rainfall and drainage length.

a. Cut channels in old road along contour lines approximately 3 by 8 in (76 by 203 mm).
b. Fill contours with permeable open-graded AC.
c. Top with permeable open-graded mixture.

ADVANTAGES

- Can be used on exposed concrete pavement or asphalt pavement.
- Clogging unlikely.
- No surface water during moderate rains.

DISADVANTAGES

- Cutting involved in the construction phase.
- Drainage capacity less than 15% of channel cross section.

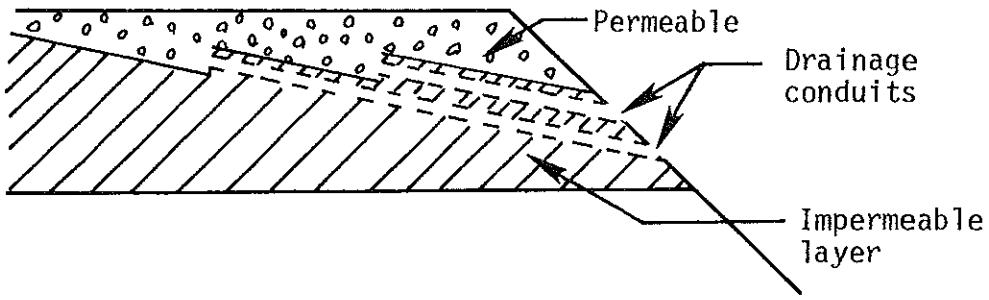

Figure 206. Subsurface individual-lane drainage, System G

ADVANTAGES

- Clogging less likely than slotted drain.
- No surface water during moderate rains.
- Multi-lane configuration.

DISADVANTAGES

- Difficult construction.
- Back slopes must be long therefore, difficult in a cut section.
- If clogging occurs then it is difficult to correct.

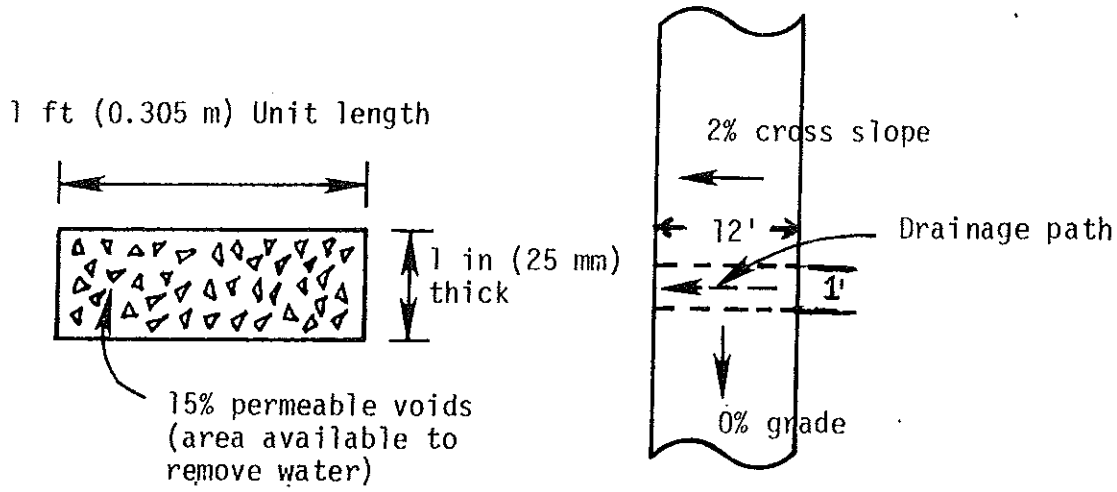

Figure 207. Longitudinal cross section

The drainage capacity, Q, needed for a pavement unit length of one foot (0.305 m), 12 feet (3.7 m) wide (See Figure 207) can be calculated as follows from the above assumptions:

$$Q = IP_A = 0.35\ ft^3/h\ (0.01\ m^3/h) \qquad \text{Eq (42)}$$

in which

Q is the outflow, ft^3/h (m^3/h),
I is the rainfall intensity, 0.35 in /h (9 mm/h), and
P_A is the pavement area being drained, ft^2(m^2).

The expected velocity through the one inch (25.4 mm) thick pavement of unit length (longitudinal cross-section of Figure 207 with 15 percent voids can be calculated from this drainage capacity as follows:

$$V = \frac{Q}{A} = 0.0078\ ft/s\ (2.38\ mm/s) \qquad \text{Eq (43)}$$

in which

V is the velocity, ft/s (mm/s), and
A is the cross-sectional area of the voids, ft^2 (m^2).

Therefore, the approximate velocity of water through the open-graded mixture is 0.0078 ft/s (2.38 mm/s). Moynahan, et. al. (44) reported a velocity of 0.002 ft/s (0.61 mm/s) for dense graded aggregate. Thus, the velocity value is of the right order of magnitude.

The thickness of the open-graded mixture needed to facilitate drainage can be estimated from an assumed horizontal velocity of 0.0078 ft/s (2.38 mm/s). The thickness continuously increases with drainage path length to a maximum t' at the pavement edge as shown in Figure 208. The thickness t', can be calculated as follows by using the same cross section as shown in Figure 207:

$$Q = VA = IP_A$$

$$V = 0.0078 \frac{ft}{s} \text{ (2.37 mm/s)}$$

$$A = 0.15\ t'y$$

$$P_A = Ly$$

in which

t' is the open-graded layer thickness, in (mm), and
y is the unit longitudinal length of the pavement section, one foot (0.305m).

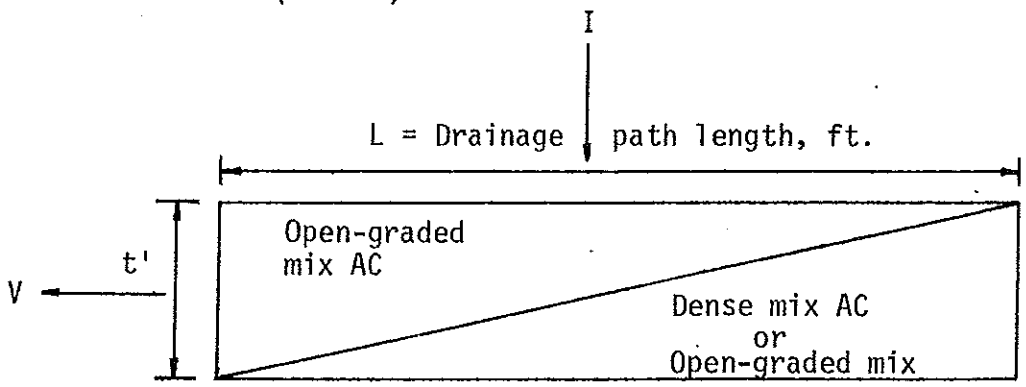

Figure 208. Thickness of open-graded pavements

Solving Equation 43 for t' the resulting equation is

$$t' = \frac{IL}{4.21} \qquad \text{Eq (44)}$$

Calculations from Equation (44) are shown in Table 23.

Table 23. Required thickness of open-graded pavement for selected rainfalls, inches (mm)

Drainage Path Length, L, feet	metres	Rainfall Intensity in/h (mm/h) 0.2 (5)	0.5 (13)	1.0 (25)	1.5 (38)	2.0 (51)
12	3.7	0.6 (15)	1.4 (36)	2.9 (74)	4.3 (109)	8.6 (218)
24	7.3	1.1 (28)	2.9 (74)	5.7 (145)	8.6 (218)	
36	11.0	1.7 (43)	4.3 (109)	8.6 (218)	12.8 (325)	
48	14.6	2.3 (58)	5.7 (145)	11.4 (290)	*Required thickness excessively large*	
60	18.3	2.9 (74)	7.1 (180)			

It is apparent from Table 23 that for design rainfalls exceeding about 1 inch (2 5 mm) per hour and drainage lengths exceeding 24 feet (7.3 m) the required thickness becomes excessive. Based on this analysis, a 1.5 inch (3 8 mm) thickness of open-graded mix is recommended for drainage of a single lane; 3 inch (7 6 mm) thickness for the drainage of two lanes; and 4.5 inch (114 mm) thickness for drainage of three lanes. The minimum cross slope should be two percent in each instance.

Where variable thickness open-graded overlays are used, the minimum thickness should be one inch (25 mm) and the maximum thickness should be consistent with the criteria presented above. The decision to increase the thickness of the open-graded mix carries with it a requirement to provide adequate drainage to the edge of the side slope. In cut sections and in the median, this can mean the use of subsurface-drainage systems. Another significant factor to consider is the increased susceptibility to compaction on the part of open-graded mixtures. This factor limits the effective thickness of open-graded paving mixtures to about 4.5 inches (114 mm). Even in this instance frequent maintenance may be required to eliminate excessive wheel path depressions.

The data presented in Table 23 illustrate that through-the-pavement drainage using an open-graded surface is very limited. This combined with the accumulation of debris and possible compaction of the mix requires that adequate cross slope of the pavement surface be maintained. As indicated in subsequent paragraphs, a minimum 2 percent cross slope is recommended for all highway pavements.

Step 3 - Evaluate The Interaction Between Grade, Pavement Cross Slope, and Pavement Deformations

A. Effect of Wheel Path Depression on the Critical Drainage Path Length

Wheel path depressions interrupt the normal flow pattern and can, if excessive, completely alter the drainage pattern on the pavement surface. This section attempts to define the conditions under which the wheel path depressions restrict the normal drainage path.

Basic Assumptions

There are two basic assumptions in the analysis process that are necessary: 1) the minimum cross slope to provide drainage is 0.5 percent and 2) the wheel path depression, WPD, is two feet (0.6 m) wide.

From the basic assumptions and Figure 209,

$$WPD \doteq S\,\frac{W}{2} - 0.005\,\frac{W}{2}. \qquad \text{Eq (45)}$$

Observed wheel path depressions have been determined as a part of this research.* These data are for asphalt surfaces on two lane highways. The data reveal that the 85th percentile wheel path depression is 0.3 inches (7.6 mm). Assuming that a minimum cross slope of 0.005 is required to provide adequate cross drainage and that the wheel path depression is approximately two feet wide, the cross slope required to provide minimum drainage on two lane rural highways of asphalt construction can be determined.

*See Chapter VI

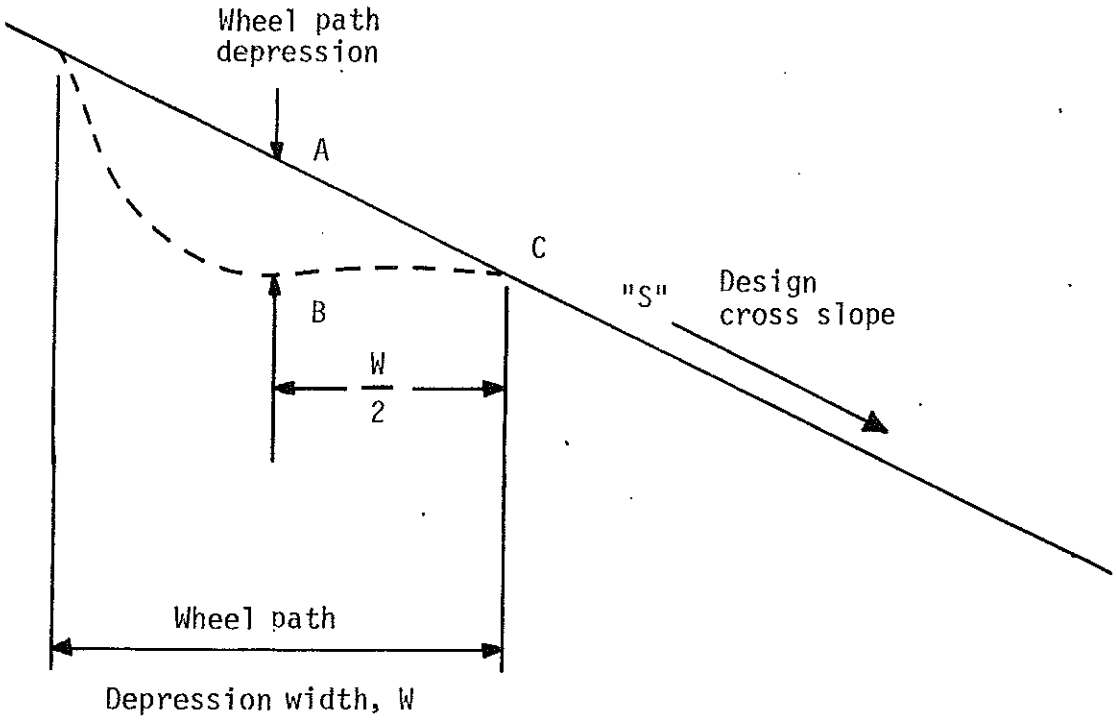

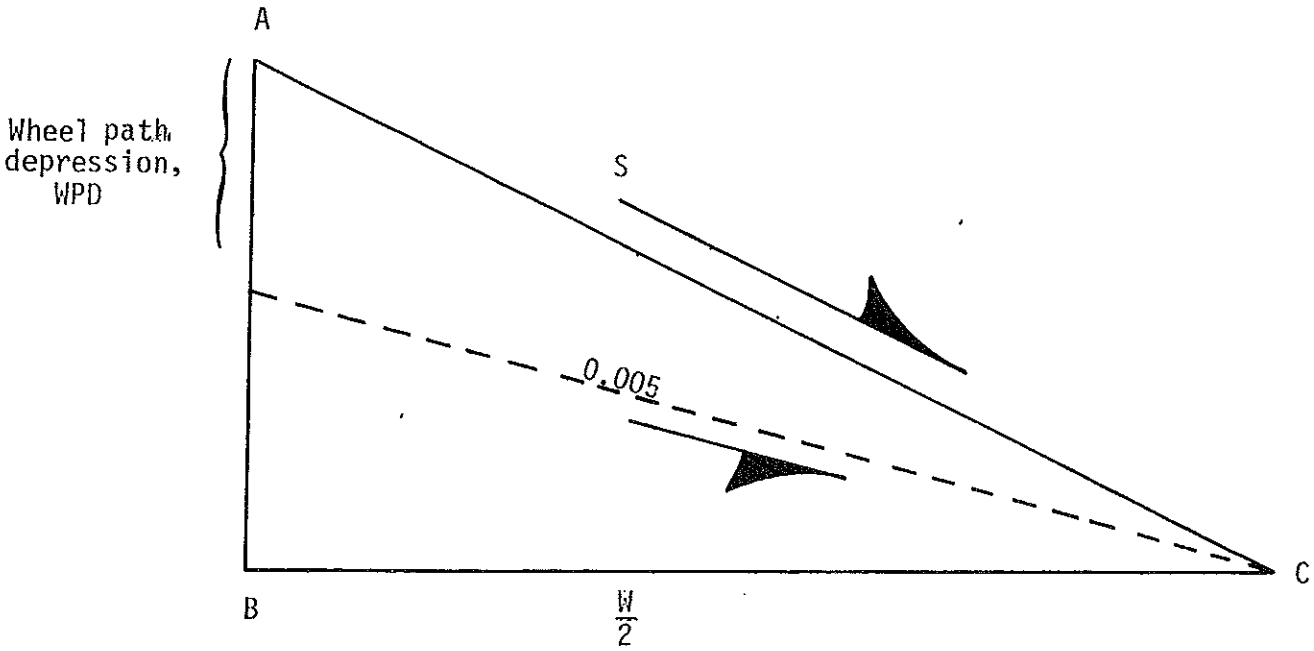

Figure 209. Basic geometry of wheel path depression

From Equation 45, and for a wheel path depression width of 2 feet (0.6 m):

$$WPD = (S - 0.005)\ (12)$$

in which

WPD is the wheel path depression, in (mm), and
S is the pavement cross slope in ft/ft (m/m).

Thus, the critical cross slope, S_c, is

$$S_c = \frac{WPD + 0.06}{12}. \qquad \text{Eq (47)}$$

For the 85th percentile depression, 0.3 in (7.6 mm),

$$S_c = \frac{0.3 + 0.06}{12} = 0.03 \text{ or } 3 \text{ percent.}$$

For the 95th percentile depression, 0.4 in (10 mm),

$$S_c = \frac{0.4 + 0.06}{12} = 0.038 \text{ or } 3.8 \text{ percent, say, } 4 \text{ percent.}$$

These data suggest that the minimum cross slope to insure adequate drainage of asphaltic concrete roadways is on the order of 3 percent.

This approach can also be used to establish the maximum allowable wheel-path depression prior to resurfacing to remove the depression. The resulting maximum wheel path depressions for various cross slope values are presented in Table 24.

Table 24. Allowable wheel path depressions

Cross Slope %	Maximum Wheel Path Depression in.	mm
1	0.06	1.5
2	0.18	4.6
3	0.30	7.6
4	0.42	10.7

B. Critical Drainage Path Length in Highway Hydroplaning

Basic Equation

$$WD = 0.00338\ \frac{TXD^{0.11}\ L^{0.43}\ I^{0.59}}{S^{0.42}} - TXD \qquad \text{Eq (16)}$$

where

WD = water depth above the top of the aggregate, in (mm/25.4)
TXD = texture depth of pavement, in (mm/25.4),
L = length of the drainage path, feet (m/0.305),
I = intensity of the rainfall, in /h ($\frac{mm}{25.4}$/h), and
S = cross slope of pavement, ft/ft (m/m).

If the above equation is solved for L, the result is

$$L = \left[\frac{(WD + TXD)\ S^{0.42}}{0.00338\ TXD^{0.11}\ I^{0.59}}\right]^{\frac{1}{0.43}}$$

and suitable numerical values of the variables are

1. Critical hydroplaning depth WD = 0.06 inches (1.52 mm);
2. Desirable water depth WD = 0.0 inches (0 mm);
3. Texture depth TXD = 0.01, 0.03, 0.06 inches (0.25, 0.76, 1.52 mm);
4. Cross slope S = 0.010, 0.015, 0.020; and
5. Rainfall intensity I = 0.15, 0.35, 0.50, 0.75, 1.0 in /h (3.8, 8.9, 12.7, 19.0, 25.4 mm/h).

Once the maximum drainage path length is calculated a critical grade can be found. The design grade cannot exceed this critical grade or the drainage path length becomes excessive and flooding results. Therefore, the design grades must be smaller than the critical grade for satisfactory performance.

The calculations for the critical grade are as follows:

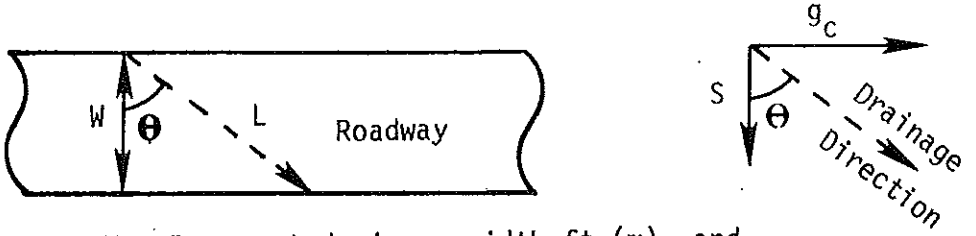

W = Pavement drainage width ft (m), and
g_c = Critical grade, percent.

Figure 210. Critical grade analysis

From Figure 210,

$$\text{Cos}\theta = \frac{W}{L} \text{ and } \text{Tan}\theta = g_c/S; \text{ therefore,}$$

$$\text{Tan}\theta = \frac{L^2 - W^2}{W} = g_c/S \text{ or } g_c = \frac{S}{W}\,[L^2 - W^2] \qquad \text{Eq (46)}$$

where: g_c = critical grade; W = pavement width; S = cross slope; L = drainage path length.

Figures 211 through 215 present these calculations graphically.

Findings from Drainage Path Analysis

As can be seen from Figures 211 through 215 the critical drainage path length is very sensitive to the water depth assumed. Desirably, the water depth would be 0.0 as a maximum and the minimum acceptable condition would be about 0.06 in (1.52 mm). A study of the 6 percent normal maximum grade for the minimum water depth of 0.06 in (1.52 mm) reveals that flooding will not occur for pavement cross slopes of 2 percent or more. Based on Figures 211 through 215, the following conclusions are drawn.

1. Water buildup on pavements up to 36 feet (11 m) wide will not be sufficient to induce hydroplaning for cross slopes of 2 percent or greater and rainfall intensities below 0.5 in /h (13 mm/h) for the assumed critical water depth of 0.06 in (1.52 mm).

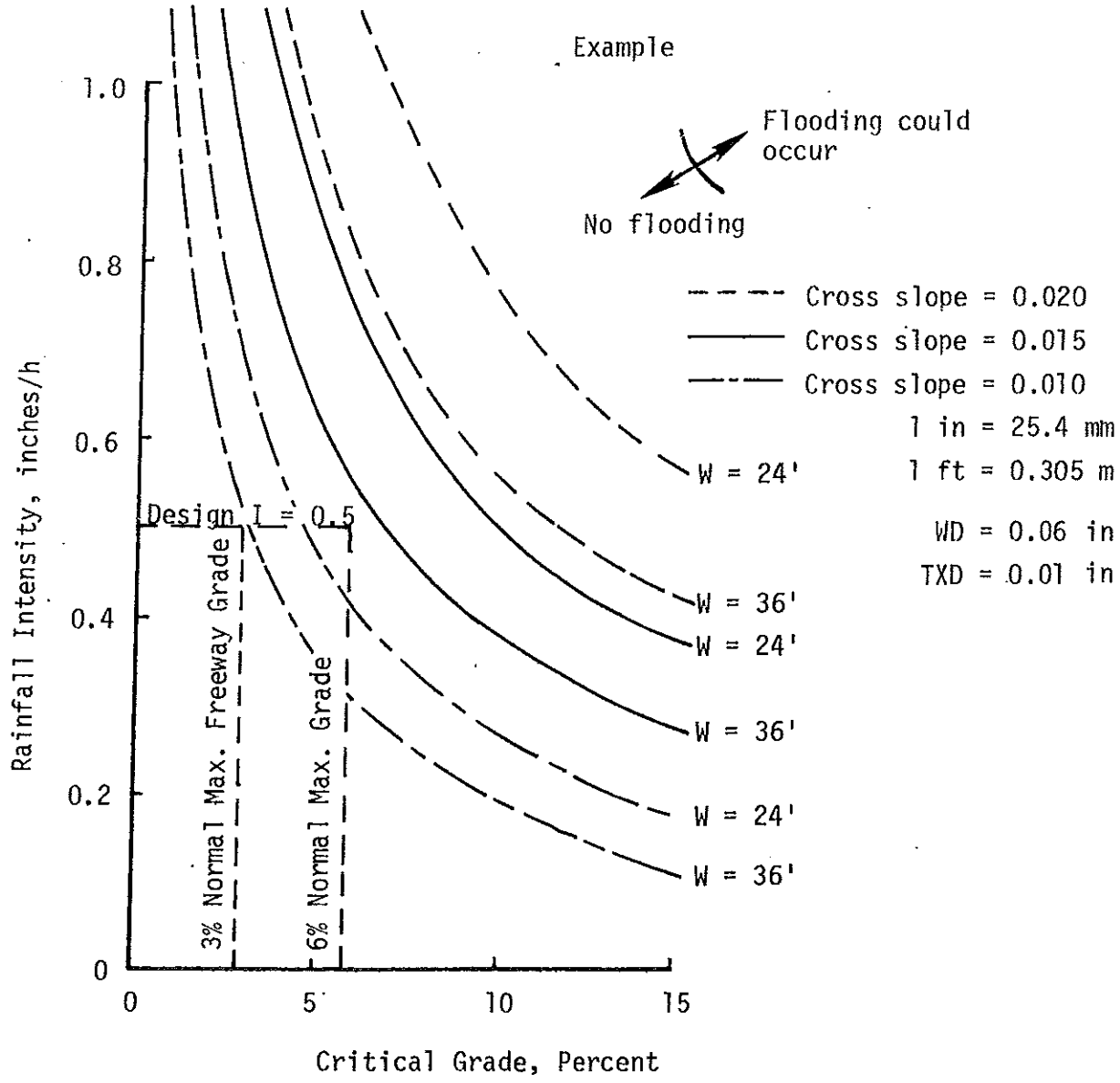

Figure 211. Rainfall intensity vs. critical grade

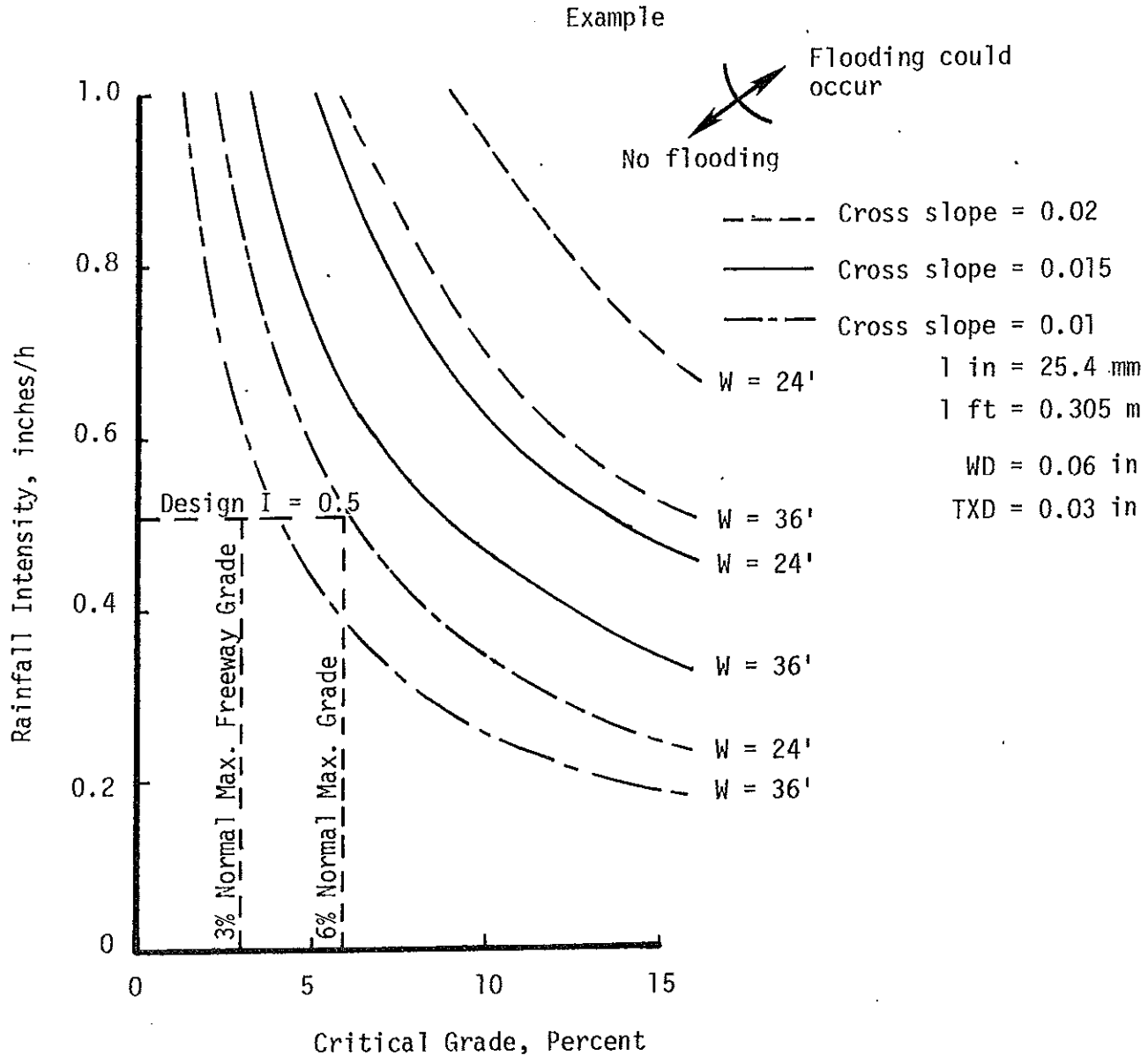

Figure 212. Rainfall intensity vs. critical grade

Machines
» Articulated Trucks
» Backhoe Loaders
» Cold Planers
» **Compactors**
» Feller Bunchers
» Forest Machines
» Forwarders
» Harvesters
» Hydraulic Excavators
» Knuckleboom Loaders
» Material Handlers
» Motor Graders
» Multi Terrain Loaders
» Off Highway Tractors
» Off Highway Trucks
» Paving Equipment
» Pipelayers
» Road Reclaimers
» Scrapers
» Skid Steer Loaders
» Skidders
» Soil Stabilizers
» Telehandlers
» Track Loaders
» Track-Type Tractors
» Underground Mining
» Wheel Dozers
» Wheel Excavators
» Wheel Loaders

CB-634D ASPHALT COMPACTOR

Select

Overview **Specifications** **Benefits & Features** **Optional Equipment**

SPECIFICATIONS

Engine	Units: US | **Metric**
Engine Model	Cat® 3116T
Gross Power	145 hp
EEC 80/1269	138 hp
ISO 9249	138 hp
Bore	4.12 in
Stroke	5 in
Net Power - SAEJ1349 (JUN 95)	138 hp
Weights	
Operating Weight with ROPS/FOPS	28160 lb
Operating Weight at Rear Drum with ROPS/FOPS	14643.09 lb
Operating Weight at Front Drum with ROPS/FOPS	13512.12 lb
Operating Weight without ROPS/FOPS	27255 lb
Shipping Weight with ROPS/FOPS	26260 lb
Shipping Weight without ROPS/FOPS	25355 lb
Service Refill Capacities	
Fuel Tank Capacity	66 gal
Water (Spray) Tank Capacity	317 gal
Operating Specifications	
Curb Clearance	15.1 in
Turning Radius Outside Drum Edge	262 in
Turning Radius Inside Drum Edge	170 in
Ground Clearance	15.1 in
Travel Speed Max	7.6 mph
Vibratory System	
Drum Width	84 in
Drum Diameter	51 in
Frequency	2640 vpm
Nominal Amplitude - High	.041 in
Nominal Amplitude - Low	.015 in
Centrifugal Force Maximum	35745 lb
Centrifugal Force Minimum	13039 lb

CONFIGURE 634D
Customize y meet your n
→ **Configure**

LOCATE YO
Get in touch dealer for m
→ **Locate Yo**

CB-634D AS COMPACTOR
Downloac Brochure (5

Vibration Selection	Independent per drum
Eccentric Weight Drive	Hydraulic direct, auto reversing

Dimensions

Overall Length	195 in
Wheelbase	124 in
Height at Steering Wheel	93 in
Height with ROPS/FOPS	123 in
Compaction Width	84 in
Overall Width	90.98 in

©2007 Caterpillar All Rights Reserved. Legal Notices Site Map [+]Site Feedback Contact

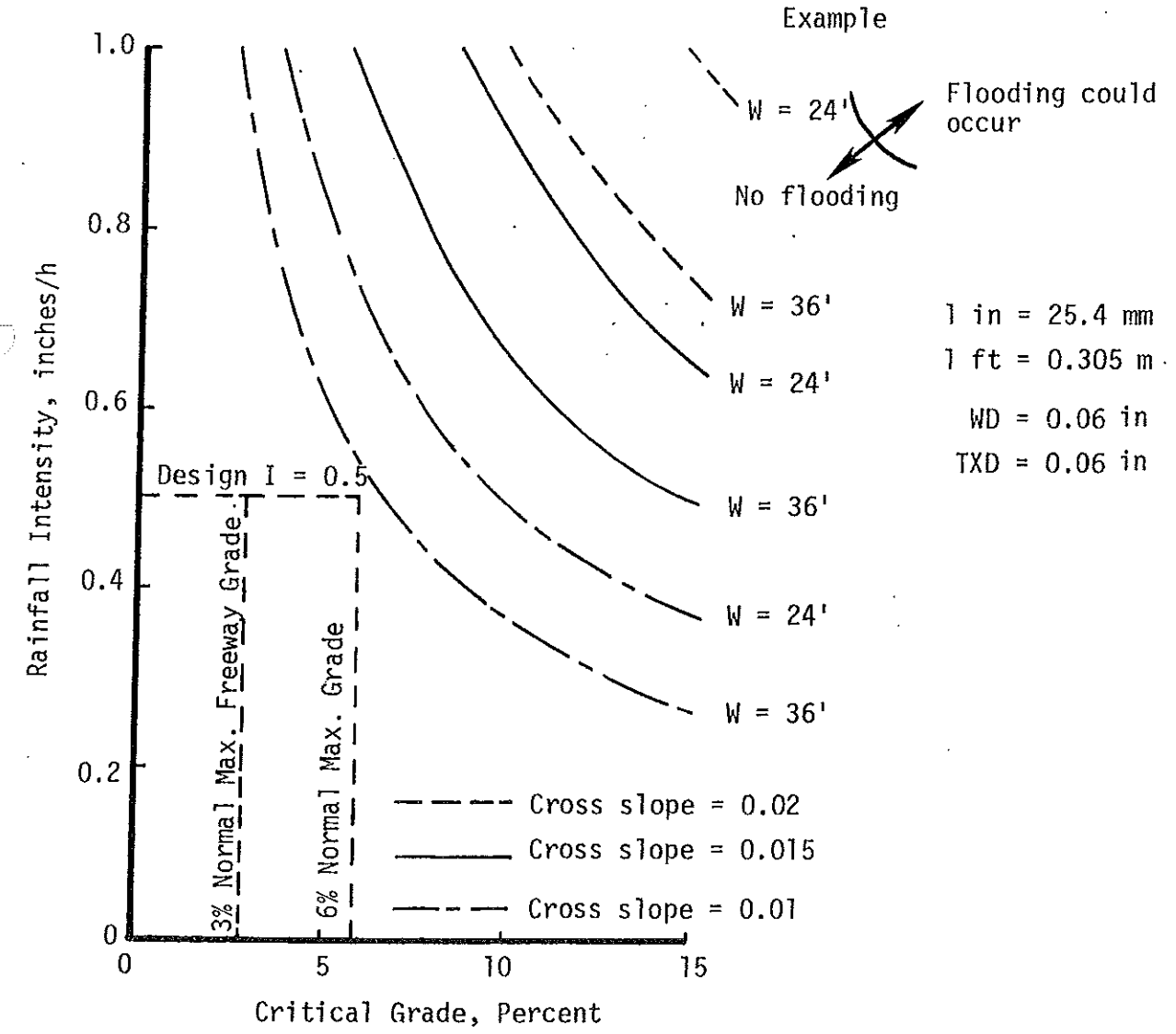

Figure 213. Rainfall intensity vs. critical grade

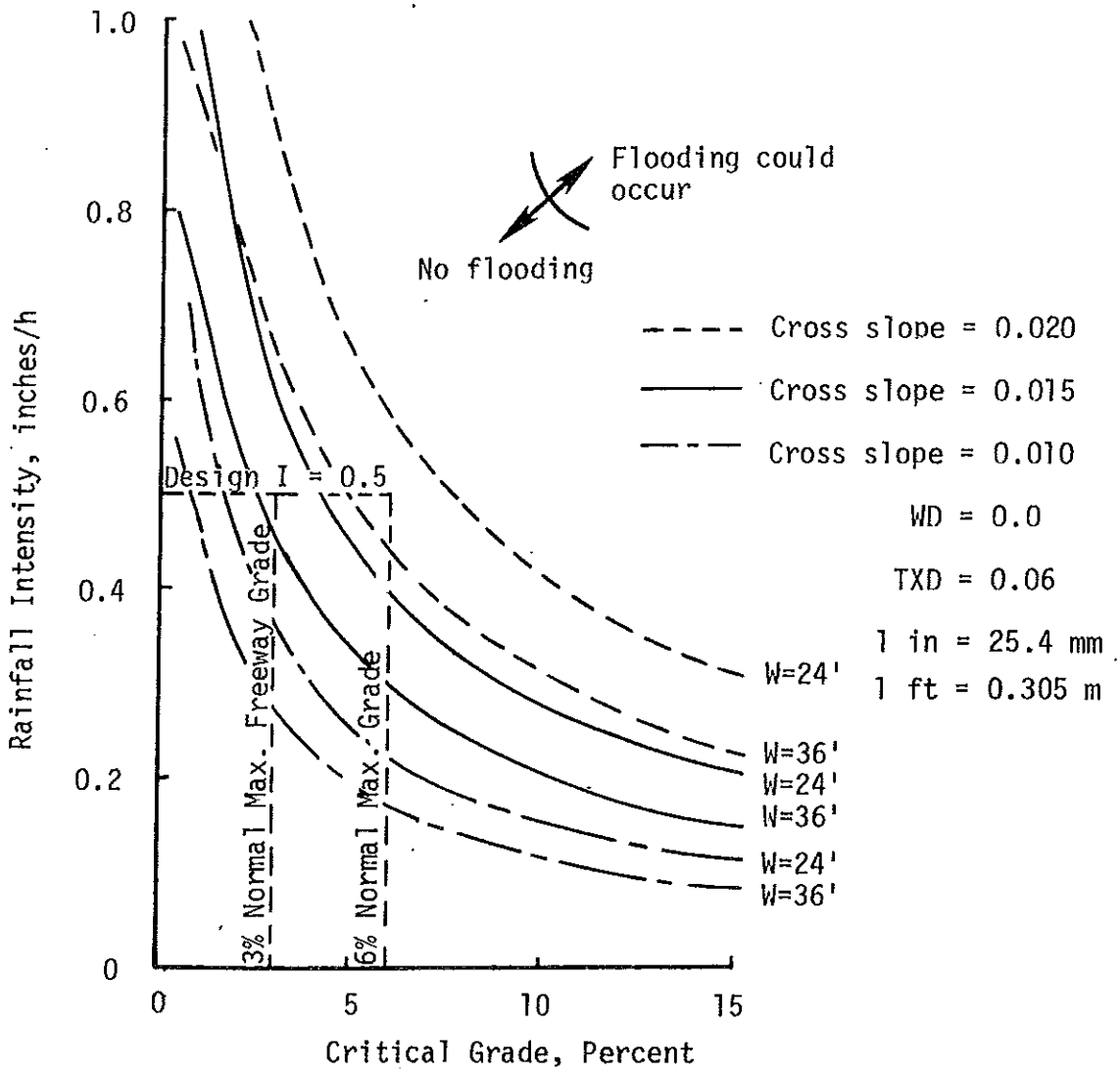

Figure 214.. Rainfall intensity vs. critical grade

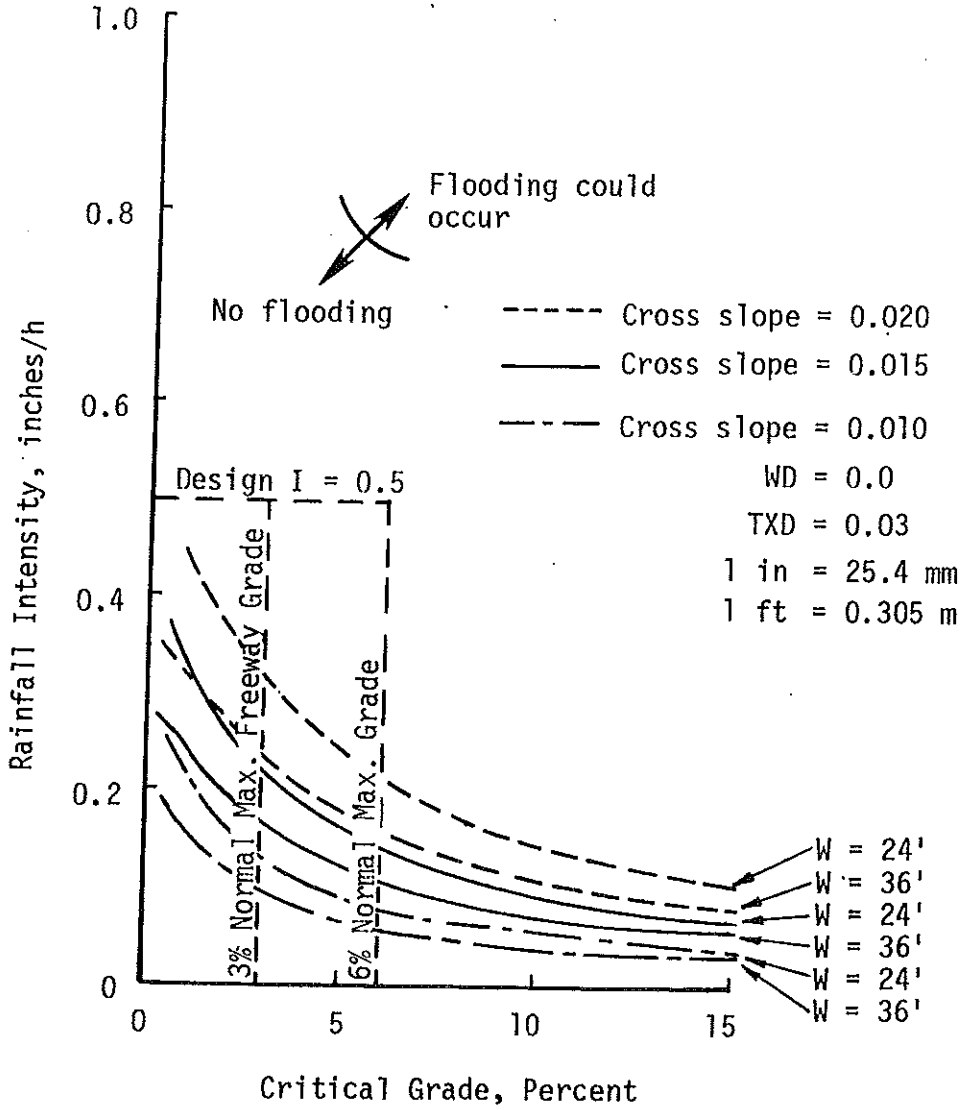

Figure 215. Rainfall intensity vs. critical grade

2. Using the desirable design value of water depth of 0.0 in (0 mm) results in critical drainage path lengths for all pavement widths when the pavement texture depth is less than 0.03 (0.8 mm). For texture depth over 0.03 (0.8 mm) no hydroplaning problem would be expected for two lane pavements. Multi-lane pavements would have a tendency to flood at normally expected rainfall intensities.
3. The cross slope is more critical than texture depth when the critical water depth assumption is 0.06 in (1.52 mm). With the 0.0 in (0 mm) critical water depth assumption, texture depth is equally important in determining the critical length of the drainage path.
4. A minimum pavement cross slope of 0.02 is suggested for all pavement sections.
5. The desirable design assumption suggests the combination of an open-graded surface course (or high texture surface) and the 0.02 minimum cross slope.

Step 4 - Rank Innovative Surface-Drainage Techniques

The seven concepts for innovative surface drainage systems have been subjectively evaluated in Table 25. A ranking of the systems is provided in Table 26.

Step 5 - Recommend A Surface-Drainage Technique For Sag-Vertical Curves

From the eight criteria in Table 25, the subjective evaluation of the surface-drainage systems suggests that the three open-graded systems without subdrain systems probably have the greatest potential for reducing hydroplaning on sag-vertical curves. The drainage-path analysis suggests, however, that an open-graded paving mixture can not substitute for adequate cross slope of the pavement section. From an economic point of view there are real advantages to using a thin lift of open-graded mixture (say 1 inch or 25 mm) with adequate cross slope in lieu of a thicker layer of open-graded mixture with little or no cross slope.

Step 6 - Review The Alternatives For Curbs

Curbs exist on many older highway sections which exhibit poor drainage characteristics. The alternative treatments available are

1. Provide additional drainage capacity on the pavement surface.
2. Provide additional subsurface drainage inlets in or near the curb.
3. Remove the curb and develop a drainage system off the main highway lanes.

The first of these alternative treatments has been discussed in detail in Step 2. The general conclusion was that drainage on the pavement surface, except through the use of open-graded mixtures, is probably not practical for high-speed operating conditions. The second alternative is practical from a hydraulic capacity point of view but unsafe on high-speed facilities. For practical purposes the removal of the curb and development of drainage facilities off the roadway combined with providing adequate cross slope to insure drainage is, therefore, the desirable approach.

Table 25 . Evaluation of innovative systems

EVALUATION	SYSTEM A	B	C	D	E	F	G	DESIRED QUALITY
1. Adaptability to wheel path depression	N	N	Y	Y	Y	Y	Y	Y
2. Susceptibility to ponding	H	M	L	L	L	L	L	L
3. Susceptibility to clogging	L	L	M	M	M	M	M	L
4. Difficulty of construction	H	H	H	M	L	M	H	L
5. Difficulty of overlaying	H	H	L	L	L	L	L	L
6. Expected degree of compaction	L	L	M	M	M	H	H	L
7. Maintenance cost	H	M	L	L	L	L	M	L
8. Difficulty in adapting to portland cement concrete (PCC) pavement	H	H	M	M	L	H	H	L
TOTAL	2	3	4.5	5.5	7	5	4	

N = no
Y = yes

L = low
M = moderate

H = high

Table 26 . Ranking of innovative surface-drainage systems for practicality

RANK	SYSTEM	SYSTEM NAME
1 (Best)	E	Subsurface Cross-Slope Drainage
2	D	Subsurface Directional Berm
3	F	Subsurface Channel Drainage
4	C	Subsurface Drop Inlet
5	G	Subsurface Individual Lane Drainage
6	B	Surface Drop Inlets
7 (Poorest)	A	Surface Transverse Slotted Pipe

Step 7 - Recommend Remedial Treatments For Sag-Vertical Curves With Curbs

The use of curb and gutter sections on older highways was a common practice. For reasons of safety, this practice is now discouraged; however, many locations still exist with the basic curb and gutter section. Where such designs exhibit a tendency to flood on a frequent basis, the remedial treatment recommended includes

1. Removal of the curb and replacement with a slotted subdrain system on a paved shoulder if required. The slotted subdrain should be located a minimum of 2 feet (0.6 m) from the edge of the traffic lane. As an alternative, remove the curb and reshape the cross section to provide a drainage channel well off the traffic lane. This channel would be drained down the grade and into a drop inlet or paved ditch near the low point of the curve and
2. Resurfacing to increase the effective cross slope to a minimum of 2 percent if the present cross slope is less than 1.5 percent. Concrete pavements not requiring an overlay may also require grooving to provide sufficient macrotexture.

The use of curbs on new design to control drainage should be kept to a minimum and when used should be located at the outside edge of a paved shoulder of sufficient width for safe operation. The minimum shoulder widths should be 10 feet (3 m) on high-volume (over 4000 VPD) roadways, 6 feet (1.8 m) intermediate volume roadways (1000-4000 VPD) and 2 feet (0.6 m) on low volume roadways (below 1000 VPD). Redirection systems provided at such locations must be located inside (i.e., traffic side) of the curb or immediately over the curb with proper approach end treatments.

Recommended Remedial Treatments for Sag-Vertical Curves Subject to Flooding

Based on the findings of this phase of the research, the suggested criteria for remedial treatment of sag-vertical curves is presented in Table 27. Similar criteria for new designs are presented in Table 28.

Summary of Major Findings

1. Of the innovative surface drainage systems considered, those featuring a permeable surface course or a high macrotexture surface course appear to have the highest potential for reducing hydroplaning accidents.
2. Based on the observed flow rates through the open-graded mixture, the thickness required to accommodate drainage through the pavement for high intensity rainfalls is too great to be economically feasible. Excessive compaction of the overlay combined with a reduced probability of high rainfall intensities are the primary reasons.
3. Pavement cross slope is the dominate factor in removing water from the pavement surface. A minimum cross slope of two percent is recommended.
4. As a guideline, a wheel-path depression in excess of 0.2 inches (5 mm) should be used as the criterion for resurfacing to reduce the pavement drainage problem when dense AC or PCC pavements are used.
5. The most likely innovative surface drainage systems are those which involve using open-graded AC surface courses without a subdrain system.

Table 27 . Recommended remedial treatment for sag-vertical curves subject to flooding

	PCC Pavements	AC Pavements
Cross Slope	Min.* 1% Max. 2% Desirable 2%	Min.* 1% Max. 2% Desirable 2%
Treatment of Surface	Longitudinal Grooving (Ref. 1) 0.1 inch (2.5 mm) grooves at 0.8 inch (20 mm) centers to a maximum depth of 0.2 inch (5 mm).	1 inch (25 mm) of open-graded AC mix or a coarse surface treatment (maximum aggregate size 0.4 inch) (10 mm)
Wheel Path Depression	Max. wheel path depression 0.20 inch (5 mm) as measured from the normal cross slope of the pavement.	Maximum wheel path depression 0.20 inch (5 mm) as measured from the normal cross slope of the pavement.

* The minimum should be used only when the rollover between adjacent lanes becomes excessive.

Table 28 . Recommended treatment for sag-vertical curves in new construction

	PCC Pavements	AC Pavements
Cross Slope	2 percent	2 percent
Treatment of Surface	High texture surface using transverse grooving of fresh concrete by metal tines. Spacing of tines 0.5 inches (13 mm) maximum and depth of groove, 0.2 inches (5 mm) maximum depth and 0.08 inches (2 mm) minimum depth. (2)	1 inch (25 mm) of open-graded AC mix or a coarse surface treatment (maximum size aggregate 0.5 inches or 13 mm).

6. Surface drains located parallel to the lane lines will probably not solve the drainge problem due to the wheel path depressions.

7. Transverse surface drains located on the pavement surface would probably result in a rough pavement, increase maintenance costs, and increased potential for ponding water. For these reasons, such systems are not recommended for general use.

CHAPTER VIII

CRITERIA TO REDUCE HYDROPLANING

Based on the information developed in preceding chapters, a clear definition has evolved concerning the influence of different factors on the full loss of control forces (dynamic hydroplaning). It is of interest now to estimate the range and distribution of these factors on the highway. Approximate distributions of these factors are given in the full report. The approximate 50 percentile values of these obviously skewed distributions are

$$TD = 7/32 \text{ in } (5.6 \text{ mm})$$
$$P = 27 \text{ psi } (186 \text{ kPa})$$
$$TXD = 0.038 \text{ in } (0.96 \text{ mm}).$$

The lower seven percentile level of the three groups is approximately

$$TD \leq 2/32 \text{ in } (1.6 \text{ mm})$$
$$P \leq 18 \text{ psi } (124 \text{ kPa})$$
$$TXD \leq 0.01 \text{ in } (0.25 \text{ mm}).$$

Two plots showing the distribution of texture depth in 1967 and in 1977 are given in Figure 216. The difference between these two plots would seem to show a remarkable (and certainly appropriate) increase in texture depths in one state over the past ten years.

Note that the plot of texture depth in terms of roadway distance is not the same as exposure rate to traffic since the more highly traveled, and thus more highly polished roads, are probably biased toward the lower texture range. Therefore, the plot given is probably more optimistic than warranted in terms of actual exposure to the lower texture values. The obvious conclusion is that significant numbers of automobiles are traveling under conditions which could produce hydroplaning at speeds less than the current speed limit of 55 mph (88 km/h).

However, there is one factor that makes the situation less critical than our initial considerations would seem to indicate. That is the comparative rarity of rainfalls intense enough to sustain significant positive water depths on the road surfaces.

Table 9, in Chapter II, shows the overall percentage of time that highways are exposed to rainfall of different intensities for Texas, Illinois and Alabama. The surprising conclusion from these data is that the exposures in these states are so similar. These data can also be estimated for other states and regions by use of two equations which fit Figures 18 and 21 reasonably well.

These equations are

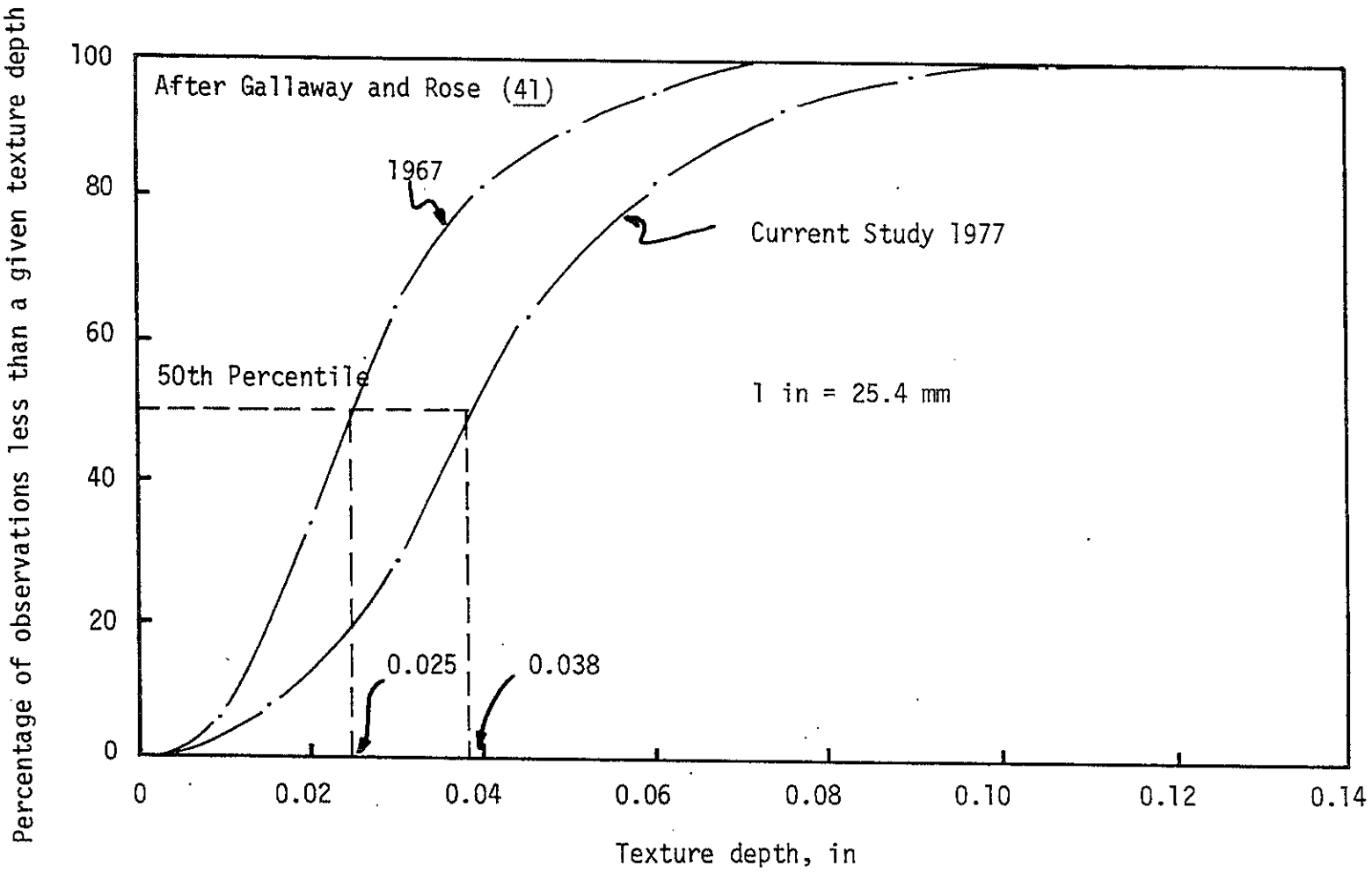

Figure 216. Approximate distribution of texture depths in one state, comparison of 1967 and 1977 data

$$T_w = 0.041 - \frac{(R_r - 60)^2}{87{,}500}$$

(1 in/y = 25.4 mm/y)

where R_r is the total annual rainfall in a specific region, r;

and T_w is the proportion of time a region is subjected to an intensity of rainfall greater than 0.01 in/h (0.25 mm/h),

and $$P_i = \frac{0.0324}{I_i} \qquad \text{Eq (48)}$$

(1 in/h = 25.4 mm/h)

where P_i is the probability of the occurrence of an intensity, I_i, during a period of rainfall.

The first produces an estimate of the proportion of time a region is subjected to rainfall equal to or greater than 0.01 in (0.25 mm) per hour based on the total annual rainfall. The second is what appears at this stage to be a conservative estimate of the probability of observing a specific intensity or greater during a period of rainfall. These two equations can be combined to produce an estimate of the proportion of time throughout a year when a rainfall of specific intensity or greater may be expected, P_{ri}, i.e.,

$$P_{ri} = P_i \, T_w$$

or $$P_{ri} = \frac{0.0324}{I_i} \left[0.041 - \frac{(R_r - 60)^2}{87{,}500} \right]. \qquad \text{Eq (49)}$$

(1 in/y = 25.4 mm/y, 1 in/h = 25.4 mm/h)

At this stage it is appropriate to discuss the selection of a "design" rainfall intensity. The purpose of a "design" intensity is twofold. First, as in the case of almost all highly variable natural phenomena, it must be recognized that it is not practical to design for all possible events. The precedent for this position is well established in many engineering disciplines. Examples are: (1) Traffic - the design of geometrics for the 85th or in some cases the 95th percentile traffic speed; (2) Hydraulics - the design of facilities based on a 25-year flood; and (3) Structures - the design for a 20-year wind, a 50-year snowfall or a 100-year earthquake.

Second, without a "design" rainfall intensity it is impossible to "design" road surfaces to preclude hydroplaning. Through experience, relatively standard practices have emerged which have reduced the hydroplaning event to a fairly low probability; but no comprehensive "design" method has emerged to provide a real direction to the effort.

Considering ways in which design rainfalls could be established, two approaches are given, with obvious preference given the latter.

Approach 1

Choose a reasonable design rainfall intensity and ask all states to design and maintain highways in such a way that this intensity will be accommodated. For example, this choice might be based on the average 95th percentile rainfall intensity throughout the nation, a value of approximately 0.5 in/h (13 mm/h). If two states are compared, one having a great deal more rainfall than the other, and all other factors being approximately equal, each state would be required to construct and maintain the same combinations of texture, cross slope and drainage path length. This would result in the lower rainfall state achieving a significantly lower probability of hydroplaning, or a much lower cost effectiveness level for efforts to decrease hydroplaning. A more versatile approach can be formulated by the "regional equalization of probability" concept; that is, design standards which would equalize the probability of hydroplaning event between different regions, e.g., between Nevada and Louisiana.

To do this, Table 29 illustrates the variables which must be considered to reduce the probability. Note only three of these factors -- surface texture, surface slope and drainage path length -- may be considered within the engineer's control. The other factors must be treated from the standpoint of probability as will be demonstrated in the following approach.

Table 29. Variables influencing hydroplaning

Factors Within Engineers Control	Factors Outside Engineers Control
Surface Texture	Rainfall
Cross Slope	Tire Tread Depths and Pressures
Drainage Path Length	Vehicle Speeds*

*Although some degree of influence may be obtained there will remain a relatively uncontrolled variation in individual vehicle speeds.

Approach 2

Choose a reasonable probability level of precluding hydroplaning and compute a design rainfall intensity for each state or geographic area to achieve that level.

As an example, consider choosing a probability level of one in one hundred thousand. This means the highway surface would be constructed

and maintained in a particular area so that the probability of hydroplaning would exist one chance in one hundred thousand. Choosing for the "design" tread depth, the minimum legal tire tread depth of 2/32 in (1.6 mm), this depth or lower occurs on 7 percent of all automobiles, a probability level of 0.07. For consistency, choosing a probability level of 0.07 for tire pressure results in a design tire pressure of approximately 18 psi (124 kPa). The probability of vehicles driving speeds necessary to achieve hydroplaning with these tire conditions is neglected on the grounds that the legal speed limit of 55 mph (88 mm/h) should be accommodated, and this speed is certainly high enough to allow hydroplaning. At this combination of tire pressure and tread depth, very small values of water depth can cause hydroplaning. Thus, a very conservative criterion to preclude such occurrence would be the allowance of no positive water depth through management of texture, cross slope and drainage path length when the highway is subjected to the "design" rainfall intensity.

The "design" rainfall intensity may be computed as follows based on the one in one hundred thousand choice of probability for the hydroplaning event.

$$P_e = P_t \times P_p \times P_{ri}$$

The probability of a specific combination of events occurring is the product of the probabilities of the individual events.*

where P_e = Probability of hydroplaning event (Selected in this example as 1×10^{-5})
P_t = Probability of the "design" tread depth (Selected in this example as 0.07)
P_p = Probability of the "design" tire pressure (Selected in this example as 0.07)
P_{ri} = Probability of the "design" rainfall intensity.

Then P_{ri} may be computed as

$$P_{ri} = \frac{P_e}{P_t \times P_p} = \frac{1 \times 10^{-5}}{7 \times 10^{-2} \times 7 \times 10^{-2}}$$

$$P_{ri} = 2 \times 10^{-3}.$$

*This assumes the individual factors are each randomly distributed and vary independently from each other. Since the variation is neglected, i.e. the probability of driving 55 mph (88 km/h) or greater is conservatively assumed to be one, the actual probability of the hydroplaning event is even less than the amount stated here. This is considered most likely since the rainfall event at design intensity levels reduces visibility and results in many vehicles slowing down. Others slow in response to the knowledge that wet pavements make vehicle control more difficult.

If the region we are considering has an annual rainfall, R_i, of 30 in, the "design" rainfall, I_d, can be calculated from the following equation:

$$I_i = I_d = \frac{0.0324}{P_{ri}} \left[0.041 - \frac{(R - 60)^2}{87,500}\right] \quad *$$

$$I_d = \frac{0.0324}{2 \times 10^{-3}} \left[0.041 - \frac{(30 - 60)^2}{87,500}\right]$$

$$I_d = \frac{32.4 \times 10^{-3}}{2 \times 10^{-3}} \cdot [0.031] = 0.5 \text{ in/h},$$

a rainfall intensity that can be accommodated by current technology.

Following the same computational method, the following design rainfall intensities would be selected for regions of the country having the annual rainfalls given. See Table 30.

Table 30. Example design rainfall intensities

Annual Rainfall in/y	Design Rainfall Intensity in/h
5	0.10
10	0.19
20	0.37
30	0.50
40	0.60
50	0.65
60	0.66

*This equation should not be used for regions where the annual rainfall is greater than 60 in (152 mm).

Although it would be more precise for each state to analyze rainfall records to develop a state or regional "design" rainfall intensity, it appears that the equations developed will provide reasonable estimates.

Once the "design" rainfall intensity is selected, information is available which will allow the prediction of water depth on the pavement as a function of surface slope, runoff length and texture. For example:

$$WD = .00338 \left[TXD^{0.11} \, L^{0.43} \, I^{0.59} \, S^{-0.42} \right] - TXD \qquad \text{Eq (16)}$$

where WD = the water depth above the top of the surface asperities in inches (25.4 mm)
L = runoff length in feet (0.305 m)
TXD = texture depth in inches (25.4 mm)
I = rainfall intensity in in/h (25.4 mm/h)
S = slope of surface in ft/ft.

Curves developed using this equation showing acceptable combinations of cross slope, drainage path length and texture depth for different rainfall intensities are given in Figures 217 through 219 . They represent combinations of the critical parameters which will result in zero water depths on a road surface. Curves of this type can be used to formulate criteria to accommodate specific "design" rainfall intensities.

For a state or region having an annual rainfall of 30 in/y (762 mm/y), criteria could take the form shown in Table 31. This is based on a rainfall intensity of 0.5 in/h (13 mm/h) as developed by "Approach 2" and on the curves shown in Figure 218.

Table 31. Example allowable combination of pavement drainage parameters

Drainage Path Length	Allowable Combinations of Slope and Texture		Nominal Texture Value 10^{-3} in
	percent	in	
12	2	≥0.022	20
12	1.5	≥0.025	25
12	1.0	≥0.031	30
12	0.5	≥0.043	45
24	2.0	≥0.031	30
24	1.5	≥0.036	35
24	1.0	≥0.043	45
24	0.5	≥0.060	60
36	2.0	≥0.039	40
36	1.5	≥0.043	45
36	1.0	≥0.052	50
36	0.5	≥0.072	70

Metric Conversion: 1 in = 25.4 mm

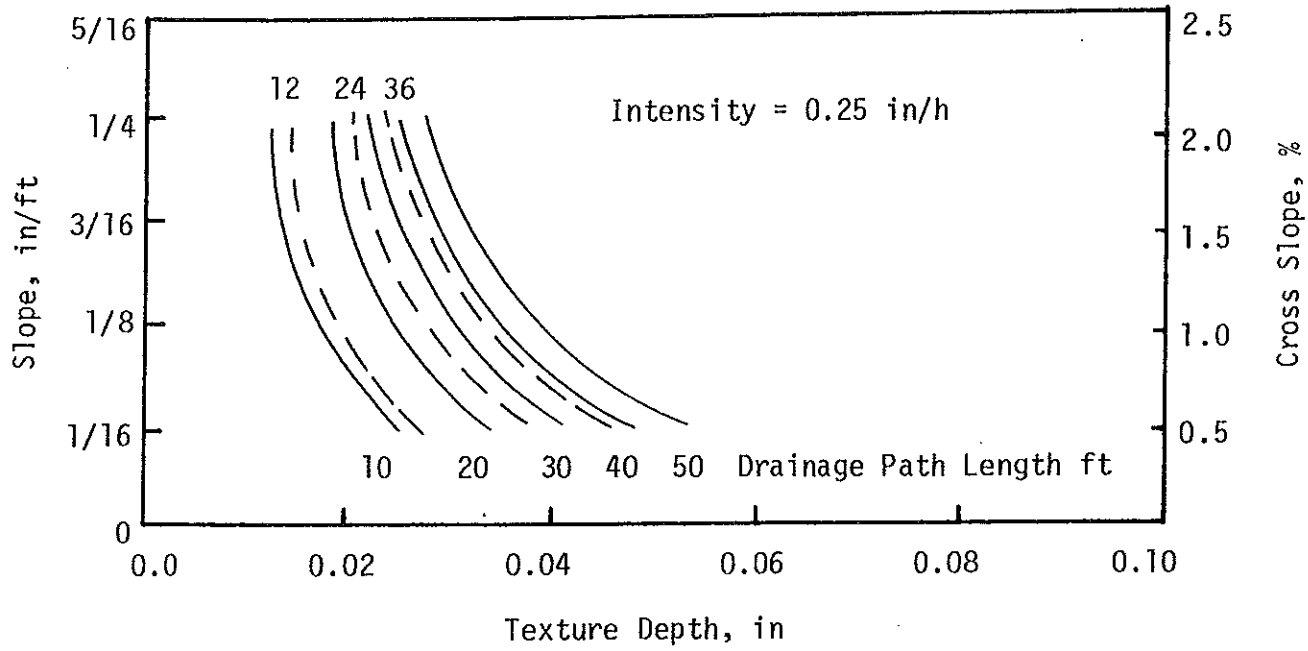

Figure 217. Curves of zero water depth for an intensity of 0.25 in/h

Metric Conversion:

1 in/h = 25.4 mm/h
1 ft = 0.305 m

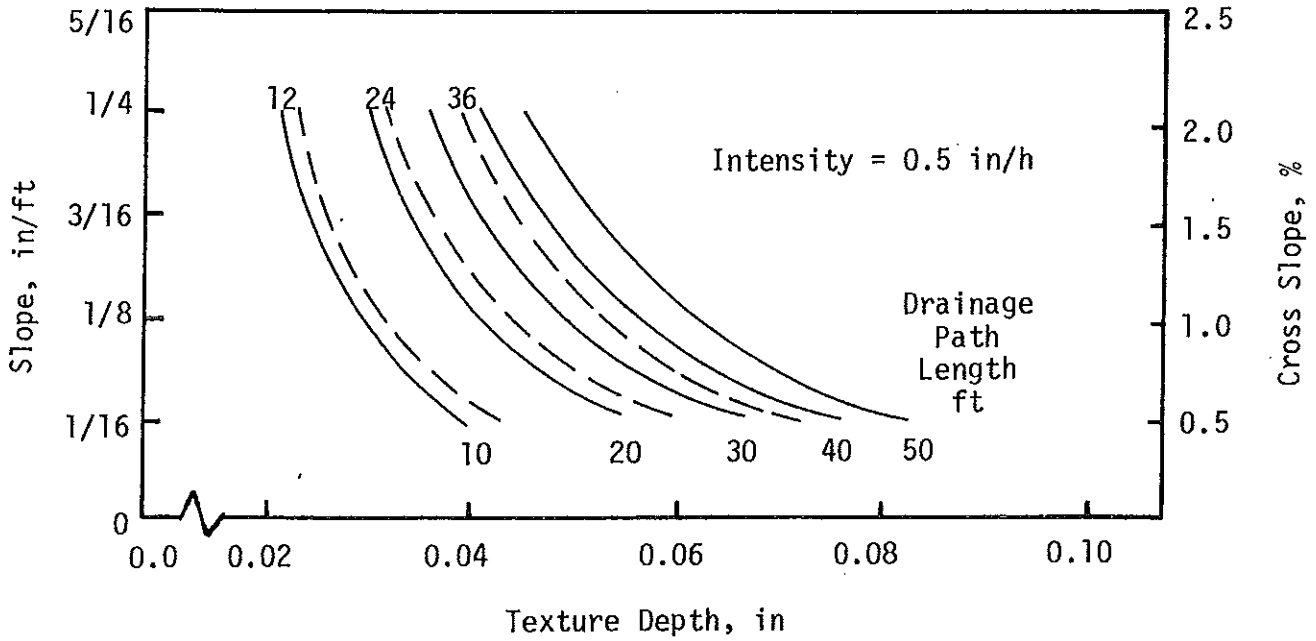

Figure 218. Curves of zero water depth for an intensity of 0.5 in/h

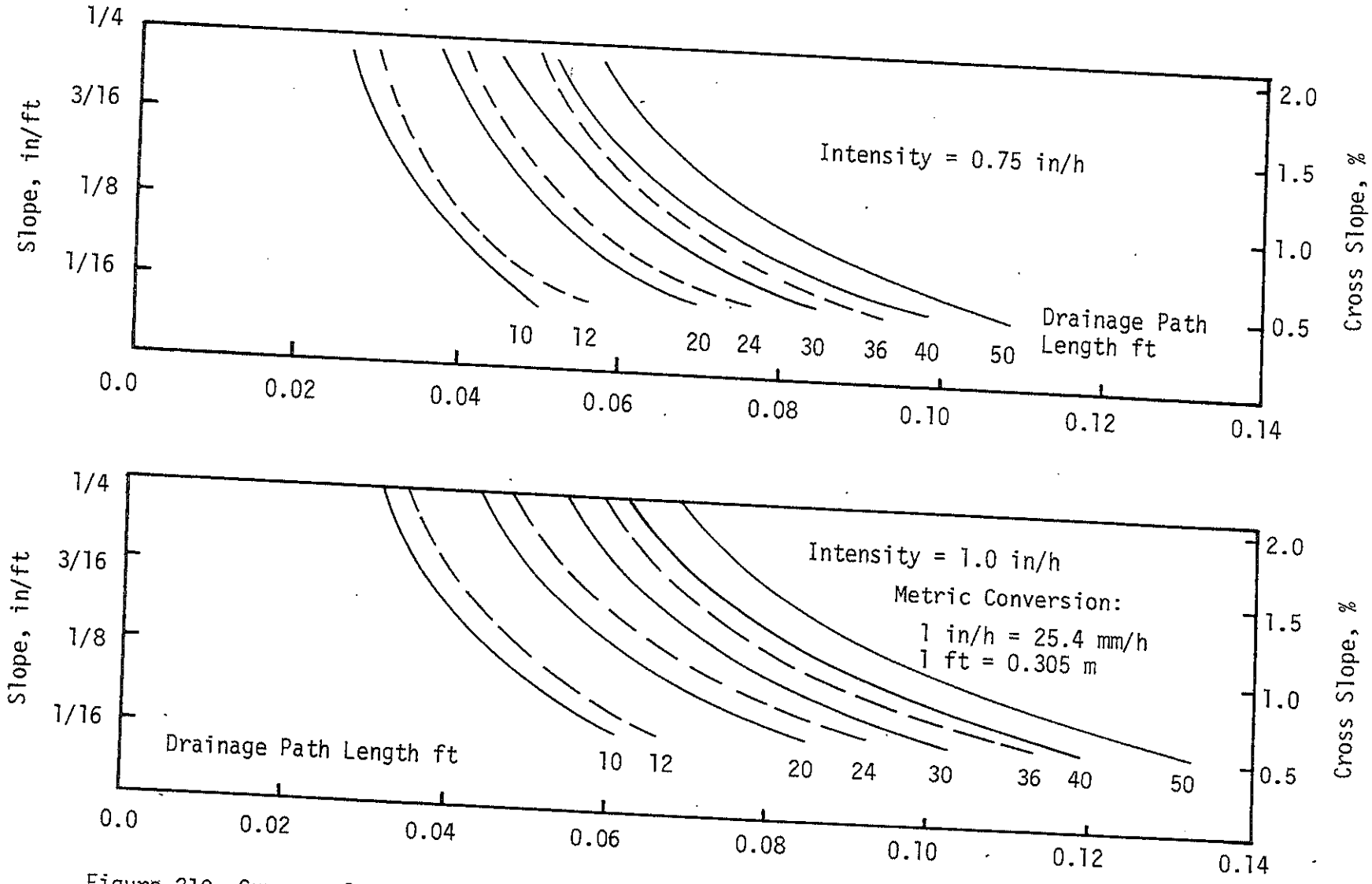

Figure 219. Curves of zero water depth for intensities of 0.75 and 1.0 in/h

When drainage path lengths are extended by significant longitudinal grade, it may not be practical to adhere to the zero water depth criteria. It is still practical through appropriate selection of cross slope and texture level to prevent water levels from exceeding 0.06 in (1.5 mm). This goal was explained in Chapter VII as a somewhat more practical goal which would not allow hydroplaning to occur over a significant length of highway except where extremely poor tire conditions are allowed by a driver. Criteria can be developed for any specified "design" rainfall from these curves or from the equations used to derive them. The following criteria can be stated for a "design" rainfall intensity of 0.5 in/h (13 mm/h).

1. Where longitudinal grades do not exceed 3 percent and drainage is not over three 12-foot lanes (36 ft or 11 m),

   a. Use values of cross slope not less than 1.5 percent.
   b. Use texture levels that will not fall below about 0.04 in (1.0 mm).

2. Where longitudinal grades are between 3 and 6 percent and drainage is not over three 12-foot lanes (36 ft or 11 m),

   a. Use values of cross slope not less than 2 percent.
   b. Use texture levels that will not fall below about 0.04 in (1 mm).

   or

   a. Use values of cross slope not less than 1.5 percent.
   b. Use texture levels that will not fall below 0.06 in (1.5 mm).

CHAPTER IX

SUMMARY AND CONCLUSIONS

The research findings of this study, relating to the pavement and geometric design criteria for minimizing hydroplaning of highway vehicles, are summarized in this chapter. Several variables such as vehicle speed, pavement surface texture, cross slope, water depth, tire inflation pressure, tread depth, etc., were thoroughly investigated using full-scale field tests. Traction tests under controlled conditions included portland cement concrete pavements of different surface textures and open-graded friction courses. The torque effect of freestanding puddles was measured by continuous recording of forces on the wheels of a specially instrumented full-scale trailer. Dangerous levels of torque were measured when freestanding puddles engaged only one side of the vehicle, thus presenting greater danger potential than puddles wide enough to engage both sides.

The primary method of investigating these variables was an instrumented two-wheel trailer. This trailer was designed to measure braking force and torque on one trailer tire and on the rotational velocity of the trailer test wheel. The freewheeling drag force is the hydrodynamic drag on an unbraked trailer tire as it moves over and through a layer of water on the road surface. The locked-wheel horizontal force is the drag force when the wheel is fully braked. Spindown and spinup refer to variations in the test wheel rotational speed compared to the rotational speed indicated by a reference fifth wheel. These force and velocity characteristics were used as indicators of hydroplaning.

Studies of a variety of pavement types and water conditions yielded fairly precise methods of predicting the occurrence of hydroplaning. In general, automobiles can hydroplane at speeds between 40 and 80 mph (64 and 129km/h) depending on specific conditions. Other observations are

1. Under the stated test conditions, the freewheeling drag force is approximately constant at 90 lbf (400 N), and is the same as the locked-wheel horizontal force above the apparent "full hydroplaning" speed of 46 mph (74 km/h). If asymmetrically distributed, this could cause unstabilizing yaw forces on a vehicle.

2. The freewheeling drag force is about 20 lbf (89 N) dry or with internal water, about 90 lbf (400 N) in 3/8 inch (9.5 mm) water and about 90 lbf (400 N) either locked or freewheeling above full hydroplaning speed.

3. Under all test conditions, the open-graded pavement provided as much, and usually more, traction than the asphalt slurry seal except at full hydroplaning where they were about equal. The open-graded surface has the added advantage of reducing the probability of positive water depths in the field.

4. With the externally applied water, the difference in traction between the two pavements was more dependent on test conditions

(water depth, tire pressure and tread depth) for the radial tire than for the ASTM E501 tire. That is, the ASTM tire produced a more consistent "ranking" of the pavements with various combinations of tire parameters and water depths.

5. Loss of contact can occur between 40 and 45 mph (64 and 72 km/h) in "puddles" of about 1 inch (25 mm) maximum depth and about 30 feet (9 m) in length. In addition, horizontal drag forces up to 300 lbf (1.3 kN) were observed. Three-eighths inch (9.5 mm) of water can produce about 90 lbf (400 N) of drag. If unevenly distributed laterally by pooling against a curb or raised shoulder on a cross slope, these forces could cause hazardous directional instability.

Pavement surface water depth is considered a most critical element for hydroplaning. As such, rainfall records of three selected states (Alabama, Illinois and Texas) were carefully examined to develop the methodology to arrive at the design rainfall intensity. Once the rainfall intensity is selected, water depth can be computed for given surface slope, runoff length and texture. Curves were also developed relating rainfall intensity, cross slope, drainage path length and texture depths so that the conditions disallowing surface accumulation of water could be determined. Curves of this type can be used to formulate allowable combinations of drainage parameters.

For given environmental conditions and pavement geometry, the water depth on the pavement surface becomes a function of the drainage capacity of the pavement. Since open-graded friction courses (OGFC) offer the best currently known method of assuring adequate and controlled surface macrotexture and some internal drainage (tests on cores indicated these surfaces are not as effective as originally hypothesized with respect to drainage), additional research was conducted under controlled conditions. The variables included speed, water depth, tire pressure, tread depth and tread design. Pavements having four values of internal voids (in the range of 15-25%) with essentially the same surface macrotexture of about 0.10 inch (2.5 mm) and all having the same open-graded overlay thickness of 1.0 inch (25 mm) were tested. Performance of these surfaces was thoroughly examined in simulated rain with intensities in the range of 0.2 to 2.0 in/h (5 to 51 mm/h). It was found that even the most open surface was flooded in the outside wheel path of the outside lane (of a two-lane facility) having 1% cross slope at rainfall intensities of 0.2 to 0.4 in/h (5 to 10 mm/h).

Specific conclusions relating to concrete highway surfaces have been drawn.

1. Water depth as a function of cross slope, texture depth and rainfall intensity can be reliably predicted for drainage lengths up to 48 feet (14.6 m), and probably considerably beyond. The direction of the texturing of portland cement concrete pavements does not significantly influence the resulting water depths.

2. Potentially hazardous positive water depths may exist for several minutes beyond the cessation of an appreciable

rainfall, and a wetted surface exists for many minutes beyond cessation of rainfall, particularly for dense surfaces. A predictive equation of the time a pavement will remain either with positive water depth or wet to any appreciable degree was developed.

3. Considering both skid number measurements and cornering slip measurements on wetted surfaces, transverse textures yield higher values than do longitudinal textures. Cornering slip tests determine the transverse or cornering force developed by a tire when the plane of the tire circumference makes an angle with the direction of movement, a slip angle. A cornering slip number (CS) is this lateral force divided by the normal force times one hundred. The logical recommendation would seem to be to require transverse textures for both tangent and horizontally curved sections of the roadway. It should be pointed out, however, that this research did not investigate the potentially hazardous maneuver of full dynamic hydroplaning of an automobile around a horizontal curve. Here the conditions are not approximated by either skid numbers or cornering slip numbers. Logic would strongly suggest that vehicle tracking could be very influential in keeping the vehicle in its respective lane. This tracking might best be obtained by providing longitudinal texturing, rather than transverse, throughout the horizontal curves. Certainly the dramatic decreases in accident rates documented in California (and elsewhere) after longitudinal grooving attests to the validity of this approach. What is not known is whether or not transverse grooving would have been as good as, worse or better than longitudinal grooving in terms of accident reduction.

   California DOT uses longitudinal grooves on horizontal curves. They report 90 to 95% reduction of spinout type of accidents. California has one installation of transverse grooves on horizontal curves and one installation with "diamond" grooves. Accident records on these sections are not conclusive at this time.

   Recently California DOT has applied transverse texturing to plastic concrete. Accident data on these installations are being collected but a conclusion at this time is premature.

   Skid number and cornering slip data clearly establish the validity of requiring transverse textures on tangent sections, but on horizontal curves the data are inconclusive.

4. Increasing texture depth provides the greatest increase in either SN or CS values. Thus deep textures should probably be constructed even though noise and tire wear increase. From a construction viewpoint, texture depths of 0.06 inch (1.5 mm) can be easily produced using tines spaced 1/4 inch (6 mm) clear distance. Initial texture depths of 0.06 inch

(1.5 mm) should be required, and the construction of texture depths below 0.05 inch (1.3 mm) should be discouraged.

5. The type of tire and tread depth significantly influence CS values. At elevated speeds and relatively high slip angles the wide oval tire developed the lowest CS values while the radial developed the highest. Shallow tread depths produced significantly lower CS values than did deeper tread depths.

Several conclusions defining performance characteristics of open-graded friction courses (OGFC) may be listed. These characteristics were determined primarily through the use of the two-wheel trailer described previously. Based on field observations as well as background information, brief summary statements regarding the interacting technical and economic factors can be stated.

1. Current OGFC mixture design procedures recommended by the Federal Highway Administration are entirely satisfactory. The inclusion of fine material in sufficient amounts that result in about 3% filler in the final mixture is a highly beneficial construction aid that permits a wider range in placement temperature.

2. For prolonged internal drainage, minimum compacted mat thickness should be about 1 inch (25.4 mm). This assumes high quality aggregates properly graded and correctly placed.

3. Open-graded mixtures offer one of the best known methods of controlling macrotexture. Large top size aggregate may be used without creating unacceptable noise levels, since the asperity peaks lie in essentially one plane and there are few percussion cups in the face of the surface mat.

4. As indicated by the hard data presented, OGFC will deliver relatively high levels of friction at legal, rural speed limits for the following conditions: (a) water depths up to 0.1 inch (2.5 mm), (b) tread depths equal to or above 0.2 inch (5 mm) and (c) tire inflation pressure at approximately 20 psi (138 kPa) or above.

5. Splash and spray are materially reduced in rainfalls ranging from about 0.2 to 0.5 in/h (5 to 13 mm/h). At lesser rainfall rates correctly designed and constructed, OGFC may be expected to present essentially completely drained surfaces with the associated performance characteristics. Sustained rainfall in excess of about 0.3 in/h (7.6 mm/h) was found to cause flooding of acceptable OGFC where the flow path exceeded about 12 feet (3.7 m); however, no serious problems were encountered in flow lengths up to 24 feet (7.3 m).

6. Sealing the outside edge of a 24-foot (7.3 m) pavement caused no significant problem with the skid performance of the surface investigated; however, long-time storage of water in the mat could cause substrate instability problems. Infiltrates may also collect with time.

7. Tires with minimum tread depth, especially the wide oval type, performed poorly at 55 mph (88 km/h) on those surfaces with water depths in excess of about 0.08 inch (2 mm), irrespective of macrotexture and internal drainage.

8. Although initial costs, maintenance costs and vehicle operating costs were not investigated in this study, these are factors that warrant consideration in a systematic friction improvement program.

Investigation of hydroplaning conditions of portland cement concrete pavement was conducted in two parts. The first part was to determine the validity of predicted water depth for drainage lengths to 48 ft (15 m) and the other was to examine skid resistance and cornering slip on textured surfaces. An equation was developed to determine the water depth from various parameters. It was also shown neither texture direction (longitudinal or transverse) nor texture type (brush, broom, burlap or tines) affected the resulting water depth to any significant degree. The water depths referred to are with respect to the tops of the pavement asperities. Thus a zero water depth would be just enough water to fill the texture but not reach a level above the top of the texture.

Some specific conclusions resulting from this work are

1. Water buildup on pavements up to 36 feet (11 m) wide will not be sufficient to induce hydroplaning for cross slopes of 2% or greater and rainfall intensities below 0.5 in/h (13 mm/h) for the assumed critical water depth of 0.06 inch (1.52 mm) or less.

2. Using the desirable design value of water depth of 0.0 inch (0 mm) results in critical drainage path lengths for all pavement widths when the pavement texture depth is less than 0.03 inch (0.8 mm). For texture depth of 0.04 inch (1.0 mm) or greater, no hydroplaning problem would be expected for two-lane pavements. Multilane pavements would have a tendency to flood at normally expected rainfall intensities.

3. The cross slope is more critical than texture depth when the critical water depth assumption is 0.06 inch (1.52 mm). With the 0.0 inch (0 mm) critical water depth assumption, texture depth is equally important in determining the critical length of the drainage path. A texture depth of 0.04 inch (1.0 mm) is recommended.

4. A minimum pavement cross slope of 1.5 % is admissible; however, 2% is recommended for most pavements.

5. The desirable design assumption suggests the combination of an open-graded surface course (or high texture surface) and an adequate pavement cross slope.

Sag-vertical curves offer areas of special consideration in any accident reduction program. Innovative concepts for improving wet-weather performance of sag-vertical curves are presented in the report which include special surface drainage devices to intercept and divert surface flow and open-graded friction courses to act as sub-surface drainage devices. Tentative sag-vertical curve drainage criteria based on a survey of existing practices are given in Table 12, and the recommendations for minimizing hydroplaning at sag-vertical curves are indicated in Tables 15 through 17.

Major findings relative to sag-vertical curves may be summarized as follows:

1. Of the innovative surface drainage systems considered, those featuring a permeable surface course or a high macrotexture surface course have the highest potential for reducing hydroplaning accidents.

2. Based on the observed flow rates through the open-graded mixture, the thickness required to accommodate drainage through the pavement for high intensity rainfalls is too great to be economically feasible.

3. Pavement cross slope is a dominant factor in removing water from the pavement surface. A minimum cross slope of 2% is recommended.

4. The most likely innovative surface drainage systems are those which involve using open-graded surface courses without a subdrain system.

5. Surface drains located parallel to the lane lines will probably not solve the drainage problem due to the wheel path depressions.

6. Transverse surface drains located on the pavement surface would probably result in a rough pavement, increase maintenance costs, and increase potential for ponding water. For these reasons, such systems are not recommended for general use.

When drainage path lengths are extended by significant longitudinal grade it may not be practical to adhere to the zero water depth criteria. It is still practical through appropriate selection of cross slope and texture level to prevent water levels from exceeding 0.06 inch (1.5 mm). This goal was explained in Chapter VII as a somewhat more practical goal which would not allow hydroplaning to occur over a significant length of highway except where extremely poor tire conditions are allowed by a driver. Criteria can be developed for any specified "design" rainfall from these curves or from the equations used to derive them. The following criteria can be stated for a "design" rainfall intensity of 0.5 in/h (13 mm/h).

1. Where longitudinal grades do not exceed 3% and drainage is not over three 12-foot lanes (36 ft or 11 m),

   a. Use values of cross slope not less than 1.5%.

b. Use texture levels that will not fall below about 0.04 inch (1.0 mm).

2. Where longitudinal grades are between 3 and 6% and drainage is not over three 12-foot lanes (36 ft or 11 m),

   a. Use values of cross slope not less than 2%.

   b. Use texture levels that will not fall below about 0.04 inch (1.0 mm).

   or

   a. Use values of cross slope not less than 1.5%.

   b. Use texture levels that will not fall below 0.06 inch (1.5 mm).

Through use of the equations, curves and examples given in this report, a state or agency should be capable of formulating an antihydroplaning road surface design policy, a policy as conservative or as liberal as the particular entity prefers. Even without specific design policies related directly to hydroplaning, states appear to be making significant progress in achieving this goal. The precepts presented here do not require impractical goals, although these goals obviously cannot be achieved in a short period of time due to the vast area of highway surfaces in this country. However, by establishing specific design goals and working toward them continuously, the time will come when surfaces that allow hydroplaning, except in extreme rainfall or in the case of extremely substandard tire use, will no longer exist.

The implementation of these recommendations will require judgment and dedication in the execution of master maintenance and reconstruction plans over a period of years. The work presented in this study has been devoted to the future realization of this goal.

REFERENCES

1. Horne, Walter B., "Tire Hydroplaning and Its Effects on Tire Traction", HRR No. 214, 1968, Washington, D.C., pp. 24-33.

2. Browne, Alan L., "A Mathematical Analysis for Pneumatic Tire Hydroplaning", General Motors, Inc., Warren, Michigan.

3. Yeager, R. W., "Tire Hydroplaning: Testing, Analysis and Design", Physics of Tire Traction, edited by D. F. Hays and A. L. Browne, Plenum Press, 1974, pp. 25-63.

4. Gengenbach, Werner, "The Effect of Wet Pavement on the Performance of Automobile Tires", Universität Karlsruhe, Deutschland (translated for limited distribution by CALSPAN, Buffalo, New York, July 1967).

5. Horne, W. B. and Joyner, U. T., "Pneumatic Tire Hydroplaning and Some Effects on Vehicle Performance", SAE International Automotive Engineering Congress, Detroit, Michigan, January 1965.

6. Horne, W. B. and Dreher, R. C., "Phenomena of Pneumatic Tire Hydroplaning", NASA Technical Note TN D-2056, Washington, D.C., November 1963.

7. Stocker, A. J., Dotson, J. T., and Ivey, D. L., "Automobile Tire Hydroplaning -- A Study of Wheel Spin-Down and Other Variables", Research Report No. 147-3F, Texas Transportation Institute, August 1974, PB 239 782/AS*.

8. Kummer, H. W. and Meyer, W. E., "Tentative Skid-Resistance Requirements for Main Rural Highways", NCHRP Report 37, Highway Research Board, Washington, D.C., 1967.

9. Gallaway, B. M., Ivey, D. L., Ross, H. E. Jr., Ledbetter, W. B., Woods, D. L., and Schiller, R. E. Jr., "Tentative Pavement and Geometric Design Criteria for Minimizing Hydroplaning", Phase I Final Report, Report No. FHWA-RD-75-11, February 1975, PB 255 748/AS.

10. Farnsworth, E. E. and Johnson, M. H., "Reduction of Wet Pavement Accidents on Los Angeles Metropolitan Freeways", California Division of Highways, June 1971, Sacramento, California, 20 pages.

11. Gallaway, Bob M., Schiller, Robert, and Rose, Jerry G., "The Effects of Rainfall Intensity, Pavement Cross Slope, Surface Texture, and Drainage Length on Pavement Water Depths", Research Report 138-5, Texas Transportation Institute, College Station, Texas.

12. Horne, W. B., "Runway Drainage Analysis", An unpublished memorandum transmitted to D. L. Ivey in 1975.

---

*NTIS accession number. Available from the National Technical Information Service, Springfield, Virginia 22161.

13. Ivey, D. L. and Lehtipuu, Eero K., "Rainfall and Visibility - The View from Behind the Wheel", Research Report 135-3, Texas Transportation Institute, August 1974, PB 241 241/AS.

14. Burns, J. C. and Peters, R. J., "Surface Friction Study of Arizona Highways", HPR-1-9 (162), Arizona Department of Transportation, Materials Services, Research Branch, Phoenix, Arizona, August 1972.

15. Ivey, D. L., et al., "Development of a Wet Weather Safety Index", Texas Transportation Institute, Report 221-1F, 1977.

16. Stocker, A. J. and Gregory, R. T., "Construction of a Facility to Study Variables Associated with Hydroplaning", Texas Transportation Institute, Study No. 2-8-70-147, HPR-1(9), Texas A&M University, College Station, Texas, March 1971.

17. Ledbetter, W. B., Meyer, A. H., and Ballard, D. E., "Evaluation of Full Scale Experimental Concrete Highway Finishes", Research Report 141-4F, Texas Transportation Institute, September 1974.

18. Moe, James A., "A Study of the Effects of Grooving on Motor Vehicle Accidents", Report No. CA-TL-78-19, California Department of Transportation, June 1978.

19. Goodwin, W. A., "Skid Resistance - An Historical Perspective", Asphalt Paving Technology, Minneapolis, Minn., Vol. 42, p. 352, 1973.

20. Nakkel, E., "Corrective Measures for Slipperiness - European View", Asphalt Paving Technology, Vol. 42, p. 366, 1973.

21. Gallaway, B. M., "A Review of Current Methods and Mechanisms for Producing Skid Resistant Pavements", Asphalt Paving Technology, Vol. 42, p. 401, 1973.

22. Huschek, S., "Interrelation Between Skid Resistance, Road Surface Texture and Water Film", International Symposium on Porous Asphalt, Proceedings, Study Centre for Roadconstruction, Arnham, The Netherlands, p. 9, 1977.

23. Welleman, T., "Porous Asphalt Against Water Nuisance", International Symposium on Porous Asphalt, Proceedings, Study Centre for Roadconstruction, Arnham, The Netherlands, p. 16, 1977.

24. Szatkowski, W. S. and Brown, J. R., "The Design and Performance of Pervious Surfacings for Roads in Britain, 1967-76", International Symposium on Porous Asphalt, Proceedings, Study Centre for Roadconstruction, Arnham, The Netherlands, p. 30, 1977.

25. Hutson, R. M., "Development of Open Textured Bitumen Macadam Friction Course for Airports in Great Britain", International Symposium on Porous Asphalt, Proceedings, Study Centre for Roadconstruction, Arnham, The Netherlands, p. 41, 1977.

26. Plancher, H., Dorrence, S. M., and Petersen, J. C., "Identification of Chemical Types in Asphalt Strongly Absorbed at the Asphalt-Aggregate Interface and Their Relative Displacement by Water", AAPT, Vol. 46, 1977.

27. Liddle, W. J., Petersen, D. E., and Wiley, M. L., "Use of Hydrated Lime in Bituminous Mixtures to Decrease Hardening of the Asphalt Cement", Final Report, Utah State Highway Department, Materials and Tests Division, Salt Lake City, December, 1971, PB 213 170.

28. Plancher, H., Green, E. L., and Petersen, J. C., "Reduction of Oxidative Hardening of Asphalts by Treatment with Hydrated Lime -- A Mechanistic Study", AAPT, Vol. 45, 1976.

29. Gallaway, B. M. and Epps, J. A., "Mixture Design Concepts, Laboratory Tests and Construction Guides for Open Graded Bituminous Overlays", Research Report 36-1F, 131 pages, Texas Transportation Institute, College Station, Texas, 1974.

30. Smith, R. W., "Examination of Factors Related to the Development and Performance of Open-Graded Asphalt Friction Course", International Symposium on Porous Asphalt, Proceedings, Study Centre for Roadconstruction, Arnham, The Netherlands, p. 91, 1977.

31. White, T. D., "Construction and Evaluation of Airfield PFC in the United States", International Symposium on Porous Asphalt, Proceedings, Study Centre for Roadconstruction, Arnham, The Netherlands, p. 136, 1977.

32. Smith, R. W., Rice, J. M., and Spelman, S. R., "Design of Open-Graded Asphalt Friction Courses", FHWA-RD-74-2, Interim Report, January 1974, PB 227 479/AS.

33. Nystrup, P., "Drainage Surfaces", International Symposium on Porous Asphalt, Proceedings, Study Centre for Roadconstruction, Arnham, The Netherlands, p. 161, 1977.

34. Gerardu, J. J. A., "Construction and Evaluation of the Porous Asphalt Experimental Sections", International Symposium on Porous Asphalt, Proceedings, Study Centre for Roadconstruction, Arnham, The Netherlands, p. 184, 1977.

35. Hatherly, L. W. and Lamb, D. R., "Friction Course Trials with Modified Binders", International Symposium on Porous Asphalt, Proceedings, Study Centre for Roadconstruction, Arnham, The Netherlands, p. 193, 1977.

36. Beaton, J. L., "Providing Skid Resistant Pavements", TRB Transportation Research Record 622, p. 39, 1976.

37. Smith, H. A., "Pavement Contributions to Wet-Weather Skidding Accident Reduction," TRB Transportation Research Record 622, p. 51, 1976.

38. Gramling, W. L., "Development and Implementation of a Program to Reduce Skid Accident", TRB Transportation Research Record 622, p. 85, 1976.

39. Hatherly, L. W. and Young, A. E., "The Location and Treatment of Urban Skidding Hazard Sites", TRB Transportation Research Record 623, p. 21, 1976.

40. Halstead, W. J., NCHRP Synthesis 49, "Open-Graded Friction Courses for Highways", Transportation Research Board, National Research Council, Washington, D.C., 1978.

41. Gallaway, Bob M. and Rose, Jerry G., "Macro-Texture, Friction, Cross Slope and Wheel Track Depression Measurements on 41 Typical Texas Highway Pavements", Research Report 138-2, Texas Transportation Institute, June 1970.

42. Epps, J. A. and Button, J. W., "Mirafi Fabric Tack Coat Requirements", Report RF 3424-1, Texas Transportation Institute, p. 6, July 1977.

43. Browne, A. L., "Tire Deformation during Dynamic Hydroplaning", A Report of the General Motors Corporation Research Laboratories, Warren, Michigan, Report No. GMR-1701, September 1974.

44. Moynahan, Thomas J. and Sternberg, Yaron M., "An Investigation of the Vertical and Horizontal Hydraulic Conductivities of Dense Graded Base Course Aggregate", A Report of the Civil Engineering Department, University of Maryland, College Park, Maryland, p. 57, July 1974, p. 57.

APPENDIX A

Table 32. Cornering Slip Data

TS	WS	TT	P	TD	TXD	TXDN	SA	CS	V	WD	I	S
F1	NAT	ASTM	24	1132	.027	TRAN	4	58	40		0.23	.29
F1	NAT	ASTM	24	1132	.027	TRAN	4	49	40		0.00	.29
F1	NAT	ASTM	24	1132	.027	TRAN	8	71	40		0.00	.29
F1	NAT	ASTM	24	1132	.027	TRAN	8	76	40		0.21	.29
F1	NAT	ASTM	24	1132	.027	TRAN	16	84	40		0.17	.29
F1	NAT	ASTM	24	1132	.027	TRAN	16	75	40		1.64	.29
F1	NAT	ASTM	24	1132	.027	TRAN	16	79	40		0.00	.29
F1	NAT	ASTM	24	1132	.027	TRAN	16	82	40		0.53	.29
F1	NAT	ASTM	24	1132	.027	TRAN	4	47	55		0.74	.29
F1	NAT	ASTM	24	1132	.027	TRAN	4	58	55		0.05	.29
F1	NAT	ASTM	24	1132	.027	TRAN	4	56	55		0.23	.29
F1	NAT	ASTM	24	1132	.027	TRAN	8	67	55		0.00	.29
F1	NAT	ASTM	24	1132	.027	TRAN	8	74	55		0.30	.29
F1	NAT	ASTM	24	1132	.027	TRAN	16	69	55		0.00	.29
F1	NAT	ASTM	24	1132	.027	TRAN	16	70	55		0.27	.29
F1	NAT	ASTM	24	1132	.027	TRAN	16	74	55		0.76	.29
F2	NAT	ASTM	24	1132	.034	TRAN	16	75	55		0.30	.29
F2	NAT	ASTM	24	1132	.034	TRAN	4	60	40		0.00	.20
F2	NAT	ASTM	24	1132	.034	TRAN	4	59	40		0.23	.20
F2	NAT	ASTM	24	1132	.034	TRAN	8	74	40		0.00	.20
F2	NAT	ASTM	24	1132	.034	TRAN	8	76	40		0.21	.20
F2	NAT	ASTM	24	1132	.034	TRAN	16	83	40		0.00	.20
F2	NAT	ASTM	24	1132	.034	TRAN	16	83	40		0.53	.20
F2	NAT	ASTM	24	1132	.034	TRAN	16	80	40		0.51	.20
F2	NAT	ASTM	24	1132	.034	TRAN	16	77	40		1.64	.20
F2	NAT	ASTM	24	1132	.034	TRAN	16	86	40		0.17	.20
F2	NAT	ASTM	24	1132	.034	TRAN	4	59	55		0.05	.20
F2	NAT	ASTM	24	1132	.034	TRAN	4	50	55		0.74	.20
F2	NAT	ASTM	24	1132	.034	TRAN	4	57	55		0.23	.20
F2	NAT	ASTM	24	1132	.034	TRAN	8	74	55		0.00	.20
F2	NAT	ASTM	24	1132	.034	TRAN	8	75	55		0.30	.20
F2	NAT	ASTM	24	1132	.034	TRAN	16	79	55		0.76	.20
F2	NAT	ASTM	24	1132	.034	TRAN	16	70	55		0.00	.20
F2	NAT	ASTM	24	1132	.034	TRAN	16	81	55		0.27	.20
F3	NAT	ASTM	24	1132	.029	LONG	16	81	55		0.30	.20
F3	NAT	ASTM	24	1132	.029	LONG	4	50	40		0.00	.22
F3	NAT	ASTM	24	1132	.029	LONG	4	58	40		0.23	.22
F3	NAT	ASTM	24	1132	.029	LONG	8	69	40		0.00	.22
F3	NAT	ASTM	24	1132	.029	LONG	8	78	40		0.21	.22
F3	NAT	ASTM	24	1132	.029	LONG	16	78	40		0.00	.22
F3	NAT	ASTM	24	1132	.029	LONG	16	72	40		0.51	.22
F3	NAT	ASTM	24	1132	.029	LONG	16	68	40		1.64	.22
F3	NAT	ASTM	24	1132	.029	LONG	16	85	40		0.53	.22
F3	NAT	ASTM	24	1132	.029	LONG	16	84	40		0.17	.22
F3	NAT	ASTM	24	1132	.029	LONG	4	47	55		0.74	.22
F3	NAT	ASTM	24	1132	.029	LONG	4	59	55		0.05	.22
F3	NAT	ASTM	24	1132	.029	LONG	8	56	55		0.23	.22
F3	NAT	ASTM	24	1132	.029	LONG	8	62	55		0.00	.22
F3	NAT	ASTM	24	1132	.029	LONG	8	74	55		0.30	.22
F3	NAT	ASTM	24	1132	.029	LONG	16	64	55		0.00	.22
F3	NAT	ASTM	24	1132	.029	LONG	16	47	55		0.27	.22
F3	NAT	ASTM	24	1132	.029	LONG	16	70	55		0.76	.22
F4	NAT	ASTM	24	1132	.056	LONG	16	75	55		0.30	.22
F4	NAT	ASTM	24	1132	.056	LONG	4	52	40		0.00	.22
							4	61	40		0.23	.22

Table 32. Cornering Slip Data (Cont.)

TS	WS	TT	P	TD	TXD	TXDN	SA	CS	V	WD	I	S
[illegible]	NAT	ASTM	24	1132	.056	LONG	8	71	40		0.00	.22
[illegible]	NAT	ASTM	24	1132	.056	LONG	8	82	40		0.00	.22
[illegible]	NAT	ASTM	24	1132	.056	LONG	8	85	40		0.21	.22
[illegible]	NAT	ASTM	24	1132	.056	LONG	16	91	40		0.00	.22
[illegible]	NAT	ASTM	24	1132	.056	LONG	16	96	40		0.53	.22
[illegible]	NAT	ASTM	24	1132	.056	LONG	16	89	40		1.64	.22
[illegible]	NAT	ASTM	24	1132	.056	LONG	16	96	40		0.51	.22
[illegible]	NAT	ASTM	24	1132	.056	LONG	16	96	40		0.53	.22
[illegible]	NAT	ASTM	24	1132	.056	LONG	16	92	40		0.17	.22
[illegible]	NAT	ASTM	24	1132	.056	LONG	4	63	55		0.05	.22
[illegible]	NAT	ASTM	24	1132	.056	LONG	4	48	55		0.74	.22
[illegible]	NAT	ASTM	24	1132	.056	LONG	4	62	55		0.05	.22
[illegible]	NAT	ASTM	24	1132	.056	LONG	4	62	55		0.23	.22
[illegible]	NAT	ASTM	24	1132	.056	LONG	8	75	55		0.00	.22
[illegible]	NAT	ASTM	24	1132	.056	LONG	8	83	55		0.30	.22
[illegible]	NAT	ASTM	24	1132	.056	LONG	16	89	55		0.00	.22
[illegible]	NAT	ASTM	24	1132	.056	LONG	16	60	55		0.27	.22
[illegible]	NAT	ASTM	24	1132	.056	LONG	16	82	55		0.76	.22
[illegible]	NAT	ASTM	24	1132	.056	LONG	16	92	55		0.30	.22
[illegible]	NAT	ASTM	24	1132	.064	LONG	4	53	40		0.00	.22
[illegible]	NAT	ASTM	24	1132	.064	LONG	4	61	40		0.23	.22
[illegible]	NAT	ASTM	24	1132	.064	LONG	8	78	40		0.00	.22
[illegible]	NAT	ASTM	24	1132	.064	LONG	8	86	40		0.21	.22
[illegible]	NAT	ASTM	24	1132	.064	LONG	16	84	40		0.51	.22
[illegible]	NAT	ASTM	24	1132	.064	LONG	16	80	40		1.64	.22
[illegible]	NAT	ASTM	24	1132	.064	LONG	16	94	40		0.00	.22
[illegible]	NAT	ASTM	24	1132	.064	LONG	16	95	40		0.17	.22
[illegible]	NAT	ASTM	24	1132	.064	LONG	4	48	55		0.74	.22
[illegible]	NAT	ASTM	24	1132	.064	LONG	4	62	55		0.23	.22
[illegible]	NAT	ASTM	24	1132	.064	LONG	8	75	55		0.00	.22
[illegible]	NAT	ASTM	24	1132	.064	LONG	8	82	55		0.30	.22
[illegible]	NAT	ASTM	24	1132	.064	LONG	16	93	55		0.00	.22
[illegible]	NAT	ASTM	24	1132	.064	LONG	16	60	55		0.27	.22
[illegible]	NAT	ASTM	24	1132	.064	LONG	16	87	55		0.76	.22
[illegible]	NAT	ASTM	24	1132	.064	LONG	16	91	55		0.30	.22
[illegible]	NAT	ASTM	24	1132	.027	LONG	4	49	40		0.00	.22
[illegible]	NAT	ASTM	24	1132	.027	LONG	4	60	40		0.23	.22
[illegible]	NAT	ASTM	24	1132	.027	LONG	8	68	40		0.00	.22
[illegible]	NAT	ASTM	24	1132	.027	LONG	8	74	40		0.21	.22
[illegible]	NAT	ASTM	24	1132	.027	LONG	16	79	40		0.53	.22
[illegible]	NAT	ASTM	24	1132	.027	LONG	16	67	40		1.64	.22
[illegible]	NAT	ASTM	24	1132	.027	LONG	16	68	40		0.51	.22
[illegible]	NAT	ASTM	24	1132	.027	LONG	16	80	40		0.00	.22
[illegible]	NAT	ASTM	24	1132	.027	LONG	16	81	40		0.17	.22
[illegible]	NAT	ASTM	24	1132	.027	LONG	4	57	55		0.05	.22
[illegible]	NAT	ASTM	24	1132	.027	LONG	4	47	55		0.74	.22
[illegible]	NAT	ASTM	24	1132	.027	LONG	4	56	55		0.23	.22
[illegible]	NAT	ASTM	24	1132	.027	LONG	8	67	55		0.00	.22
[illegible]	NAT	ASTM	24	1132	.027	LONG	8	71	55		0.30	.22
[illegible]	NAT	ASTM	24	1132	.027	LONG	16	71	55		0.76	.22
[illegible]	NAT	ASTM	24	1132	.027	LONG	16	67	55		0.27	.22
[illegible]	NAT	ASTM	24	1132	.027	LONG	16	69	55		0.00	.22
[illegible]	NAT	ASTM	24	1132	.027	LONG	16	59	55		0.30	.22
[illegible]	NAT	ASTM	24	1132	.031	TRAN	4	50	40		0.00	.22
[illegible]	NAT	ASTM	24	1132	.031	TRAN	4	60	40		0.23	.22

Reproduced from best available copy.

Reproduced from best available copy.

Table 32. Cornering Slip Data (Cont.)

TS	WS	TT	D	TD	TXD	TXDN	SA	CS	V	WD	I	S
7	NAT	ASTM	26	1132	.031	TRAN	8	71	40		0.00	.22
7	NAT	ASTM	26	1132	.031	TRAN	8	75	40		0.21	.22
7	NAT	ASTM	24	1132	.031	TRAN	16	73	40		1.64	.22
7	NAT	ASTM	24	1132	.031	TRAN	16	78	40		0.51	.22
7	NAT	ASTM	24	1132	.031	TRAN	16	80	40		0.00	.22
7	NAT	ASTM	24	1132	.031	TRAN	16	85	40		0.17	.22
7	NAT	ASTM	24	1132	.031	TRAN	16	80	40		0.53	.22
7	NAT	ASTM	24	1132	.031	TRAN	4	48	55		0.74	.22
7	NAT	ASTM	24	1132	.031	TRAN	4	56	55		0.23	.22
7	NAT	ASTM	24	1132	.031	TRAN	4	58	55		0.05	.22
7	NAT	ASTM	26	1132	.031	TRAN	8	70	55		0.00	.22
7	NAT	ASTM	24	1132	.031	TRAN	8	73	55		0.30	.22
7	NAT	ASTM	24	1132	.031	TRAN	16	74	55		0.27	.22
7	NAT	ASTM	24	1132	.031	TRAN	16	69	55		0.00	.22
7	NAT	ASTM	24	1132	.031	TRAN	16	78	55		0.30	.22
7	NAT	ASTM	24	1132	.031	TRAN	16	72	55		0.76	.22
1	TRK	BELT	26	232	.027	TRAN	4	56	40	0		.29
1	TRK	BELT	18	232	.027	TRAN	4	55	40	0		.29
1	TRK	OVAL	24	232	.027	TRAN	4	63	40	0		.29
1	TRK	OVAL	32	232	.027	TRAN	4	50	40	0		.29
1	TRK	ASTM	24	232	.027	TRAN	4	57	40	0		.29
1	TRK	ASTM	32	232	.027	TRAN	4	56	40	0		.29
1	TRK	ASTM	18	232	.027	TRAN	4	44	40	0		.29
1	TRK	RADL	24	232	.027	TRAN	4	49	40	0		.29
1	TRK	RADL	18	232	.027	TRAN	4	44	40	0		.29
1	TRK	BELT	24	232	.027	TRAN	8	72	40	0		.29
1	TRK	BELT	18	232	.027	TRAN	8	73	40	0		.29
1	TRK	OVAL	24	232	.027	TRAN	8	69	40	0		.29
1	TRK	OVAL	32	232	.027	TRAN	8	67	40	0		.29
1	TRK	ASTM	24	232	.027	TRAN	8	68	40	0		.29
1	TRK	ASTM	32	232	.027	TRAN	8	61	40	0		.29
1	TRK	ASTM	18	232	.027	TRAN	8	58	40	0		.29
1	TRK	RADL	24	232	.027	TRAN	8	79	40	0		.29
1	TRK	RADL	18	232	.027	TRAN	8	72	40	0		.29
1	TRK	BELT	24	232	.027	TRAN	16	73	40	0		.29
1	TRK	BELT	18	232	.027	TRAN	16	80	40	0		.29
1	TRK	OVAL	24	232	.027	TRAN	16	67	40	0		.29
1	TRK	OVAL	32	232	.027	TRAN	16	63	40	0		.29
1	TRK	ASTM	24	232	.027	TRAN	16	76	40	0		.29
1	TRK	ASTM	32	232	.027	TRAN	16	73	40	0		.29
1	TRK	ASTM	18	232	.027	TRAN	16	73	40	0		.29
1	TRK	RADL	24	232	.027	TRAN	16	75	40	0		.29
1	TRK	RADL	18	232	.027	TRAN	16	76	40	0		.29
1	TRK	ASTM	18	232	.027	TRAN	4	52	55	0		.29
1	TRK	BELT	18	232	.027	TRAN	4	52	55	0		.29
1	TRK	RADL	18	232	.027	TRAN	4	52	55	0		.29
1	TRK	OVAL	32	232	.027	TRAN	4	61	55	0		.29
1	TRK	ASTM	32	232	.027	TRAN	4	63	55	0		.29
1	TRK	BELT	24	232	.027	TRAN	4	59	55	0		.29
1	TRK	ASTM	24	232	.027	TRAN	4	51	55	0		.29
1	TRK	RADL	24	232	.027	TRAN	4	52	55	0		.29
1	TRK	OVAL	24	232	.027	TRAN	4	59	55	0		.29
1	TRK	ASTM	18	232	.027	TRAN	8	67	55	0		.29
1	TRK	BELT	18	232	.027	TRAN	8	70	55	0		.29
1	TRK	RADL	18	232	.027	TRAN	8	69	55	0		.29

Table 32. Cornering Slip ... a (Cont.)

TS	WS	TT	P	TD	TXD	TXDN	SA	CS	V	WD	I	S
[illegible]	[illegible]RK	OVAL	32	232	.027	TRAN	8	56	55	0		.29
[illegible]	TRK	ASTM	32	232	.027	TRAN	8	57	55	0		.29
[illegible]	TRK	BELT	24	232	.027	TRAN	8	71	55	0		.29
[illegible]	TRK	ASTM	24	232	.027	TRAN	8	53	55	0		.29
[illegible]	TRK	RADL	24	232	.027	TRAN	8	51	55	0		.29
[illegible]	TRK	OVAL	24	232	.027	TRAN	8	69	55	0		.29
[illegible]	TRK	ASTM	18	232	.027	TRAN	16	59	55	0		.29
[illegible]	TRK	BELT	18	232	.027	TRAN	16	77	55	0		.29
[illegible]	TRK	RADL	18	232	.027	TRAN	16	66	55	0		.29
[illegible]	TRK	OVAL	32	232	.027	TRAN	16	63	55	0		.29
[illegible]	TRK	ASTM	32	232	.027	TRAN	16	63	55	0		.29
[illegible]	TRK	BELT	24	232	.027	TRAN	16	70	55	0		.29
[illegible]	TRK	ASTM	24	232	.027	TRAN	16	61	55	0		.29
[illegible]	TRK	RADL	24	232	.027	TRAN	16	64	55	0		.29
[illegible]	TRK	OVAL	24	232	.027	TRAN	16	66	55	0		.29
[illegible]	TRK	BELT	24	232	.034	TRAN	4	60	40	0		.20
[illegible]	TRK	BELT	18	232	.034	TRAN	4	59	40	0		.20
[illegible]	TRK	OVAL	32	232	.034	TRAN	4	71	40	0		.20
[illegible]	TRK	OVAL	24	232	.034	TRAN	4	66	40	0		.20
[illegible]	TRK	ASTM	32	232	.034	TRAN	4	65	40	0		.20
[illegible]	TRK	ASTM	24	232	.034	TRAN	4	63	40	0		.20
[illegible]	TRK	ASTM	18	232	.034	TRAN	4	58	40	0		.20
[illegible]	TRK	RADL	24	232	.034	TRAN	4	57	40	0		.20
[illegible]	TRK	RADL	18	232	.034	TRAN	4	44	40	0		.20
[illegible]	TRK	BELT	24	232	.034	TRAN	8	77	40	0		.20
[illegible]	TRK	BELT	18	232	.034	TRAN	8	76	40	0		.20
[illegible]	TRK	OVAL	32	232	.034	TRAN	8	73	40	0		.20
[illegible]	TRK	OVAL	24	232	.034	TRAN	8	73	40	0		.20
[illegible]	TRK	ASTM	32	232	.034	TRAN	8	78	40	0		.20
[illegible]	TRK	ASTM	24	232	.034	TRAN	8	90	40	0		.20
[illegible]	TRK	ASTM	18	232	.034	TRAN	8	78	40	0		.20
[illegible]	TRK	RADL	24	232	.034	TRAN	8	83	40	0		.20
[illegible]	TRK	RADL	18	232	.034	TRAN	8	76	40	0		.20
[illegible]	TRK	BELT	24	232	.034	TRAN	16	80	40	0		.20
[illegible]	TRK	BELT	18	232	.034	TRAN	16	87	40	0		.20
[illegible]	TRK	OVAL	32	232	.034	TRAN	16	75	40	0		.20
[illegible]	TRK	OVAL	24	232	.034	TRAN	16	76	40	0		.20
[illegible]	TRK	ASTM	32	232	.034	TRAN	16	75	40	0		.20
[illegible]	TRK	ASTM	24	232	.034	TRAN	16	86	40	0		.20
[illegible]	TRK	ASTM	16	232	.034	TRAN	16	82	40	0		.20
[illegible]	TRK	RADL	24	232	.034	TRAN	16	83	40	0		.20
[illegible]	TRK	RADL	18	232	.034	TRAN	16	80	40	0		.20
[illegible]	TRK	ASTM	18	232	.034	TRAN	4	55	55	0		.20
[illegible]	TRK	RADL	18	232	.034	TRAN	4	55	55	0		.20
[illegible]	TRK	BELT	18	232	.034	TRAN	4	54	55	0		.20
[illegible]	TRK	BELT	24	232	.034	TRAN	4	65	55	0		.20
[illegible]	TRK	ASTM	24	232	.034	TRAN	4	60	55	0		.20
[illegible]	TRK	OVAL	24	232	.034	TRAN	4	65	55	0		.20
[illegible]	TRK	RADL	24	232	.034	TRAN	4	55	55	0		.20
[illegible]	TRK	ASTM	32	232	.034	TRAN	4	65	55	0		.20
[illegible]	TRK	OVAL	32	232	.034	TRAN	4	68	55	0		.20
[illegible]	TRK	ASTM	18	232	.034	TRAN	8	71	55	0		.20
[illegible]	TRK	RADL	18	232	.034	TRAN	8	72	55	0		.20
[illegible]	TRK	BELT	18	232	.034	TRAN	8	76	55	0		.20
[illegible]	TRK	BELT	24	232	.034	TRAN	8	79	55	0		.20

Reproduced from best available copy.

Reproduced from best available copy.

Table 32. Cornering Slip Data (Cont.)

TS	WS	TT	P	TD	TXD	TXDN	SA	CS	V	WD	I	S
F2	TRK	ASTM	24	232	.034	TRAN	8	71	55	0		.20
F2	TRK	OVAL	24	232	.034	TRAN	8	77	55	0		.20
F2	TRK	RADL	24	232	.034	TRAN	8	72	55	0		.20
F2	TRK	ASTM	32	232	.034	TRAN	8	69	55	0		.20
F2	TRK	OVAL	32	232	.034	TRAN	8	61	55	0		.20
F2	TRK	ASTM	18	232	.034	TRAN	16	67	55	0		.20
F2	TRK	RADL	18	232	.034	TRAN	16	71	55	0		.20
F2	TRK	BFLT	18	232	.034	TRAN	16	86	55	0		.20
F2	TRK	BELT	24	232	.034	TRAN	16	80	55	0		.20
F2	TRK	ASTM	24	232	.034	TRAN	16	75	55	0		.20
F2	TRK	OVAL	24	232	.034	TRAN	16	79	55	0		.20
F2	TRK	RADL	24	232	.034	TRAN	16	78	55	0		.20
F2	TRK	ASTM	32	232	.034	TRAN	16	67	55	0		.20
F2	TRK	OVAL	32	232	.034	TRAN	16	76	55	0		.20
F3	TRK	OVAL	24	232	.029	LONG	4	61	40	0		.22
F3	TRK	OVAL	32	232	.029	LONG	4	51	40	0		.22
F3	TRK	ASTM	32	232	.029	LONG	4	46	40	0		.22
F3	TRK	ASTM	24	232	.029	LONG	4	48	40	0		.22
F3	TRK	ASTM	18	232	.029	LONG	4	51	40	0		.22
F3	TRK	BELT	24	232	.029	LONG	4	60	40	0		.22
F3	TRK	BELT	18	232	.029	LONG	4	54	40	0		.22
F3	TRK	RADL	24	232	.029	LONG	4	50	40	0		.22
F3	TRK	RADL	18	232	.029	LONG	4	48	40	0		.22
F3	TRK	OVAL	24	232	.029	LONG	8	69	40	0		.22
F3	TRK	ASTM	32	232	.029	LONG	8	57	40	0		.22
F3	TRK	ASTM	24	232	.029	LONG	8	65	40	0		.22
F3	TRK	ASTM	18	232	.029	LONG	8	64	40	0		.22
F3	TRK	BFLT	24	232	.029	LONG	8	72	40	0		.22
F3	TRK	BELT	18	232	.029	LONG	8	79	40	0		.22
F3	TRK	RADL	24	232	.029	LONG	8	83	40	0		.22
F3	TRK	RADL	18	232	.029	LONG	8	78	40	0		.22
F3	TRK	OVAL	32	232	.029	LONG	8	59	40	0		.22
F3	TRK	ASTM	24	232	.029	LONG	16	83	40	0		.22
F3	TRK	ASTM	32	232	.029	LONG	16	56	40	0		.22
F3	TRK	ASTM	18	232	.029	LONG	16	70	40	0		.22
F3	TRK	OVAL	24	232	.029	LONG	16	64	40	0		.22
F3	TRK	BELT	24	232	.029	LONG	16	72	40	0		.22
F3	TRK	BELT	18	232	.029	LONG	16	78	40	0		.22
F3	TRK	RADL	24	232	.029	LONG	16	77	40	0		.22
F3	TRK	RADL	18	232	.029	LONG	16	89	40	0		.22
F3	TRK	OVAL	32	232	.029	LONG	16	59	40	0		.22
F3	TRK	OVAL	32	232	.029	LONG	4	59	55	0		.22
F3	TRK	ASTM	32	232	.029	LONG	4	43	55	0		.22
F3	TRK	ASTM	24	232	.029	LONG	4	48	55	0		.22
F3	TRK	OVAL	24	232	.029	LONG	4	56	55	0		.22
F3	TRK	ASTM	18	232	.029	LONG	4	49	55	0		.22
F3	TRK	RADL	18	232	.029	LONG	4	53	55	0		.22
F3	TRK	BELT	18	232	.029	LONG	4	55	55	0		.22
F3	TRK	BFLT	24	232	.029	LONG	4	56	55	0		.22
F3	TRK	RADL	24	232	.029	LONG	4	52	55	0		.22
F3	TRK	ASTM	32	232	.029	LONG	8	51	55	0		.22
F3	TRK	ASTM	24	232	.029	LONG	8	47	55	0		.22
F3	TRK	OVAL	24	232	.029	LONG	8	63	55	0		.22
F3	TRK	ASTM	18	232	.029	LONG	8	66	55	0		.22
F3	TRK	RADL	18	232	.029	LONG	8	74	55	0		.22

Table 32. Cornering Slip a (Cont.)

TS	WS	TT	P	TD	TXD	TXDN	SA	CS	V	WD	I	S
[illegible]	TRK	BELT	13	232	.029	LONG	8	70	55	0		.22
	TRK	BELT	24	232	.029	LONG	8	78	55	0		.22
	TRK	RADL	24	232	.029	LONG	8	69	55	0		.22
	TRK	OVAL	32	232	.029	LONG	8	51	55	0		.22
	TRK	ASTM	32	232	.029	LONG	16	57	55	0		.22
	TRK	ASTM	24	232	.029	LONG	16	53	55	0		.22
	TRK	OVAL	24	232	.029	LONG	16	63	55	0		.22
	TRK	ASTM	18	232	.029	LONG	16	48	55	0		.22
	TRK	RADL	18	232	.029	LONG	16	68	55	0		.22
	TRK	BELT	18	232	.029	LONG	16	73	55	0		.22
	TRK	BELT	24	232	.029	LONG	16	68	55	0		.22
	TRK	RADL	24	232	.029	LONG	16	64	55	0		.22
	TRK	OVAL	32	232	.029	LONG	16	63	55	0		.22
	TRK	BELT	24	232	.056	LONG	4	67	40	0		.22
	TRK	BELT	18	232	.056	LONG	4	57	40	0		.22
	TRK	ASTM	32	232	.056	LONG	4	72	40	0		.22
	TRK	ASTM	24	232	.056	LONG	4	75	40	0		.22
	TRK	ASTM	18	232	.056	LONG	4	64	40	0		.22
	TRK	RADL	24	232	.056	LONG	4	56	40	0		.22
	TRK	RADL	18	232	.056	LONG	4	48	40	0		.22
	TRK	OVAL	32	232	.056	LONG	4	78	40	0		.22
	TRK	OVAL	24	232	.056	LONG	4	75	40	0		.22
	TRK	BELT	24	232	.056	LONG	8	93	40	0		.22
	TRK	BELT	18	232	.056	LONG	8	82	40	0		.22
	TRK	ASTM	32	232	.056	LONG	8	87	40	0		.22
	TRK	ASTM	24	232	.056	LONG	8	93	40	0		.22
	TRK	ASTM	18	232	.056	LONG	8	94	40	0		.22
	TRK	RADL	24	232	.056	LONG	8	97	40	0		.22
	TRK	RADL	18	232	.056	LONG	8	87	40	0		.22
	TRK	OVAL	32	232	.056	LONG	8	83	40	0		.22
	TRK	OVAL	24	232	.056	LONG	8	87	40	0		.22
	TRK	BELT	24	232	.056	LONG	16	94	40	0		.22
	TRK	BELT	18	232	.056	LONG	16	95	40	0		.22
	TRK	ASTM	32	232	.056	LONG	16	83	40	0		.22
	TRK	ASTM	24	232	.056	LONG	16	82	40	0		.22
	TRK	ASTM	18	232	.056	LONG	16	97	40	0		.22
	TRK	RADL	24	232	.056	LONG	16	91	40	0		.22
	TRK	RADL	18	232	.056	LONG	16	95	40	0		.22
	TRK	OVAL	32	232	.056	LONG	16	88	40	0		.22
	TRK	OVAL	24	232	.056	LONG	16	83	40	0		.22
	TRK	ASTM	18	232	.056	LONG	4	53	55	0		.22
	TRK	RADL	18	232	.056	LONG	4	58	55	0		.22
	TRK	BELT	18	232	.056	LONG	4	57	55	0		.22
	TRK	BELT	24	232	.056	LONG	4	67	55	0		.22
	TRK	BELT	24	232	.064	LONG	4	68	55	0		.22
	TRK	ASTM	24	232	.056	LONG	4	66	55	0		.22
	TRK	OVAL	24	232	.056	LONG	4	69	55	0		.22
	TRK	RADL	24	232	.056	LONG	4	56	55	0		.22
	TRK	ASTM	32	232	.056	LONG	4	69	55	0		.22
	TRK	OVAL	32	232	.056	LONG	4	75	55	0		.22
	TRK	ASTM	18	232	.056	LONG	8	80	55	0		.22
	TRK	RADL	18	232	.056	LONG	8	82	55	0		.22
	TRK	BELT	18	232	.056	LONG	8	80	55	0		.22
	TRK	BELT	24	232	.056	LONG	8	85	55	0		.22
	TRK	BELT	24	232	.064	LONG	8	88	55	0		.22

Reproduced from best available copy.

Reproduced from best available copy.

Table 32. Cornering Slip Data (Cont.)

TS	WS	TT	D	TD	TXD	TXDN	SA	CS	V	WD	I	S
	TRK	JVAL	32	232	.027	LONG	9	52	55	0		.22
	TRK	ASTM	18	232	.027	LONG	16	48	55	0		.22
	TRK	RADL	18	232	.027	LONG	16	55	55	0		.22
	TRK	BELT	18	232	.027	LONG	16	64	55	0		.22
	TRK	ASTM	24	232	.027	LONG	16	43	55	0		.22
	TRK	JVAL	24	232	.027	LONG	16	58	55	0		.22
	TRK	RADL	24	232	.027	LONG	16	53	55	0		.22
	TRK	BELT	24	232	.027	LONG	16	53	55	0		.22
	TRK	ASTM	32	232	.027	LONG	16	48	55	0		.22
	TRK	JVAL	32	232	.027	LONG	16	52	55	0		.22
	TRK	BELT	18	232	.031	TRAN	4	55	40	0		.22
	TRK	BELT	24	232	.031	TRAN	4	52	40	0		.22
	TRK	JVAL	32	232	.031	TRAN	4	47	40	0		.22
	TRK	JVAL	24	232	.031	TRAN	4	63	40	0		.22
	TRK	ASTM	32	232	.031	TRAN	4	49	40	0		.22
	TRK	ASTM	18	232	.031	TRAN	4	46	40	0		.22
	TRK	ASTM	24	232	.031	TRAN	4	46	40	0		.22
	TRK	RADL	18	232	.031	TRAN	4	45	40	0		.22
	TRK	RADL	24	232	.031	TRAN	4	46	40	0		.22
	TRK	BELT	18	232	.031	TRAN	8	68	40	0		.22
	TRK	BELT	24	232	.031	TRAN	8	68	40	0		.22
	TRK	JVAL	32	232	.031	TRAN	8	67	40	0		.22
	TRK	JVAL	24	232	.031	TRAN	8	69	40	0		.22
	TRK	ASTM	32	232	.031	TRAN	8	62	40	0		.22
	TRK	ASTM	18	232	.031	TRAN	8	55	40	0		.22
	TRK	ASTM	24	232	.031	TRAN	8	68	40	0		.22
	TRK	RADL	18	232	.031	TRAN	8	57	40	0		.22
	TRK	RADL	24	232	.031	TRAN	8	76	40	0		.22
	TRK	BELT	18	232	.031	TRAN	16	78	40	0		.22
	TRK	BELT	24	232	.031	TRAN	16	70	40	0		.22
	TRK	JVAL	32	232	.031	TRAN	16	67	40	0		.22
	TRK	JVAL	24	232	.031	TRAN	16	69	40	0		.22
	TRK	ASTM	32	232	.031	TRAN	16	69	40	0		.22
	TRK	ASTM	18	232	.031	TRAN	16	65	40	0		.22
	TRK	ASTM	24	232	.031	TRAN	16	72	40	0		.22
	TRK	RADL	18	232	.031	TRAN	16	77	40	0		.22
	TRK	RADL	24	232	.031	TRAN	16	75	40	0		.22
	TRK	BELT	24	232	.031	TRAN	4	57	55	0		.22
	TRK	ASTM	24	232	.031	TRAN	4	49	55	0		.22
	TRK	JVAL	24	232	.031	TRAN	4	57	55	0		.22
	TRK	RADL	24	232	.031	TRAN	4	53	55	0		.22
	TRK	ASTM	18	232	.031	TRAN	4	53	55	0		.22
	TRK	RADL	18	232	.031	TRAN	4	64	55	0		.22
	TRK	BELT	18	232	.031	TRAN	4	50	55	0		.22
	TRK	ASTM	32	232	.031	TRAN	4	56	55	0		.22
	TRK	JVAL	32	232	.031	TRAN	4	53	55	0		.22
	TRK	BELT	24	232	.031	TRAN	8	68	55	0		.22
	TRK	ASTM	24	232	.031	TRAN	8	53	55	0		.22
	TRK	JVAL	24	232	.031	TRAN	8	71	55	0		.22
	TRK	RADL	24	232	.031	TRAN	8	67	55	0		.22
	TRK	ASTM	18	232	.031	TRAN	8	63	55	0		.22
	TRK	RADL	18	232	.031	TRAN	8	66	55	0		.22
	TRK	BELT	18	232	.031	TRAN	8	67	55	0		.22
	TRK	ASTM	32	232	.031	TRAN	8	56	55	0		.22
	TRK	JVAL	32	232	.031	TRAN	8	59	55	0		.22

Table 32. Cornering Slip Data (Cont.)

TS	WS	TT	P	TD	TXD	TXDN	SA	CS	V	WD	I	S
17	TRK	BELT	24	232	.031	TRAN	16	57	55	0		.22
17	TRK	ASTM	24	232	.031	TRAN	16	56	55	0		.22
17	TRK	OVAL	24	232	.031	TRAN	16	70	55	0		.22
17	TRK	RADL	24	232	.031	TRAN	16	61	55	0		.22
17	TRK	ASTM	18	232	.031	TRAN	16	53	55	0		.22
17	TRK	RADL	18	232	.031	TRAN	16	63	55	0		.22
17	TRK	BELT	18	232	.031	TRAN	16	72	55	0		.22
17	TRK	ASTM	32	232	.031	TRAN	16	64	55	0		.22
17	TRK	OVAL	32	232	.031	TRAN	16	70	55	0		.22

TS - Test Section
WS - Water Source: TRK - truck water
NAT - natural
TT - Test Tire Type (RADL - Radial, ASTM - ASTM Standard, OVAL - Wide oval, BELT - Bias belted)
P - Tire Pressure, psi (1 psi = 6.9 kPa)
TD - Tread Depth: 1132 - 11/32 in (8.7 mm)
232 - 2/32 in (1.6 mm)
TXD - Texture Depth, in. (1 in = 25.4 mm)
TXDN - Texture Direction: TRAN - Transverse
LONG - Longitudinal
SA - Slip Angle, Degrees
CS - Measured Cornering Slip Number
V - Test Vehicle Speed, mph (1 mph = 1.6 km/h)
WD - Water Depth, in. (1 in = 25.4 mm)
I - Rainfall Intensity, in/h (1 in = 25.4 mm)
S - Cross Slope, in/ft

APPENDIX B

MEASUREMENT OF TEXTURE DEPTH BY THE SILICONE PUTTY METHOD

Scope

This method describes a procedure for determining the average macrotexture depth of a selected portion of a highway pavement surface.

Significance

The friction between a tire and the highway surface required for various vehicle maneuvers on a wet pavement, particularly in braking, depends in part on the thickness of the water film between the contact surfaces. This thickness, in turn, is controlled by the water drainage characteristics of the pavement as well as tire tread design and condition. Pavement drainage is influenced strongly by its surface macrotexture, one measure of which is the so-called texture depth. Additionally, an important contribution to friction at the tire-pavement interface is the hysteresis energy losses which occur as a result of cyclic deformation of the tread rubber; these are also influenced by texture depth.

Summary of Method

A known volume of silicone putty is formed into an approximate sphere and placed on the pavement surface. A 6-inch (15.2-cm) plate with a 4-inch (10.2-cm) diameter by 1/16-inch (0.16-cm) deep recess is centered over the putty and pressed down firmly against the pavement surface. The average diameter of the flattened putty is recorded. The volume of putty is selected so that on a smooth, flat surface with no texture the silicone putty will completely fill the 4-inch (10.2-cm) diameter recess. A decrease in diameter of the deformed putty is related to an increase in texture depth thus giving a rapid and simple index of pavement macrotexture.

The texture depth determined by this method is a number representing the ratio of the volume of the putty used to the resultant measured circular area covered. Accordingly, it is only an indirect measure of pavement macrotexture wavelength and amplitude, and gives no information on shape, distribution or other factors which may influence pavement surface drainage or hysteresis losses. Additionally, it is assumed that the putty completely fills all voids under the measured circular area.

Apparatus

The apparatus required for calibration and texture depth measurement consists of the following:

1. A circular plate 6 inches (15.2 cm) in diameter by 1 inch (2.5 cm) thick machined from flat acrylic plastic sheet* with a centrally machined, 4-inch (10.2 cm) diameter by 1/16-inch (0.16 cm) deep recess on one side.
2. 50-pound (22.7 kg) weight with convenient handle.**
3. Steel-wire bristle brush.
4. Stiff-bristle general-utility scrubbing brush.
5. 250-ml polyethylene "squeeze" washing or dispensing bottle fitted with a delivery tip drawn to give a fine, directed stream of dewetting agent.
6. Synthetically produced, wear-resistant cellulose, polyurethane, or other type of polymer foam sponge suitable for quick removal of excess dewetting agent from the pavement surface.
7. An engineer's scale capable of measuring putty diameter to 0.01 inch (0.025 cm).
8. A metal pry bar (for separation of the circular plate from the pavement at the end of test).
9. 3-ounce (88.7 cm^3) seamless tin plate containers with fitted lid (such as used in ASTM D 6).
10. Flat plateglass plate for use as a reference check surface, approximately 8 inch by 8 inch by 1/2 inch (20.3 cm by 20.3 cm by 1.3 cm).

Materials

The following materials are required to conduct this test:

---

*Plastic sheets, usually known as "plexiglas", manufactured by the Rohm & Haas Co., Philadelphia, Pa., or "Lucite", manufactured by E. I. DuPont de Nemours Co., Wilmington, Delaware, have been used satisfactorily.

**Such weights made by Fairbanks-Morse have been found to be satisfactory for this purpose.

1. A filled high-viscosity polysiloxane polymer, known as silicone putty*. Approximately 16 grams of this material will be required to completely fill the recess in the test plate on a flat smooth surface. It is usually possible to completely remove the putty from most pavement surfaces after a test is completed, and reuse this material in subsequent tests. However, it has proven to be advantageous to provide a number of pre-weighed putty specimens at the test site, transported in the covered 3-ounce (88.7 cm^3) containers described in 9 above.

2. Dilute solution of dioctyl sodium sulfosuccinate for use as a wetting and parting agent between the pavement surface and silicone putty test specimen. This solution can be made by mixing 5 ml of 75 percent aqueous Aerosol OT solution** with 5 gallons (19 litres) of distilled water.

Sampling

It is well known that in a given nominally uniform section of highway pavement, surface macrotexture may vary significantly from spot to spot. On the other hand, the area covered by the putty in this test is only a small fraction of the total pavement surface to be evaluated. Accordingly, appropriate selection of test locations will be a significant factor in achieving the objective of this test procedure. In a given section of pavement, putty depth measurement shall be made on at least 10 different locations. These may be selected as follows:

1. Random sampling procedure (preferred method). On a diagram of the pavement surface section to be measured, place a rectangular grid producing at least 1000 square cells, each designating a location on the pavement surface, and number these cells serially by any systematic method. Select 10 of these numbers from a table of random digits, and make tests at the center of the cell numbers so indicated.

2. Selective sampling (for preliminary or quick evaluation tests only). Visually inspect the pavement section to be evaluated, and select, on the basis of such observation, 10 locations which appear to be most representative of the texture of the entire section.

---

*A material marketed as "Silly Putty", available from Arnold Clark, Inc., Box 741, New Haven, Conn., has been found suitable for this purpose.

**Available from many general laboratory supply houses.

Procedure

At the locations selected for texture depth measurements, proceed as follows:

1. Remove all loose stones, other debris and contaminants by vigorous application of the steel wire brush.
2. Remove remaining sand and dust from the surface by careful dry brushing with the scrubbing brush.
3. Wet a section at least as large as the test plate with a spray of dilute Aerosol OT solution from a squeeze bottle.
4. Remove excess Aerosol OT solution by dipping and wiping the surface with the sponge.
5. Form silicone putty into an approximate sphere and place on the pavement surface.
6. Center the recess of the test plate over the putty and press the plate down in firm contact with the road surface. Use of the 50-pound (22.7 kg) weight to exert pressure for approximately 1 minute will usually suffice to bring the edges of the test plate into contact with the pavement surfact. Time intervals over 5 minutes should be avoided.
7. Make four diameter measurements with an angular spacing of 45°, with an engineer's scale to the nearest 0.01 inch (0.25 mm). The average of these readings is taken as the diameter of the flattened putty.
8. Remove the test plate from the pavement surface, using a pry bar if necessary. At the same time the putty also should be removed from the surface. In most instances, complete removal of the putty can be achieved by lightly pressing the putty ball against the few fragments which are clinging to the surface. In the few cases where more than a few hundredths of a gram of putty cannot be removed, it will be necessary to use a fresh putty specimen of the correct weight.

Calibration

Before the apparatus is used for field measurements, the standard procedure shall be followed in the laboratory, using the flat plateglass surface as a standard. If the putty has been weighed out correctly, it should completely fill the test plate recess, i.e., the putty shall have a diameter of 4 inches (10.2 cm).

Calculation of Texture Depth or Volume of Texture per Unit Area

Texture depth is calculated from the putty diameter by the following equation:

$$T_p = \frac{1}{D^2} - 0.0625 \quad [=] \frac{in^3}{in^2}$$

where:

T_p = texture depth, inches

D = average putty circle diameter, inches

or

$$T_p = \frac{2.54}{D^2} - 0.15875$$

where:

T_p = texture depth, cm

D = average putty circle diameter, cm

☆ U.S. GOVERNMENT PRINTING OFFICE: 1980 O— 620-871/805 REGION 3-1

FEDERALLY COORDINATED PROGRAM OF HIGHWAY RESEARCH AND DEVELOPMENT (FCP)

The Offices of Research and Development of the Federal Highway Administration are responsible for a broad program of research with resources including its own staff, contract programs, and a Federal-Aid program which is conducted by or through the State highway departments and which also finances the National Cooperative Highway Research Program managed by the Transportation Research Board. The Federally Coordinated Program of Highway Research and Development (FCP) is a carefully selected group of projects aimed at urgent, national problems, which concentrates these resources on these problems to obtain timely solutions. Virtually all of the available funds and staff resources are a part of the FCP, together with as much of the Federal-aid research funds of the States and the NCHRP resources as the States agree to devote to these projects.*

FCP Category Descriptions

1. Improved Highway Design and Operation for Safety

Safety R&D addresses problems connected with the responsibilities of the Federal Highway Administration under the Highway Safety Act and includes investigation of appropriate design standards, roadside hardware, signing, and physical and scientific data for the formulation of improved safety regulations.

2. Reduction of Traffic Congestion and Improved Operational Efficiency

Traffic R&D is concerned with increasing the operational efficiency of existing highways by advancing technology, by improving designs for existing as well as new facilities, and by keeping the demand-capacity relationship in better balance through traffic management techniques such as bus and carpool preferential treatment, motorist information, and rerouting of traffic.

3. Environmental Considerations in Highway Design, Location, Construction, and Operation

Environmental R&D is directed toward identifying and evaluating highway elements which affect the quality of the human environment. The ultimate goals are reduction of adverse highway and traffic impacts, and protection and enhancement of the environment.

4. Improved Materials Utilization and Durability

Materials R&D is concerned with expanding the knowledge of materials properties and technology to fully utilize available naturally occurring materials, to develop extender or substitute materials for materials in short supply, and to devise procedures for converting industrial and other wastes into useful highway products. These activities are all directed toward the common goals of lowering the cost of highway construction and extending the period of maintenance-free operation.

5. Improved Design to Reduce Costs, Extend Life Expectancy, and Insure Structural Safety

Structural R&D is concerned with furthering the latest technological advances in structural designs, fabrication processes, and construction techniques, to provide safe, efficient highways at reasonable cost.

6. Prototype Development and Implementation of Research

This category is concerned with developing and transferring research and technology into practice, or, as it has been commonly identified, "technology transfer."

7. Improved Technology for Highway Maintenance

Maintenance R&D objectives include the development and application of new technology to improve management, to augment the utilization of resources, and to increase operational efficiency and safety in the maintenance of highway facilities.

* The complete 7-volume official statement of the FCP is available from the National Technical Information Service (NTIS), Springfield, Virginia 22161 (Order No. PB 242057, price $45 postpaid). Single copies of the introductory volume are obtainable without charge from Program Analysis (HRD-2), Offices of Research and Development, Federal Highway Administration, Washington, D.C. 20590.

NTIS does not permit return of items for credit or refund. A replacement will be provided if an error is made in filling your order, if the item was received in damaged condition, or if the item is defective.

Reproduced by NTIS
National Technical Information Service
U.S. Department of Commerce
Springfield, VA 22161

This report was printed specifically for your order from our collection of more than 2 million technical reports.

For economy and efficiency, NTIS does not maintain stock of its vast collection of technical reports. Rather, most documents are printed for each order. Your copy is the best possible reproduction available from our master archive. If you have any questions concerning this document or any order you placed with NTIS, please call our Customer Services Department at (703)487-4660.

Always think of NTIS when you want:
• Access to the technical, scientific, and engineering results generated by the ongoing multibillion dollar R&D program of the U.S. Government.
• R&D results from Japan, West Germany, Great Britain, and some 20 other countries, most of it reported in English.

NTIS also operates two centers that can provide you with valuable information:
• The Federal Computer Products Center - offers software and datafiles produced by Federal agencies.
• The Center for the Utilization of Federal Technology - gives you access to the best of Federal technologies and laboratory resources.

For more information about NTIS, send for our FREE *NTIS Products and Services Catalog* which describes how you can access this U.S. and foreign Government technology. Call (703)487-4650 or send this sheet to NTIS, U.S. Department of Commerce, Springfield, VA 22161. Ask for catalog, PR-827.

Name _____
Address _____
_____
_____
Telephone _____

- Your Source to U.S. and Foreign Government Research and Technology.

U.S. DEPARTMENT OF COMMERCE
Technology Administration
National Technical Information Service
Springfield, VA 22161 (703) 487-4650

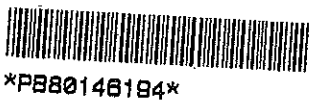

PB80146194

BX

BIN: M36 03-12-03
INVOICE: 1253285
SHIPTO: 1*152401
PAYMENT: CSH*CP